

Some pages of this thesis may have been removed for copyright restrictions.

If you have discovered material in Aston Research Explorer which is unlawful e.g. breaches copyright, (either yours or that of a third party) or any other law, including but not limited to those relating to patent, trademark, confidentiality, data protection, obscenity, defamation, libel, then please read our [Takedown policy](#) and contact the service immediately (openaccess@aston.ac.uk)

NEURONAL NETWORK DYNAMICS DURING EPILEPTOGENESIS IN THE MEDIAL TEMPORAL LOBE

**Tamara Modebadze
Doctor of Philosophy**

Aston University

September 2014

©Tamara Modebadze, 2014

Tamara Modebadze asserts her moral right to be identified as the author of this
thesis

This copy of the thesis has been supplied on condition that anyone who consults it is understood to recognise that its copyright rests with its author and that no quotation from the thesis and no information derived from it may be published without proper acknowledgement.

Aston University

Neuronal network dynamics during epileptogenesis in the medial temporal lobe

Tamara Modebadze

Doctor of Philosophy

2014

Epilepsy is one of the most common neurological disorders, a large fraction of which is resistant to pharmacotherapy. In this light, understanding the mechanisms of epilepsy and its intractable forms in particular could create new targets for pharmacotherapeutic intervention. The current project explores the dynamic changes in neuronal network function in the chronic temporal lobe epilepsy (TLE) in rat and human brain *in vitro*. I focused on the process of establishment of epilepsy (epileptogenesis) in the temporal lobe.

Rhythmic behaviour of the hippocampal neuronal networks in healthy animals was explored using spontaneous oscillations in the gamma frequency band (SyO). The use of an improved brain slice preparation technique resulted in the natural occurrence (in the absence of pharmacological stimulation) of rhythmic activity, which was then pharmacologically characterised and compared to other models of gamma oscillations (KA- and CCh-induced oscillations) using local field potential recording technique. The results showed that SyO differed from pharmacologically driven models, suggesting higher physiological relevance of SyO. Network activity was also explored in the medial entorhinal cortex (mEC), where spontaneous slow wave oscillations (SWO) were detected.

To investigate the course of chronic TLE establishment, a refined Li-pilocarpine-based model of epilepsy (RISE) was developed. The model significantly reduced animal mortality and demonstrated reduced intensity, yet high morbidity with almost 70% mean success rate of developing spontaneous recurrent seizures. We used SyO to characterize changes in the hippocampal neuronal networks throughout the epileptogenesis. The results showed that the network remained largely intact, demonstrating the subtle nature of the RISE model. Despite this, a reduction in network activity was detected during the so-called latent (no seizure) period, which was hypothesized to occur due to network fragmentation and an abnormal function of kainate receptors (KAr). We therefore explored the function of KAr by challenging SyO with kainic acid (KA). The results demonstrated a remarkable decrease in KAr response during the latent period, suggesting KAr dysfunction or altered expression, which will be further investigated using a variety of electrophysiological and immunocytochemical methods.

The entorhinal cortex, together with the hippocampus, is known to play an important role in the TLE. Considering this, we investigated neuronal network function of the mEC during epileptogenesis using SWO. The results demonstrated a striking difference in AMPAR function, with possible receptor upregulation or abnormal composition in the early development of epilepsy. Alterations in receptor function inevitably lead to changes in the network function, which may play an important role in the development of epilepsy. Preliminary investigations were made using slices of human brain tissue taken following surgery for intractable epilepsy. Initial results showed that oscillogenesis could be induced in human brain slices and that such network activity was pharmacologically similar to that observed in rodent brain.

Overall, our findings suggest that excitatory glutamatergic transmission is heavily involved in the process of epileptogenesis. Together with other types of receptors, KAr and AMPAR contribute to epilepsy establishment and may be the key to uncovering its mechanism.

Acknowledgements

I would like to express my biggest gratitude to my supervisor, Prof. Gavin Woodhall, for being the best supervisor one could dream of having. His guidance, support and great sense of humor have made my PhD so enjoyable. I admire his passion for science, and this is something for me to look up to. A big thank you goes to my associate supervisor, Prof. Ian Stanford, for giving advice and support whenever I needed it, and for his always honest opinions.

I would like to thank everyone who taught me so many things when I started. Most of all, Emma (Dr. Prokic!), thank you so much for all the lab and not-so-lab times and for always taking time to answer my million questions! I want to thank Craig (Dr. McAllister), Dr. Stephen Hall, Kim (Dr. Ronnqvist), Drs. Rhein Parri and Rob Sims. Many thanks to the guys from the biomed facilities, Wayne, Jeffrey, Kathryn and Brian, for always being ready to help. A special thank you goes to Gerard for the analysis of my data and his endless patience!

Big thanks to my friends and current lab mates Emma (again), Nick, Jane, Darshna (especially, for helping me finish some of the experiments!), Swetha and Serena! Those long long hours in the lab (and outside of it) were so much more fun with you guys! I would also like to thank my dear friends Korjik, Belka and Vova, who were miles away but were still supporting me in my good and bad times.

A very big thank you goes to my dear Andreas, who always encouraged me to move forward, who was always there for me. Thank you so much for your patience and all the tea and food that you made for me while I was writing up!

Finally, the most important thank you goes to my parents and my family, for always believing in me, for encouraging me, for loving and supporting me, most importantly for making me the person I am today. For that I am endlessly grateful.

Table of Contents

Acknowledgements	3
Table of Contents	4
List of Figures	9
List of Tables	12
Abbreviations	13
Chapter 1 Introduction	17
1.1. Neuronal network oscillations	18
1.1.1. What are brain rhythms?	18
1.1.2. Gamma rhythm (30 – 100 Hz)	19
1.1.2.1. ING model	20
1.1.2.2. PING model	21
1.1.2.3. Gamma oscillations in brain physiology	23
1.1.2.4. Gamma oscillations in brain pathology	24
1.1.3. Slow rhythm (0.1 – 0.5 Hz)	25
1.1.3.1. Mechanism of SWO generation	26
1.1.3.2. Pharmacology of SWO	27
1.1.3.3. SWO in brain physiology	29
1.1.3.4. SWO in brain pathology	29
1.2. Kainate receptors and oscillogenesis	30
1.2.1. KA _r in the hippocampus	30
1.2.2. KA _r in the EC	32
1.2.3. KA _r pharmacology	33
1.2.4. KA _r in gamma oscillations	34
1.2.5. KA _r in epilepsy	36
1.3. Aims and objectives	38
Chapter 2 Methods	39
2.1. Brain slice preparation	40
2.2. Reduced intensity model of chronic epilepsy	41
2.2.1. Model protocol	41
2.2.2. Experimental timeline	42
2.2.3. SRS development	43
2.3. Human brain tissue electrophysiology	43
2.4. Electrophysiological Recordings	44

2.4.1. Extracellular recording	44
2.4.2. Evoked field potential recording	45
2.4.3. Patch-clamp recording	46
2.5. Data Collection and Analysis	46
2.5.1. Spontaneous gamma oscillations	46
2.5.2. Phase analysis	47
2.5.3. SWO analysis	50
2.5.4. Evoked field potential and patch-clamp analysis	51
2.6. Drugs	51

Chapter 3 Spontaneous gamma oscillations in CA3

hippocampus	52
3.1. Introduction	53
3.1.1. <i>In vitro</i> models of induced gamma oscillations and pharmacology	53
3.1.2. Spontaneous gamma oscillations	55
3.1.3. Improved brain slice preparation technique	56
3.2. Results	57
3.2.1. Traditional vs. improved brain slice preparation	57
3.2.2. Basic profile of SyO, KA- and CCh-induced gamma oscillations	58
3.2.3. Characterisation of SyO	62
3.2.4. Pharmacological profile of SyO, KyO and CChyO	62
3.2.4.1. GABAergic pharmacology	63
3.2.4.2. Glutamatergic pharmacology	65
3.2.4.3. Cholinergic pharmacology	69
3.2.4.4. Gap junctions	69
3.2.5. Phase profile of SyO, KyO and CChyO	71
3.2.5.1. Phase characterisation	71
3.2.5.2. Volume conduction problem	74
3.2.5.3. Dose-dependent phase effects of KA and CCh on SyO	74
3.2.6. Laminar profile of SyO and KyO	78
3.3. Discussion	78
3.3.1. SyO in improved brain slice preparation	78
3.3.2. Basic profile of SyO, KyO and CChyO	80
3.3.3. Characterisation of SyO	82
3.3.4. Comparative Pharmacology	83
3.3.4. Phase analysis of SyO	87
3.3.5. Laminar characterisation of SyO and KyO	87
3.3.7. SyO as a physiologically relevant model of gamma oscillations	88

3.4. Conclusion	88
Chapter 4 The Reduced Intensity Status Epilepticus (RISE)	
model of chronic epilepsy	90
4.1. Introduction	91
4.1.1. Epilepsy models in animals.....	92
4.1.1.1. <i>In vitro</i> models of seizures	93
4.1.1.2. Models of acute seizures	94
4.1.1.3. Kindling model of epilepsy	94
4.1.1.4. Post SE epilepsy models	94
4.1.1.4.1. KA-induced SE model of epilepsy.....	96
4.1.1.4.2. Pilocarpine/Li-pilocarpine model of epilepsy	96
4.1.2. Epilepsy in human brain slices <i>in vitro</i>	100
4.1.3. Necessity for improvement and refinement	101
4.2. Results	102
4.2.1. Model refinement	102
4.2.1.1. Low mortality and high morbidity.....	103
4.2.2. Behavioural studies.....	105
4.2.3. <i>In vitro</i> studies in the hippocampus.....	107
4.2.3.1. Morphology and staining	107
4.2.3.2. SyO in healthy and epileptic rats.....	110
4.2.3.2.1. 24h post-SE	110
4.2.3.2.2. 7d post-SE	112
4.2.3.2.3. 6-8 wks post-SE	114
4.2.3.2.4. 90+d post-SE	116
4.2.3.3. VFO as a biomarker of epilepsy.....	118
4.2.3.4. Ictal and interictal activity in CA3	119
4.2.3.5. Spontaneous ictal activity in the mEC in PSE 7d.....	121
4.3. Discussion.....	122
4.3.1. Model refinement	122
4.3.2. Reduced mortality in RISE.....	123
4.3.3. Behavioural studies.....	123
4.3.4. <i>In vitro</i> studies of neuronal networks	124
4.3.4.1. Early post-insult alterations in network function	124
4.3.4.2. Neuronal network function during the latent period	126
4.3.4.3. Neuronal network function during SRS period	127
4.3.4.4. Ictal activity in the mEC.....	128
4.4. Conclusion	128

Chapter 5 KAr studies in RISE	130
5.1. Introduction	131
5.1.1. KAr expression in human epilepsy.....	132
5.1.2. KAr expression in animal models of epilepsy	134
5.2. Results.....	135
5.2.1. Extracellular recordings	135
5.2.2. KAr function in evoked field potential recording.....	145
5.2.3. KAr function in whole-cell patch-clamp recordings	148
5.2.3.1. Attempts to increase CA3 viability.....	148
5.2.3.2. KAr effects on GABA release.....	149
5.3 Discussion.....	153
5.4. Conclusion	156
Chapter 6 Spontaneous rhythmic activity in layer II mEC	157
6.1. Introduction	158
6.1.1. The EC and epilepsy.....	158
6.1.2. The EC and SWO	158
6.2. Results.....	160
6.2.1. Basic profile in control slices.....	160
6.2.2. Pharmacological characterisation	165
6.2.3. Spontaneous SWO in RISE	171
6.2.4. Pharmacology of SWO in epileptic slices	172
6.3. Discussion.....	173
6.3.1. Basic profile of SWO in control vs. epileptic slices	173
6.3.2. Pharmacology of SWO in control vs. epileptic slices	175
6.3.3. Functional significance and relation to <i>in vivo</i> studies	179
6.4. Conclusions	181
Chapter 7 Electrophysiology of paediatric brain tissue resected from patients with intractable epilepsy	182
7.1. Introduction	183
7.2. Results.....	184
7.2.1. Basic profile of neuronal network oscillations	184
7.2.2. Pharmacological characterisation	188
7.2.3. VFO and ictal activity	192
7.2.4. IPSC kinetics in human cortical slices	194
7.3. Discussion.....	195
7.3.1. Basic profile of human tissue oscillations	195

7.3.2. Pharmacology of human tissue oscillations	200
7.3.3. VFO and ictal activity	200
7.4. Conclusion	201
Chapter 8 General discussion and future work.....	202
References.....	207
Appendix	244
Appendix 1.....	245
Appendix 2.....	248

List of Figures

Figure 1.1. Schematic representation of ING and PING models of gamma oscillations.	21
Figure 1.2. Schematic diagram of interconnected pyramidal cell and different types of interneurons in hippocampal CA3 region.....	22
Figure 1.3. KAr localisation in the hippocampus.....	31
Figure 1.4. KAr localisation in the EC	33
Figure 2.1. Experimental timeline.	42
Figure 2.2. Schematic diagram of combined hippocampal-EC brain slice.	44
Figure 2.3. Electrophysiology rig setup.....	45
Figure 2.4. PLV for random and unimodal distribution of phase angle difference.	48
Figure 2.5. Method limitation: bimodal phase angle difference distribution.	49
Figure 3.1. Improved brain slice preparation increases slice viability and exposes natural SyO.	58
Figure 3.2. Basic profile of SyO, KyO and CChyO.	59
Figure 3.3. Time-frequency analysis of SyO, KyO and CChyO.....	59
Figure 3.4. Mean power-frequency characterisation of SyO, KyO and CChyO.....	60
Figure 3.5. SyO survive prolonged storage.	61
Figure 3.6. Weight-dependent profile of SyO.	62
Figure 3.7. Abolition of SyO, KyO and CChyO by 20 μ M PTX.	63
Figure 3.8. The effects of GABA-Ar modulators on SyO, KyO and CChyO.	64
Figure 3.9. Differential effects of GluK1,3 KAr antagonist UBP310 (3 μ M) on SyO, KyO and CChyO.	65
Figure 3.10. Differential effects of NMDAr antagonist on SyO, KyO and CChyO.....	67
Figure 3.11. The effects of glutamatergic antagonists on SyO, KyO and CChyO.....	68
Figure 3.12. Differential effects of mAChr antagonist on SyO, KyO and CChyO.	69
Figure 3.13. The effects of mGluR and mAChr antagonists and gap junction blocker SyO, KyO and CChyO.	70
Figure 3.14. Phase coupling of SyO, KyO and CChyO across CA3.....	72
Figure 3.15. Short- and long-range connectivity in SyO.	73
Figure 3.16. Volume conduction issue.....	74
Figure 3.17. Phase synchrony-power relationship for increasing concentrations of KA and CCh.....	76
Figure 3.18. Phase synchrony-power-concentration relationship for KyO.....	77
Figure 3.19. Laminar profile of SyO and KyO.	78
Figure 4.2. The mechanism of pilocarpine model of chronic TLE.....	94
Figure 4.2. SRS frequency is variable and follows a weekly cycle.	104
Figure 4.3. Behavioural measurements of epilepsy following induction.	106

Figure 4.4. Morphology of epileptic brains.	109
Figure 4.5. At PSE 24h LFP recordings show SyO and fast bursts in CA3.	111
Figure 4.6. SyO in CA3 at PSE 7d.	113
Figure 4.7. SyO in CA3 during PSE 6wks.	115
Figure 4.8. SyO in CA3 during PSE 90d.	117
Figure 4.9. VFO as a biomarker of increased excitability in PSE 24h and PSE 90d.	118
Figure 4.10. Spontaneous ictal activity in the hippocampal CA3 region in PSE 24h.	120
Figure 4.11. Interictal activity in the hippocampal CA3 region in PSE 24h.	121
Figure 4.12. Spontaneous ictal events in layers II/III mEC in PSE 7d slices.	121
Figure 5.2. Basic profile of SyO and KyO in AMC and PSE 24h.	136
Figure 5.3. Basic profile of SyO and KyO in AMC and PSE 7d.	137
Figure 5.4. Basic profile of SyO and KyO in AMC and PSE 6wks shows compromised KA- induced activity.	140
Figure 5.5. Basic profile of SyO and KyO in AMC and PSE 90d.	141
Figure 5.5. Pooled peak frequency and peak power plots for SyO and KyO in control and epileptic conditions.	144
Figure 5.6. KAr response is compromised during PSE 6wks.	145
Figure 5.7. Evoked field potential in the hippocampal CA3 region.	147
Figure 5.8. Poor survival of the hippocampal CA3 in control adult slices.	148
Figure 5.9. KAr effects on GABA release in CA3 of control slices.	151
Figure 5.10. KAr effects on GABA release in CA3 of epileptic slices.	152
Figure 6.1. Basic profile of SWO in layers II/III of the mEC.	161
Figure 6.2. Variety of electrographic patterns of SWO in control and PSE 24h/7d slices. ..	162
Figure 6.3. SWO in deep and superficial layers of the mEC.	163
Figure 6.4. Differences in the developmental profile of SWO in control and epileptic slices.	164
Figure 6.5. Reducing $[Mg^{2+}]_o$ promotes SWO in control adult slices.	164
Figure 6.6. Differential effects of GABA-Ar blockade on SWO in control and PSE 24h/7d slices.	165
Figure 6.7. The effects of GABA-Br blockade on SWO in control and PSE 24h/7d slices. .	166
Figure 6.8. NMDAr blockade reduces the interburst frequency but increases burst amplitude in control and PSE 24h/7d.	167
Figure 6.9. AMPAr/KAr blockade abolishes SWO in control and PSE 24h/7d slices.	167
Figure 6.10. GluK1,3 KAr blockade abolishes SWO in control and PSE 24h/7d slices.	168
Figure 6.11. The effect of KAr activation on SWO in PSE 24h/7d.	168
Figure 6.12. AMPAr blockade abolishes SWO in PSE 24h/7d but not control slices	169
Figure 6.13. mGluR ₅ blockade promotes intraburst synchrony in control and PSE 24h/7d.	170

Figure 6.14. mGluR groups II/III blockade promotes intraburst synchrony in control and PSE 24h/7d.	170
Figure 6.15. Gap junction blockade abolishes SWO in control and PSE 24h/7d.	171
Figure 7.1. Human brain tissue slice morphology and KA-induced rhythmic activity	186
Figure 7.2. KA- and CCh-induced rhythmic activity in human cortical brain tissue.	187
Figure 7.3. Rhythmic activity in the human cortex is mediated by GABA-Ar.	188
Figure 7.7.4. Pharmacological profile of pharmacologically-induced rhythmic activity in the human cortical tissue.	190
Figure 7.5. VFOs are not mediated via gap junctions.....	191
Figure 7.6. Similarities between VFO in PSE 24h slices and epileptic human tissue.....	192
Figure 7.7. Ictal event in epileptic cortical tissue from a human brain.	193
Figure 7.8. GABA sIPSC kinetic properties of the individual cells in normal and dysplastic human tissues.	194
Figure 7.9. KAr modulated GABA release.	195
Figure A.1.	245

List of Tables

Table 1.1. KAr ligands.....	34
Table 2.1. Racine scale of seizures.....	42
Table 2.2. Patient data.....	43
Table 4.1 PSBB tasks.....	105
Table A.1. Choline chloride-based cutting solution recipe.....	248
Table A.2. NMDG-based cutting solution recipe.....	248
Table A.3. Modified HEPES holding aCSF recipe.....	249
Table A.4 Recording aCSF recipe.....	249

Abbreviations

ACh - Acetylcholine

aCSF – Artificial Cerebrospinal Fluid

ADP – Adenosine Triphosphate

AMC – Age-Matched Control

AMPA_r - 2-amino-3-(5-methyl-3-oxo-1, 2- oxazol-4-yl) propanoic acid receptor

AP-5 - D-(-)-2-Amino-5-phosphonopentanoic acid

Arb. Unit – Arbitrary Unit

ATP – Adenosine Triphosphate

Av. - Average

Ca²⁺ - Calcium Ion

CaCl₂ – Calcium Chloride

CBX - Carbenoxolone

CCh – Carbachol

CChyO – CCh-induced Gamma Oscillations

CHPG - (RS)-2-Chloro-5-hydroxyphenylglycine

Cl⁻ - Chloride Ion

CNQX - 6-Cyano-7-nitroquinoxaline-2,3-dione

D - Day

DG – Dentate Gyrus

DHPG- (S)-3,5-Dihydroxyphenylglycine

e.g. – *Exempli Gratia*

EC – Entorhinal Cortex

EEG- Electroencephalogram

EPSCs – Excitatory Postsynaptic Currents

eEPSCs – Evoked excitatory Postsynaptic Currents

FFT – Fast Fourier Transform

FIR – Finite Impulse Response

GABA - Gamma (γ)-Aminobutyric Acid

GABA-A_r - Gamma (γ)-Aminobutyric Acid - A receptor

GABA-B_r Gamma (γ)-Aminobutyric Acid – B receptor

GBZ - Gabazine

h - Hour

HCO₃⁻ - Bicarbonate Ion
HEPES - 4-(2-Hydroxyethyl)piperazine-1-ethanesulfonic acid
i.e. – *Id est*
I_{CAN} - Calcium-sensitive Non-selective Cation Current
IEI – Interevent Interval
IEM 1460 - N, N, H,-Trimethyl-5-[(tricyclo [3.3.1.1^{3,7}] dec-1-ylmethyl) amino]-1-entanaminiumbromide hydrobromide
iGluR – Ionotropic Glutamate Receptor
ILAE – International League Against Epilepsy
i/m - Intramuscular
I_{Na(p)} – Persistent Sodium Channel
ING - Interneuron Network Gamma
IP₃ – Inositol 1,4,5-trisphosphate
IPSCs – Inhibitory Postsynaptic Currents
IPSPs- Inhibitory Postsynaptic Potentials
IR-DIC – Infrared light/Differential Interference Contrast
K⁺ - Potassium Ion
KA – Kainic Acid
KAr – Kainate Receptor
KCl – Potassium Chloride
Kg - Kilogram
K_γO – KA-induced Gamma Oscillations
KO – Knock Out
LFP – Local Field Potential
Li – Lithium
LiCl – Lithium Chloride
mAChRs – Muscarinic Acetylcholine Receptors
MEG - Magnetoencephalography
Mg²⁺ - Magnesium Ion
mGluR – Metabotropic Glutamate Receptor
MgSO₄ – Magnesium Sulphate
mEC – Medial Entorhinal Cortex
mEPSPs – Miniature Excitatory Postsynaptic Potentials
MEST - Maximal Electroshock Seizure Threshold

Min - Minute
mIPSC - Miniature Inhibitory Postsynaptic Current
ml - Millilitre
mM - Millimolar
 μ M - Micromolar
M Ω - Megaohm 12
Ms - Millisecond
NA - Noradrenaline
Na⁺ - Sodium Ion
NaCl – Sodium Chloride
NaH₂PO₄ – Sodium Phosphate
NaHCO₃ – Sodium Hydrogen Carbonate
nM - Nanomolar
NMDAr - N-Methyl-D-aspartic acid receptor
NMDG - N-methyl d-glucamine chloride
P – Postnatal Day
PING – Pyramidal Interneuron Network Gamma
PLV – Phase-Locking Value
PPS – Proportionate Phase Synchrony
PSBB – Post-seizure Behavioural Battery
PSE 24h – 24 Hours Post *Status Epilepticus*
PSE 7d – 7 Days Post *Status Epilepticus*
PSE 6wks – 6 weeks Post *Status Epilepticus*
PSE 90d – 90 Days Post *Status Epilepticus*
PSd – Phase-Locking Value for KA- or CCh- induced gamma oscillations
PSs – Phase-Locking Value for Spontaneous gamma oscillations
PTX - Picrotoxin
PTZ - Pentylentetrazol
PV - Parvalbumin
RISE – Reduced Intensity *Status Epilepticus*
RMS – Root Mean Square
s – Second
s. - *Stratum*
s/c - Subcutaneous

SE – *Status Epilepticus*

S.E.M. – Standard Error of the Mean

SyO – Spontaneous Gamma Oscillations

sIPSC – Spontaneous Inhibitory Postsynaptic Current

sPSC – Spontaneous Postsynaptic Currents

SRS – Spontaneous Recurrent Seizures

SWO – Slow Wave Oscillations

TTX - Tetrodotoxin

TLE – Temporal Lobe Epilepsy

uIPSC – Unitary Inhibitory Postsynaptic Current

VFO – Very Fast Oscillations

vs. - Versus

wks - Weeks

Chapter 1 Introduction

1.1. Neuronal network oscillations

As early as 1875, the first electrical signals were recorded from the exposed brains of animals by Richard Canton, a Liverpool physician. However, it was not until 50 years later that such signals were recorded from a human brain. An Austrian psychiatrist, Hans Berger, was one of the pioneers in electroencephalography (EEG), having invented the EEG device, which allowed recording rhythmic activity of the brain. Since then much effort has been put into exploring various brain rhythms, their functions and mechanisms, roles in physiological and pathological states, as well as ways of altering rhythmic activity, using pharmacotherapy, deep brain stimulation and transcranial magnetic stimulation.

In the past 20 years, the field of neuronal network oscillations has become very popular, it has been able to attract neuroscientists from different areas by providing the opportunity to study brain function at multiple organisational levels: from understanding cellular and synaptic mechanisms underlying neuronal network behaviour, through interactions between networks at regional and interregional levels, to how network oscillations correlate with higher brain functions and pathological conditions. The development of *in vitro* electrophysiology has broadened the horizons of neuroscientific research. Using a combination of *in vivo* and *in vitro* approaches provides an opportunity to bring insights from different techniques together, working towards a larger picture of neuronal network function.

1.1.1. What are brain rhythms?

Brain rhythms represent extracellular voltage changes, which originate from the summation of electrical activity of neuronal assemblies, and are shaped by the geometry and alignment of those neurons (Buzsaki, 2006). The complexity of human/animal behaviour and cognitive functions requires neuronal networks in different areas of the brain to work together, which in turn requires populations of neurons engaged in a task to fire synchronously and repeatedly. This neuronal network activity is synchronized into particular rhythms. These rhythms can be detected and measured *in vivo* e.g. through EEG and magnetoencephalography (MEG), and *in vitro* e.g. local field potential recording (LFP). The mechanisms

underlying the generation of specific brain rhythms and the role(s) they play in the brain remain key questions in neuroscience.

Neuronal network oscillations are known to occur at characteristic frequencies ranging from 0.05 to ~600 Hz (Buzsaki and Draguhn, 2004). The EEG classification of brain rhythms divides them into frequency bands:

- ✚ delta (1 – 4 Hz)
- ✚ theta (4 – 7 Hz)
- ✚ alpha (8 – 13 Hz)
- ✚ beta (13 – 30 Hz)
- ✚ gamma (30 – 100 Hz)

Frequencies beyond this classification such as slow-wave (<1 Hz) oscillations (SWO) and very fast (>100 Hz) oscillations (VFOs) have also been observed (Steriade *et al.*, 1993c,d; Curio *et al.*, 1994). Each of the frequency bands correlates with specific brain functions, and various physiological and pathological states. For instance, delta rhythm can be observed during the deepest stages of sleep, whereas alpha wave represents a wakeful relaxation with closed eyes (Kandel *et al.*, 2000). Faster rhythms are thought to be involved in the process of memory formation and cognition, feature binding and, more globally, in a large-scale integration (Thallon-Baudry and Bertrand, 1999; Singer, 1999). Furthermore, some neurological disorders like epilepsy, Alzheimer's disease, schizophrenia and Parkinson's disease, are associated with abnormalities in synchronised brain activity (for review see Herrmann and Demiralp, 2005; Ulhaas and Singer, 2006). There is clear evidence that neuronal network oscillations play one of the key roles in the operation of the brain; exploring these network oscillations will lead to a better understanding of mechanisms underlying higher brain functions. Below, I will briefly review neuronal network oscillations of high (gamma) and very low (SWO) frequencies in terms of their mechanisms and biological functions.

1.1.2. Gamma rhythm (30 – 100 Hz)

Probably the most extensively studied rhythm in the brain *in vitro* is the gamma rhythm. It is commonly observed in various regions of the brain during wakefulness

and is most often associated with cognitive function (for reviews see Singer and Gray, 1995; Engel *et al.*, 2001). In terms of *in vitro* gamma rhythmogenesis, the most explored oscillations have been those occurring in the hippocampus. This is due to its accessibility, its clearly defined laminar organisation and its densely packed pyramidal cells, which give rise to large-amplitude oscillations. *In vivo*, hippocampal gamma oscillations are known to arise during specific behavioural states like exploration, when they usually co-occur with theta oscillations; therefore, there is an opportunity to study the relationship between oscillations and behaviour (Bragin *et al.*, 1995). Due to a large amount of work done on gamma activity in hippocampus, many underlying mechanisms have been already uncovered.

From the results of *in vivo* studies, two independent generators of gamma oscillations in the hippocampus have been identified, the first one being in the dentate gyrus (DG) receiving inputs from the entorhinal cortex (EC) and another one being in CA3 region propagating to CA1 (Csicsvari *et al.*, 2003). Over the years, ways of artificially inducing gamma oscillations in brain slices have been discovered: kainic acid (KA), carbachol (CCh) or (*RS*)-2-Chloro-5-hydroxyphenylglycine (CHPG, metabotropic glutamate receptor agonist), hypertonic potassium (K^+) solution, as well as by tetanic stimulation (Whittington *et al.*, 1995; Fisahn *et al.*, 1998; Fisahn *et al.*, 2004; Hajos and Paulsen, 2009). Overall, the general mechanism has been established and it is known that gamma oscillations arise from the interaction of the inhibitory interneuronal network and pyramidal cells. One of the crucial conditions for gamma rhythm generation in hippocampus is the presence of γ -Aminobutyric acid (GABA)-mediated inhibition by interneurons. Two models of gamma oscillations include interneuron network gamma (ING) and pyramidal-interneuron network gamma (PING) and have been reviewed by Whittington *et al.* (2000).

1.1.2.1. ING model

Gamma oscillations can be generated by a group of inhibitory interneurons (Fig. 1.1A). The prerequisites for the emergence of gamma oscillations are: 1. interconnected inhibitory interneurons, 2. GABA-A receptor (GABA-Ar) mediated inhibitory postsynaptic potentials (IPSPs) with an exponential decay time constant and 3. an excitatory drive to elicit spiking in the interneurons (Wang and Rinzel,

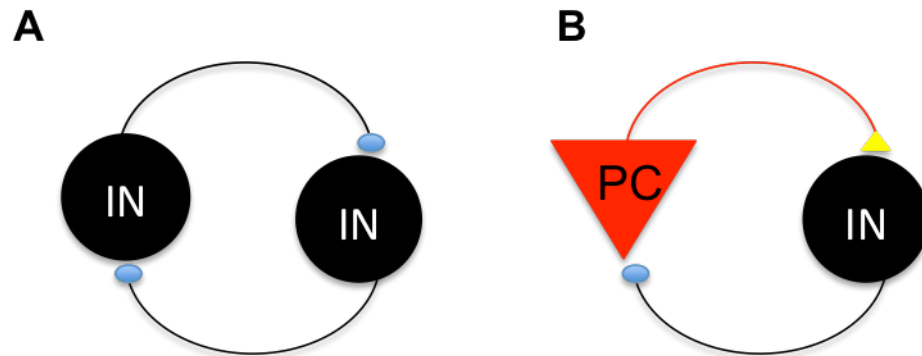


Figure 1.1. Schematic representation of ING and PING models of gamma oscillations. ING (A), PING (B). Adapted from Mann *et al.*, 2005a.

1992; Whittington *et al.*, 1995; Traub *et al.*, 1996a). When the interneurons receive either a tonic or stochastic excitatory input, they start firing spikes. The synchrony comes about when a group of interneurons starts discharging together and thus generate IPSPs in the coupled interneurons, which respond with a rebound spiking after the decay of GABA-Ar-mediated hyperpolarisation, and the process is repeated (Buzsaki and Wang, 2012). Single interneurons spike with the frequency of approximately 40 Hz (Wang and Buzsaki, 1996). Such mutual inhibition takes all the interneurons to zero-phase synchrony, when the activity is synchronous without any temporal delays. The frequency of oscillations essentially depends on the kinetics of IPSPs. Experiments with increased decay time constant have demonstrated a decrease in the frequency of oscillations whilst manipulations, which speed up the decay time constant, have the opposite effect (Traub *et al.*, 1996a).

1.1.2.2. PING model

Compared to a simple ING model, a more complex PING model (Fig. 1.1B), which adds to the system pyramidal cells reciprocally connected to the interneurons, demonstrates how the whole network can be phase-locked to gamma frequency. It is believed that with certain strength of the fast excitation coupled with delayed inhibition, activity in the two populations of cells can alternate in a cyclic manner (Buzsaki and Wang, 2012). In the PING model, three different types of interneurons are distinguished: targeting either other interneurons, perisomatic regions of pyramidal cells, or pyramidal cell dendrites (Fig. 1.2) (Buhl *et al.*, 1994; Halasy *et al.*, 1996; Acsady *et al.*, 1996; Cobb *et al.*, 1997). After numerous studies on the possible mechanism of PING model, it was identified that of all the different types of

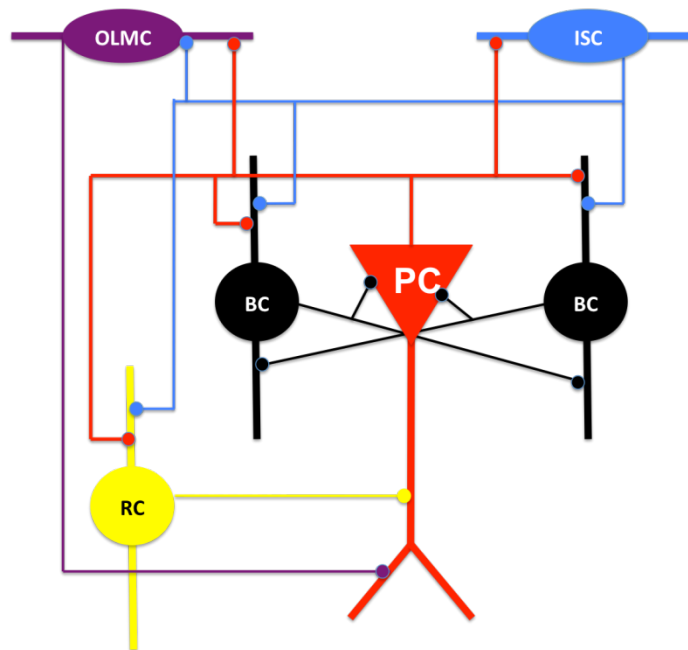


Figure 1.2. Schematic diagram of interconnected pyramidal cell and different types of interneurons in hippocampal CA3 region (adapted from Hajos *et al.*, 2004). PC, pyramidal cell; BC, basket cell, IS, interneuron-selective cell; OLM, oriens-lacunosum-moleculare cell; RC, radiatum cell.

interneurons, the fast spiking parvalbumin-containing (PV) basket cells projecting to the pyramidal cell soma have the putative role of generating gamma rhythm (Lyttton and Sejnowski, 1991; Penttonen *et al.*, 1998; Csicsvari *et al.*, 2003; Gloveli *et al.*, 2005; Mann *et al.*, 2005b). The basket cells impose rhythmic IPSPs on the pyramidal cells, thus making their firing become binned into narrow time windows (Penttonen *et al.*, 1998; Gloveli *et al.*, 2005, Hasenstaub *et al.*, 2005, Mann *et al.*, 2005a). Among different types of interneurons, basket cells stand out because of their low spike threshold, ability to fire quickly, and their resonance in gamma frequency band in response to stochastic excitation (Gulyas *et al.*, 1993; Buzsaki *et al.*, 1983; McCormick *et al.*, 1985; Pike *et al.*, 2000). The role of other interneuron types in generating gamma oscillations is less understood. Miles and colleagues (1996) compared the roles of somatic and dendritic targeting interneurons and concluded that while somatic interneurons control pyramidal cell output, the dendritic interneurons regulate the efficacy of dendritic inputs.

Receiving the excitatory drive from pyramidal cells, individual interneurons become synchronised. With the coordinated involvement of interneuron-selective interneurons and basket cell coupling with each other via synapses and gap junctions, the interneuronal network activity becomes synchronised with gamma frequency (Cobb

et al., 1997; Fukuda and Kosaka, 2000; Meyer *et al.*, 2002). Electrical coupling between the interneurons does not seem to be a prerequisite for the generation of gamma oscillations. However, knocking out (KO) gap junction protein connexin 36, which is expressed between interneurons (Galarreta and Hestrin, 1999, 2002), greatly reduced the amplitude of oscillations (Hormuzdi *et al.*, 2001; Buhl *et al.*, 2003). Similarly, pharmacological blockade of gap junctions reduced oscillatory power as well (Traub *et al.*, 2000, 2001a).

Interestingly, the intracellular recordings from the basket and pyramidal cells during gamma oscillations revealed that pyramidal cells phase-locked to the oscillation fired at a very low frequency (approximately 3 Hz), while the phase-coupled interneurons fire with a delay at higher frequencies (Fisahn *et al.*, 1998; Hajos *et al.*, 2004). Interneurons terminating in the perisomatic region exhibited firing at high frequencies and were strongly phase-coupled, whereas interneurons projecting to the dendrites displayed firing at lower frequency and weaker phase coupling (Hajos *et al.*, 2004). To investigate whether the pyramidal cells firing at low frequencies are able to support gamma oscillations, Mann and colleagues (2005a) designed a network model of 400 pyramidal cell and 40 interneurons. They concluded that with the phasic excitation of interneurons provided by pyramidal cells, the recurrent feedback inhibition appeared to be a plausible mechanism for network activity synchronisation and that pyramidal cells were not required to fire on every cycle of an oscillation.

1.1.2.3. Gamma oscillations in brain physiology

The role of gamma oscillations in the brain is still being uncovered, however, they are most often observed during attentive states such as focused wakefulness, sensory perception, object recognition, and language perception (Bouyer *et al.*, 1981; Sheer *et al.*, 1989; Murthy and Fetz, 1992; Pfurtscheller and Neuper, 1992). Gamma frequency oscillations have been implicated in fast coordination of neurons required in such hippocampal processes as input selection, arranging cells into functional groups, memory storage and retrieval (Colgin and Moser, 2010). These operations require activation of certain neuronal populations, as well as selective elimination of unnecessary inputs. Hence, hippocampal pyramidal cells are known not to fire on every cycle of the gamma rhythm (Senior *et al.*, 2008; Colgin *et al.*, 2009; de Almeida *et al.*, 2009). It is believed that gamma is involved in temporal encoding and sensory

binding of features, as well as learning and memory processes (Hopfield *et al.*, 1995; Buzsaki and Chrobak, 1995; Lisman and Idiart, 1995; Lisman, 1999). On a global scale, gamma frequency oscillations are thought to indicate integration mechanisms in the brain (Herrmann *et al.*, 2004). It is clear that gamma oscillations play a substantial role in cognitive brain functions, however this area requires further exploration.

1.1.2.4. Gamma oscillations in brain pathology

Apart from the physiological role of gamma oscillations, gamma rhythm alterations are also observed during various pathological states. For example, synchronous activity of neuronal networks is a key player in epilepsy, as it has long been thought that hypersynchronisation was the main feature underlying this condition (Penfield and Jasper, 1954). In this context, high frequency oscillations in the gamma range have been observed both before and at the onset of ictal events (Fisher *et al.*, 1992; Allen *et al.*, 1992). A special place in epilepsy disorder is taken by VFOs observed both *in vivo* and *in vitro* in humans and animals at the onset of seizures and have been proposed to play a role of biomarkers of epilepsy (Fisher *et al.*, 1992; Bragin *et al.*, 1999a,b; Traub *et al.*, 2001b; Grenier *et al.*, 2003; Worrell *et al.*, 2008). Several studies explored changes in synchrony associated with epilepsy and showed enhanced local phase synchrony (van Putten, 2003; Garcia Dominguez *et al.*, 2005). In contrast to hypersynchrony in epilepsy, schizophrenia is one of the disorders closely associated with the impairment of neuronal network beta and gamma frequency range oscillation and their synchronisation over long distances, leading to disturbed cognitive functions (Kwon *et al.*, 1999; Krishnan *et al.*, 2005; Ulhaas *et al.*, 2006). Abnormalities of GABA-ergic transmission, as well as NMDAr dysfunction have been proposed to play a role in the mechanism of disrupted synchronisation in schizophrenia (Lewis *et al.*, 2005; Moghaddam *et al.*, 2003). Herrmann and Demiralp (2005), as well as Ulhaas and Singer (2006), have published extensive reviews of abnormal gamma rhythms in the context of neuropsychiatric disorders. Several studies also suggested that impaired long-range synchronisation was implicated in Alzheimer's disease, and this, together with neuronal loss, was leading to cognitive dysfunctions (Babiloni *et al.*, 2004; Koenig *et al.*, 2005; Stam *et al.*, 2006). Gamma rhythm activity has also been shown to play a role in such disorders as autism (Brock *et al.*, 2002) and attention deficit hyperactivity disorder (Yordanova *et al.*, 2001).

1.1.3. Slow rhythm (0.1 – 0.5 Hz)

Studies in behaving animals have investigated oscillatory neuronal network activity in the two fundamental brain states: sleep and arousal. The state of arousal in animals is represented by attentiveness and alertness and appears on EEG as low-voltage high-frequency activity (Moruzzi and Magoun, 1949). Quiescent states, on the other hand, are observed during sleep or anaesthesia and are accompanied by high-voltage low-frequency oscillatory activity. During deep sleep and anaesthesia, the cortex does not simply remain in an idle state, but rather engages in a characteristic pattern of activity consisting of periods of silence (DOWN state) and intensive cell firing (UP state) alternating at 0.1–0.5 Hz. In humans the frequency range may be slightly broader (Achermann and Borbely, 1997; Iber *et al.*, 2007). Steriade (2006) suggested that SWO *in vivo* played a role in grouping other rhythms creating complex, nested waveforms. Human studies demonstrated that UP states of SWO were accompanied by elevated activity in almost all frequency bands (Csécsa *et al.*, 2010). Cortical activity of such low frequency has been reported both *in vivo* in anaesthetised and sleeping animals and *in vitro* in cortical slices of various species (Steriade *et al.*, 1993a-d; Timofeev *et al.*, 1996; Sanchez-Vives and McCormick, 2000; Shu *et al.*, 2003; Dickson *et al.*, 2003; Cunningham *et al.*, 2006; Sheroziya *et al.*, 2009). Due to the occurrence of SWO in various cortical regions (in neo- and allocortex), different functional properties have been assigned to observed cortical activity (from implications in development and metabolism to information processing and memory consolidation). Nevertheless, SWO show striking similarities regardless of the brain area, and it is commonly agreed that the more recently described SWO recorded *in vitro* resemble those recorded by Steriade *et al.* (1993c,d) during sleep and anaesthesia.

SWO are generated within the cortex. Experiments with lesioned thalamocortical connections revealed that SWO persisted in the cortex in the absence of reciprocal connections and does not appear in the thalamus of decorticated animals (Timofeev and Steriade, 1996). Different views exist regarding the layer-specific origin of this activity. Several reports from *in vitro* and *in vivo* studies suggest that activity is generated in the deep cortical layers (in particular layer V of the neocortex), spreading to layer VI and later to the superficial layers (Sanchez-Vives and McCormick, 2000, Chauvette *et al.*, 2010). On the other hand, the current-source

density analysis of human recordings from prefrontal and parietal cortices revealed a large sink in supragranular layers, indicating superficial origin of UP state generation (Csercsa *et al.*, 2010). Furthermore, studies in the entorhinal cortex demonstrate that SWO activity is generated by interaction of superficial neurons and interneurons (Dickson *et al.*, 2003; Gnatkovsky *et al.*, 2007). The discrepancies, however, could arise from the differences in species, the cytoarchitectonics of recorded cortical areas, as well as recording conditions.

Nir and colleagues (2011) investigated whether the human cortical SWO activity was a global or localised phenomenon. Their results demonstrated a localised nature of this activity, favouring the theory of sleep being controlled by local circuits (Krueger *et al.*, 2008). Nir *et al.* (2011) also showed that slow waves could propagate along different anatomic pathways. At the cellular level, the following questions arise: what causes persistent firing during UP states of SWO? Does it occur due to intrinsic membrane properties or barrages of synaptic activity? Some experimental results demonstrated that intracellular injection of hyperpolarising or depolarising currents did not alter the parameters of SWO, indicating that network mechanisms may underly this rhythm (Sanchez-Vives and McCormick, 2000).

1.1.3.1. Mechanism of SWO generation

Numerous studies dedicated to unraveling how SWO activity is generated yielded two plausible cellular mechanisms. UP states are initiated by spontaneous firing of layer V neurons (in conditions of increased excitability) and sustained through recurrent excitatory connections (Sanchez-Vives and McCormick, 2000; Compte *et al.*, 2003). Being the largest cortical cells, layer V neurons have the largest number of inputs, which increases the probability of UP state generation. Another proposed mechanism involves occasional summation of miniature excitatory postsynaptic potentials (mEPSPs), which activates persistent sodium (Na^+) current ($I_{\text{Na(p)}}$) leading to the depolarisation of cortical pyramidal cells, activation of calcium (Ca^{2+})-sensitive non-selective cation current (I_{CAN}) (Sheroziya *et al.*, 2009) and subsequent spike generation. This process triggers an UP state of prolonged bursts maintained by $I_{\text{Na(p)}}$, I_{CAN} and synaptic activity (Timofeev *et al.*, 2000; Bazhenov *et al.*, 2002; Sheroziya *et al.*, 2009; Chauvette *et al.*, 2010). $I_{\text{Na(p)}}$ is a small but long-lasting Na^+ current, which is activated by subthreshold voltages and persists for hundreds of

milliseconds (ms), thus enhancing excitability of other depolarising currents and maintaining repetitive firing (Stafstrom *et al.*, 1985; Beck and Yaari, 2008).

DOWN states are known to be refractory periods of hyperpolarisation occurring due to Na⁺- and Ca²⁺-activated K⁺ currents and synaptic fatigue (possibly due to depletion of extracellular Ca²⁺ after a prolonged UP state) (Steriade *et al.*, 1993d; Sanchez-Vives and McCormick, 2000; Bazhenov *et al.*, 2002; Compte *et al.*, 2003; Sheroziya *et al.*, 2009). Cunningham and colleagues (2006) suggested that the initiation of DOWN states occurred due to a K⁺ current activated by metabolic demands [ATP]/[ADP] (adenosine triphosphate/adenosine diphosphate) during UP states. Overall, activation of K⁺ currents leads to cell hyperpolarisation. It has been reported that the switch to silent (DOWN) state was highly synchronous, which implied involvement of widespread inhibition mediated by interneurons (Volgushev *et al.*, 2006). A later study demonstrated that almost half of the fast-spiking cell population started firing at a higher rate towards the end of UP states (Puig *et al.*, 2008).

1.1.3.2. Pharmacology of SWO

In a combined *in vitro* and *in vivo* study, Sanchez-Vives and McCormick (2000) suggested that UP states of SWO were generated by both excitatory and inhibitory postsynaptic potentials. A detailed pharmacological analysis of SWO helped tease apart various components of synaptic transmission involved in their generation and maintenance. Several studies suggested that spontaneous SWO in the cortex depended heavily on N-Methyl-D-aspartic acid receptors (NMDAr), being blocked by NMDAr antagonist AP-5 (Sanchez-Vives and McCormick, 2000; Shu *et al.*, 2003; Allene *et al.*, 2008; Sheroziya *et al.*, 2009). Conversely, Cunningham and colleagues (2006) demonstrated that neither NMDAr nor 2-Amino-3-(5-methyl-3-oxo-1,2-oxazol-4-yl) propanoic acid receptors (AMPAr) were involved in SWO. CNQX, a non-selective AMPAr/KAr antagonist, reliably abolished SWO activity in most studies, indicating a crucial role of KAr-mediated excitation (Sanchez-Vives and McCormick, 2000; Shu *et al.*, 2003; Cunningham *et al.*, 2006; Sheroziya *et al.*, 2009). Cunningham and colleagues (2006) further investigated KAr role by applying UBP302 (a selective GluK1 antagonist), which readily blocked spontaneous SWO.

Together with excitatory components, the role of GABA-ergic inhibition was investigated in several studies. It is generally accepted that GABA-Ar blockade enhances SWO activity before transforming it into interictal (epileptiform) discharges (Sanchez-Vives and McCormick, 2000; Shu *et al.*, 2003; Allene *et al.*, 2008; Sheroziya *et al.*, 2009). Similar results were demonstrated with a decrease in magnesium (Mg^{2+}) concentration in artificial cerebro-spinal fluid (aCSF) causing a gradual rise in the frequency of rhythmic activity and a rapid switch to prolonged epileptiform bursts (Sanchez-Vives and McCormick, *et al.*, 2000). Recently, Allene *et al.* (2008) reported two distinct types of SWO occurring at different stages of development (cortical early network oscillations and cortical giant depolarising potentials). Interestingly, while the early network oscillations were considered to be glutamate-driven (abolished by NMDAr blockade, but enhanced by GABA-Ar blockade), the giant depolarising potentials were less sensitive to NMDAr block and were abolished by GABA-Ar antagonists (Allene *et al.*, 2008).

Resemblance of SWO *in vitro* with those observed during sleep and anaesthesia encouraged researchers to explore potential cholinergic and noradrenergic modulation of this activity. It is known that these two systems are at least partially involved in cortical arousal, since slow rhythmic patterns of activity can be disrupted by brainstem stimulation of cholinergic and noradrenergic nuclei (Moruzzi and Magoun 1949; Steriade *et al.* 1993a; Steriade and Contreras 1995). Several studies demonstrated that the same results could be reproduced *in vitro* by application of either CCh or noradrenaline (NA) (Shu *et al.*, 2003; Favero *et al.*, 2012). These results indicated that cortical SWO recorded in brain slices related in some way to slow wave sleep oscillations, and possibly represented the same phenomenon at the mechanistic level.

Together with obvious similarities between various reported slow oscillations, there are certain discrepancies in their properties. Hence, it is not clear whether the disparities arise from exploring different brain regions in different species under different conditions or because investigators are actually observing different types of cortical activity.

1.1.3.3. SWO in brain physiology

Several research groups study rather similar patterns of SWO, but diverge in their views on the nature and the functional significance of this activity. For instance, the laboratories of Yehezkel Ben-Ari, Rosa Cossart and others suggest a developmental role of SWO during the maturation of the cortex. Furthermore, Sheroziya *et al.* (2009) also suggest an important role played by bursting neurons (in the EC) in cortical and hippocampal development. Although Allene and colleagues (2008) draw a parallel between cENO and *in vivo* rhythms observed during sleep, they do not make any definite conclusions. Steriade, Timofeev, McCormick and others, on the other hand, focus on the SWO occurring during sleep and anaesthesia and suggest implications in information processing and memory consolidation (Sanchez-Vives and McCormick, 2000; Tononi and Cirelli, 2006; Stickgold and Walker, 2007). These sleep-related SWO may exhibit an age-dependent pattern of their own. For example, Massimini and colleagues (2004) demonstrated that in humans this activity originated mostly from frontal cortical areas. Supporting these findings, Kurth *et al.* (2010) showed how the SWO propagation changed with age, starting from occipital regions in toddlers and gradually switching from posterior to anterior cortical brain regions until late adolescence. These results suggested changing levels of cortical excitability throughout development, which could potentially explain recording spontaneous SWO in the EC only in young animals (Sheroziya *et al.*, 2009) or in adult animals under the conditions of increased excitability (Cunningham *et al.*, 2006).

1.1.3.4. SWO in brain pathology

A potential link between SWO and epilepsy has been investigated in several studies in humans and animals. Vanhatalo and colleagues (2004) used EEG recording to detect slow activity (0.02 – 0.2 Hz) in the brains of epileptic patients during sleep. The study demonstrated that interictal activity was synchronised with SWO in cortical regions, preferentially appearing on the negative peak of SWO. The authors suggested that these results might help develop new diagnostic and therapeutic approaches to epilepsy. In animals, for instance, Steriade and Contreras (1995) showed that normal sleep-like synchronous activity in the cortex could develop into ictal activity, represented by typical 2 – 4 Hz spike-and-wave complexes. This type of pathological activity is normally observed on the EEG during absence seizures. Assuming SWO are a developmental phenomenon, it is possible to explore this

rhythmic activity in epileptic animals to determine any developmental changes occurring in pathological conditions.

1.2. Kainate receptors and oscillogenesis

Glutamate is a major excitatory neurotransmitter in the mammalian brain. Metabotropic and ionotropic glutamate receptors (mGluR and iGluR) are two classes of receptors mediating excitatory transmission through G-proteins and ion channels, respectively. KAR, together with AMPAR and NMDAR, constitute a class of ligand-gated iGluRs, which are mostly permeable to Na⁺, K⁺ and Ca²⁺. KAR are homo- and heteromeric tetramers, comprised of the combinations of 5 receptor subunits GluK1-5, formerly known as GluR5-7 and KA1-2 (Bettler and Mulle, 1995). KAR have been shown to give rise to excitatory postsynaptic currents (EPSCs) with kinetics much slower compared to AMPAR (Castillo *et al.*, 1997; Vignes and Collingridge, 1997). While AMPAR and NMDAR, located postsynaptically, mostly mediate basal excitatory synaptic transmission, KAR produce a variety of regulatory effects in neuronal communication. This type of receptors is found both pre- and postsynaptically. Postsynaptic KAR, due to their slow kinetics, have a role of regulating neuronal excitability and information processing by integrating excitatory synaptic inputs (Frerking and Nicoll, 2000; Frerking and Oligher-Frerking, 2002, Goldin *et al.*, 2007, Pinheiro *et al.*, 2013). Presynaptic KAR, on the other hand, bidirectionally regulate neurotransmitter release at both inhibitory and excitatory synapses (Schmitz *et al.*, 2000; Lauri *et al.*, 2001; Rodriguez-Moreno *et al.*, 1998; Frerking *et al.*, 1999; Cossart *et al.*, 2001). For extensive updated reviews on KAR in the brain see Perrais *et al.* (2010), Contractor *et al.* (2011), Lerma and Marques (2013).

1.2.1. KAR in the hippocampus

Despite the abundance of KAR across diverse brain regions, possibly the most studied area remains the hippocampus (for review see Carta *et al.*, 2014). Early studies demonstrated high densities of KAR, with all 5 subunit types expressed in rat hippocampus (Monaghan and Cotman, 1982; Wisden and Seeburg, 1993). Studies reported expression of GluK1 KAR subunits on the hippocampal interneurons, GluK2 were found in pyramidal cell layers and interneurons, GluK3 were expressed mostly in the DG, GluK4 on pyramidal cells, while GluK5 were widely found throughout the

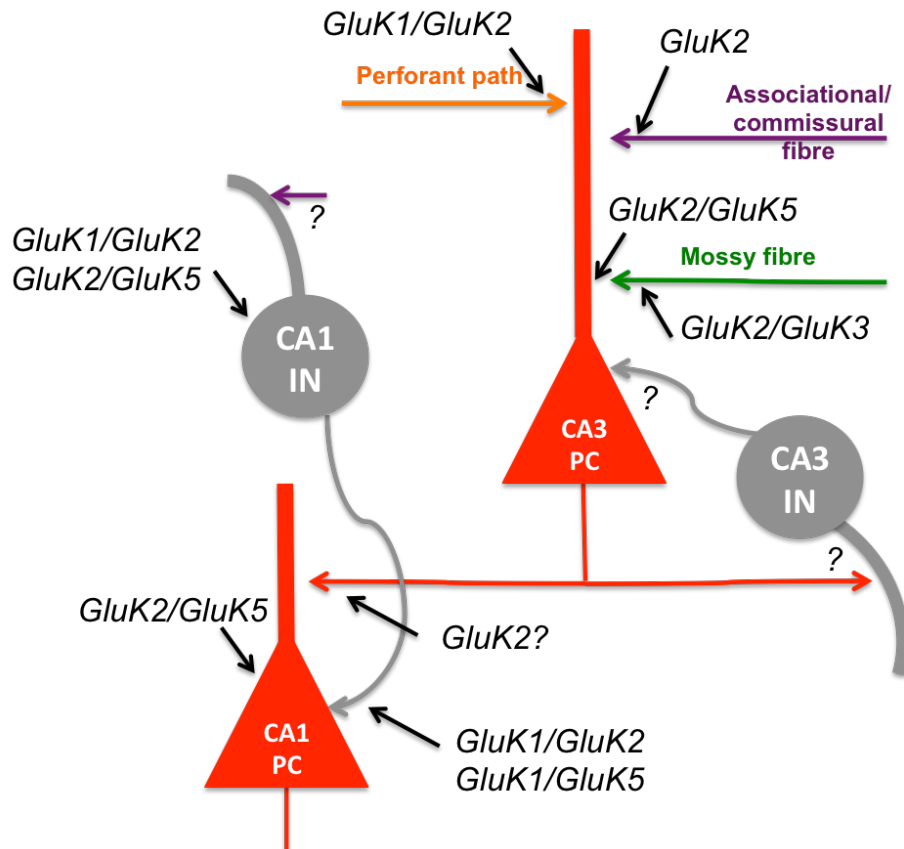


Figure 1.3. KAR localisation in the hippocampus. IN, interneuron; PC, pyramidal cell (adapted from Pinheiro and Mulle, 2006 and Carta *et al.*, 2014).

hippocampus (for review see Carta *et al.*, 2014). The lack of subunit-selective KAR antagonists presents an issue in determining subunit-specific effects. In the hippocampal CA3 region, postsynaptic KAR function has been explored at mossy fibres projecting to CA3 pyramidal cells (Castillo *et al.*, 1997; Vignes and Collingridge, 1997). Mulle and colleagues demonstrated that slow EPSCs on CA3 pyramidal cells were mediated by GluK2 KAR. Mossy fibres have also been shown to carry presynaptic KAR autoreceptors (Represa *et al.*, 1987; Schmitz *et al.*, 2001). Presynaptic effects of KAR on mossy fibres include facilitation of transmitter release (Contractor *et al.*, 2001; Pinheiro *et al.*, 2007). Darstein and colleagues (2003) carried out a subunit-specific analysis of pre- and postsynaptic KAR at mossy fibres. The results showed that GluK4 were expressed presynaptically, while GluK5 were found at the postsynaptic membrane, however both types were co-expressed with GluK2 (Darstein *et al.*, 2003). The lack of studies on interneuronal KAR in the CA3 region does not allow a review of KAR function in this area.

Together with the CA3 region, KAr localisation and function were explored in CA1. Early reports demonstrated presynaptic inhibition of glutamate release at Schaffer collateral – CA1 pyramidal cell synapses (Chittajallu *et al.*, 1996; Kamiya and Ozawa, 1998). Later studies proposed that presynaptic modulation was conducted by metabotropic KAr (Rodriguez-Moreno and Lerma, 1998; Frerking *et al.*, 2001). Interestingly, postsynaptic KAr responses (KAr EPSCs) could not be evoked at CA1 pyramidal cells, indicating the absence of KAr on the postsynaptic membrane (Cossart *et al.*, 1998; Frerking *et al.*, 1998; Cossart *et al.*, 2002). Early studies reported that micromolar (μM) concentration of KA presynaptically reduced inhibitory transmission of CA1 interneurons onto the pyramidal cells (Fisher and Alger, 1984; Kehl *et al.*, 1984; Rodriguez-Moreno *et al.*, 1997). Later studies using submicromolar concentrations reported an increase of inhibition (Cossart *et al.*, 2001; Jiang *et al.*, 2001). Rodriguez-Moreno and colleagues (1997) suggested metabotropic nature of presynaptic KAr. Somato-dendritic KAr have been found on CA1 interneurons, contributing to the postsynaptic excitatory inputs to interneurons. Semyanov and Kullmann (2001), however, suggest axonal localisation of KAr on CA1 interneurons.

KAr localisation and function in the hippocampus is summarised in Fig. 1.3, adapted from Vincent and Mulle (2009) and Carta *et al.* (2014).

1.2.2. KAr in the EC

KAr function in the EC has been described only by a small number of studies (West *et al.*, 2007; Beed *et al.*, 2009 and Chamberlain *et al.*, 2012). The most extensive characterisation of pre- and postsynaptic KAr in layer III of the EC was presented by Chamberlain and colleagues (2012). Authors reported that glutamate terminals carried presynaptic KAr, which facilitated glutamate release and were likely to be assembled of GluK1 and possibly GluK2 subunits, similarly to mossy fibre autoreceptor reports. The authors did not exclude the possibility of non-GluK1 KAr inhibiting glutamate release. It was also suggested that GluK1 KAr were unlikely to participate in postsynaptic transmission. KAr were shown to mediate slow EPSCs in layer III neurons via GluK2, but not GluK1-containing KAr (Beed *et al.*, 2009; Chamberlain *et al.*, 2012). It was suggested that postsynaptic KAr in the EC could be located peri- or extrasynaptically (Chamberlain *et al.*, 2012). The role of KAr in GABA-ergic transmission was also investigated in layer III EC. The results

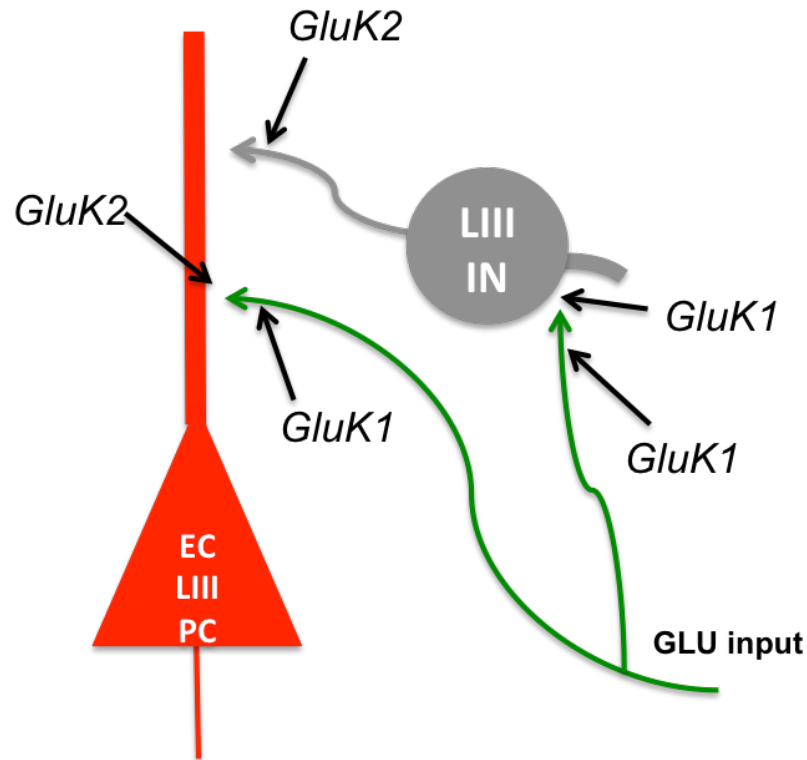


Figure 1.4. KAR localisation in the EC LIII IN, mEC layer III interneuron; EC LIII PC, mEC layer III pyramidal cell; GLU input, glutamatergic input (adapted from Chamberlain *et al.*, 2012).

demonstrated that KAR stimulation increased GABA release, as a result of increased firing of interneurons due to activation of somato-dendritic GluK1-containing KAR on interneurons (Chamberlain *et al.*, 2012). Same study suggested the existence of presynaptic non-GluK1 KAR heteroreceptors inducing GABA release. The effects of KAR in the EC are summarized in Fig. 1.4, adapted from Chamberlain *et al.* (2012).

1.2.3. KAR pharmacology

Uncovering the functions of KAR has always been restricted by the lack of selective pharmacological agents that could first distinguish between AMPAR and KAR and then between the different subunits within KAR. With the development of selective AMPAR antagonists like GYKI 53655 (Paternain *et al.*, 1995) and SYM 2206 (Pelletier *et al.*, 1996), it was possible to extract KAR-mediated currents and their slow kinetics (Castillo *et al.*, 1997). Pharmacological advancement resulted in the development of subunit-selective KAR agonists and antagonists, which are summarised in Table 1.1,

adapted from Jane *et al.* (2009). Certain KAr subunits like GluK2 or GluK5 remain without selective antagonists, which complicates KAr characterisation.

Table 1.1. KAr ligands. Adapted from Jane *et al.*, (2009).

Compound	Activity	Selectivity	References
KA	Agonist	KAr ($EC_{50} < 10\mu M$)	Watkins, 1981; Alt <i>et al.</i> , 2004
AMPA	Agonist	AMPAr ($EC_{50} > 100\mu M$)	Hansen <i>et al.</i> , 1983; Alt <i>et al.</i> , 2004
ATPA	Agonist	GluK1	Clarke <i>et al.</i> , 1997; Alt <i>et al.</i> , 2004
ACET	Antagonist	GluK1, GluK1/5	Dolman <i>et al.</i> , 2007; Perrais <i>et al.</i> , 2009
UBP310	Antagonist	GluK1, GluK3	Dolman <i>et al.</i> , 2007; Perrais <i>et al.</i> , 2009
UBP304	Antagonist	GluK1	Dolman <i>et al.</i> , 2006
UBP296	Antagonist	GluK1, GluK1/2, GluK1/5	More <i>et al.</i> , 2004; Dolman <i>et al.</i> , 2006
LY382884	Antagonist	GluK1, GluK1/2, GluK1/5	Alt <i>et al.</i> , 2004

1.2.4. KAr in gamma oscillations

The fast excitation provided for interneurons by the pyramidal cells is mediated *via* glutamatergic synapses. There are contradicting reports on the role of glutamatergic AMPAr in generation and maintenance of gamma oscillations in the brain. Some reports demonstrated that gamma oscillations were greatly decreased in power with genetically reduced AMPA currents and were greatly diminished or blocked by AMPA receptor antagonists (Fuchs *et al.*, 2007; Cunningham *et al.*, 2003, 2004; Palhalmi *et al.*, 2004). By contrast, Fisahn *et al.* (2004) reported that AMPAr antagonist did not produce any effect, implying that AMPAr were not involved in gamma oscillations. The discrepancies, however, could be species- (rats vs. mice), area- (hippocampus vs. EC), AMPAr antagonism- (GYKI 53655 vs. SYM2206 vs. AMPAr KO) and gamma type-specific (KA- vs. CCh- vs. DHPG-induced).

Another mediator of glutamatergic transmission is KAr, abundantly expressed both in the hippocampus and EC and playing an important role in neuronal communication. KAr also appear to be crucial for neuronal network synchronisation in the gamma frequency band. Application of nanomolar doses of KA produces persistent gamma oscillation in brain slices, which has been observed in the cortex (Buhl *et al.*, 1998; Cunningham *et al.*, 2003), hippocampus (Hajos *et al.*, 2000; Hormuzdi *et al.*, 2001; Fisahn *et al.*, 2004) and other areas. Several studies were dedicated to uncovering the roles of each receptor subunit. Fisahn and colleagues (2004) studied the hippocampus of GluK1 and GluK2 KO mice and discovered that in the absence of GluK2, KA was not able to induce oscillations. It was suggested that GluK2 subunit-containing KAr were located in the somato-dendritic region of interneurons and pyramidal cells and, when activated by KA, increased action potential firing and consequent GABA and glutamate release. KAr containing GluK1, on the other hand, were located on the axons of interneurons and did not seem to be critical for induction of oscillatory activity, but instead set the inhibition level, preventing epileptiform activity. A slightly different picture was presented by Brown *et al.* (2006) in the hippocampus and Stanger *et al.* (2008) in the medial EC (mEC). In those studies, KAr GluK1 subunit function was pharmacologically tested using selective GluK1 antagonists and it was revealed that while it might not be sufficient to *generate* oscillatory activity, it played an important role in *maintaining* gamma oscillations in the temporal lobe.

It was demonstrated that KAr played a crucial role not only in gamma frequency oscillations but also in the generation of SWO in the EC. SWO are known to be shaped by the balance between excitation and inhibition. Contributing to this balance may be KAr, since SWO was abolished by CNQX, as well as by GluK1-selective KAr antagonist UBP302 (Cunningham *et al.*, 2006; Sheroziya *et al.*, 2009). Taking into account the work of Chamberlain and colleagues (2012), it appears that it is either tonically active presynaptic KAr autoreceptors or somato-dendritic KAr receptors on layer III interneurons that are involved in SWO generation. Further studies would be required to determine the exact role of KAr in this type of rhythmic activity.

1.2.5. KAr in epilepsy

Interestingly, application of KA can produce not only oscillatory, but also epileptiform activity. For many years local and systemic administration of KA has been used as a model of seizures/epilepsy, which resemble those observed in temporal lobe epilepsy (TLE) patients (Ben-Ari *et al.*, 1985). The role of KAr in epilepsy and its link to oscillogenesis have been explored. The variety of pre- and postsynaptic effects exerted by KAr on different cells populations in the temporal lobe introduces possibilities of KAr involvement in regulating the excitation and inhibition balance (Ben-Ari and Cossart, 2000). Several studies indicated a dual nature of KA effects, depending on the subunit composition. GluK1 subunit KAr are located mostly on interneurons and act to decrease excitability of pyramidal neurons by increasing tonic and phasic inhibition (Khalilov *et al.*, 2002; Fisahn *et al.*, 2004). The GluK1 subunit specific agonist ATPA was shown to augment the firing of interneurons and subsequent GABA release, which inhibited pyramidal cells. Authors also reported that ATPA was able to stop propagation of paroxysmal discharges in hippocampal regions. There are, however, studies showing that GluK1 antagonist prevented pilocarpine- and 6 Hz stimulation-induced seizures (Smolders *et al.*, 2002; Barton *et al.*, 2003). GluK2-containing KAr, on the other hand, are found in mossy fibre synapses and are considered to be involved in seizure generation, since KO studies show a significant increase in seizure threshold and a reduced sensitivity to KA (Cossart *et al.*, 1998; Mulle *et al.*, 1998; Fisahn *et al.*, 2004). Telfeian and colleagues (2000) reported that overexpression of GluK2 receptors in the hippocampus produced limbic seizures *in vivo*.

A study by Behr *et al.* (2002) demonstrated inhibitory presynaptic KAr effects on GABA release in DG. As the results suggest, this effect was augmented in kindled animals, indicating elevated KAr sensitivity or expression. Epsztein *et al.* (2010) discovered KAr-related differences between dentate granule cells in TLE and healthy animals. It was reported that in TLE, unlike controls, recurrent mossy fibre synapses relied on KA transmission, which changed the firing of dentate granule cells from sparse to sustained rhythmic pattern. Since the DG gates information flow from EC to hippocampus, its altered activity in TLE may disrupt normal neuronal processing and coding (Artinian *et al.*, 2011).

Much effort has been put into exploring the effects of KAR agents in both healthy and epileptic animals, providing new possibilities for drug discovery process. A large part of research focused on the roles of GluK1 and GluK2 subunits. For instance, it was demonstrated that the anticonvulsant, topiramate, was able to block both electrophysiological and clinical GluK1-mediated effects (Gryder and Rogawski, 2003; Kaminski *et al.*, 2004). It also reduced KA-induced seizures (Kaminski *et al.*, 2004). The role of GluK1 was also explored by Smolders and colleagues (2002) both *in vivo* and *in vitro*. GluK1 antagonists were found to reduce and prevent population spikes elicited by KA or pilocarpine in hippocampal regions. Similar anticonvulsant effects were achieved by GluK1 antagonists *in vivo*, when tested against pilocarpine- and 6 Hz stimulation-induced seizures. Both electrical stimulation- and picrotoxin-induced epileptiform events in CA3 were reduced by GluK1 antagonists, although the compounds were found to be ineffective against seizures caused by intravenous injection of picrotoxin (PTX). Barton and colleagues (2003) demonstrated that one of those GluK1 antagonists, although ineffective against generalised MES seizures, produced a decrease in seizures induced by 6 Hz stimulation. Furthermore, studies on soman-induced seizure model revealed that GluK1 antagonists could block pathological rhythmic activity both *in vitro* and *in vivo* (Apland *et al.*, 2009; Apland *et al.*, 2013; Figueiredo *et al.*, 2011).

Apart from GluK1 and GluK2, the role of GluK3 was investigated by Loscher *et al.* (1999). It was reported that a relatively selective GluK3 antagonist reduced seizures elicited by kindling in rats, however, did not produce any significant effect in MES model.

Altogether, studies in the literature demonstrate that KAR are tightly involved in an essential brain function, such as rhythmogenesis, by exerting a variety of their regulatory effects due to differential subunit composition and receptor localisation on different types of neurons. Moreover, growing evidence shows a complex role of KAR in the processes of icto- and epileptogeneses and the potential for unravelling the mechanism of epilepsy and developing new therapeutic approaches.

1.3. Aims and objectives

1. To develop a physiologically-relevant model of neuronal network activity in the hippocampus *in vitro* and compare it to existing models.
2. To develop a model reflecting natural activity of neuronal networks in the EC *in vitro*.
3. To develop a refined model of chronic TLE in the rat.
4. To characterise changes in the temporal lobe network function in the refined model of epilepsy using models 1 and 2.
5. To investigate the role of excitatory neurotransmission in epileptogenesis.
6. To characterise neuronal network activity in human epileptic brain *in vitro* and compare it to the refined animal model of epilepsy.

Chapter 2 Methods

2.1. Brain slice preparation

Combined hippocampal-EC slices were obtained from male Wistar rats (50 – 500 g). Each rat was anaesthetized firstly with 2% isoflurane in N₂/O₂ and then with injection of pentobarbital (~600 mg/kg) and ketamine (~100 mg/kg) + xylazine (10 mg/kg) until the paw pinch, tail pinch and corneal reflexes disappeared. Then the rat was transcardially perfused with ice-cold sucrose aCSF, which contained (mM): 180 sucrose, 2.5 KCl, 10 MgSO₄, 25 NaHCO₃, 1.25 NaH₂PO₄, 0.5 CaCl₂, 10 glucose, 1 L-ascorbic acid, 2 N-acetyl-L-cysteine, 1 taurine, 20 ethyl pyruvate, 0.04 indomethacin, 0.4 uric acid, 0.01 aminoguanidine, 0.19 ketamine and saturated with carbogen (95% O₂, 5% CO₂). To obtain brain tissue free of spontaneous activity, basic sucrose solution composition was used for perfusion and cutting (mM): 206 sucrose, 2 KCl, 1.6 MgSO₄, 26 NaHCO₃, 1.25 NaH₂PO₄, 2.25 CaCl₂, 10 glucose, and 5 sodium pyruvate. After the perfusion, the brain was rapidly and carefully extracted and placed in the same solution. Horizontal slices 450 μm (for extracellular recording) and 400 μm (for patch-clamp recording) thick were cut in chilled (5 – 10°C) sucrose aCSF using Vibroslice (Campden Instruments, UK). Following the cutting, slices were placed into an interface (for extracellular recording) or submersion (for patch-clamp recording) chambers, which were constantly bubbled with carbogen and were filled with room-temperature sodium chloride based aCSF of the following composition (mM): 126 NaCl, 3 KCl, 1.6 MgSO₄, 26 NaHCO₃, 1.25 NaH₂PO₄, 2 CaCl₂, 10 glucose. 0.04 mM indomethacin and 0.4 mM uric acid were also added to the storage solution. Slices for patch-clamp recording were kept in the submerged storing chamber for one hour (h) prior to being placed in the recording chamber. Slices for extracellular recordings were placed into the recording chamber immediately after slicing (Scientific System Design Inc., Canada), where they were perfused with sodium chloride aCSF for one hour at 33 – 34 °C, which was maintained by PTC03 proportional temperature controller (Scientific System Design Inc., Canada).

2.2. Reduced intensity model of chronic epilepsy

2.2.1. Model protocol

The current epilepsy model is based on a modified version of the lithium(Li)/low-dose pilocarpine model originally described in rats by Glien *et al.* (2001). The described model involved a pre-dose of lithium chloride (LiCl) 24 h prior to repeated (30 minutes) low-doses of pilocarpine. The model employs a similar protocol but combined this with administration of the sedative and muscle relaxant drug, xylazine, during the acute seizure phase and rapid termination of the acute seizure phase with an anticonvulsant/antiepileptic cocktail.

Rats (male Wistar, 45–80g) were housed in temperature and humidity controlled conditions with a 12/12 light/dark cycle and were allowed to feed and drink *ad libitum*. On day 1, rats were treated with 127 mg/kg LiCl via subcutaneous (s/c) injection. Twenty-four hours following the LiCl injection, α -methyl scopolamine 1mg/kg (s/c) was administered to reduce peripheral effects of muscarinic cholinergic (mAChR) receptor activation. Thirty minutes later, a low dose of pilocarpine (15–25 mg/kg, s/c) was given. Animals were then closely observed for signs of seizure activity, which was ranked using Racine's scale (Table 2.1, Racine, 1972). Animals failing to reach Racine Stage 4 were dosed again with pilocarpine, up to a maximum of 3 doses given at 30–45 minute intervals. When a seizure severity rating of >3 on Racine's scale was reached (bilateral forelimb clonus with rearing), xylazine (2.5 mg/kg intramuscularly – i/m) was immediately administered. To reduce seizure severity, rats were allowed to remain in xylazine-modified *status epilepticus* (SE) for no more than one hour, at which point seizure activity was arrested using a 'stop' solution, given s/c at 1 ml/Kg, and containing MK-801 (0.1 mg/kg; R&D systems, UK), diazepam (2.5 mg/kg; ethanolic solution; Bayer, De) and MPEP (20 mg/kg Abcam Biochemicals, UK). SE ceased within 30 min and animals were then closely monitored during subsequent recovery. During the recovery period, rats were kept on a heat pad to maintain body temperature and visually monitored until ambulatory and able to consume water and moistened, powdered food. Where necessary, 0.9% w/v saline was given s/c to rehydrate animals. In most cases recovery was near complete at 4 h and all rats were fully recovered within 12 h. Regular checks were made to ensure animals were recovering well, and animals were weighed at 24 h and 48 h to monitor

recovery. The end-point for weight loss was 20% of weight at induction, and this was not reached at any point. The low severity of the protocol precluded the requirement for eye drops to prevent ocular keratitis. At approximately 48–72 h after recovery, rats were housed in groups of 2–5 and allowed to feed and drink *ad libitum*.

Table 2.1. Racine scale of seizures. Adapted from Racine *et al.*, 1972)

Stage 1.	Mouth and facial movements
Stage 2.	Head nodding
Stage 3.	Forelimb clonus
Stage 4.	Rearing
Stage 5.	Rearing and falling

2.2.2. Experimental timeline

For experimental purposes, comparison of network activity was conducted between epileptic rats and age-matched control rats (often litter mates) that received no pharmacological treatments. Animals were taken for experiments 24 h, 5–7 days, 6–8 weeks and 90+ d post-SE (PSE 24h, PSE 7d, PSE 6wks, PSE 90d), which roughly fell into the following phases of epileptogenesis: SE and some breakthrough seizures, latent period and spontaneous recurrent seizures (SRS) period (Fig. 2.1). For brain slice preparation see Section 2.1.

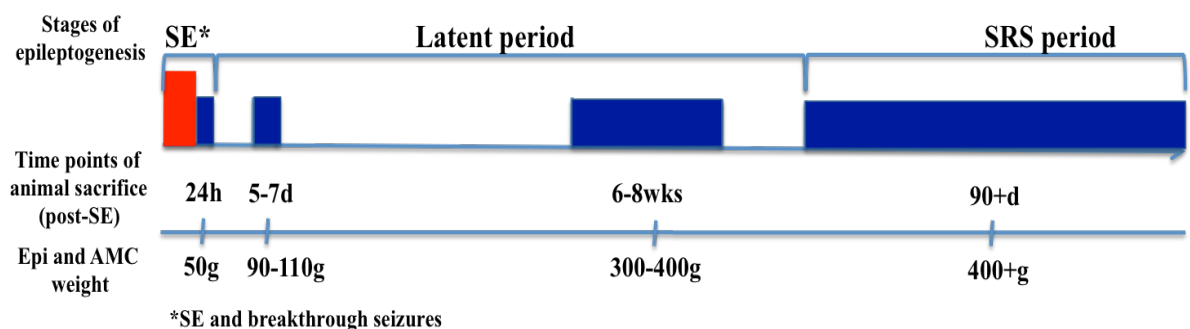


Figure 2.1. Experimental timeline. Red box represents SE period, blue boxes indicate periods (PSE 24h, PSE 7d, PSE 6wks, PSE 90d), during which animals were sacrificed for experiments

2.2.3. SRS development

In the absence of post-seizure behavioural battery (PSBB), the development of the SRS stage was determined by exposing an animal to either new environment (a box) or a strong stimulus (e.g. a loud clap) to evoke a seizure episode of stage 2–3 Racine scale. Animals that exhibited seizures were considered to have entered the SRS stage. The tests were carried out one day prior to sacrificing the animal for experiments.

2.3. Human brain tissue electrophysiology

Human brain tissue was obtained from paediatric patients undergoing surgical brain resection due to intractable epilepsy. The tissue was obtained via collaboration with Birmingham Children's Hospital and with the approval of, and according to the terms specified by, both the Black Country LREC (protocol 'Cellular studies in epilepsy' 10/H1202/23), and the Birmingham Children's Hospital NHS Trust (RECREP 10/H1202/23) (see Appendix 1). The work was undertaken with Aston University's ethical permission Project number 328. Briefly, surgically removed tissue from locations predetermined using intraoperative and/or implanted electrocorticography was placed in cooled aCSF and slices prepared as described in Section 2.1. Patient data are presented in Table 2.2.

Table 2.2. Patient data.

Patient	Diagnosis/pathological substrate	Nature of resected brain tissue
1	Heterotopia	Control tissue above the lesion
2	Cortical dysplasia	Dysplastic tissue
3	Cortical dysplasia	Control tissue
4	Cortical dysplasia	Control and dysplastic cortex
5	Cortical dysplasia	Dysplastic cortex

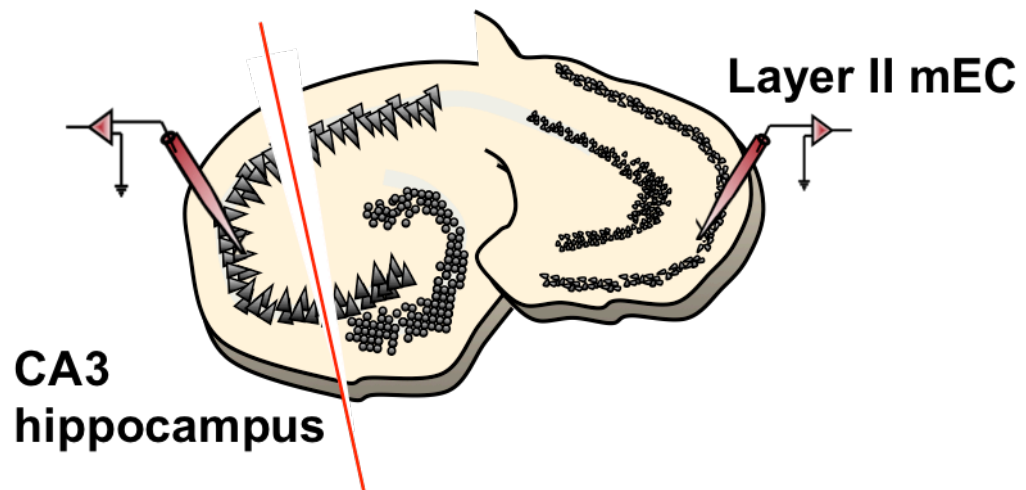


Figure 2.2. Schematic diagram of combined hippocampal-EC brain slice. Two recording electrodes placed in CA3 and layer II regions. Red line shows a cut made to disconnect the two areas in some experiments.

2.4. Electrophysiological Recordings

2.4.1. Extracellular recording

LFP of neuronal networks were measured using an extracellular recording technique. Borosilicate microelectrodes filled with aCSF were used to record LFPs from brain slices. Microelectrodes with an open tip resistance of 1–3 M Ω were fabricated using a Flaming/Brown micropipette puller (P-97, Sutter instruments Co, USA). A silver wire electroplated with silver chloride was inserted into the microelectrode and then placed on a manually operated micro-manipulator (Narishige MM-3, Japan). Synchronised activity of neuronal networks could be detected within the 250 μ m radius from the electrode tip (Katzner *et al.*, 2009; Xing *et al.*, 2009).

LFPs were simultaneously recorded from 4 slices using 4 microelectrodes placed under the Olympus SZ51 microscope (Olympus, Japan) into either CA3 *s. pyramidale* of the hippocampus to record spontaneous gamma oscillations (SyO) or layers II/III of the mEC to record SWO (Fig. 2.2). The signal was amplified by 100 times and low-pass filtered at 1 KHz through EXT-02F amplifier (NPI, Germany). It was further amplified by 10 times and low-pass filtered at 700 Hz through LHBF-48X amplifier/filter (NPI, Germany). Environmental noise was reduced by Hum Bug 50/60 Hz noise eliminators (Quest Scientific Instruments Inc, Canada). Signals were digitised to a PC at 10 KHz using an Axon Digidata 1400A (Axon Instruments, USA) or Micro-1401 (Cambridge Electronic Device, UK) analog to digital converter and

recorded by Clampex 10.2 or Spike2 7.0 software, respectively (Fig. 2.3.). The data were analysed using Clampfit 10.2, Spike2 7.0, Mini Analysis (Synaptosoft Inc, USA) and GraphPad Prism 5, MatLab software.

To explore phase properties of SyO, KA- and CCh-induced gamma oscillations (KyO and CChyO), the same equipment was used for data acquisition. However, the experimental setup was different: 4 evenly separated microelectrodes were placed into the hippocampal CA3 *s. pyramidale* of a single slice. When SyO were stable, either a single dose or increasing doses of KA or CCh were bath-applied. Epochs of data for analysis were taken when the oscillations were stable.

2.4.2. Evoked field potential recording

Evoked field potentials were recorded from CA3 hippocampus in order to study KAR-mediated response induced by electrical stimulation. Stimulation was delivered by ISO STIM01D (NPI, Germany) through a bipolar electrode made from 80/20 nichrome wire, which was placed in granule cell layer to stimulate mossy fibres. Different stimulation protocols were employed (see section 5.2.2.). Evoked field potentials were recorded by Clampex 10.2 software and analysed in Clampfit 10.2.

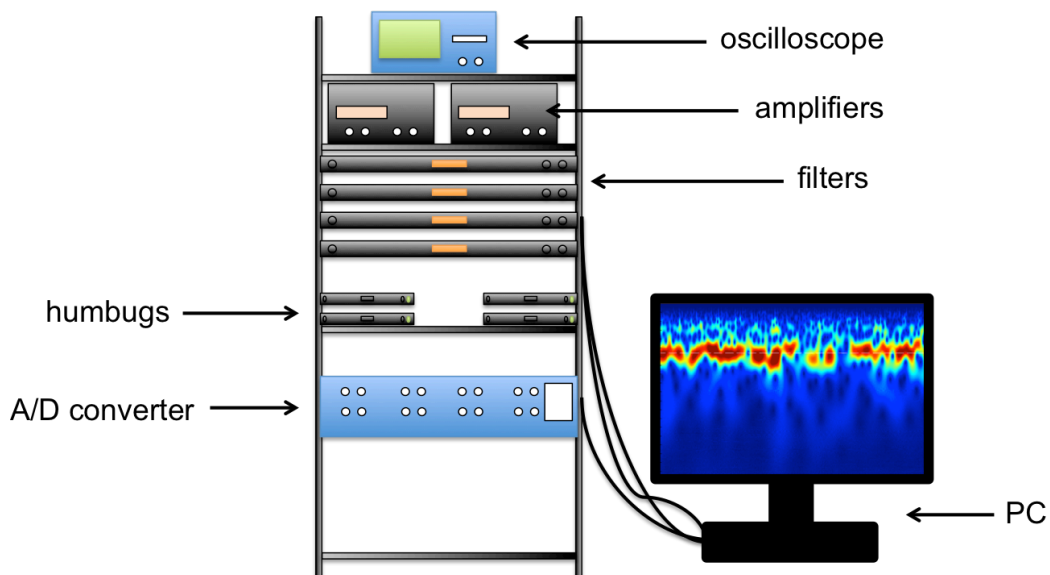


Figure 2.3. Electrophysiology rig setup. Electrophysiology rig for LFP and evoked field potential recordings.

2.4.3. Patch-clamp recording

Borosilicate glass microelectrodes pulled with a P-2000 laser puller (Sutter Instruments, USA) were used for the current technique. Microelectrodes with tip resistance of 5–7 M Ω were filled with internal solution of the following composition (in nM): 100 CsCl, 40 HEPES, 1.0 QX-314, 0.6 EGTA, 5.0 MgCl₂, 10 TEA-Cl, 80 ATP-Na, 6 GTP-Na, 1 IEM1460. The microelectrode was connected to an Axon CV-2 headstage, which was in turn connected to an Axopatch 200B amplifier (Molecular Devices, USA). Recording was made in the submerged chamber continuously perfused with sodium chloride aCSF at 5-7 ml/min, 32 °C. Prior to the recording, the neurons of hippocampal CA3 region, layer II/III of the mEC or human cortex in the slice were visualized using differential interference contrast optics and infrared camera (IR-DIC). The internal solution composition allowed the observation of inhibitory postsynaptic currents (IPSCs) at a holding potential of -65 mV.

2.5. Data Collection and Analysis

2.5.1. Spontaneous gamma oscillations

All data from extracellular experiments were converted to a digital waveform and recorded in Clampex 10.2 and Spike 2 (version 7.0). The data were analysed in Clampfit 10.2 and Spike 2 using the Fast Fourier Transform (FFT) algorithm, which created power spectrum where the waveform was split into frequency components. 30 seconds (s) epochs of sampled data were analysed. Pooled data were analysed in GraphPad Prism 5 and presented as mean normalized peak power change (with control value taken for 100%) and mean peak frequency change. Statistical significance was determined using paired non-parametric Wilcoxon matched-pairs signed rank test. All data are expressed as mean \pm standard error of the mean (S.E.M.). For RISE model and KAr LFP studies, statistical significance was determined using Mann-Whitney test between the epileptic and AMC groups.

MatLab software was used to conduct a time-frequency analysis. For analysis of SyO, KyO and CChyO, Morlet wavelet spectrograms were created using a script written by Dr. Stephen Hall (Aston University, Plymouth University).

2.5.2. Phase analysis

Frequency-specific synchronisation is a part of brain coding and is important in both physiological and pathological conditions (e.g. epilepsy). The idea was to use phase synchrony to characterise SyO in CA3. The main question was asked: are SyO different from KyO and CChyO? We are planning to further use this analysis to characterise epilepsy development, as we hypothesise that during a seizure-free period network synchrony is disrupted and recovers during the SRS stage.

The method called phase-locking statistics, which allows measuring phase synchrony between two signals, was developed by Lachaux *et al.* (1999) and has advantages over the traditional method of spectral coherence by separating phase and amplitude components. It is important because coherence increases with amplitude covariance, which does not allow an independent phase component estimation.

The phase analysis of SyO, KyO and CChyO was carried out by our collaborator Gerard Gooding-Williams (Aston University). Epochs of 60 s of data were processed using Matlab software. Down-sampled to 1 kHz, the data were filtered to the frequency of interest (± 2.5 Hz) using a zero phase finite impulse response (FIR) filter function. Instantaneous phase values were estimated using Hilbert transform. Phase angle difference and phase synchronisation as measured by phase-locking value (PLV) were calculated using the following formulas (Lachaux *et al.*, 1999):

$$\Delta\theta = \theta_1(t) - \theta_2(t),$$

where $\Delta\theta(t)$ is instantaneous phase angle difference between the 2 signals, $\theta_2(t)$ instantaneous phase angle of signal 2, $\theta_1(t)$ instantaneous phase angle of signal 1.

$$\Delta\theta = \theta_1(t) - \theta_2(t) \quad PLV = \frac{1}{N} \sum_{n=1}^N |e^{i\Delta\theta_n}|,$$

where PLV is phase-locking value (phase synchronisation), $\Delta\theta$ is phase angle difference.

PLVs were normalised to a scale of 0 to 1, with a score of 0 meaning no phase-locking between the two signals measured, a score of 1 implying a perfect phase-locking between the signals. Fig. 2.4. presents two examples of phase angle difference distributions (3000 points) and resulting PLVs: a random sample (no phase synchrony) and an example of phase synchrony centred around 90 degrees (unimodal distribution). Fig. 2.5. demonstrates an example of method limitation, where it is not able to resolve a bimodal distribution and therefore produces a false result.

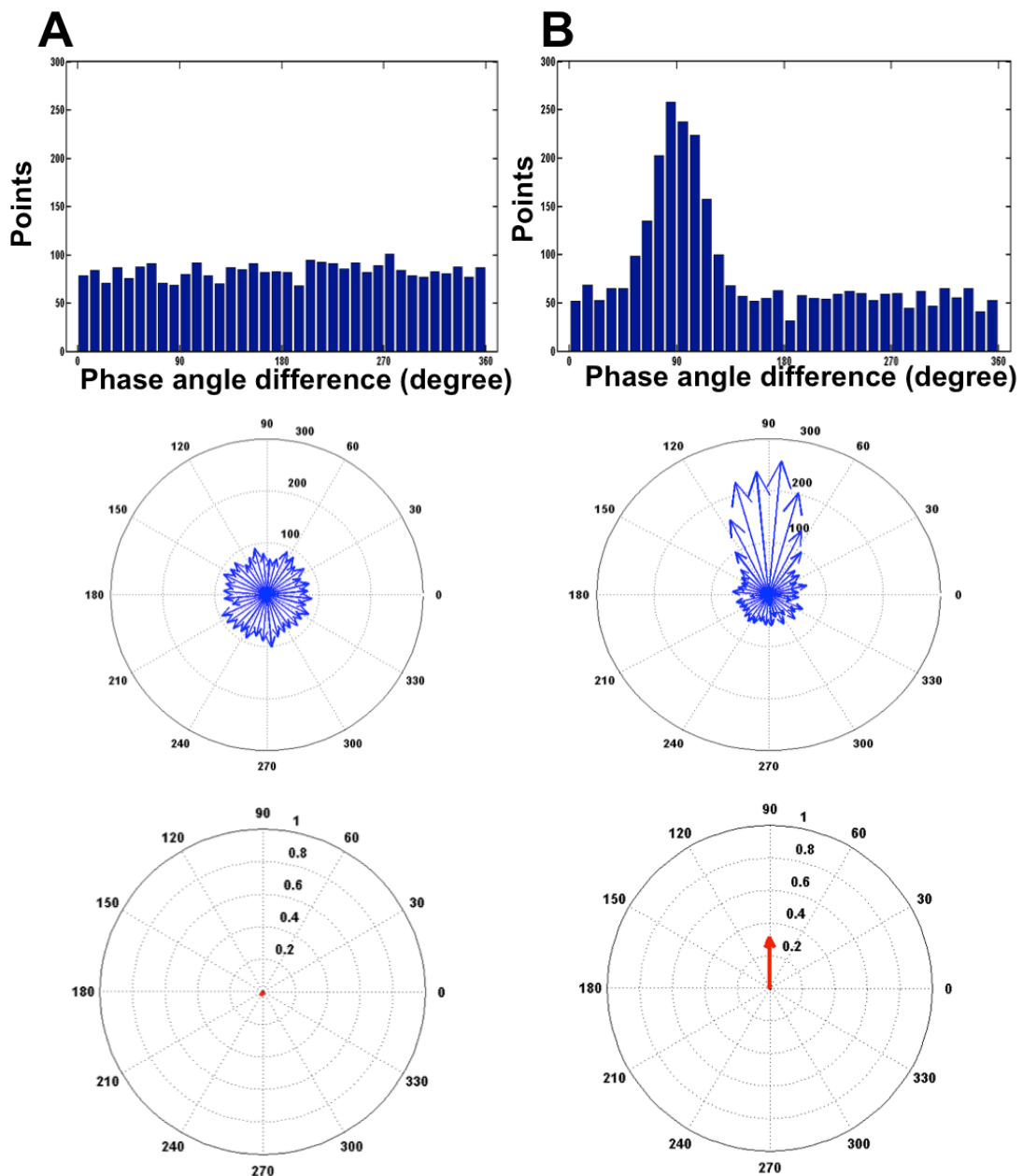


Figure 2.4. PLV for random and unimodal distribution of phase angle difference. A. Random phase angle difference distribution histogram (top), histogram plotted onto circular plot (middle), generated PLV (bottom). **B.** Unimodal phase angle difference distribution histogram (top), histogram plotted onto circular plot (middle), generated PLV (bottom).

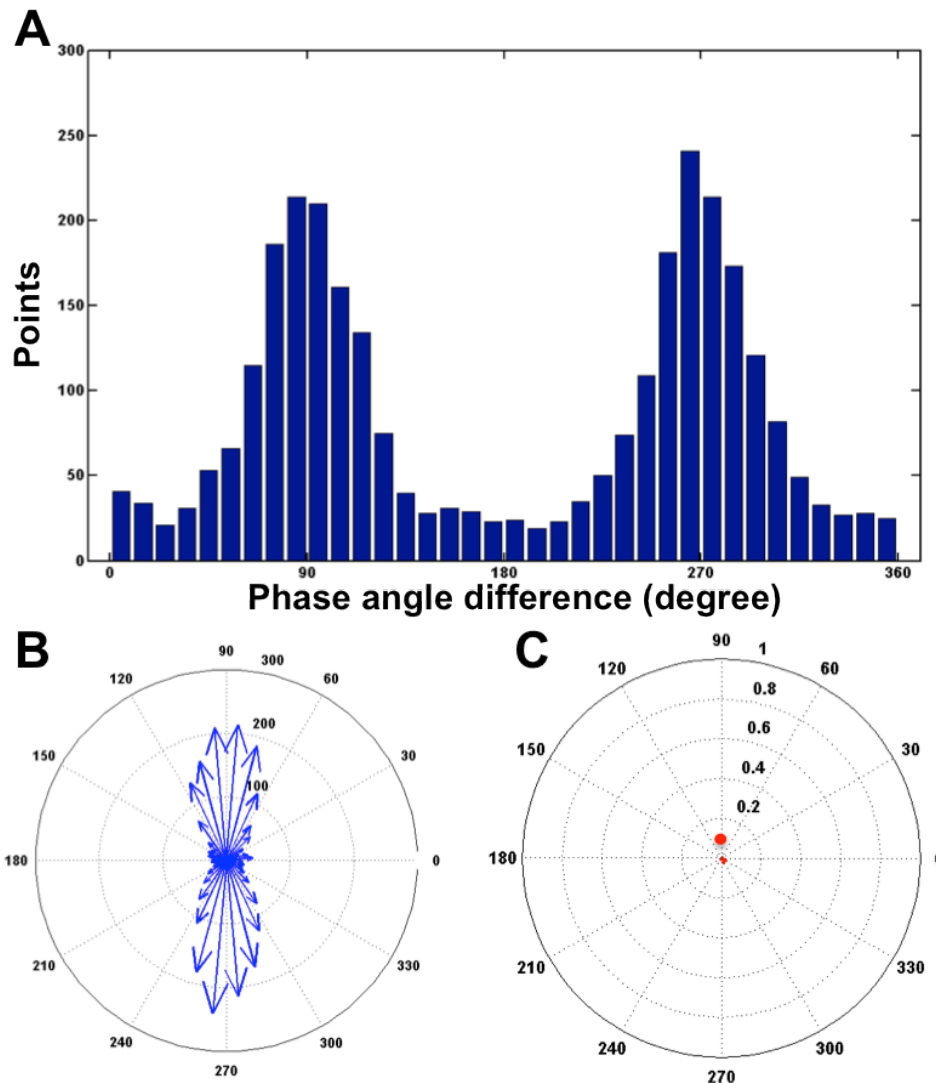


Figure 2.5. Method limitation: bimodal phase angle difference distribution. **A.** Phase angle difference distribution histogram, phase-locking shared between 90 and 270 degree angles. **B.** Histogram plotted onto circular plot. **C.** Generated PLV being close to zero due to phase angle difference cancelling out.

Phase synchrony is presented for each pairing of adjacent electrodes (i.e. 1-2, 2-3, 3-4) as a set of PLVs for 20–70 Hz range (51 values at 1 Hz step).

A single trial method requires a null data set to be created, in order to calculate the phase synchrony threshold value for a particular significance level (Hurtado *et al.*, 2004). For this analysis, null data sets were developed and were based on a Gaussian distributed random process. The validity of the null data sets was tested against synthetic surrogate data and *in vitro* test data for both correlated and uncorrelated data. Good agreement was found between phase synchrony and phase entropy measures across the test data and for various significance levels tested

(although only PLV data are presented here). A multiple comparison correction was applied to the phase coherence significance threshold for the plots presented.

Both linear and non-linear measurements of phase analysis, such as phase synchrony and phase entropy, were employed in the analysis. Different approaches produced equivalent results at the same significance level, as the phase difference data were unimodal. Presented data are the result of phase synchrony analysis.

To account for the variability of phase synchrony between the tissue samples, a new value 'proportional phase synchrony' (PPS) was adopted. For each frequency and electrode pair there is a phase synchrony PLV for spontaneous (PSs) and corresponding KA- or CCh- driven (PSd) oscillations.

For PLV increase from spontaneous to driven, **PPS = (PSd-PSs)/(1-PSs)**

For PLV decrease from spontaneous to driven, **PPS = (PSd-PSs)/PSs**

Using the same filter parameters as in the calculation of phase synchrony, the root mean square (RMS) power was calculated at each frequency (20 – 70 Hz) for spontaneous and driven (KA or CCh) conditions. A measure is produced by the following ratio:

(driven RMS power)/(spontaneous RMS power)

To derive an aggregated value across electrodes, the PPS and RMS power values were averaged. Graphs were produced by plotting RMS power against PPS measured at 1 Hz intervals across 20 – 70 Hz for different concentrations of KA and CCh.

2.5.3. SWO analysis

For SWO, a burst analysis was carried out in Mini-Analysis software. It allowed to determine burst duration, peak amplitude, interburst interval, interevent interval (intra-burst interval), and the number of events in a burst. The data were compared between control and drug conditions within both healthy and epileptic groups, as well as healthy versus (vs.) epileptic. Statistical significance was determined using

Wilcoxon matched pairs signed rank test within the group and Mann-Whitney test between the groups. The data are presented as percentage of change from control to drug (with control value taken for 100%) \pm S.E.M. for each measured parameter in both groups (healthy and epileptic).

2.5.4. Evoked field potential and patch-clamp analysis

Recorded evoked field potentials were low-pass filtered at 10 Hz in Clampfit 10.2 to eliminate stimulation artefacts. The amplitude of evoked response was measured in the same software.

For patch-clamp recording IPSCs were recorded using Clampex 10.2 and later analysed in Mini Analysis software. A minimum of 200 events were taken from the recordings in order to calculate the amplitude, the decay time and the interevent interval (IEI) of the IPSCs. The cumulative probability distributions were plotted for each of the variables in control and drug. The two-sample Kolmogorov-Smirnov (KS) test was used to determine whether the difference between two distributions was significant.

2.6. Drugs

The drugs were purchased from Tocris Bioscience, Bristol, UK. Stock solutions of each drug were prepared at a certain concentration and stored at $-20\text{ }^{\circ}\text{C}$ prior to being used. The drugs were directly applied to the perfusing aCSF, for approximately 50 – 60 min or depending on the experiment design.

Chapter 3 Spontaneous gamma oscillations in CA3 hippocampus

3.1. Introduction

3.1.1. *In vitro* models of induced gamma oscillations and pharmacology

Knowledge accumulated over the last 20 years demonstrates that rhythmic electrical activity of gamma frequency arises from the interaction of inhibitory interneuronal network and pyramidal cells. Critical conditions for gamma rhythm generation are the presence of GABA-Ar-mediated inhibition by interneurons and the excitatory glutamatergic drive (Wang and Rinzel, 1992; Whittington *et al.*, 1995; Traub *et al.*, 1996a). In addition to that, other mechanisms were found to be involved leading to various ways of eliciting different forms of gamma oscillations *in vitro*: using CCh (Fisahn *et al.*, 1998), KA (Buhl *et al.*, 1998; Hajos *et al.*, 2000; Fisahn *et al.*, 2004), mGluR activation (Whittington *et al.*, 1995; Whittington *et al.*, 1997; Palhalmi *et al.*, 2004) and hypertonic K⁺ solution (LeBeau *et al.*, 2002).

One of the first discovered ways of inducing gamma oscillations *in vitro* in the hippocampus was by activation of mGluRs either by an agonist (Whittington *et al.*, 1995) or by tetanic stimulation (Whittington *et al.*, 1995; Whittington *et al.*, 1997). This type of gamma oscillations is of transient nature, because of time-limited nature of the stimulus and subsequent glutamate reuptake and/or mGluR desensitisation. However, despite the transience of this rhythm, it was established that the oscillations were phase-locked over the distance of 1–2 mm and dependent on the inhibition mediated by GABA-Ar. Oscillations remained in the presence of GABA-B receptor (GABA-Br) and iGluR antagonists, further supporting this point. Whittington *et al.* (1995) suggested a crucial role of tonic activation (mGluRs) projecting excitatory effects on inhibitory interneurons. The role of gap junctions was studied and it was concluded that while electrical cell coupling was not essential, it significantly enhanced the network synchrony. Several years later, persistent dose-dependent gamma oscillations in the hippocampus could be elicited by activation of mGluRs with DHPG (group I mGluR agonist). Palhalmi *et al.* (2004) pharmacologically characterised this rhythmic activity and drew a conclusion that DHPG-induced gamma depended both on excitation and inhibition, as it was blocked by a broad-spectrum mGluR antagonist, LY341495, and an AMPA antagonist, GYKI53655, as well as by a GABA-Ar antagonist, bicuculline (Palhalmi *et al.*, 2004).

Shortly after the discovery of mGluR role in inducing gamma oscillations, a different way of providing excitatory input in the hippocampus was suggested by Buhl and colleagues (1998) – pharmacological stimulation with the combination of CCh and KA (in somatosensory cortex), or with either CCh (Fisahn *et al.*, 1998) or KA (Hajos *et al.*, 2000; Fisahn *et al.*, 2004) independently. Application of micromolar concentrations of mAChr agonist CCh consistently elicited persistent 40 Hz gamma oscillations in the hippocampus (Fisahn *et al.*, 1998). CChγO were abolished by a non-selective mAChr antagonist, atropine, and an M1 mAChr antagonist, pirenzepine. Once again indicating the crucial role of inhibition and excitation, GABA-Ar, AMPAr and KAR antagonists blocked CChγO. NMDAr and mGluR, on the other hand, did not produce any effect, the latter suggesting the differences in models of oscillations *in vitro*. This work was yet another milestone in *in vitro* network activity research.

Following the work of Buhl *et al.* (1998), Hajos *et al.* (2000) explored persistent hippocampal gamma oscillations induced by nanomolar application of KA. They described the modulation of KγO by the cannabinoid system. This model was further characterized in connexin-36 KO studies performed by Hormuzdi *et al.* (2001). It was discovered that oscillations in the wild-type mice were sensitive to GABA-Ar and gap junction blockers. KO mice, however, demonstrated reduced amplitude oscillations with preserved frequency and synchrony within the area. Several years later, Fisahn and colleagues (2004) further characterised the pharmacology of KγO and explored the role of different KAR subunits in generation and maintenance of oscillations. KγO persisted in the presence of GYKI53655, AP-5 and MCPG, which suggests AMPAr, NMDAr and group I mGluR respectively, are not involved in this model of network oscillations. DNQX, a non-selective AMPAr/KAR antagonist, and bicuculline, GABA-Ar antagonist, abolished the activity, indicating the prerequisite components common to all models. Studies with M1 mAChr knockout mice demonstrated that CCh could not generate oscillations, while induction with KA remained intact, proving these two models have an independent generation mechanism (Fisahn *et al.*, 2004).

3.1.2. Spontaneous gamma oscillations

The diversity of *in vitro* models brings up such questions as which model represents best the *in vivo* gamma oscillations or whether all of them contribute to the actual gamma rhythm mechanism, reflecting the difference in regions and states. Apart from the absence of proper network connectivity and a higher degree of spatial coherence compared to the intact brain, *in vitro* gamma oscillations are induced through artificial stimulation. In this light, the latest model described in literature – SyO occurring in the hippocampus *in vitro* (Trevino *et al.*, 2007; Pietersen *et al.*, 2009; Case and Broberger, 2012) – seems to be a better physiological model, free of any external intervention. SyO are observed in the healthiest slices, therefore improving brain slice preparation techniques and increasing viability of the slices results in uncovering a persistent gamma rhythm in the hippocampal CA3 region. Hajos and Mody (2009) suggested possible modifications of aCSF composition in order to create physiological environment resembling that of neurons in an intact brain. Inclusion of such neuroprotective agents as NMDAr antagonists, antioxidants and anti-inflammatory drugs reduces the processes of excitotoxicity, oxidative stress and neuroinflammation taking place in the slice (Farooqui, 2008). Improved aCSF composition combined with transcatheter perfusion of the animal appear to be the key factors in obtaining brain slices with increased viability and longevity, which allows neuronal populations to exhibit their natural spontaneous activity.

One of the most extensive reports on SyO was done by Pietersen *et al.* (2009), where SyO were compared to KyO in murine hippocampus. The analysis revealed common features of the basic mechanism in both models, demonstrating once again that oscillations arise from the interplay of excitation and inhibition. Gap junction blockers demonstrate that both models rely on electrical coupling between the cells. AMPAr antagonist SYM2206 was reported to block SyO, while it only partially decreased KyO. Furthermore, NMDAr antagonist also did not produce similar effects in the two models, causing a decrease in SyO and an increase in KyO. A broad-spectrum mGluR antagonist did not produce any significant effect in either of the models, demonstrating that mGluR activation was not required for maintenance of gamma oscillations. Partial block of SyO was observed in atropine, suggesting the involvement of mAChR. Based on the current-source density analysis, Pietersen and colleagues (2009) reported that SyO relied on the perisomatic inhibition less in

comparison to KyO. Moreover, cross-correlation and phase studies revealed that KyO were coherent across the CA3 region, whereas phase changed between the regions in SyO. Overall, they concluded that both oscillation models arise from the same local network mechanism; however, they show differences in the pharmacological properties. In this light, it was suggested that SyO is used as a new physiologically relevant model of gamma oscillations *in vitro*. Unfortunately, this report has major discrepancies between tabulated effects and results/discussion in the main text, and this makes interpretation of these data difficult.

3.1.3. Improved brain slice preparation technique

The acute brain slice technique (Yamamoto and McIlwain, 1966; Andersen *et al.*, 1972; Alger *et al.*, 1984) has contributed substantially to the investigation of the electrical and morphological properties of neurons and synapses. More recently, the *in vitro* slice approach has provided insights into neuronal network oscillations (Whittington *et al.*; 1995; Traub *et al.*, 1996a; Buhl *et al.*, 1998; Cunningham *et al.*, 2003), allowing the understanding of fundamental mechanisms underlying network function and the EEG.

A brain slice is a preparation containing local neuronal networks, yet in such preparation a great number of input and output connections with other brain regions are either cut off due to the size of a brain slice or severed as a result of performed manipulations (e.g. brain extraction, cutting procedures). These manipulations are stressful for brain tissue, as they trigger a cascade of excitotoxic and neuroinflammatory reactions, which alters electrical properties of the cells and eventually leads to cell death. In order for *in vitro* brain slice research to be translational, it is crucial to obtain healthy and viable brain slices with well-preserved brain cells and networks, so that the networks resemble those found *in vivo*. Traditionally, rhythmic activity in a brain slice has been induced by either pharmacological or electrical stimulation to mimic excitatory inputs or by alteration of ionic concentrations to set the right level of neuronal excitability. However, I noticed that upon improvement of preparation techniques, brain slices started exhibiting spontaneous rhythmic activity (free of any pharmacological or electrical stimulation), suggesting a sufficient presence of network elements required for the generation of oscillations by the system itself.

Having obtained these spontaneous oscillations, it was of interest to investigate their nature more thoroughly and compare them to the most commonly used models in the literature (K γ O and CCh γ O). Naturally occurring gamma activity in the slices presented an opportunity to investigate a physiologically relevant *in vitro* model of hippocampal oscillations that can be correlated with *in vivo* observations in animals and EEG recordings in humans. To determine the differences between the three models of oscillations, we examined their pharmacology using standard LFP recording techniques. Time-series analysis was used to investigate the phase relationships between neighbouring local networks in the models of gamma oscillations.

3.2. Results

3.2.1. Traditional vs. improved brain slice preparation

Spontaneous activity in the gamma frequency range (S γ O) was observed in CA3 hippocampus in brain slices obtained using improved methods described in Prokic (2012). The method included transcardial perfusion and alteration of aCSF recipe to include various neuroprotectants, including taurine, aminoguanidine and ethyl pyruvate, which significantly improved the viability of Betz cells in M1 brain slices. We compared horizontal hippocampal-entorhinal slices obtained with traditional method to the ones obtained using the modified method. In young adult rats, the hippocampal CA3 region (usually the most vulnerable area) generally survived better in modified preparation, compared to the traditional one (Fig. 3.1A,B). We then explored whether S γ O were present in CA3 hippocampus *s.pyramidale* in slices made using standard methods, and it appeared that the activity was still present in some slices. However, it did not appear reliably and, when present, was low in power and variable in frequency (Fig. 3.1C,D). S γ O were observed in 22.9% (11/48) of traditional method slices, whereas this increased to 87.7% (142/162) slices obtained with the modified technique.

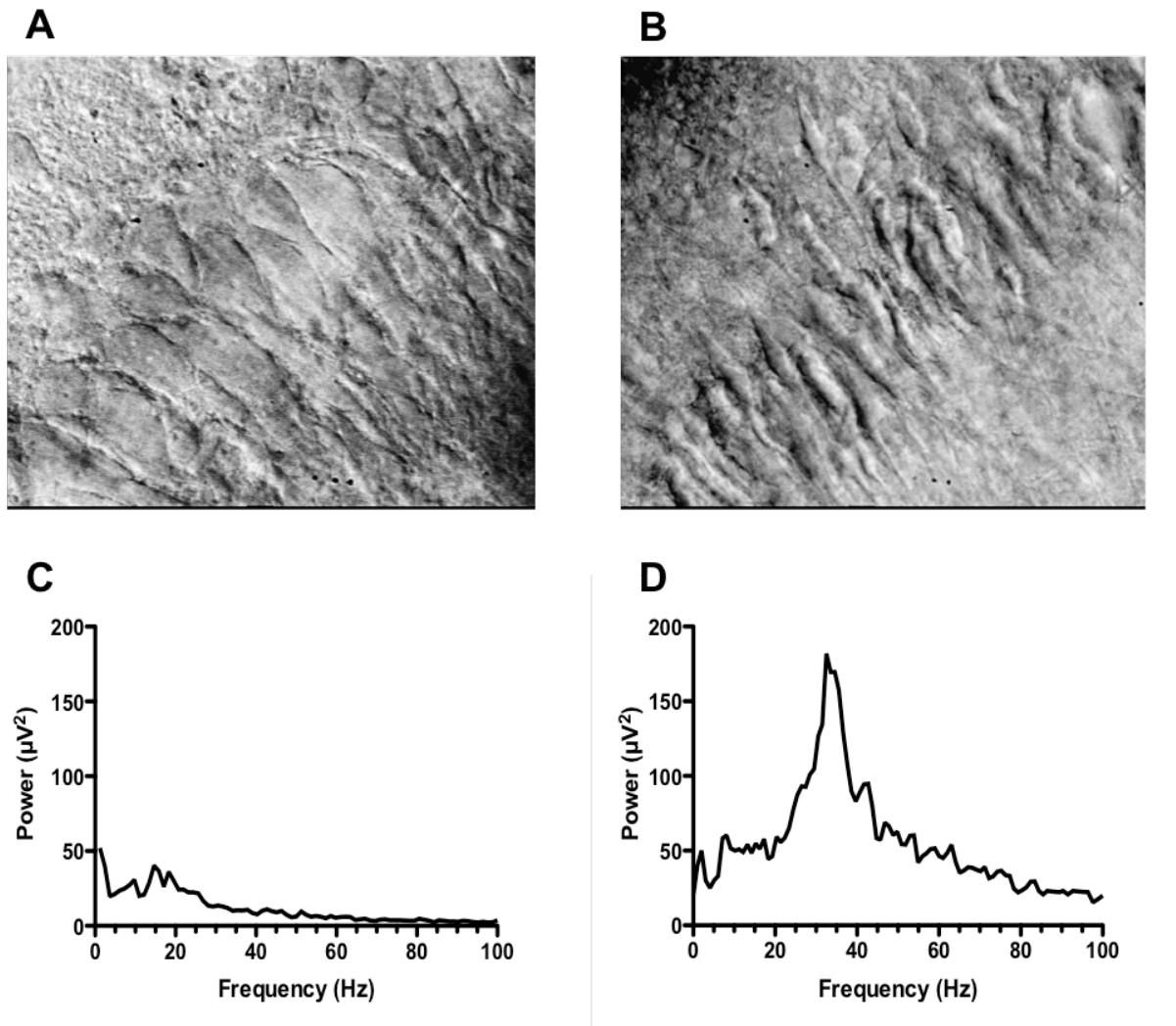


Figure 3.1. Improved brain slice preparation increases slice viability and exposes natural SyO. A. and B. Images of the hippocampal CA3 region in traditional and improved brain slice preparation, respectively. **C. and D.** FFT power spectra of spontaneous rhythmic activity in slices from traditional and improved preparations.

3.2.2. Basic profile of SyO, KA- and CCh-induced gamma oscillations

SyO were studied and compared to K γ O (50 nM KA) and their CCh γ O (1 μ M CCh). Oscillations were recorded from *s.pyramidale* of CA3 hippocampus of 80 – 120 g Wistar rats (Fig. 3.2). Time-frequency relationship of all gamma oscillation models was explored using Morlet wavelet analysis. The results demonstrated that the peak frequency was stable over time and oscillation amplitude showed low-frequency modulation (Fig. 3.3). The average peak frequency of SyO was 31.8 ± 0.4 Hz and average peak power 55.2 ± 6.1 μV (n=121), compared to the frequency and amplitude range of oscillations induced by 50 nM KA (37.4 ± 0.8 Hz and 596.3 ± 167.2 μV [n=58]) or 1 μ M CCh (38.1 ± 0.5 Hz and 151.9 ± 23.7 μV [n=69]) (Fig. 3.4).

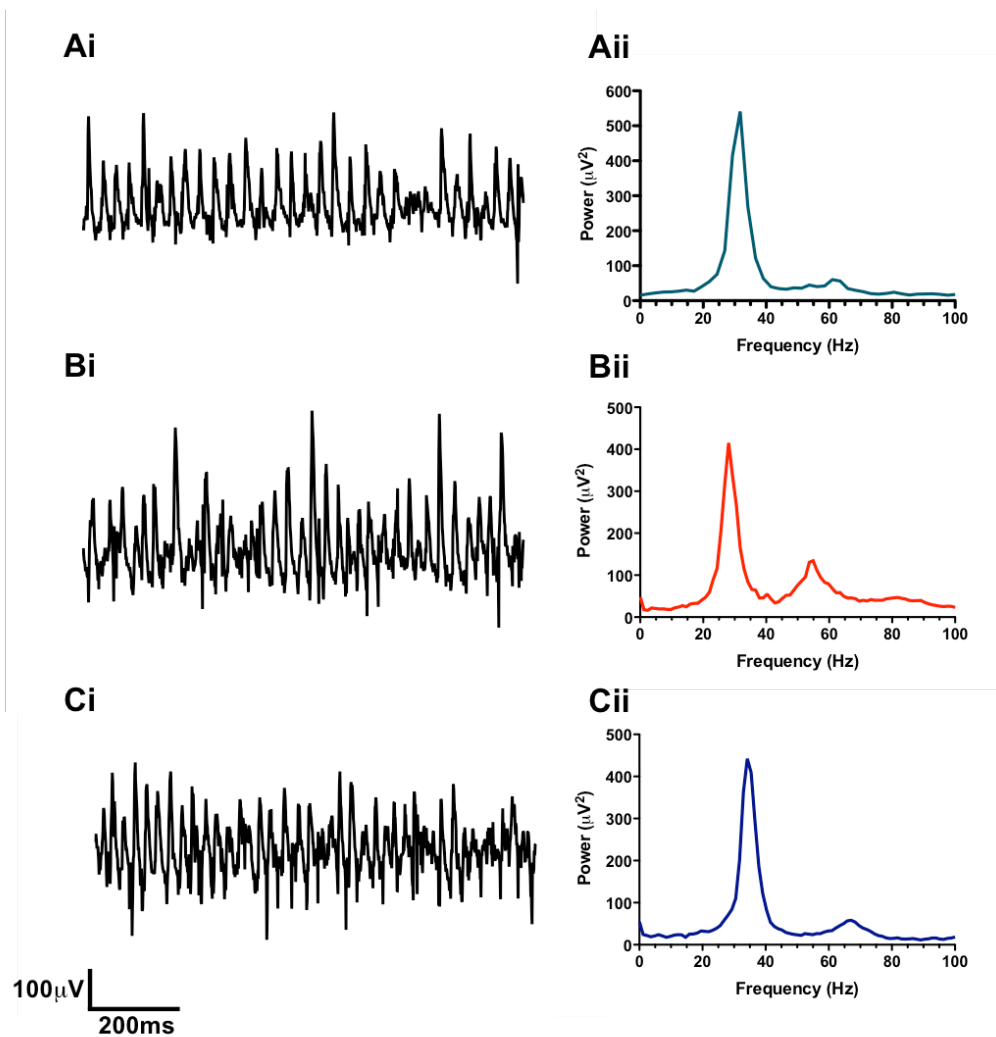


Figure 3.2. Basic profile of SyO, KyO and CChyO. . Ai., Bi. and Ci. Unfiltered raw traces of SyO, KyO (75 nM KA) and CChyO (1 μM CCh), respectively. **Aii., Bii. and Cii.** Representative FFT power spectra of SyO, KyO and CChyO, respectively.

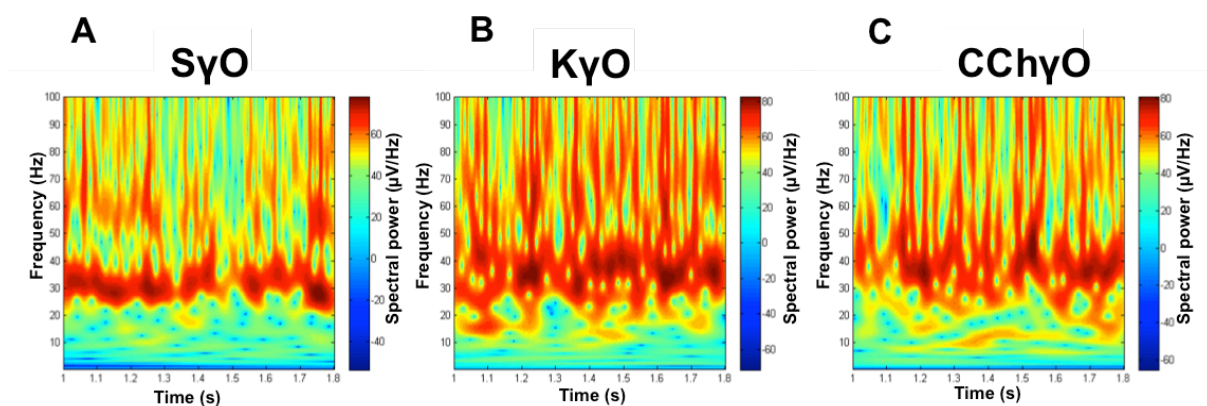


Figure 3.3. Time-frequency analysis of SyO, KyO and CChyO. A., B. and C. Morlet wavelet time-frequency plots for SyO, KyO and CChyO, respectively.

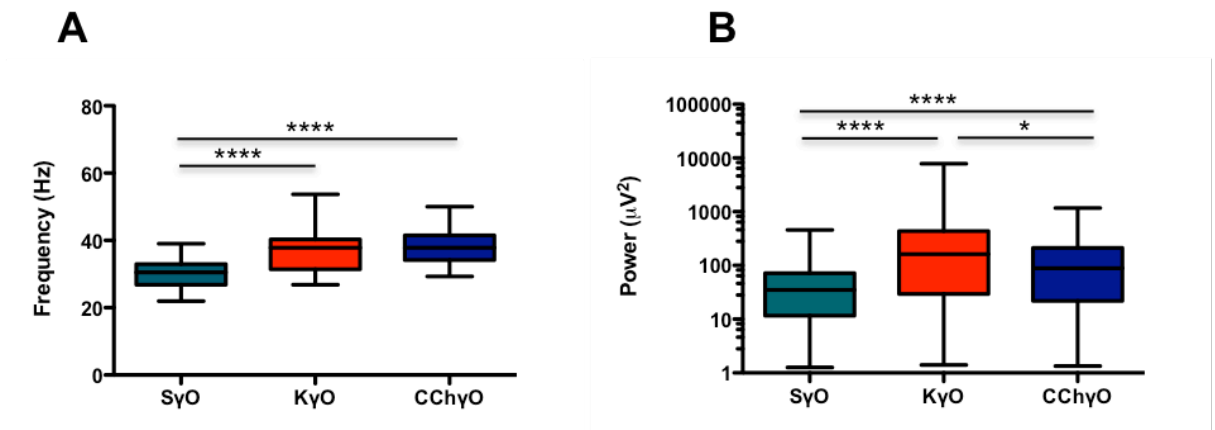


Figure 3.4. Mean power-frequency characterisation of SyO, KyO and CChyO. Mean peak frequency (**A.**) and power (**B.**) of SyO (teal), KyO (red) and CChyO (blue). **** represent $p < 0.0001$, * represents $p < 0.05$.

SyO appeared from the start of the recording (1 h after slicing), peaked in power after 1–1.5 h and persisted in this stable state for several hours, with the longest recording of stable SyO being >7 hrs. KyO and CChyO emerged approximately 10 minutes after bath application of either KA or CCh, reached stable state 1.5–2 h later and again persisted for several hours.

Observation of SyO over time demonstrated a gradual increase in power until reaching a stable state. Addition of KA or CCh to pre-existing SyO in majority of slices resulted in initial acceleration of oscillations and rapid power escalation. As the power was reaching its peak, the frequency decreased slightly, before settling, usually at a point above the pre-drug level. Shifts in frequency upon transition could probably be explained by elevated level of excitation produced by KA and CCh in the slice (Wang and Buzsaki, 1996). Exploratory KA and CCh dose-response curve experiments demonstrated that the power of gamma oscillation induced by 25 nM KA corresponded approximately to the power induced by 1 μ M CCh, however, CCh induced a different input-output curve, inducing rhythmic activity of different frequencies, depending on the dose.

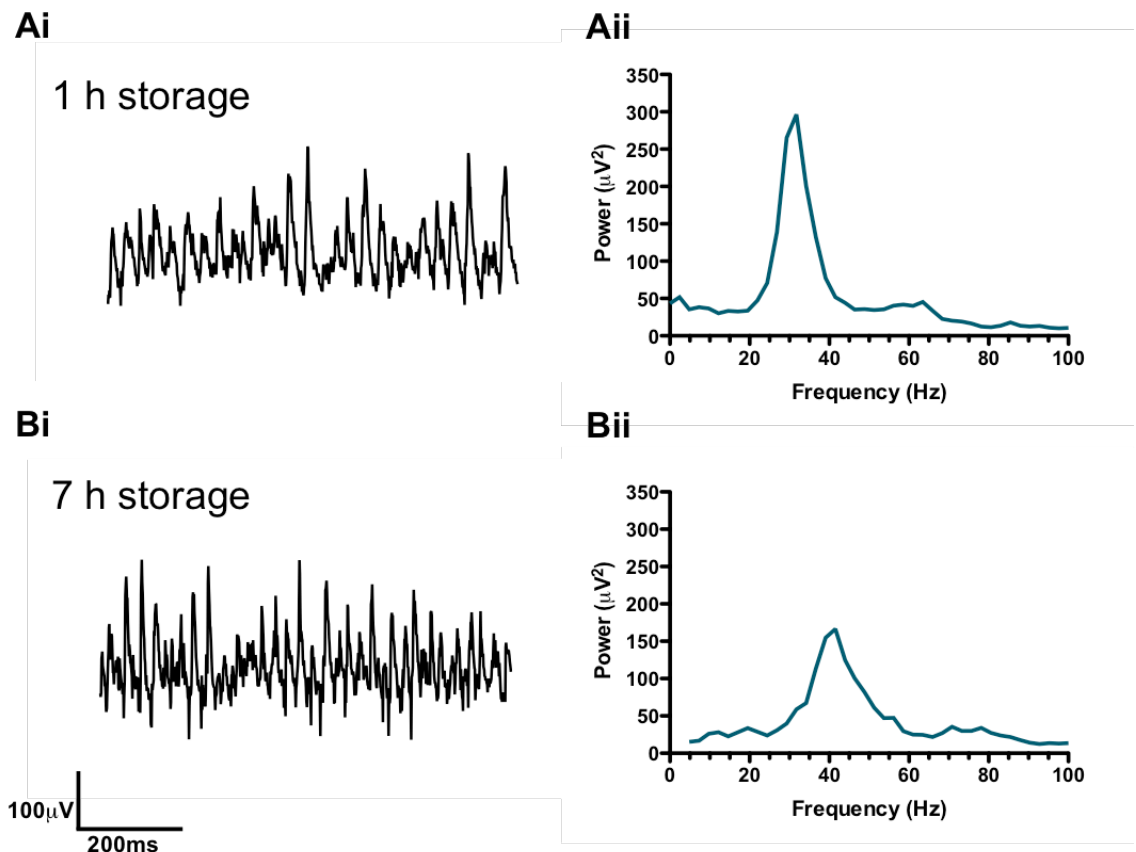


Figure 3.5. SyO survive prolonged storage. **Ai.** and **Aii.** Unfiltered raw trace and FFT power spectrum of SyO recorded from a slice stored for 1 h. **Bi.** and **Bii.** Unfiltered raw trace and FFT power spectrum of SyO preserved in a slice stored for 7 h.

SyO appeared in almost all hippocampal slices immediately after 1 h of recovery period, as well as after a prolonged (even up to >6h) storage (Fig. 3.5). The oscillations in stored slices varied in peak power and frequency, but were generally smaller and slower compared to freshly-cut slices. In stored slices, gamma oscillations could also be induced with as little as 25 nM KA and 500 nM CCh, indicating higher sensitivity of CA3 to KA. Generally there was a positive correlation between the size and frequency of SyO and chemically induced gamma oscillations in the same slice.

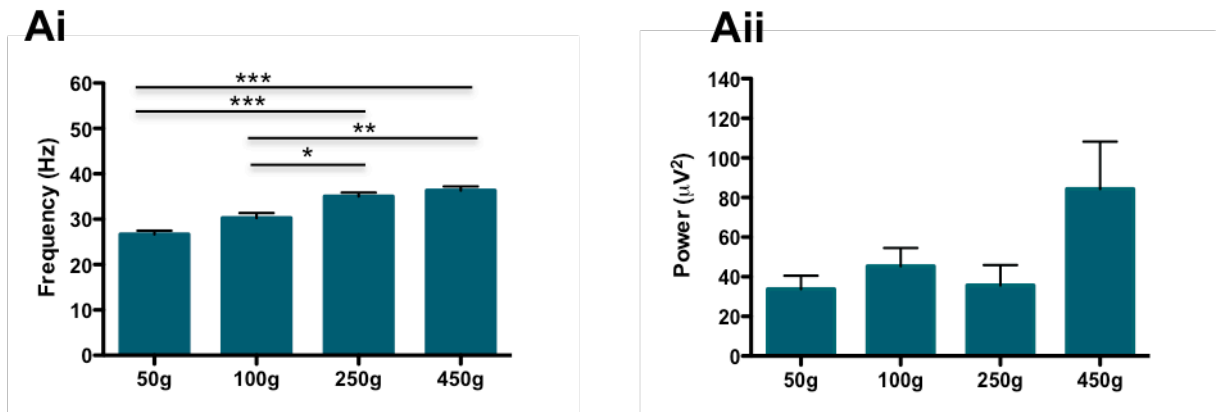


Figure 3.6. Weight-dependent profile of SyO. Ai. and Aii. Bar charts showing mean peak frequency and peak power of SyO in slices from 50 g, 100 g, 250 g and 450 g animals. *** indicate $p < 0.001$, ** indicate $p < 0.01$, * indicates $p < 0.05$.

3.2.3. Characterisation of SyO

SyO were more readily observed towards the dorsal side of the hippocampus. To determine the origin of SyO, LFP recordings were obtained from slices with the cut made through the perforant path/mossy fibres and Schaffer collateral to disconnect CA3 region from the EC, DG and CA1, respectively. Persistent SyO could still be observed in CA3 region, suggesting that spontaneous activity was intrinsic to this area.

SyO were studied across different weight groups (50g, 100g, 250g, 450g). These studies showed that the average peak frequency significantly increased with weight from 26.6 ± 0.8 Hz ($n=13$) in 50g animals to 31.8 ± 0.4 Hz ($n=26$) in 100g, 34.7 ± 0.8 Hz ($n=17$) in 250g and 36.3 ± 0.8 Hz ($n=14$) in 450g animals (Fig. 3.6). Generally the FFT peaks appeared sharper in older rats. The average peak power, though quite variable, did not exhibit statistically significant differences across all age groups.

3.2.4. Pharmacological profile of SyO, KyO and CChyO

Pharmacological properties of three gamma oscillation models were characterized and compared. We explored the roles of inhibitory and excitatory systems in generation and maintenance of SyO, KyO and CChyO.

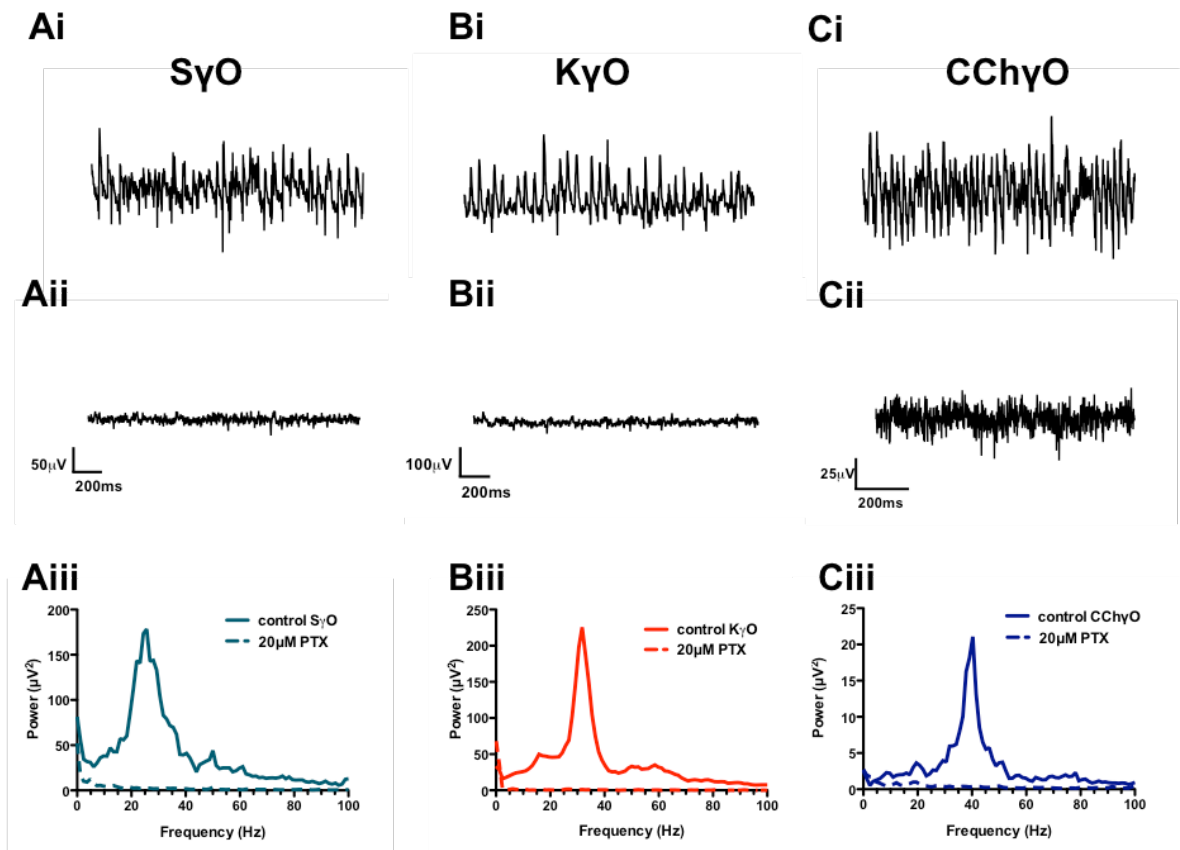


Figure 3.7. Abolition of SyO, KyO and CChyO by 20 μ M PTX. **A.**, **B.** and **C.** Unfiltered raw traces of SyO (teal), KyO (red) and CChyO (blue) under control and 20 μ M PTX.

3.2.4.1. GABAergic pharmacology

It is known that GABA-mediated inhibition is critical for induced gamma oscillation generation and maintenance *in vitro* (Whittington *et al.*, 1995; Fisahn *et al.*, 1998; Pietersen *et al.*, 2009). We explored the role of GABA-Ar in SyO observed in our slices and compared it to chemically induced gamma oscillations. In all experiments, the GABA-Ar antagonist bicuculline (20 μ M) and GABA-Ar blocker PTX (20 μ M) reliably abolished gamma oscillations, demonstrating the crucial role of the GABAergic system (Fig. 3.7). Hence, in the majority of slices, gamma rhythm was replaced by slow interictal-like activity, appearing once the effect of GABA-Ar blockade had stabilised. Benzodiazepine site agonist zolpidem (100 nM) significantly augmented the peak power of SyO, KyO and CChyO by $44.5 \pm 25.2\%$ ($n=10$, $p<0.01$), $21.0 \pm 18.6\%$ ($n=9$, $p<0.05$), $46.8 \pm 25.4\%$ ($n=8$, $p<0.05$), respectively (Fig. 3.8A). A decrease in the peak frequency was also observed in all three models: Δ Hz - 1.95 ± 1.6 , $p<0.01$ in SyO, -1.2 ± 0.9 , $p<0.05$ in KyO and -1.4 ± 0.8 , $p<0.05$ in CChyO. We then investigated the effects of GABA-Ar modulator pentobarbital (10 μ M), which produced a significant change in peak power only in CChyO (increase by $21 \pm 14.6\%$

$p < 0.01$, $n = 10$), although a characteristic significant decrease in the peak frequency was observed in all three models ($\Delta\text{Hz} -3.5 \pm 1.9\text{Hz}$, $n = 9$, $p < 0.01$ in SyO, $-4.8 \pm 1.8\text{Hz}$, $n = 9$, $p < 0.01$ in KyO and $-2.3 \pm 1.1\text{Hz}$, $n = 10$, $p < 0.01$ in CChyO) [Fig. 3.8B].

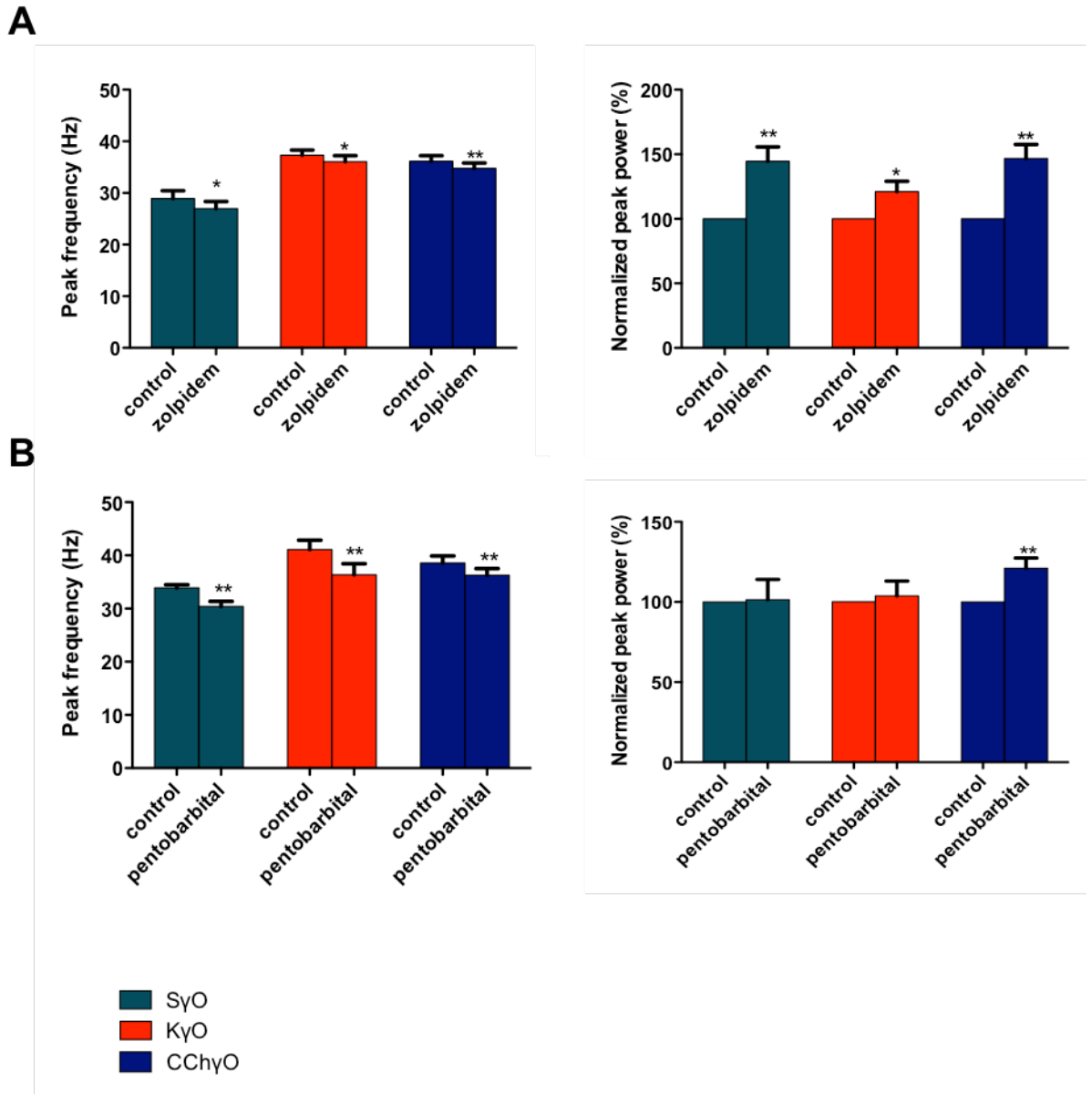


Figure 3.8. The effects of GABA-Ar modulators on SyO, KyO and CChyO. A. Bar charts illustrating a significant reduction of peak frequency and an increase in the peak power of SyO (teal), KyO (red) and CChyO (blue) upon the application of 100 nM zolpidem. **B.** Bar charts showing a significant reduction of SyO (teal), KyO (red) and CChyO (blue) peak frequency upon the application of 10 μM pentobarbital. A significant increase in peak power observed only in CChyO. ** indicate $p < 0.01$, * indicates $p < 0.05$.

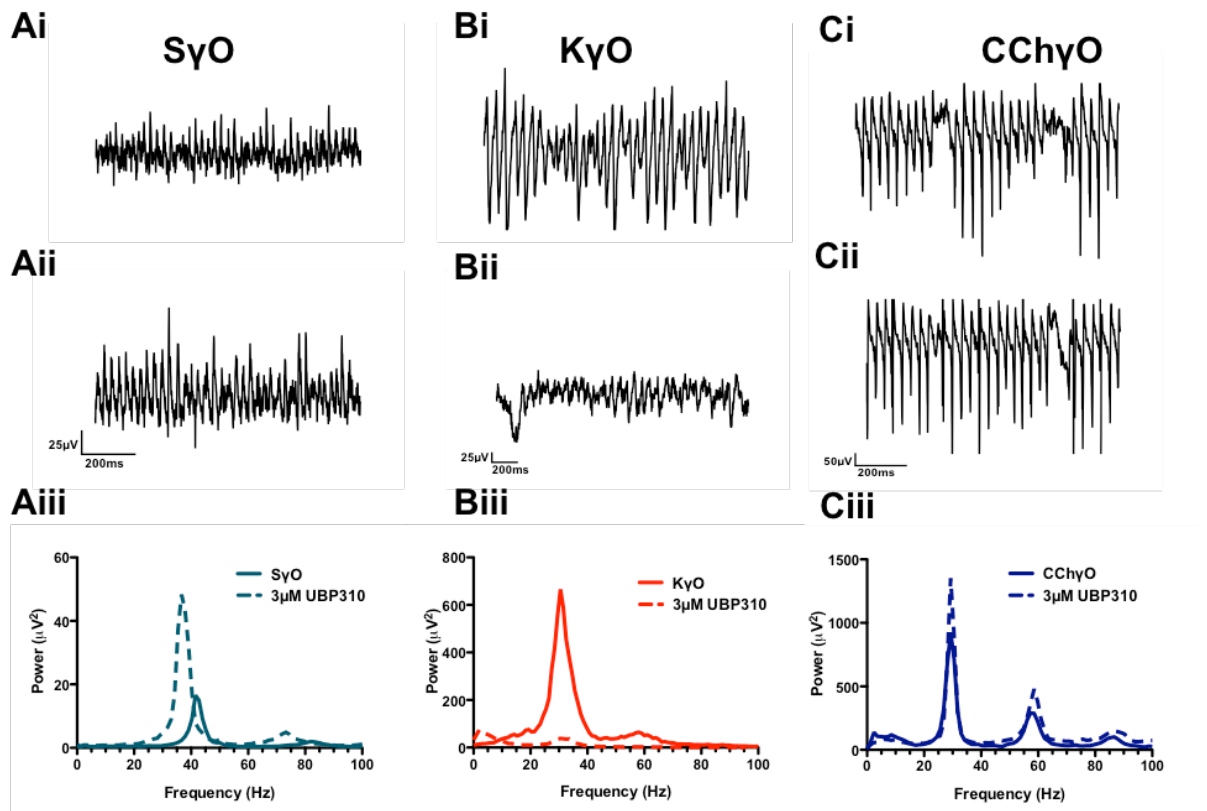


Figure 3.9. Differential effects of GluK1,3 KAR antagonist UBP310 (3 μ M) on SyO, KyO and CChyO. Ai., Bi. and Ci. Unfiltered raw traces of SyO, KyO and CChyO under control conditions. Aii., Bii. and Cii. Unfiltered raw traces of SyO, KyO and CChyO after 3 μ M UBP310 application. Aiii., Biii. and Ciii. FFT power spectra for control and UBP310 conditions in SyO, KyO and CChyO, respectively. The figure demonstrates a marked reduction of KyO power in UBP310, while an increase in SyO and CChyO.

3.2.4.2. Glutamatergic pharmacology

The role of phasic excitatory inputs in oscillogenesis was established in the works of Buhl *et al.* (1998) and Fisahn *et al.* (1998). To explore the involvement of excitatory glutamatergic system in the generation of spontaneous and other types of gamma oscillations, a KAR/AMPA antagonist, CNQX (20 μ M), was bath applied. CNQX caused a significant reduction of gamma band power in all three models, however, a broad peak in theta/beta bands was introduced instead with mean peak frequencies 13.22 ± 2.1 Hz for SyO (n=12), 11.39 ± 2.9 Hz for KyO (n=3) and 17.5 ± 1.5 Hz for CChyO (n=12). The mean peak power of the theta oscillation was significantly lower compared to initial gamma peak in both KyO (by 69.3 ± 10.6 %, $p < 0.05$) and CChyO (by 68.24 ± 10.6 %, $p < 0.001$), but did not change significantly in SyO ($p < 0.05$), as illustrated by Fig. 3.11A. The role of GluK1 and/or GluK3-containing KAR in the generation of gamma oscillations by the administration of a selective antagonist, UBP310 (3 μ M). The effects produced by UBP310 application differed significantly

between the models. The antagonist produced an increase in mean peak power of S γ O by $68\pm 21.4\%$ ($n=12$, $p<0.05$) and a decrease in the mean peak frequency by 4.5 ± 2.4 Hz ($n=12$, $p<0.01$), as illustrated by Figs. 3.9A and 3.11C. In contrast, application of UBP310 dramatically reduced the peak power of K γ O (by $78.9\pm 6.25\%$, $n=11$, $p=0.001$) and insignificantly increased the peak frequency (Figs. 3.9B and 3.11C). CCh γ O did not change significantly upon the blockade of GluK1,3 KAr (Figs. 3.9C and 3.14C).

In addition to KA type glutamate receptors, mammalian neurones express AMPAr, which mediate fast synaptic transmission. We examined the role of AMPAr by applying AMPAr antagonist, SYM2206 (Pelletier *et al.*, 1996). Application of SYM2206 (20 μ M) did not demonstrate consistent results. Initially, SYM2206 produced a significant increase in all types of gamma oscillations, however, when experiments were repeated, it showed abolition of gamma rhythm in all models. Therefore it was decided to block AMPAr with the combination of 20 μ M SYM2206 and 2.5 μ M NBQX. At such a low concentration NBQX is known to be selective for AMPAr, although higher doses also act on KAr. SYM2206+NBQX reliably abolished gamma oscillations in S γ O ($n=9$), K γ O ($n=8$) and CCh γ O ($n=10$) but introduced a low amplitude theta peak (10 – 15 Hz) afterwards (Fig. 3.11B). The mean peak frequencies after AMPAr blockade were 10.26 ± 0.7 ($p<0.01$) Hz in S γ O, 11.32 ± 0.9 ($p<0.01$) in K γ O and 13.94 ± 2.6 ($p<0.01$) in CCh γ O. We also investigated whether another type of ionotropic glutamate receptors, NMDAr, were involved in the mechanism of gamma oscillations. DL-AP-5 (25 μ M), an NMDAr antagonist, increased the peak power of only CCh γ O by $56.2\pm 20.8\%$ ($n=11$, $p<0.01$), and caused no significant effect in other models (Figs. 3.10 and 3.11D). Despite no changes in power, DL-AP-5 significantly reduced the peak frequency of S γ O and K γ O (by 3.78 ± 1.1 Hz [$n=10$, $p<0.01$] and 1.0 ± 0.6 Hz [$n=9$, $p<0.05$], respectively). Apart from ionotropic glutamate receptors, mammalian neurones express a variety of metabotropic glutamate receptors, which exert their effects on excitability and synaptic function through G-proteins. The main mGluRs can be divided into 3 groups,

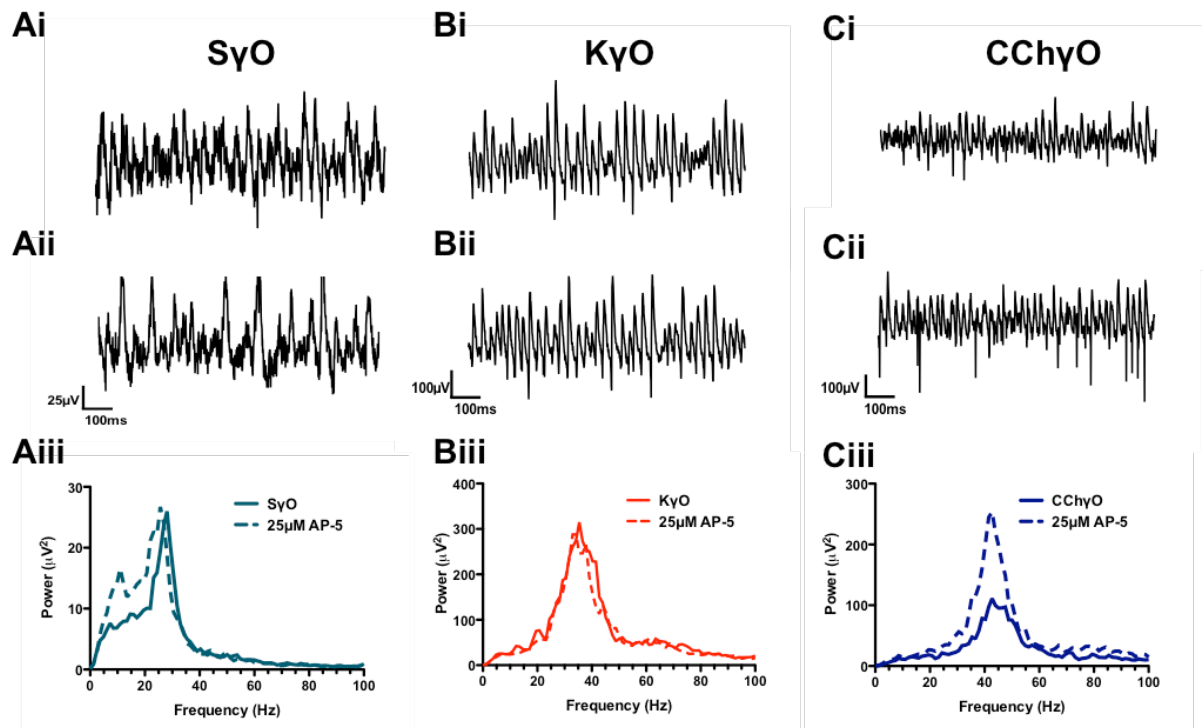


Figure 3.10. Differential effects of NMDA receptor antagonist on SyO, KyO and CChyO. Ai., Bi. and Ci. Unfiltered raw traces of SyO, KyO and CChyO under control conditions. Aii., Bii. and Cii. Unfiltered raw traces of SyO, KyO and CChyO after 25 μ M AP-5 application. Aiii., Biii. and Ciii. FFT power spectra for control and AP-5 conditions in SyO, KyO and CChyO, respectively. The figure demonstrates a marked increase of CChyO power in AP-5, while no significant change in SyO and KyO.

groups I contains mGluRs 1 and 5, group II is comprised of mGluRs 2 and 3, while group III contains mGluR4, mGluR6-8. The role of metabotropic receptors, mediating slow excitation and presynaptic inhibition of transmitter release, was explored using a selective antagonist, MPEP (mGlu₅ antagonist), and a group II/III mGluR antagonist, LY341495. MPEP (20 μ M) increased γ oscillation peak power in SyO, KyO and CChyO by $60.3 \pm 27.6\%$ ($n=9$, $p<0.01$), $48.9 \pm 27.5\%$ ($n=10$, $p=0.01$) and $31.9 \pm 21.9\%$ ($n=11$, $p<0.05$), respectively (Fig. 3.13A). Furthermore, results demonstrated that MPEP reduced the peak frequency of SyO and KyO by 3.8 ± 0.7 Hz ($p<0.01$) and 2.3 ± 1.7 Hz ($p<0.05$), respectively (Fig 3.13A). Application of LY341495 (5 μ M) did not result in a significant effect in any of the three models, yet it significantly decreased the peak frequency of gamma oscillations by 2.17 ± 1.4 Hz ($n=9$, $p<0.05$) in SyO and 1.6 ± 0.9 Hz ($p<0.05$) in KyO (Fig. 3.13B).

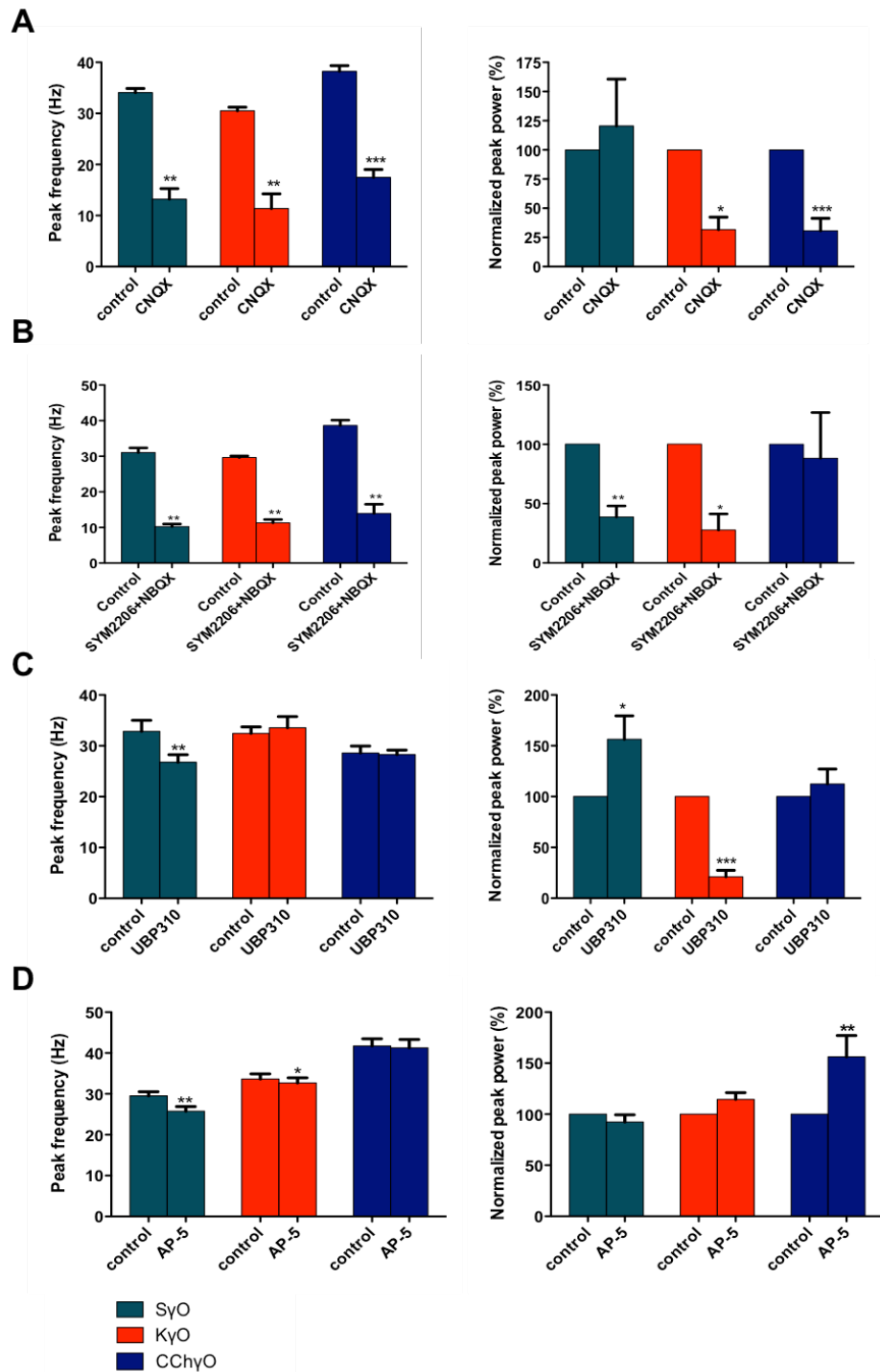


Figure 3.11. The effects of glutamatergic antagonists on S γ O, K γ O and CCh γ O. **A.** Bar charts illustrating a significant reduction of peak frequency in S γ O (teal), K γ O (red) and CCh γ O (blue) and peak power of K γ O and CCh γ O, but not S γ O upon the application of AMPAR/KAR antagonist CNQX (20 μ M). **B.** Bar charts illustrating a similar reduction in the peak frequency of all three models, while a reduction in power only in S γ O and K γ O, but not CCh γ O upon administration of AMPAR antagonists SYM2206+NBQX (20 μ M and 2.5 μ M, respectively). **C.** Bar charts showing significant decrease in peak frequency and an increase of peak power of S γ O upon administration of 3 μ M UBP310 (GluK1,3 Kar antagonist). UBP310 nearly abolished K γ O. **D.** Bar charts showing the effects of NMDAR antagonist AP-5 (25 μ M), which reduced the peak frequency of S γ O and K γ O and increased the peak power of CCh γ O. *** indicate $p < 0.001$, ** $p < 0.01$, * $p < 0.05$.

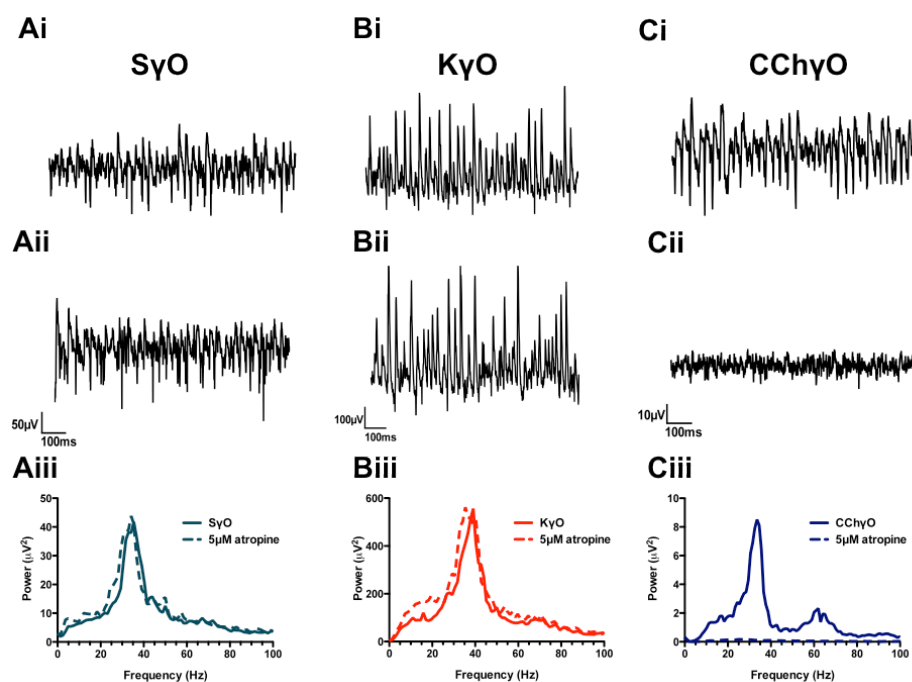


Figure 3.12. Differential effects of mAChR antagonist on SyO, KyO and CChyO. Ai., Bi. and Ci. Unfiltered raw traces of SyO, KyO and CChyO under control conditions. **Aii., Bii. and Cii.** Unfiltered raw traces of SyO, KyO and CChyO after 5 μ M atropine application. **Aiii., Biii. and Ciii.** FFT power spectra for control and atropine conditions in SyO, KyO and CChyO, respectively. The figure demonstrates abolition of CChyO by atropine, while no significant change in SyO and KyO.

3.2.4.3. Cholinergic pharmacology

According to Fisahn and colleagues (1998), atropine blocked CChyO, suggesting this model of oscillations heavily depends on cholinergic system. We investigated, whether this was the case for SyO or KyO. We first established that atropine (5 μ M) abolished CChyO, confirming previous reports in literature (Fig. 3.13C). The muscarinic receptor antagonist, however, produced no significant effect on the power of SyO and KyO (Fig. 3.12). Despite that, it still significantly reduced the frequency of SyO by 2.77 ± 0.9 Hz ($n=11$, $p<0.01$).

3.2.4.4. Gap junctions

Early work on *in vitro* gamma oscillations demonstrated that electrical coupling between neurons is an important part of neuronal network oscillations (Traub *et al.*, 2000; Hormuzdi *et al.*, 2001). We bath applied 200 μ M carbenoxolone (CBX), a gap junction blocker, and it significantly decreased SyO, KyO and CChyO by $83.3 \pm 7.21\%$ ($n=15$, $p<0.0001$), $61.2 \pm 21.4\%$ ($n=10$, $p<0.01$) and $60.4 \pm 20.5\%$ ($n=8$, $p>0.05$), respectively (Fig. 3.13D).

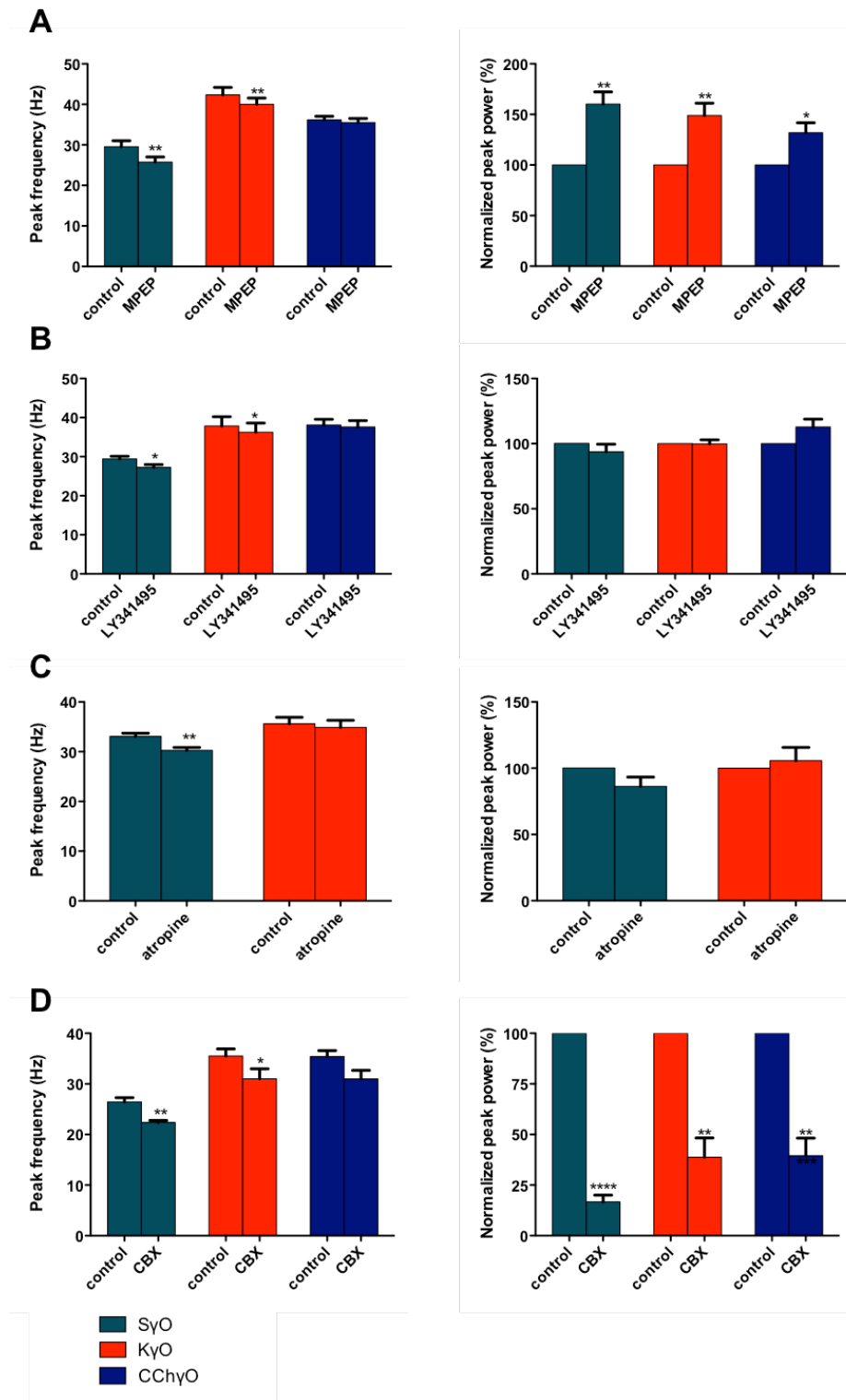


Figure 3.13. The effects of mGluR and mAChR antagonists and gap junction blocker SyO, KγO and CChγO. A. Bar charts showing a significant reduction of peak frequency in SyO and KγO and an increase in peak power of all three models produced by an mGluR₅ antagonist, MPEP (20 μM). **B.** Bar charts showing a significant reduction in the peak frequency of SyO and KγO upon the application of mGluR group II and III antagonist LY341495. **C.** Bar charts demonstrating a decrease of SyO peak frequency produced by mAChR antagonist atropine (5 μM). **D.** Bar charts showing a reduction of peak frequency in SyO and KγO produced by a gap junction blocker CBX (200 μM). CBX caused a dramatic decrease in the peak power of all three models. *** indicate p<0.001, ** p<0.01, * p<0.05.

3.2.5. Phase profile of SyO, KyO and CChyO

3.2.5.1. Phase characterisation

Phase analysis of SyO, KyO and CChyO was carried out to determine the difference between the three models of gamma oscillations. Phase synchrony differences were explored by adding various doses of KA or CCh to existing SyO, thus investigating SyO->KyO and SyO->CChyO transitions. As a first stage of analysis, three parameters were considered: phase synchrony (PLV), dominant frequency and phase angle difference. Phase synchrony and phase angle difference plots for adjacent electrodes recording SyO, KyO and CChyO are presented in Fig. 3.14. The results showed that SyO had high degree of phase synchronisation between all electrodes within a single slice. Between adjacent electrodes (e.g. 1-2) the phase coupling generally occurred across the 20 – 70 Hz range, with a dominant frequency of approximately 5 Hz bandwidth between 30 Hz and 40 Hz. As for the long-range phase relations (electrodes 1-4), phase coupling was reduced, yet the dominant frequency was still preserved (Fig. 3.15). Phase angle difference between adjacent pairs of electrodes was consistent across the frequency range.

Addition of either 50 nM KA or 1 μ M CCh increased the intrinsic phase coupling across the measured frequency band. The effect of phase angle difference, however, was not consistent, either increasing or remaining unchanged. At this stage of analysis, no differences were detected between KA and CCh in their effect on SyO in the CA3 hippocampus.

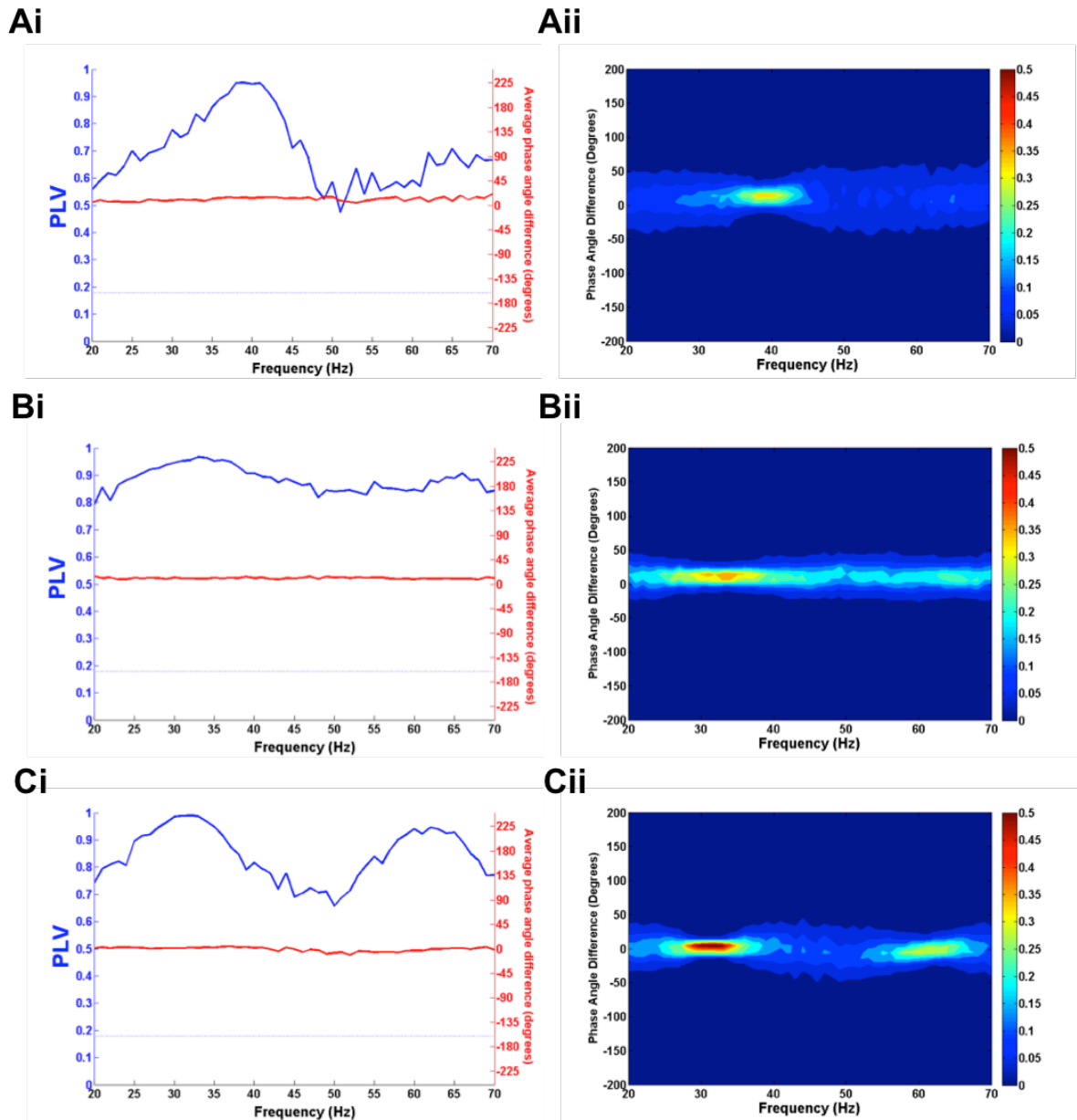


Figure 3.14. Phase coupling of SyO, KyO and CChyO across CA3. Ai., Bi. and Ci. Strong phase coupling at gamma frequency between the neighbouring local CA3 networks in SyO, KyO and CChyO, respectively. The plots show strong phase coupling in all models of gamma oscillations. **Aii., Bii. and Cii.** Small phase angle difference between the two signals in SyO, KyO and CChyO, respectively.

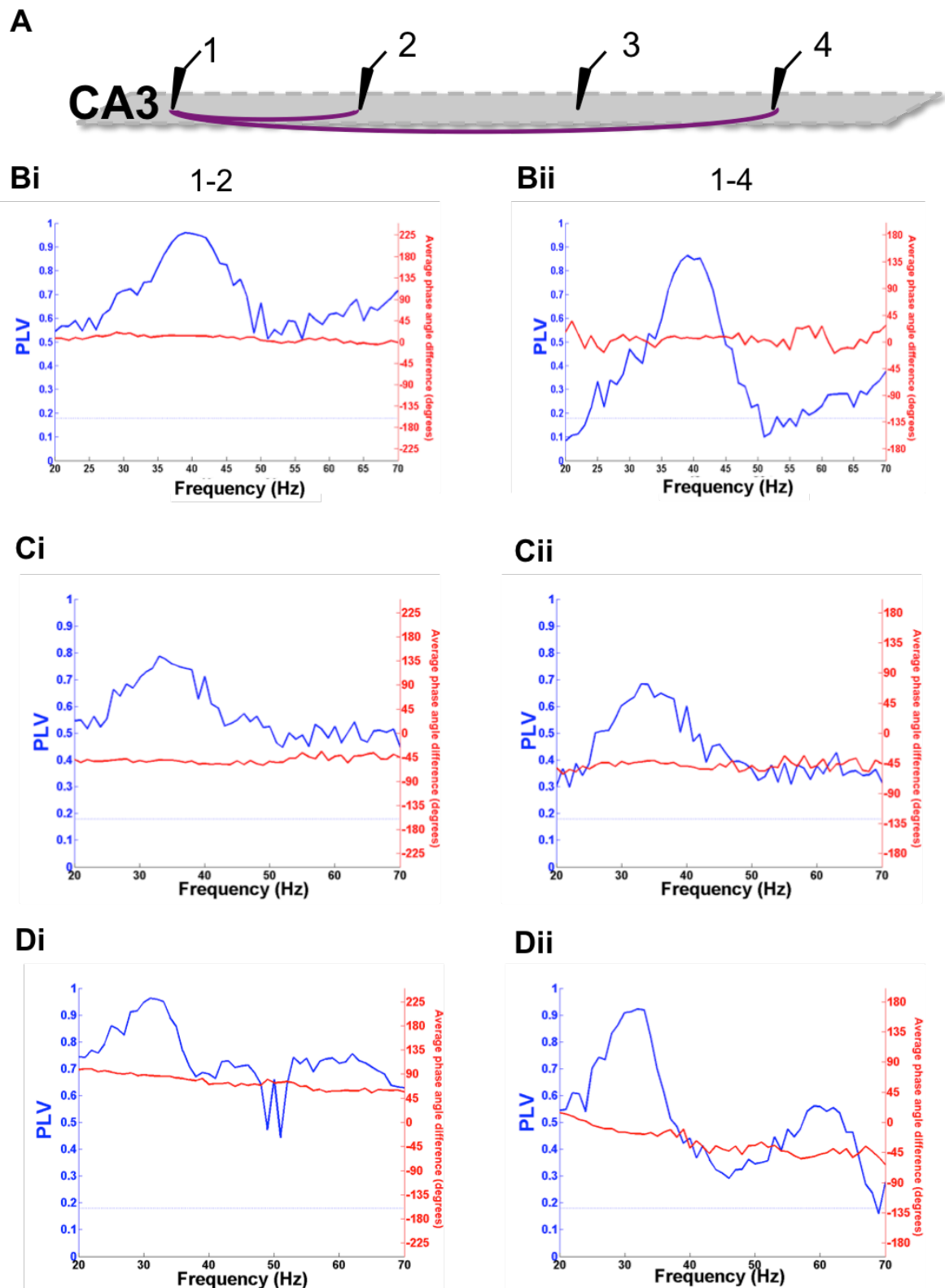


Figure 3.15. Short- and long-range connectivity in SyO. **A.** A schematic representation of 4 recording electrodes in the hippocampal CA3 region. **Bi. and Bii.** Phase synchrony between the adjacent (1-2) and distal (1-4) electrodes in SyO, demonstrating stronger phase coupling between the adjacent electrodes. **Ci. and Cii.** Phase synchrony between the adjacent and distal electrodes in KyO demonstrating stronger phase coupling between the adjacent electrodes. **Di. and Dii.** Phase synchrony between the adjacent and distal electrodes in CChyO, demonstrating stronger phase coupling between the adjacent electrodes.

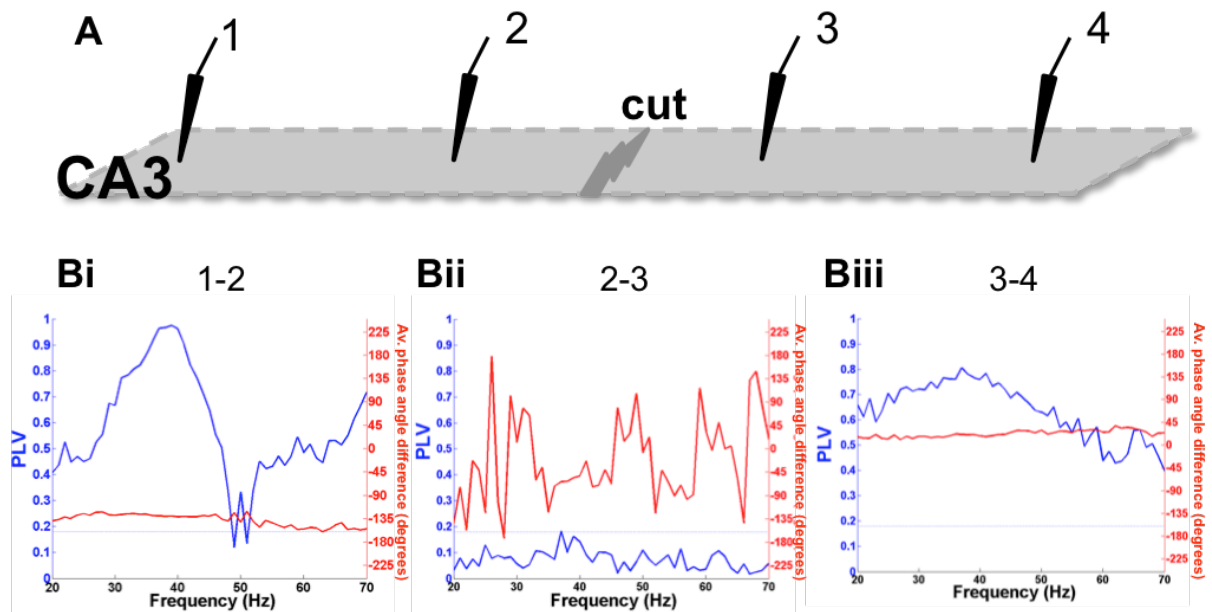


Figure 3.16. Volume conduction issue. **A.** A schematic representation of 4 recording electrodes in the hippocampal CA3 region with an incision made between electrodes 2 and 3. **Bi., Bii. and Biii.** PLV plots demonstrating preservation of SyO phase coupling between electrodes 1 and 2, 3 and 4, while a disruption of phase coupling between electrodes 2 and 3, demonstrating no volume conduction effect.

3.2.5.2. Volume conduction problem

High values of phase synchrony, as mentioned above, raise the possibility that the data were compromised by volume conduction phenomenon and might not represent the real network activity recorded by the electrodes. To test this possibility, a cut was made in the slice through CA3b region, thus separating electrodes 2 and 3. The hypothesis was that the incision would sever neuronal connection disrupting neuronal communication between electrodes 2 and 3; however, the touching sides of the lesioned tissue would allow volume conduction phenomenon to occur, if present. The results demonstrated that the phase synchrony between electrodes 2 and 3 was below significance level, whereas electrode pairs on either side of the cut presented high degree of phase coupling, which suggested a disrupted link between the two middle electrodes (Fig. 3.16). Results demonstrated that volume conduction played little or no role in generating the phase-locking data observed.

3.2.5.3. Dose-dependent phase effects of KA and CCh on SyO

Phase synchrony and oscillatory power relationship was explored using increasing concentrations of KA (0.5 – 125 nM) and CCh (0.5 – 50 μ M) applied to SyO. Scatter

plots were built for each agent concentration (each dot representing PPS-RMS power relationship for every frequency value between 20 Hz and 70 Hz). The plots for KA and CCh are presented in Fig. 3.17. Results suggested that the relationship between power and phase were linear across frequencies at a particular drug concentration, hence could be described by the parameters of a linear equation $y=mx+c$ for each dose of a driving agent, where m determines the slope of the line (i.e. the relationship between phase synchrony and power), while c determines the y-intercept (i.e. the gain in power at each concentration). Plotting gradients (m) and constants (c) for different concentrations of driving agents (in this case KA) produces the following graph presented in Fig. 3.18. The plot shows the behaviour of CA3 network oscillations under different concentrations of KA. By the created definition of phase-power relationship, at 0 nM KA (essentially, SyO) no phase-power relationship ($m=0$) and no gain in power ($c=1$) would be expected. This was confirmed experimentally (within the measurement error), as at near zero concentration c is close to 1, whereas m is approaching 0 (Fig. 3.18). While the power (c line) appears to increase linearly with added doses of KA, the phase-power relationship (m curve) demonstrates dose-dependent differences, suggesting different modes of oscillations at low concentrations compared a higher (>20 nM) KA drive. Nevertheless, at concentrations above 20 nM KA, which are commonly used for KyO induction, m seems to change in a linear fashion. To test the hypothesis that SyO are mechanistically the same as KyO, only smaller, we extrapolated from the linear region (20 – 100 nM KA) back to 0 nM KA (i.e. SyO). Fig. 3.18 shows that extrapolation does not produce $c=1$, $m=0$ for SyO, which would be the case, if SyO were the same as KyO. Although the results are preliminary, they suggest that SyO are different from KyO elicited by 20-100 nM KA. Although pharmacologically they appeared similar to KyO, the effects of UBP310 confirmed our interpretation of fundamental differences between induced and spontaneous gamma activity.

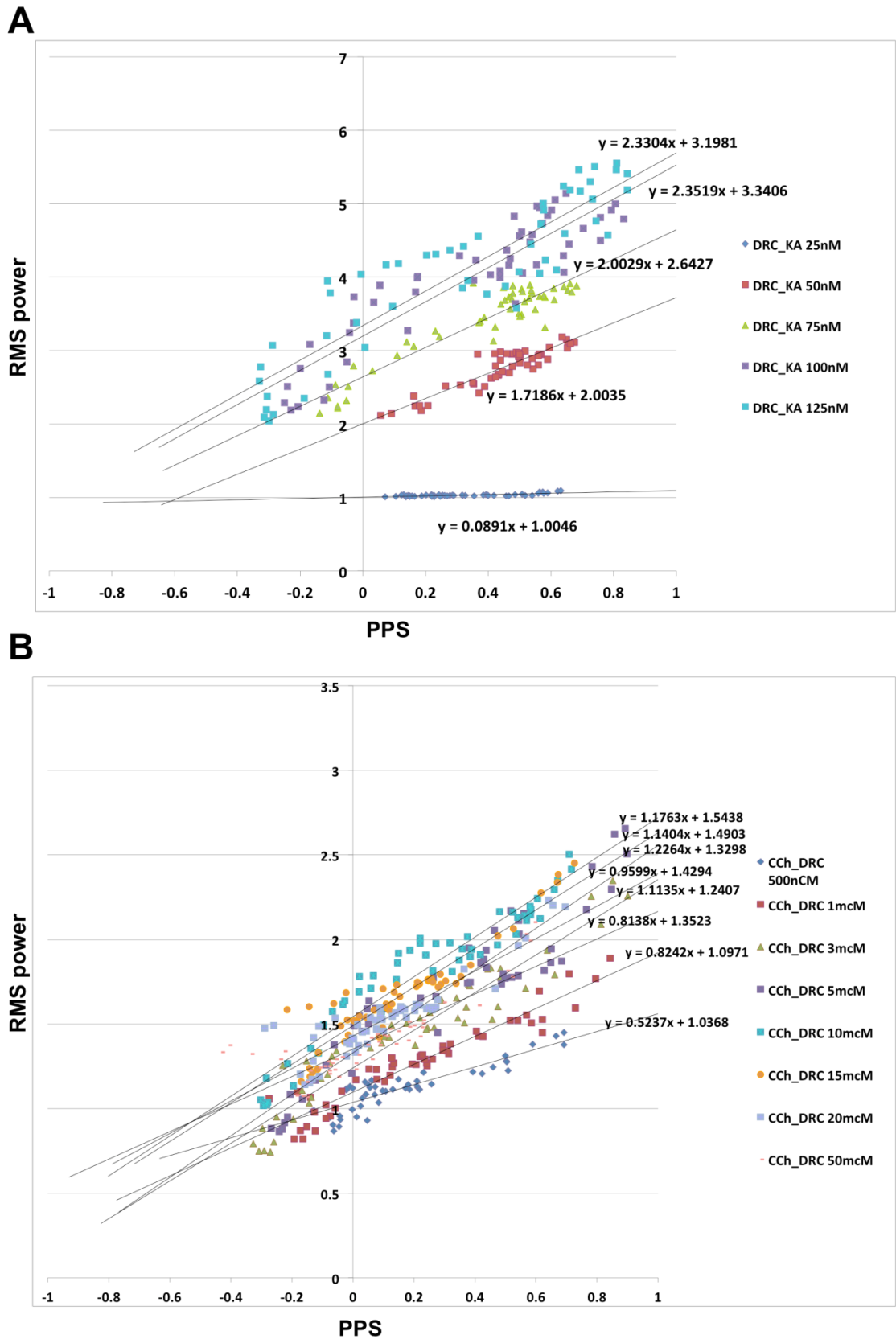


Figure 3.17. Phase synchrony-power relationship for increasing concentrations of KA and CCh. A. Scatter plot showing phase synchrony (PPS) and KyO oscillation power relationship at different concentrations of KA. **B.** Scatter plot showing phase synchrony (PPS) and CChyO oscillation power relationship at different concentrations of CCh.

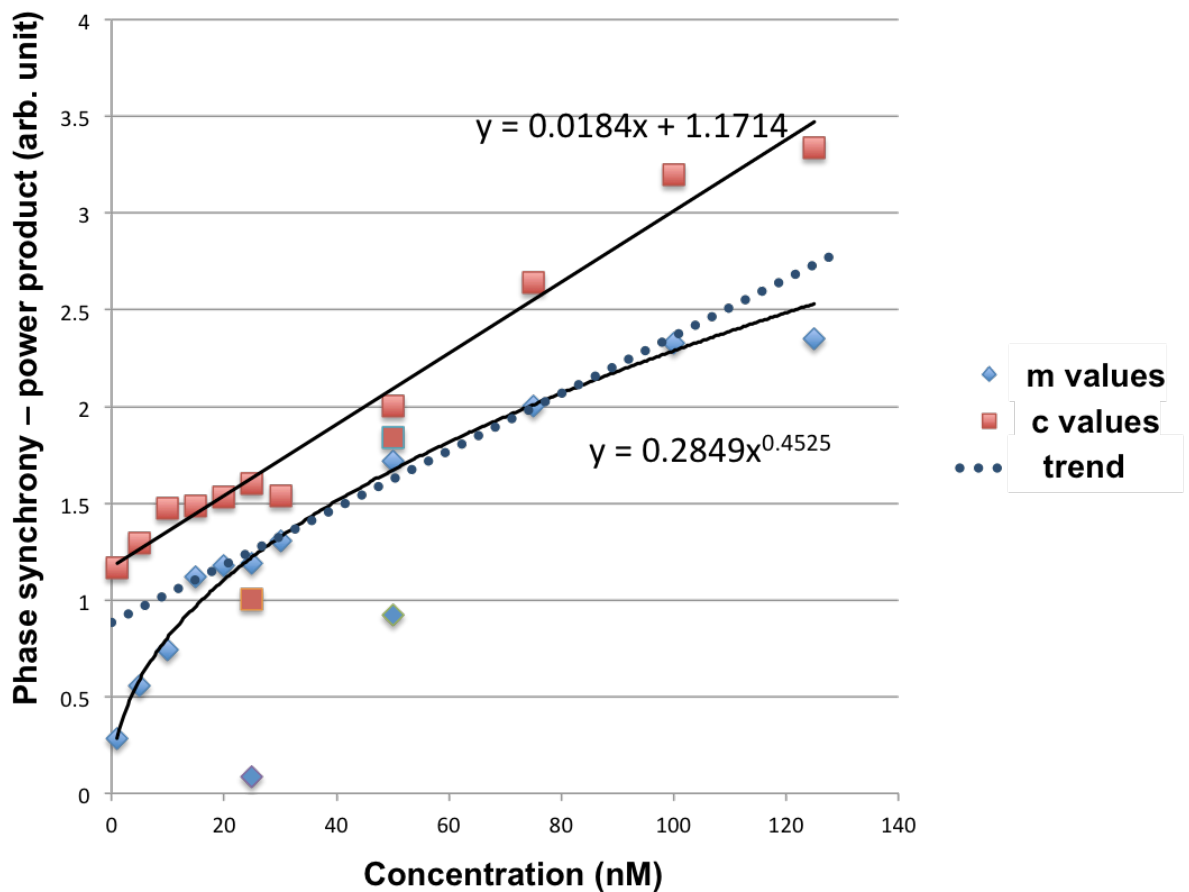


Figure 3.18. Phase synchrony-power-concentration relationship for KyO. A. **c** (red) values representing the power change of KA and **m** (blue) values showing phasepower relationship change with increasing concentrations for KA. The graph demonstrates linear increase in power, while a curvilinear phase-power relationship change. Extrapolation (blue dotted line) from the linear part of **m** (20–100 nM KA) to zero concentration gives $m=0.8841$ instead of predicted $m=0$ if SyO were the same as KyO (induced by 20–100 nM KA).

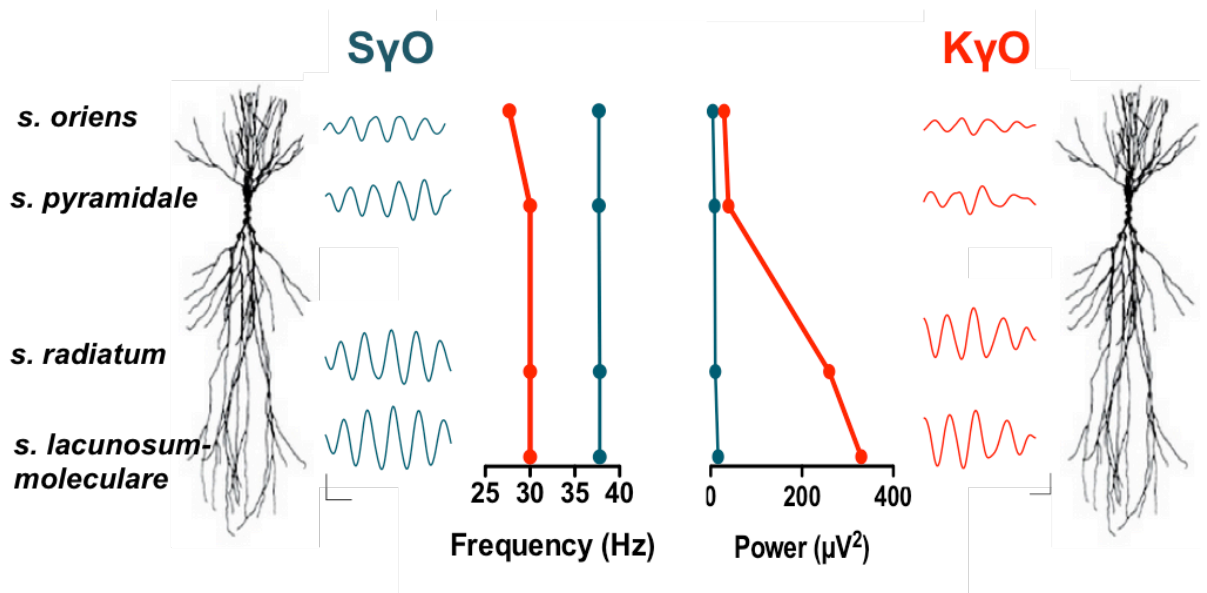


Figure 3.19. Laminar profile of SyO and KyO. A. Band-pass filtered (20–60 Hz) raw traces of SyO (teal) and KyO (red) recorded from the hippocampal CA3 layers (single recording). The peak frequency of SyO remains the same throughout the layers, whereas KyO in *s. oriens* showed lower frequency compared to other layers. Largest peak power for both SyO and KyO was observed in *s. lacunosum-moleculare*. Scale bars 20µV×25ms for SyO (left) and 100µV×25ms for KyO (right).

3.2.6. Laminar profile of SyO and KyO

The laminar profile of SyO and KyO was studied in the same slice by placing recording electrodes in *s. oriens*, *s. pyramidale*, *s. radiatum* and *s. lacunosum-moleculare* (distal *s. radiatum*) of the CA3 region. The largest power of both SyO and KyO was observed in *s. lacunosum-moleculare* and declined further away from the layer (Fig. 3.19). The frequency remained the same throughout the layers, although *s. oriens* showed lower frequency in KyO. Phase analysis demonstrated phase reversal between *s. pyramidale* and *s. radiatum* in both SyO and KyO (data not shown).

3.3. Discussion

3.3.1. SyO in improved brain slice preparation

In vitro brain slice research in rodents has always been criticised by researchers occupying “higher” levels of research pyramid, working on whole-brain preparations, on larger mammals, on *in vivo* preparations and finally on humans. Obvious limitations of brain slices include reduced size of the preparation, isolated neuronal

networks, absence of long-range connectivity, artificial conditions, not to mention the differences in species. Despite all these factors, so much information that we possess today has been acquired through *in vitro* research, and many mechanisms were uncovered because of the work that otherwise would not be possible due to ethical and practical considerations. Yet discrepancies still exist between the *in vitro* and *in vivo* sides of research, and it is our responsibility to make research more translational. One of the first steps towards this process should be increasing the quality of *in vitro* research by maximising the quality of brain preparations.

Increasing the viability and longevity of brain slices by improving slice preparation and storage techniques resulted in uncovering a natural gamma frequency rhythm in the hippocampal CA3 region. During the traumatic brain injury like brain extraction and cutting, brain cells undergo a stressful insult, which triggers a cascade of excitotoxic reactions aggravated by neuroinflammation and oxidative stress. These factors compromise cell well-being and result in cell death. In our lab, much effort is put into creating conditions for brain slices resembling the conditions found in more intact 'physiological' systems. Our goal is obtaining healthy slices and, hence good quality recordings. In their review Hajos and Mody (2009) proposed several modifications to the aCSF that would significantly improve tissue preservation. Altering aCSF composition was one of the first steps: using different aCSF solutions for cutting and recording (sucrose- and NaCl-based, respectively). Replacing NaCl with sucrose prevents cell swelling and lysis during the damaging procedure of cutting slices (Aghajanian and Rassmussen, 1989). Furthermore, inclusion into the aCSF of various neuroprotectants, neuromodulators and antioxidants, like indomethacin, uric acid, aminoguanidine, L-ascorbic acid, ketamine, N-acetylcysteine and taurine substantially improved cell viability and longevity (Pakhotin *et al.*, 1997; Tutak *et al.*, 2005; Proctor, 2008; Griffiths *et al.*, 1993; Rice, 2000; Green and Cote, 2009; Tian *et al.*, 2003; Kreisman and Olson, 2003). Changing the dissection technique, employing transcardial perfusion with ice-cold cutting aCSF caused remarkable changes in slice visualisation and endurance. These modified techniques, combined and utilised by Prokic (2012) allowed us to minimize excitotoxicity and neuronal death in the slice, which resulted in the observed spontaneous activity in the CA3. Pietersen *et al.* (2009) also reported that using

transcardial perfusion with sucrose-based aCSF substantially increased the occurrence of SyO in the hippocampal slices.

Spontaneous activity observed in brain slices in the absence of any pharmacological intervention allows us to study the natural “preferred” rhythm of a particular network. This way we are able to exclude from the process a biased step of artificial promotion of activity, a forceful drive of a network, which might not necessarily be the case *in vivo*. SyO present an opportunity to study a more physiologically relevant model of gamma oscillations and broaden our understanding of this phenomenon. Another potential application of this model is in the drug discovery/development process for increasing cognitive functions, as gamma waves in hippocampus are known to be involved in learning and memory.

3.3.2. Basic profile of SyO, KyO and CChyO

Due to the fact that SyO were persistently observed in the majority of slices, in order to independently measure and compare KyO and CChyO models, we had to go back to the basic aCSF composition for slice preparation, in order to create a clear baseline prior to induction of oscillatory activity. In the absence of additional neuroprotectants and neuromodulators, spontaneous activity was mostly absent or significantly reduced, suggesting that slice viability was a key factor in observations of spontaneous oscillatory activity. SyO have been reported previously in a preparation of murine hippocampus, however, they appeared only in 32.9% of slices and persisted for only 20 – 40 min, which makes pharmacological characterisation of this activity difficult (Pietersen *et al.*, 2009). In contrast to this, SyO described in this report readily appeared in the majority (>85%) of slices and lasted for several (up to 7) h, which could be explained by using improved brain slice preparation techniques. The basic profiles of explored gamma models appear to be very similar, although SyO frequency is significantly lower than induced oscillations. The mean peak frequencies of gamma rhythm models observed by Pietersen and colleagues (2009) were comparable to SyO and KyO recorded from our slices, suggesting to some extent a similar nature of SyO studied in both laboratories. There are several possible reasons that could account for frequency difference between spontaneous and induced activity. On the one hand, the oscillations could involve same core mechanisms, but different levels of excitatory drive. Hence, increasing the tonic

excitatory drive by addition of KA or CCh and recruiting larger networks makes chemically-induced gamma oscillations faster and more powerful compared to SyO (Buzsaki and Wang, 1996). On the other hand, the studied models could involve different microcircuits and interneuron types in the generation of gamma oscillations (Middleton *et al.*, 2008; Pietersen *et al.*, 2009). In this scenario, different interneurons would have different connectivity, IPSP decay kinetics or excitability, which might alter the rhythm created upon their activation. The contrast in the frequency of rhythmic activity is observed not only during the independent comparison, but also when KA/CCh are added to pre-existing SyO. The frequency shift marks the transition from one type of oscillation to another for the possible reasons described above. It is worth mentioning the positive correlation between the quality of SyO and induced gamma in the same slice, indirectly implying involvement of similar basic mechanism (Pietersen *et al.*, 2009), although it can also reflect good general survival of different network elements.

The differences in the peak power of oscillations between the three models arise due to uneven strength of excitatory drives provided by 50 nM KA and 1 μ M CCh. As identified from the input-output curves, application of 25 nM KA produces gamma frequency oscillations of a comparable power to the ones produced by 1 μ M CCh. Concentrations of driving agents used to elicit gamma oscillations in our experiments were considerably lower than the ones reported in original studies, indicating higher sensitivity for KA and CCh (Fisahn *et al.*, 1998; Hajos *et al.*, 2000; Hormuzdi *et al.*, 2001). Possibly due to enhanced slice viability and network preservation, minimal excitation was sufficient to generate network oscillations. Despite seemingly increased excitability, the hippocampal network appeared to be relatively stable, as it was impossible to induce any epileptiform activity, even at high concentrations of KA and CCh. Increasing driving force usually reached a point when oscillations gradually ceased, which was in line with early studies on hippocampal oscillations (Traub *et al.*, 1996a). A project carried out by Darshna Shah, another member of the laboratory, in collaboration with Newcastle University has revealed that the modified brain slice preparation contained more PV-positive interneurons (usually vulnerable to injury) and was less susceptible to epileptiform activity compared to traditional slice preparations.

Early studies on brain slice preparation techniques (methodology) revealed that immediately after cutting brain, slices required a minimum of 1 h rest prior to recording, during which a structural recovery of the slice took place (Garthwaite *et al.*, 1980; Hajos *et al.*, 1989; Kirov *et al.*, 1999). This technique is also used in our laboratory, and we found that when the LFP was recorded after the recovery period, SyO were already present in the hippocampal CA3 region. By contrast, when recorded straight after slicing, no activity was observed in the slices, however, it still emerged after approximately 1 h, upon the completion of “synaptically silent” period of recovery (Kirov *et al.*, 1999). In all three models, gamma oscillations became stable within 1.5–2 h of recording and usually lasted for several hours. Even though we conducted no direct studies measuring the maximum life span of oscillations in our slices, it was obvious from dose-response/sham experiments that SyO persisted for up to 7 h, while oscillations sustained by pharmacological stimulation could persist for 10 h and possibly longer. These observations once again point out high level of brain cell preservation. Even slices exposed to prolonged storage (>6h) exhibited SyO, further supporting this interpretation.

It is interesting how hippocampal rhythmic activity undergoes changes in frequency, depending on applied KA/CCh dose. Dose-response experiments demonstrated that at higher concentrations of KA and CCh, together with gamma oscillations, slow rhythms were introduced (either theta or delta). It has been reported previously in experimental and modeling conditions that different concentrations of CCh (4–60 μ M) were able to elicit transient delta, theta and gamma rhythm oscillations (Fellous and Sejnowski, 2000; Tiesinga *et al.*, 2001). Theta oscillations have been widely observed in the hippocampus of rodents during active behaviour. Of a particular interest is co-occurrence of gamma and theta rhythms, the so-called nesting of rhythms (Soltesz and Deschenes, 1993; Bragin *et al.*, 1995; Colgin *et al.*, 2009; Belluscio *et al.*, 2012). It is believed that such dual oscillation is involved in coding information, memory and sensory processes (Lisman and Jensen, 2013).

3.3.3. Characterisation of SyO

Apart from the CA3 region, spontaneous oscillatory activity has not been detected in any other hippocampal regions in our slices. It is known that spontaneous oscillations emerge from the areas with a substantial system of recurrent excitatory collaterals, a

characteristic feature of the hippocampal CA3 region. Our results from experiments with cut slices (to isolate CA3) support the idea of intrinsically generated SyO.

Exploring SyO occurrence across different age groups has revealed that spontaneous activity is present throughout the life of an animal, although reports exist in the literature about gamma rhythm decline in aged animals (Vreugdenhil and Toescu, 2005; Lu *et al.*, 2009). In contrast to this, our experiments show that SyO become stronger and increase in frequency, as the rats get older. It is probably important to establish whether it is the development or the aging of the system, as by P20 (50g rat) the most fundamental developmental processes are already completed. Pharmacological analysis showed that SyO peak frequencies were altered significantly in response to any modulation, even when the power of oscillations remained unchanged. This might indicate that oscillation frequency is sensitive to even slight changes in the network balance, which provides generation/maintenance of gamma oscillations. It is possible that some network elements undergo fine age-dependent alterations, which modulate the frequency of rhythmic neuronal activity. One of the potential contributors is the change in kinetic properties of GABA-Ar, as the frequency of gamma oscillations is determined by the decay time constant of GABA-mediated IPSCs (Whittington *et al.*, 1995; Buzsaki *et al.*, 1996). Some of our data show that spontaneous IPSCs recorded from CA3 pyramidal cells of 50g rats have a longer decay time compared to 100g animals, hence slower gamma frequency oscillations (see Section 5.2.3.2.). This difference could potentially be traced in older animals, however more experiments are required. Other studies have demonstrated faster IPSC kinetics in mature animals compared to young ones, which was associated with an increase in $\alpha 1$ subunit content of postsynaptic GABA-Ar (Doischer *et al.*, 2008; Lazarus and Huang, 2011). The frequency of SyO could also depend on the overall level of interneuron excitation mediated by AMPAr (Wallenstein and Hasselmo, 1997), which could change throughout development/aging.

3.3.4. Comparative Pharmacology

Together with basic characterisation of *in vitro* gamma oscillations models, we carried out a pharmacological analysis of SyO, KyO and CChyO, which revealed that the three models were pharmacologically different. The results showed that

GABAergic system was essential for gamma oscillations generation and maintenance in all studied models, as GABA-Ar antagonists PTX and bicuculline readily abolished all oscillatory activity. These findings were in line with the original studies on SyO, KyO and CChyO in the hippocampus and cortical regions (Fisahn *et al.*, 1998; Fisahn *et al.*, 2004; Palhalmi *et al.*, 2004; Cunningham *et al.*, 2003; Yamawaki *et al.*, 2008; Pietersen *et al.*, 2009). Increased power of gamma oscillations caused by the positive allosteric modulator of GABA-Ar zolpidem (100 nM) further supported the importance of GABA involvement. Similar effect was observed by Heistek *et al.* (2010) in the hippocampus and Yamawaki *et al.* (2008), Prokic (2012) and Ronnqvist *et al.* (2013) in M1 motor cortex. Palhalmi *et al.*, 2004, on the other hand, reported an opposite effect in CA3 area, which may be due to a 100-fold difference in zolpidem concentration. In accordance with previous pharmacological studies (Fisahn *et al.*, 1998; Cunningham *et al.*, 2003; Yamawaki *et al.*, 2008; Pietersen *et al.*, 2009), GABA-Ar modulator pentobarbital produced a characteristic decrease in frequency of all three types of gamma oscillations due to its ability to prolong the decay time of GABAergic IPSCs (Segal and Barker, 1984). A significant shift in power was observed only in CChyO, which could indicate that this model might be more dependent on GABAergic IPSCs. Together these findings demonstrate that in SyO, like other gamma oscillations models, GABA-mediated inhibition is a prerequisite for neuronal network synchronisation.

We also explored the role of excitatory glutamatergic system in the generation of SyO and compared it to traditional KyO and CChyO models. Our findings show that fast excitation mediated by ionotropic AMPAr was necessary for gamma oscillations generation in all studied models. In all models, a non-selective AMPAr and KAR antagonist, CNQX, abolished gamma rhythm, and replaced it with theta oscillations 6-15 Hz and ripples (150-200 Hz). This effect was similar to the one observed with the combination of selective AMPAr blockers NBQX+SYM2206, although the theta rhythm seemed to be more pronounced, whereas ripples were less prominent. Theta oscillations occurring under the conditions of suppressed AMPAr activity were reported by Gillies *et al.* (2002) and have been suggested to be generated by intrinsic theta-frequency spiking subset of hippocampal interneurons. A remarkable difference between the models appeared when GluK1,3-containing KAR were blocked by UBP310 and the expected reduction in KyO power was contrasted with an *increase*

in SyO power. The lack of literature on KAr in CA3 means we may only speculate on the possible mechanism of UBP310 action on SyO. It seems likely that the effect occurs on a local CA3 interneuron/pyramidal cell level. Based on the studies of KAr in the hippocampus (for reviews see Pinheiro and Mulle, 2006 and Carta *et al.*, 2014), pyramidal cells mostly express GluK2-containing KAr, while GluK1 KAr are found on the interneurons. An increase in SyO peak power could arise from blocking the suppressive effect of presynaptic GluK1,3 on GABA release. For example, Rodríguez-Moreno and colleagues (1997) showed that presynaptic KA-heteroreceptors decreased GABA release by 90% in hippocampus *in vitro* and in *in vivo*. Jiang *et al.* (2001) further demonstrated that high levels of KAr activity depressed GABA inhibition in CA1, whilst low levels of activity facilitated inhibition in the form of increased success rate of unitary IPSCs (uIPSCs). Hence, during SyO, low levels of KAr activity may favour inhibition of pyramidal cell activity and this would be relieved by KAr blockade with UBP310, leading to increased principal cell excitability and enhanced oscillatory power, whilst during KA-driven activity, inhibition would already be suppressed to some extent and the effects of UBP310 would be dominated by depressant effects on network excitation – leading to a reduction in KyO power. This mechanism is necessarily speculative, since the work cited above was performed in CA1, however, we might predict that CChyO activity, which also lacks direct KAr activation, might resemble SyO in its response to UBP310. This was indeed observed in some experiments (see Fig. 3.9C) but not in others and the mixed effects may indicate that CCh drive places the network at the threshold for significant indirect KAr activation, placing this model somewhere between SyO and KyO in this regard.

Due to the lack of selective GluK2 KAr antagonists, it is difficult to evaluate the role of GluK2 subunit in the generation of gamma oscillations. However, Fisahn and colleagues (2004) showed that in GluK2 KO mice, KA application failed to elicit gamma oscillations. Most studies suggest that KAr and AMPAR-mediated excitation was required for the generation of various types of gamma oscillations (Fisahn *et al.*, 1998; Whittington *et al.*, 2000; Cunningham *et al.*, 2003; Khazipov and Holmes, 2003; Fisahn *et al.*, 2004; Brown *et al.*, 2006; Pietersen *et al.*, 2009). Fisahn and colleagues (2004), however, argued that AMPAR activation was not necessary for

KyO, although discrepancies could possibly occur due to different AMPAR antagonists used.

Our results demonstrated that NMDAR did not significantly contribute to SyO or KyO, the latter being supported by the original pharmacological study (Fisahn *et al.*, 2004). On the contrary, Pietersen *et al.* (2009) showed SyO suppression and KyO enhancement with NMDAR antagonist AP-5. Interestingly, our CChyO increased significantly after NMDAR were blocked.

The involvement of metabotropic glutamate receptors was explored using MPEP and LY341495 to block mGlu₁, mGlu₅ and groups II and III, respectively. Our findings showed that groups II and III did not actively contribute to gamma oscillations in either of explored models. Blockade of mGlu₅, on the other hand, resulted in a substantial increase in oscillation power in all three models, possibly due to indirect effects leading to increased synaptic inhibition, which boosted the oscillations (Desai *et al.*, 1994).

Apart from the synaptic mechanism, all three models of gamma oscillations heavily relied on the non-synaptic component, as the gap junction blocker either greatly decreased or abolished gamma oscillations in all experiments. These observations were in line with previous reports (Traub *et al.*, 2000, 2003; Hormuzdi *et al.*, 2001; Buhl *et al.*, 2003; Pietersen *et al.*, 2009). Generally, previous reports demonstrated that electrical coupling dramatically increased the power of gamma frequency oscillations, however were not required for the generation of rhythmic activity.

Atropine, as an mACh antagonist, was used to determine whether these receptors were required for maintaining gamma rhythm oscillations. The results demonstrated that while activation of cholinergic system was able to induce oscillatory activity, its presence was not required for the naturally occurring rhythm in the slices (SyO). The fact that atropine blocked CChyO (Fisahn *et al.*, 1998), but not SyO and KyO (Fisahn *et al.*, 2004) indicated that SyO were more comparable to KyO than CChyO. Our observations led us to an assumption that KyO represented a more physiologically relevant *in vitro* model of gamma oscillations in comparison to CChyO, however as

the system is capable of generating different types of gamma activity, we cannot exclude the possibility of K γ O or CCh γ O occurrence in an intact brain.

Overall, pharmacological characterisation shows fundamental differences in the mechanism of the three models. S γ O, K γ O, CCh γ O seem to share some basic elements taking part in rhythmogenesis, such as dependence on GABAergic inhibition. However, the independence of S γ O from GluK1 KAr and mAChr, which are essential for K γ O and CCh γ O maintenance, respectively, suggests that S γ O constitute a distinct class of rhythmic activity.

3.3.4. Phase analysis of S γ O

Phase synchrony analysis provided some insights into the nature of S γ O and their spatial profile. Similarly to driven oscillation, S γ O were strongly phase coupled throughout the CA3 region. Although it decreased in the long range, the coupling was still rather strong. The fact that upon addition of pharmacological agents the phase synchrony became slightly stronger suggested either the recruitment of more cells or a more synchronised cell firing. To address the issue of volume conductance, we carried out experiments with the cut between adjacent electrodes, which showed that strong coupling was produced by the network activity recorded by the electrodes. The analysis of short- and long-range connectivity is in progress, and should provide more knowledge on the spatial properties of S γ O, in comparison to K γ O and CCh γ O.

Based on the KA dose-dependent phase synchrony-power relationship, it appeared that S γ O were different from K γ O, as S γ O behaviour did not fit into the predicted 0 nM KA K γ O. More experiments are required to investigate whether S γ O are a 'small version' of CCh γ O.

3.3.5. Laminar characterisation of S γ O and K γ O

The laminar profile of S γ O suggested that the change in polarity from *s. pyramidale* to *s. radiatum* reflected the flow of currents in somato-dendritic regions of CA3 pyramidal cells. Original studies demonstrated phase reversal from body to apical dendrites of hippocampal pyramidal cells in K γ O and CCh γ O (Csicsvari *et al.*, 2003; Buzsaki *et al.*, 2003; Hajos *et al.*, 2004; Mann *et al.*, 2005a; Vreugdenhil and Toescu, 2005). Current-source density (CSD) studies revealed that gamma oscillations were

associated with alternating current sink and source pairs in *s. pyramidale* and *s. radiatum* (Csicsvari *et al.*, 2003; Hajos *et al.*, 2004; Mann *et al.*, 2005a). The investigation carried out by Vreugdenhil and Toescu (2005) on KyO and CChyO revealed certain differences in characteristics of these two models. Although some observation from the study did not fit with other literature (in particular regarding CChyO), the authors concluded that despite similar mechanisms between KyO and CChyO, they involved different networks (Vreughdenhil and Toescu, 2005). The same research group investigated laminar CSD profile of SyO in comparison to KyO, their results showed less pronounced sinks and sources in SyO and authors suggested that KyO additionally recruited perisomatic IPSCs (Pietersen *et al.*, 2009).

3.3.7. SyO as a physiologically relevant model of gamma oscillations

Electrophysiological and pharmacological comparison of three types of gamma oscillations (SyO, KyO and CChyO), combined with previous reports, suggest that, compared to KyO and CChyO, SyO more closely resemble the gamma oscillations observed *in vivo* (Csicsvari *et al.*, 2003; Buzsaki *et al.*, 2003; Vreugdenhil and Toescu, 2005; Pietersen *et al.*, 2009). We demonstrate that SyO are pharmacologically different, and thus could be used for exploring rhythmic activity in the hippocampus *in vitro*. Although SyO have been observed previously, it had a transient nature and did not appear regularly. For these reasons, characterisation of such SyO and interpretation of results appear to be difficult. Despite this limitation, Pietersen and colleagues (2009) suggest that SyO and KyO arise from the same basic network, but are different in the types of involved interneurons and pharmacological properties, although it is difficult to make conclusions. Nevertheless, the main idea taken from spontaneous activity observation is that SyO represent a physiologically-relevant model of oscillations, as it is naturally produced by the local neuronal networks preserved in a brain slice. Due to the existence of only two characterisation studies on SyO, much information about this rhythm is still unknown.

3.4. Conclusion

In this report we explore a model of persistent spontaneous gamma oscillations in CA3 area of the hippocampus. We suggest that improving slice viability by altering

methodology (techniques) uncovers this natural rhythm. We compare its electrophysiological and pharmacological properties to traditional K γ O and CCh γ O models of gamma oscillations. We conclude that SyO in CA3 hippocampus appear to employ the same basic inhibition-based mechanism as K γ O, however, significant difference in KAr dependence is observed. Similarly, SyO differs from Cch γ O in their independence from cholinergic system. Based on the pharmacological and phase analyses, we conclude that SyO are a distinct type of gamma rhythmic activity, and hence, due to their natural occurrence, are more physiologically relevant. These findings present an opportunity to work on a reliable physiological model of neuronal network oscillations, partially solving the problem of large discrepancies between *in vitro* and *in vivo* research.

Chapter 4 The Reduced Intensity Status Epilepticus (RISE) model of chronic epilepsy

4.1. Introduction

Epilepsy is a pathological condition, characterized by the occurrence of SRS, which appear as a result of abnormal neuronal excitability and synchrony. Electrographic seizures are associated with large amplitude oscillatory activity, suggesting hypersynchrony, at least on a local level (Timofeev *et al.*, 2012). Due to a large variety of seizure and epilepsy types in humans, as well as a large variety of studied brain regions, different types of rhythmic activity have been associated with seizures (either preceding or superimposed upon them): spike-wave complexes (2 – 3 Hz) and fast runs at 10 – 20 Hz (Steriade *et al.*, 1998; Neckelmann *et al.*, 1998), 50 – 80 Hz rhythmic activity (Allen *et al.*, 1992); 80 – 200 Hz ripples (Fisher *et al.*, 1992; Traub *et al.*, 2001b; Grenier *et al.*, 2003) and 200 – 500 Hz fast ripples (Bragin *et al.*, 1999b). Overall, much information has been accumulated from both human and animal studies over the years; however, more research exploring the role of different oscillatory patterns in epilepsy is yet to come. It is becoming clear that high-frequency oscillations are tightly associated with seizure activity and might indicate epileptogenic properties of the tissue and identify the focus of seizure generation.

From a clinical point of view, as defined by the International League Against Epilepsy (ILAE), epilepsy is “a condition characterized by two or more recurrent epileptic seizures over a period longer than 24 h, unprovoked by any immediate identified cause” (Sander, 1997). Various classifications of epilepsy exist in the literature and clinics, including the localisation of the focus, aetiology, as well as the seizure types. According to seizure manifestation, seizures can be motor, sensory (auditory, visual, olfactory), autonomic (sweating, piloerection, epigastric sensation), psychic (cognitive, illusions, hallucinations). There are two types of seizures: partial, occurring in a specific area of the brain (focal), and generalised, when the pathological activity spreads across the brain regions. Partial seizures are further divided into simple (maintained consciousness) and complex (loss of consciousness). Generalised seizures actively involve motor system, hence are accompanied by convulsive state with tonic /clonic phases. Based on the aetiology, epilepsy is classified into idiopathic (e.g. absence epilepsy), provoked, cryptogenic and the largest group symptomatic, which includes genetic/developmental and

acquired (e.g. head trauma, infection, brain tumors) (Shorvon, 2011). Depending on the brain area producing the seizures, epilepsies are classified into temporal, frontal, parietal and occipital lobe epilepsies. TLE is the most common type among localisation-related epilepsies, occurring in 66% cases (Semah *et al.*, 1998). Furthermore, TLE is known to be the most common type of intractable epilepsy, occurring in 50 – 70% of the cases (Wass *et al.*, 1985; Guldvog *et al.*, 1994; Keene *et al.*, 1997). As suggested by its name, TLE involves temporal lobe brain structures like the hippocampus and amygdala, its symptoms usually include motionless staring (freezing) and oroalimentary automatisms (Engel, 1996). TLE is usually accompanied by characteristic neuropathological alterations like hippocampal sclerosis with excessive gliosis and cell death, neuronal circuit reorganisation with axonal sprouting and synaptogenesis (Sutula *et al.*, 1988, 1989; Mikkonen *et al.*, 1998).

4.1.1. Epilepsy models in animals

A number of questions have been formulated in the epilepsy research over the years. What leads to cell hyperexcitability, what causes abnormal synchronous neuronal discharges, what underlies the transition from interictal to ictal activity, why do seizures propagate, how do they stop, how is intractable epilepsy different from other types, and, of course, developing new antiepileptic drugs (AEDs) – these are the main questions the research has been trying to answer (Mody and Schwartzkroin, 1997).

One might understand that human studies are not suitable for extensive epilepsy research, due to obvious ethical issues. These limitations have led to the development of a wide variety of epilepsy and seizure models in animals. The search for new effective AEDs and the necessity to unravel the mechanism of epileptogenesis have been the main factors pushing forward the development of different epilepsy models up to this date. One of the critical moments of epilepsy animal research is to distinguish between seizure and epilepsy models. Both types are widely used nowadays, however they serve different purposes. Seizure models are mainly utilised for new AED screening in the pharmaceutical industry, when certain model properties like cost- and time-effectiveness are essential. Epilepsy models, on the other hand, are mostly used by research groups exploring the

mechanisms of epileptogenesis in search for new targets for pharmacotherapeutic intervention.

One of the main challenges in the field has been the questionable validity of epilepsy models. As summarised by Sarkisian (2001), some people reasonably argue that many investigations are carried out on healthy rather than epileptic brains, some of the seizure manifestations, both behavioural and at the level of brain recording, do not resemble those observed in humans, and finally, it may be asked: how translational is animal research in epilepsy? So what are the criteria for a good epilepsy model? Again, as pointed out by Sarkisian (2001), an epilepsy model should exhibit the same or at least similar behavioural and EEG patterns of seizures, as in human epilepsy. Furthermore, a valid epilepsy model should mimic the aetiology of the corresponding human condition. The model should have a similar age of epilepsy onset and exhibit the same pathological changes characteristic for a certain type of human epilepsy. Logically, a valid epilepsy model should respond to the same AEDs as the human epilepsy.

A brief description of the most commonly used models of seizures and epilepsy will be given now.

4.1.1.1. *In vitro* models of seizures

In vitro brain slice preparations allow modelling and studying epileptiform discharges at the cellular and network levels, which can be a solid support for epilepsy model findings and the mechanism(s) of action of AEDs. *In vitro* models of seizures are a good basis for exploring seizure initiation, propagation and cessation within a localised area. These models clearly lack the most important features of *in vivo* models, such as long-range connectivity of the brain, as well as behavioural and motor components, and therefore can produce only limited aspects of seizures. These seizure equivalents are achieved by altering electrical activity and ionic concentrations in slices. In brain slices, acute seizure-like activity can be elicited with low Ca^{2+} (Jefferys and Haas, 1982), low Mg^{2+} (Stanton *et al.*, 1987) or elevated K^+ (Jensen and Yaari, 1988) medium, as well as 4-aminopyridine (4-AP) (Avoli *et al.*, 1996) and/or electrical stimulation (Rafiq *et al.*, 1995). It is peculiar that seizures are induced in slices from healthy tissues, yet it is often very difficult to elicit seizures in

the same way in human tissue from epileptic brain (Gabriel *et al.*, 2004; Huberfeld *et al.*, 2011). When using brain slice preparations to study seizure-like events, one should always keep in mind the disadvantages of this model, such as the tissue undergoing acute lesioning/ischemia, disturbed networks, severed connections, reduced oxygen and nutrients diffusion in slices, differences in brain physiology/anatomy between species (Heinemann *et al.*, 2006).

4.1.1.2. Models of acute seizures

Different models of seizures and epilepsy are used based on the aims of conducted research. For the purpose of screening a large number of compounds for anticonvulsant properties, a new class of models termed models of acute seizures was developed. These models include induction of seizures with chemical agents like pentylenetetrazol (PTZ), antibiotics, metals and toxins or with electrical stimulation, such as maximal electroshock seizure threshold (MEST) and 6-Hz seizure test (for review see Velisek, 2006; Mares and Kubova, 2006).

4.1.1.3. Kindling model of epilepsy

The kindling phenomenon was discovered by Graham Goddard in 1967, and it has been widely used in epilepsy research as a model of chronic TLE, since the most significant changes appear in the temporal lobe regions like the amygdala and piriform, perirhinal, entorhinal, and insular cortices (Goddard *et al.*, 1969; McIntyre *et al.*, 1999). The kindling phenomenon occurs when a repeated induction of focal seizures results in a gradually increasing response to the stimulating agent, producing electrographic and behavioural changes and leading to the kindled state. Eventually, after a long period of time, epileptic seizures start appearing spontaneously, as the brain region becomes 'overkindled' and truly epileptic. For an extensive review of kindling models see Morimoto *et al.* (2004).

4.1.1.4. Post SE epilepsy models

TLEs exhibit several features that have been incorporated into different animal models. These hallmarks include seizure foci in the temporal lobe (Bartolomei *et al.*, 2005), an initial insult (so-called 'initial precipitating injury') [Mathern *et al.*, 2002] followed by a seizure-free period and certain histopathological changes (Mathern *et*

al., 1997). SE models of epilepsy constitute a large field of animal epilepsy research, due to the common properties they share with TLE. They allow exploration of truly epileptic animals exhibiting SRS some time after systemic administration of convulsant agents like KA or pilocarpine. These models, although employing different mechanisms, progress through the same stages: an initial hours-long SE characterised by continuous recurrent seizures, followed by a quiescent period of a few weeks or months with no seizures (the so-called latent period), and finally SRS, when an animal becomes epileptic. During the SRS phase, researchers can observe seizures lasting 1 – 3 min and resembling complex partial seizures with secondary generalisation, which increase in frequency with epilepsy progression. The most explored stages are either SRS period or the transition from latent period to SRS. It is believed that all neuropathological changes take place during the latent period. The duration of latent period can not be precisely calculated, however, its mean duration is around 40 d (Gliem *et al.*, 2001) and it can be manipulated through the dose of inducing agent, lasting from several days at high doses to months after SE induction at lower doses (Hamani and Mello, 2002). Moreover, Navarro Mora *et al.* (2009) suggest that in pilocarpine model a prolonged SE is not required for an animal to become epileptic. They demonstrate that even after not having experienced SE still, lesioned animals develop SRS after latent periods of up to a year.

SE models are widely used to study TLE, as they closely mimic the changes occurring in human mesial TLE, even though animal models may produce extensive brain damage. Indeed, severe brain damage and animal mortality during the induction are serious disadvantages and problems of these models. Klitgaard and colleagues (2002) report that in pilocarpine model minimum 30 min SE is necessary for SRS development later on, however, the longer the SE period is, the more extensive cellular death is observed (Inoue *et al.*, 1992). It is known that SE might be difficult to control, and it is further exacerbated by the variability in sensitivity towards convulsant agents among animals. These factors often result in high animal mortality. On the other hand, reducing the dose of an agent most of the times leads to a low success rate, therefore, when working with these models, it is essential to find the right balance.

4.1.1.4.1. KA-induced SE model of epilepsy

In 1978 Nadler and colleagues discovered that focal injection of KA induced seizure and neuropathological changes in the hippocampus. This model became a powerful tool in the epilepsy field. KA-induced epilepsy in animals closely resemble acquired human epilepsy and TLE condition, sharing the same morphological alterations such as significant neuronal death, hippocampal gliosis, and axonal sprouting (Wieser *et al.*, 2004). Furthermore, a similar etiology was documented in humans, when an outbreak of amnesic shellfish poisoning took place in Canada in 1987. Acute domoic acid (a KA analogue) poisoning resulted in affected people exhibiting various seizure manifestations from chewing and grimacing to a prolonged SE (Teitelbaum *et al.*, 1990; Cendes *et al.*, 1995). The patients who had undergone SE had a seizure-free period of about a year before developing TLE (Cendes *et al.*, 1995). The postmortem examinations of patients with fatal outcome revealed specific neuropathological changes in the hippocampus and amygdala, similar to KA-induced damage in animals (Teitelbaum *et al.*, 1990).

4.1.1.4.2. Pilocarpine/Li-pilocarpine model of epilepsy

The pilocarpine model of chronic epilepsy was first described by Turski and colleagues in 1983, and since then has been used extensively as a model of human TLE. The fact that pilocarpine-induced epilepsies demonstrate circuit reorganisation in limbic structures (e.g. the loss of interneurons, mossy fibre sprouting and reactive gliosis) and are poorly controlled by AEDs further supports the use of this model for exploring TLE (Wieser, 2004; Glien *et al.*, 2002; Chakir *et al.*, 2006). Studies show that pilocarpine produces its epileptogenic effects via M1 mAChR, since seizures can not be induced with pilocarpine in M1 receptor KO mice (Hamilton *et al.*, 1997). Furthermore, administration of atropine prior to SE induction is able to prevent the development of seizures (Clifford *et al.*, 1987). Interestingly, atropine loses its effectiveness once the seizures are initiated, suggesting that their maintenance relies on mechanisms other than muscarinic receptor activation (Clifford *et al.*, 1987). Extensive research on the mechanism of pilocarpine effects has been conducted for years now, and it has been summarised by Cavalheiro *et al.* (2006) and presented in Fig. 4.1. When examining the whole picture, it becomes clear that pilocarpine triggers a massive cascade of reactions in neurons and glial cells. These reactions affect signal transduction pathways, ionic concentrations, receptor and neurotransmitter

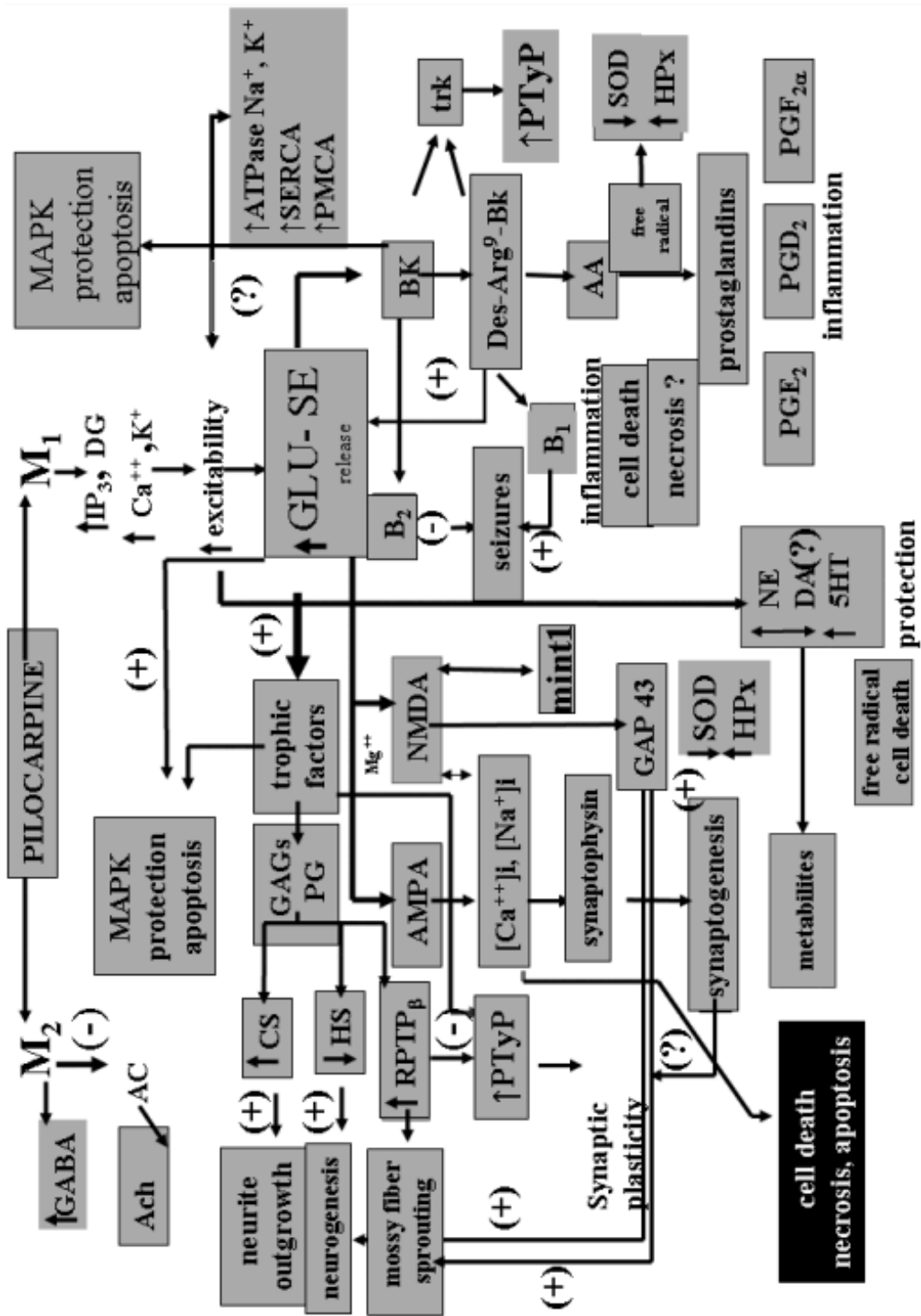


Figure 4.1. The mechanism of pilocarpine model of chronic TLE. The chart shows a cascade of neuroinflammatory reactions triggered by pilocarpine administration (adapted from Cavalheiro *et al.*, 2006).

activity, and inflammation, which lead to increased excitability, development of SE, cellular death and neuronal reorganisation.

Many epilepsy models, including the pilocarpine model, initially induce SE, which progresses through the Racine stages, culminates in generalised tonic-clonic seizures and persists for hours before spontaneously subsiding. Before and during SE, EEG recordings initially demonstrate theta rhythm in the hippocampus, which turns into large amplitude and high frequency activity, as the seizures worsen. Later on, high voltage spiking appears prior to seizures, hence both ictal and interictal activity can be observed on the EEG. Once SE remits, the EEG goes back to normal. Studies suggest that the epileptiform activity originates in hippocampus and spreads to the amygdala and the cortex (Turski *et al.*, 1983).

The SRS phase is characterised by the occurrence of spontaneous seizures, which begin with partial seizures such as staring, oroalimentary automatism, forelimb clonus and later turn into generalized seizures, including bilateral forelimb clonus, rearing, falling and tonic-clonic seizures (Veliskova, 2006; Goffin *et al.*, 2007). It has been noted that SRS appear in a cyclic manner every 5–8 days (Goffin *et al.*, 2007). EEG manifestations include bursts of spikes originating in the hippocampus and propagating to the cortex; ictal activity is followed by interictal activity with suppressed background activity with spikes (Cavalheiro *et al.*, 1991).

Since the pilocarpine model of epilepsy has been in use for decades now, it has inevitably undergone modification and improvement. Different research groups add their own components and change the protocol according to desired outcomes. One of the most popular modifications of the model is administration of Li 24 h prior to pilocarpine induction (Honchar *et al.*, 1983). It was suggested that Li and pilocarpine exert synergistic effects, increasing inositol 1,4,5-trisphosphate (IP₃) production and subsequent acetylcholine (ACh) release and mAChR signalling (Honchar *et al.*, 1983; Jope *et al.*, 1986). Administration of Li allows reducing the dose of pilocarpine from 300–400 mg/kg to only 30 mg/kg. The models seem to be indistinguishable in all their parameters, apart from increased sensitivity to pilocarpine and increased success rate (Clifford *et al.*, 1987; Goffin *et al.*, 2007). Despite all its advantages, the Li-pilocarpine still caused very high (>90%) mortality among the animals (Jope *et al.*,

1986; Morissett *et al.*, 1987). To reduce mortality, different methods have been suggested, such as repeated injections of low doses of pilocarpine over time and shortening SE by termination with drugs (diazepam, pentobarbital and phenytoin).

Neuropathological alterations occurring under the influence of pilocarpine induction of epilepsy are similar to those observed in KA-induced model and human TLE. Following SE, the changes appear in many areas of the brain, including olfactory cortex, the amygdala, hippocampus, thalamus, and neocortex (Turski *et al.*, 1983a,b). Cell death has been reported in different limbic structures like amygdala, subiculum and entorhinal cortex, particular loss of interneurons was found in the hippocampus (Turski *et al.*, 1983a,b; Du *et al.*, 1995; Mello and Covolan, 1996; Knopp *et al.*, 2005). Neocortex has been reported to undergo significant neuropathological changes like sprouting, reorganisation, abnormal morphology, reactive gliosis, disruption of cortical organisation, and reduction in the cortical thickness (Sanabria *et al.*, 2002; Silva *et al.*, 2002). It is still not clear what role those changes play in the reorganisation and seizure development, since sprouting can occur without extensive cell loss, and epileptogenesis itself has been suggested to occur without neuronal damage (Zhang *et al.*, 2002). This observation can be true, since there is a minority of TLE patients without gross histopathological changes (Margerison and Corsellis, 1966; Lehericy *et al.*, 1997; Liu *et al.*, 2002; Jackson *et al.*, 2004; and other).

Much effort has been put into trying to unravel the mechanism(s) of epileptogenesis. Different theories have been proposed and explored, including reduction in synaptic inhibition, increase of excitation, and changes in receptors and ion channels (for review see Dudek *et al.*, 2006). Researchers have employed a variety of *in vitro* and *in vivo* electrophysiological and histological methods in their attempts to disentangle mechanisms, however, there is a daunting level of complexity. For example, some research groups have been focusing on exploring axonal sprouting and development of new recurrent excitatory circuits during epileptogenesis (Dudek *et al.*, 2002; Dudek and Shao, 2003; Nadler, 2003). Other laboratories have pursued a different path, focusing on the possible selective loss of interneurons, leading to subsequent disinhibition of pyramidal cells (Best *et al.*, 1994; Morin *et al.*, 1998; Buckmaster and Jongen-Relo, 1999). In their review, Bernard and colleagues (2000) reasonably point

out that alterations observed in the brain are area-, pathway-, time- and model-specific, which adds an incredible number of variables that have to be taken into account when researching in this field. On the one hand, it would be extremely helpful to have a unified model of epilepsy. On the other hand, so much variability exists among the human epilepsy itself, that it may justify the existence and usage of different animal models. Finally, identifying the mechanisms/findings that are common across models could potentially be the most fruitful approach.

4.1.2. Epilepsy in human brain slices *in vitro*

A handful of laboratories around the world explore mechanisms underlying epilepsy in a preparation of human brain slices. The tissue is usually obtained from surgical resections of epileptogenic brain foci in patients with pharmacoresistant epilepsies, most commonly mesial TLEs. Significant amount of information on the human brain tissue physiology has been accumulated thanks to the works of Köhling, Schwartzkroin, Avoli, Miles, Cunningham and others. A variety of electrophysiological techniques, including intracellular and field potential recordings (commonly utilising multielectrode arrays), have been used to study ionic concentrations, voltage-gated currents, cellular, synaptic, and network properties of epileptic human brain tissue (Köhling *et al.*, 2006). Apart from electrophysiological techniques, a wide range of histochemical and immunohistochemical, optical imaging and pharmacological methods have been implemented as well. Despite best efforts, human brain slices do not exhibit spontaneous epileptiform activity, however, electrical and pharmacological stimulation, as well as changes of ionic concentration were found to elicit epileptiform activity (Masukawa *et al.*, 1989, Avoli *et al.*, 1991; Hwa *et al.*, 1991, Avoli *et al.*, 1994).

One of the greatest advantages of this specimen compared to the models discussed previously is the true nature of human epilepsy. The findings derived from the epileptic human tissue would never be under the attack of animal model criticism or skepticism regarding the actual relation to human disease. However, together with strengths, certain limitations of this preparation exist. Firstly, it is extremely difficult to obtain non-epileptic human brain tissue to use as a negative control. Researchers have, however, sometimes used tumour resections or healthy tissue taken to gain access to deep epileptic areas. Secondly, resected tissues are always minimised in

size and often do not contain preserved networks, which might be crucial in the context of epilepsy. Possibly due to these reasons, little or no spontaneous ictal activity has ever been observed in epileptic human brain slices. Thirdly, access to this kind of material is usually limited and only a small number of laboratories have the opportunity conduct human tissue research.

4.1.3. Necessity for improvement and refinement

“The sheer mass of data now available on the subject of temporal lobe epilepsy is emblematic of the modern problem of having so much information on any given subject that it is significant conceptual challenge to separate facts from notions, associations from causes, and to discriminate between the possibly important and the probably unimportant. The enormous information now available to us, taken together with the natural desire we have to get clear and unambiguous answers to all of the questions we ask, makes simple answers appealing, and may explain, in part, the general hesitancy we have to admit that we may know far less than we actually do”. (Sloviter 2005)

After decades of researching epilepsy, it appears that we are still in the very beginning of our understanding. Numerous discrepancies and inconsistencies arising from epilepsy animal research prevent it from moving forward. The use of a wide array of different seizure and epilepsy models, which are time- and cost-effective, but which often fail to reflect the natural history of epilepsy only further exacerbates the problem. All models of seizures and epilepsy undoubtedly demonstrate both advantages and disadvantages. For instance, kindling and focal lesioning are known to be less severe, compared to systemic injections of proconvulsants. Systemic injections, on the other hand, allow a “self-selection” of brain regions most vulnerable to seizures. Despite this advantage, some systemic protocols may involve a very intense and/or prolonged seizure activity resulting in a severe neuronal damage all over the brain, which is not found in the majority of epilepsy patients, hence, is not a prerequisite for idiopathic epilepsy. Sloviter (2005) has questioned the validity of epilepsy models that rely upon prolonged SE for the induction of the disease. The amount of research conducted and information accumulated over the past years compared to the overall progress made suggests the necessity of employing a multidisciplinary approach, with active integration of existing models with the only

truly epileptic material i.e. human brain tissue. The adoption of 3Rs (Reduction, Refinement and Replacement of animals) principles into the research ethics framework of many EU and non-EU nations has provided an encouragement to seek more refined animal models that not only reduce animal usage and suffering but also aim to improve the scientific basis for models through, for example, closer homology to the natural history of a disease (Russell and Burch, 1959).

The disadvantages of existing epilepsy models encouraged us to attempt to improve the Li-pilocarpine model to mimic the human condition more closely. The severity of existing models and the extent of neuropathological brain damage were the key factors that required refining, as pointed out by Sloviter (2005, 2008). As mentioned earlier, high animal mortality also remains an important issue, as it undermines both ethical principles, as well as physiological relevance of the model. Therefore, we developed a model of acquired TLE with a better control of induced SE and, thus, minimised brain damage and mortality. We characterised it in behavioural and *in vitro* studies, demonstrating that the refined model is of low severity, yet high morbidity, which makes it a good tool to explore the mechanisms of epileptogenesis.

4.2. Results

4.2.1. Model refinement

The current Li/low-dose pilocarpine epilepsy model is based on a modified version of the model originally described in rats by Glien *et al.* (2001). The original model involved a pre-dose of Li 24 h prior to repeated (30 min intervals) low doses of pilocarpine. The reduced-intensity *status epilepticus* (RISE) model described and utilised here employs a similar protocol but combines this with administration of the sedative and muscle relaxant drug, xylazine, during the acute seizure phase and rapid termination of the acute seizure phase with an anticonvulsant/antiepileptic cocktail.

The original studies used high-dose pilocarpine (300–400 mg/kg) model, which was very common and was associated with the development of a full syndrome, yet with a very high mortality (Turski *et al.*, 1983b, 1989; Cavalheiro *et al.*, 1991; Liu *et al.*,

1994). Honchar and colleagues (1983) discovered that administration of relatively low doses of pilocarpine to Li-treated rats produced sustained limbic seizures. Li was found to have a potentiating effect on pilocarpine-produced seizures, when pre-administered 24 h before pilocarpine (Honchar *et al.*, 1983; Jope *et al.*, 1986; Clifford *et al.*, 1987). Studies have reported that Li-pilocarpine model produces similar behavioural and electrographic seizures, as well as neuropathological changes, as those seen in animals treated only with high doses of pilocarpine, but appears to be more consistent in seizure onset latency and success rate (Jope *et al.*, 1986; Clifford *et al.*, 1987). Hence, the Li-pilocarpine model of chronic epilepsy was used as a foundation for the current model. After pre-dosing with Li (127 mg/kg), we used 30 mg/kg pilocarpine (s/c) to induce SE. A-methylscopolamine was administered (s/c) prior pilocarpine to block peripheral cholinergic effects like piloerection, salivation, tremor and diarrhoea. Once the animals experienced two periods of stage 4–5 Racine scale seizures, behavioural seizure manifestations and clonic muscle contractions were attenuated by administration of a low dose (2.5 mg/kg) of the central muscle relaxant xylazine (Yang *et al.*, 2006; Thompson *et al.*, 2007). Administration of xylazine helped minimise animal suffering and the severity of the model. Glien and colleagues (2001) conducted a study showing that the majority of animals exhibit SRS even after 1h of SE, which is significantly shorter than used by some laboratories (Lemos and Cavalheiro, 1995). Therefore, to reduce neuropathological damage and animal suffering, after 1h of xylazine-modified SE, a STOP cocktail containing diazepam (allosteric modulator at GABA-Ar benzodiazepine site), MPEP (mGluR₅ antagonist), MK-801 (selective and non-competitive NMDAr antagonist) and ethanol was administered s/c to terminate SE, as diazepam and MK-801 are known to produce anticonvulsant effects (Walton and Treiman, 1988, 1991; Ormandy *et al.*, 1989). The rats were recovering during the next 6 h and were back to normal within 24 h. Close monitoring of animals during the recovery period was a critical condition for high survival of animals after lesioning.

4.2.1.1. Low mortality and high morbidity

The current model of chronic epilepsy has been tested on a total of 396 rats, which resulted in 12 losses during initial SE and 39 animals were sacrificed for health and welfare reasons. Once the model protocol was fully established from a total of 196 rats only 2 losses were recorded, showing a very low mortality rate (~1%) across the

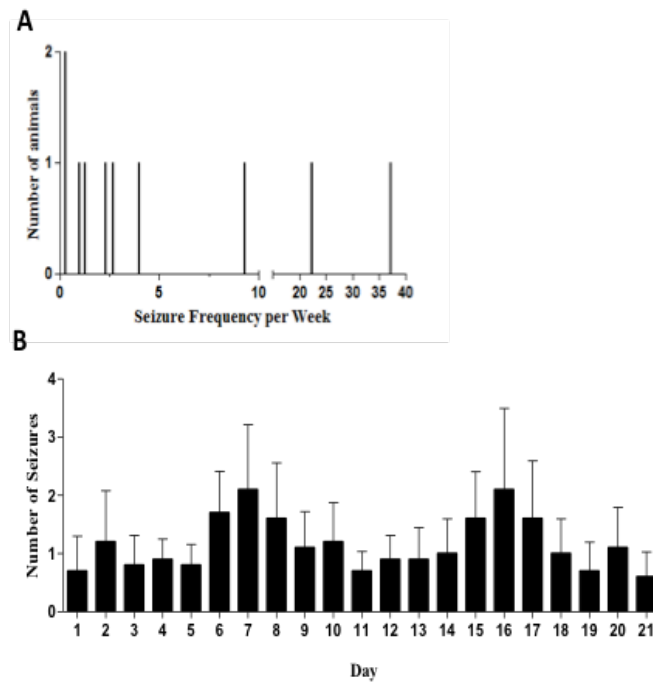


Figure 4.2. SRS frequency is variable and follows a weekly cycle. **A.** Distribution of weekly seizure frequency as observed during video monitoring (n=10). **B.** Mean daily seizure frequency of animals during the recording period, data are expressed as mean \pm S.E.M. (n=10).

two laboratories in which it has been used. Overall, using a combination of Lipilocarpine and decreasing the duration of SE to only 1 h, resulted in a lower mortality rate during and after SE, when compared to previous reports: 40–50% (Gliem *et al.*, 2001; Turski *et al.*, 1989) and 50–80% (Jope *et al.*, 1986). In order to determine the fraction of animals undergoing SRS, our collaborators from Reading University used behavioural assessment (discussed below) and demonstrated that 40–100% of surviving animals in any cohort (mean 69% overall) successfully developed SRS. After it was confirmed by PSBB (see below) and video monitoring that animals exhibited SRS, the group in Reading explored the course of SRS development in behaviourally monitored animals (n=10). The results showed a large variability of seizure occurrence among the animals (range: 1–37; mean: 8.1 ± 3.5 seizures per week), however the frequency of seizures also varied in a characteristic periodic way peaking every 5–7 days (Fig. 4.2). It should be noted that the observed animals were from different batches and exhibited SRS at different times. Hence the rats were video monitored on different schedules, which made it impossible for any external factors to interfere with these results.

4.2.2. Behavioural studies

SRS detection and assessment are associated with time-consuming continuous video monitoring or implantation of electrodes for continuous electrographic monitoring for seizures. Addressing this issue, our colleagues in Reading University designed a series of behavioural tests (PSBB) to confirm the occurrence of SRS in animals exposed to the RISE model of chronic epilepsy. Previous studies revealed that epileptic animals showed signs of hyperexcitability and aggression in comparison to healthy controls (Rice *et al.*, 1998; Polascheck *et al.*, 2010; Huang *et al.*, 2012). The PSBB used by our colleagues was based on the behavioural battery introduced by Moser (1988) and adapted by Rice *et al.* (1998). The PSBB included the touch task (gently nudging the animal with a blunt instrument) and the pickup task (picking up the animal by grasping around the body), responses to which were rated according to the scale in Table 4.1.

Table 4.1 PSBB tasks.

Score	Touch task	Pickup task
1	No reaction	Very easy pickup
2	Rat turns toward instrument	Easy pickup with vocalisation
3	Rat moves away from instrument	Some difficulty in pickup (rat rears and faces the hand)
4	Rat freezes	Rat freezes
5	Rat turns toward the touch	Difficult pickup (rat moves away)
6	Rat turns away from the touch	Very difficult pickup (rat behaves defensively or attacks the hand)
7	Rat jumps (with or without vocalisation)	-

Our collaborators video monitored and PSBB assessed 8 animals during latent and SRS periods. It was confirmed by video monitoring that 6 out of 8 studied animals exhibited SRS. The results of PSBB revealed that epileptic animals consistently showed high PSBB scores in both tasks (touch x pickup: 12.6 ± 1.4 ; pickup time bin: 4.2 ± 0.2 ; $n=6$), in contrast to age-matched controls (AMC) that demonstrated significantly lower scores (touch x pickup: 1.3 ± 0.1 ; pickup time bin: 1.1 ± 0.0 ; $n=12$). Animals that did not develop SRS following the induction exhibited PSBB scores that were between fully epileptic and AMC (touch x pickup: 5.2 ± 0.8 ; pickup time bin: 3.4 ± 0.3). Based on the obtained results, our colleagues developed the criteria that

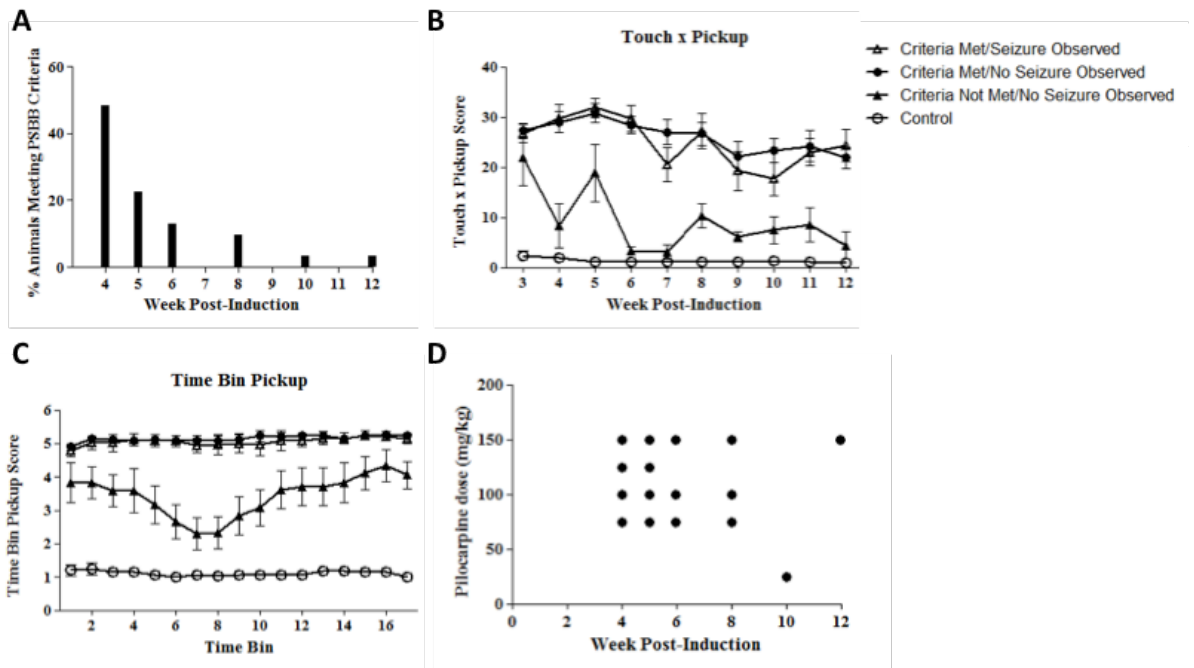


Figure 4.3. Behavioural measurements of epilepsy following induction. **A.** The percentage of animals meeting PSBB criteria at various weeks post-induction (n=31). **B.** Touch x pickup and **C.** time bin pickup PSBB scores of animals having undergone *status epilepticus* induction (n=37) and age-matched controls (criteria met/seizure observed, n=13; criteria met/no seizure observed, n=18; criteria not met/no seizure observed, n=6; control, n=12). **D.** Correlation between pilocarpine dose administered during SE dose and the week animals met PSBB criteria. A Spearman's rank analysis was conducted showing no statistical correlation ($p > 0.05$; n=31).

would help easily identify animals in the SRS stage: touch x pickup score is >10 or time-bin pickup score is ≥ 4 for 4 consecutive trials. According to this scale, 83% of animals with confirmed SRS fulfilled these criteria and none of the non-epileptic animals did so. These findings indicate the possibility of false negative, however not false positive, results.

Using PSBB criteria assessment, the Reading group determined the duration of the seizure-free latent period. The results showed that, following a successful SE induction (n=37), 84% of the animals fulfilled the SRS criteria by 12 weeks post-SE. It was revealed that a large number of animals developed SRS within 4 and 5 weeks post-induction (48% and 23%, respectively) [Fig. 4.3]. When compared to AMC (n=12), all the animals that fulfilled the SRS criteria showed a significantly higher PSBB score ($p < 0.001$). It is worth mentioning that even though no significant difference was observed between non-epileptic rats (not meeting the SRS criteria) and AMC ($p > 0.05$), non-epileptic ones showed greater variability in scores. This could indicate individual differences in the speed of SRS development in those

animals (e.g. >12 week). The findings described here validate the use of PSBB independently of visual monitoring for identification of SRS. It was also investigated whether the dose of injected pilocarpine during the induction could influence the duration of the latent period, however, no significant correlation was observed ($p>0.05$).

4.2.3. *In vitro* studies in the hippocampus

Following a period of RISE not exceeding 60 minutes, we sacrificed animals and made recordings at specific time points PSE 24h, PSE 7d, PSE 6wks, PSE 90d. We made horizontal brain slices containing both hippocampus and EC (Jones and Heinemann, 1988), cut such that connections around the extended circuitry remained intact. These two regions are known to be heavily involved in and affected by TLE. Recordings were made in the hippocampal area CA3 at the indicated time-points in order to track the progress of epileptogenesis and to monitor the functional state of neuronal networks in CA3. During the post-insult development of SRS, we noted clear differences between the activities of neuronal networks relevant to TLE.

4.2.3.1. Morphology and staining

High doses of inducing agents and prolonged SE in traditional unrefined models of epileptogenesis are known to induce gross neuropathological damage, which do not necessarily reflect changes occurring in human epilepsy (Sloviter, 2005). We compared horizontal brain slices taken from animals that underwent epilepsy induction (PSE 24h, PSE 7d, PSE 90d) to those from AMC. When viewed with IR-DIC optics, both healthy and lesioned hippocampal slices showed no severe cell loss in hippocampal CA3 region. Slices from animals that, for the reasons of individual hypersensitivity, exhibited severe and difficult to control SE exhibited clear microhemorrhages, which appeared in the piriform, perirhinal, entorhinal cortices and the hippocampus (Fig. 4.4E,F). The hemorrhages were visible to the naked eye and were not removed by transcardial perfusion, indicating that those areas could be ischemic in the live animal. The slices taken from severe cases of SE and studied under the microscope did not present viable tissue either; it appeared inflamed, rough and had no cells. When rats received higher doses of pilocarpine (37.5 mg/kg compared to 25 mg/kg), it has a pronounced effect on the temporal lobe, when

explored PSE 24h. The ventral part of the temporal lobe exhibited significant tissue sclerosis (Fig. 4.4C,D).

Generally, no significant differences were observed in the morphology of CA3 pyramidal cells between PSE 24h and AMC animals (Fig. 4.4A,B). It was a challenge to preserve CA3 area in adult slices from both epileptic and control animals, as the region becomes very sensitive to any external intervention, especially mechanical damage. Our collaborators from Newcastle University performed a histological analysis of the brains of epileptic rats and demonstrated that there was no gross cell loss in the CA3 region in PSE 90d (data not shown). Overall, we showed that our model demonstrated reduced severity due to high survival rate and low neuropathological damage, yet high morbidity due to the good success rate of animals developing SRS.

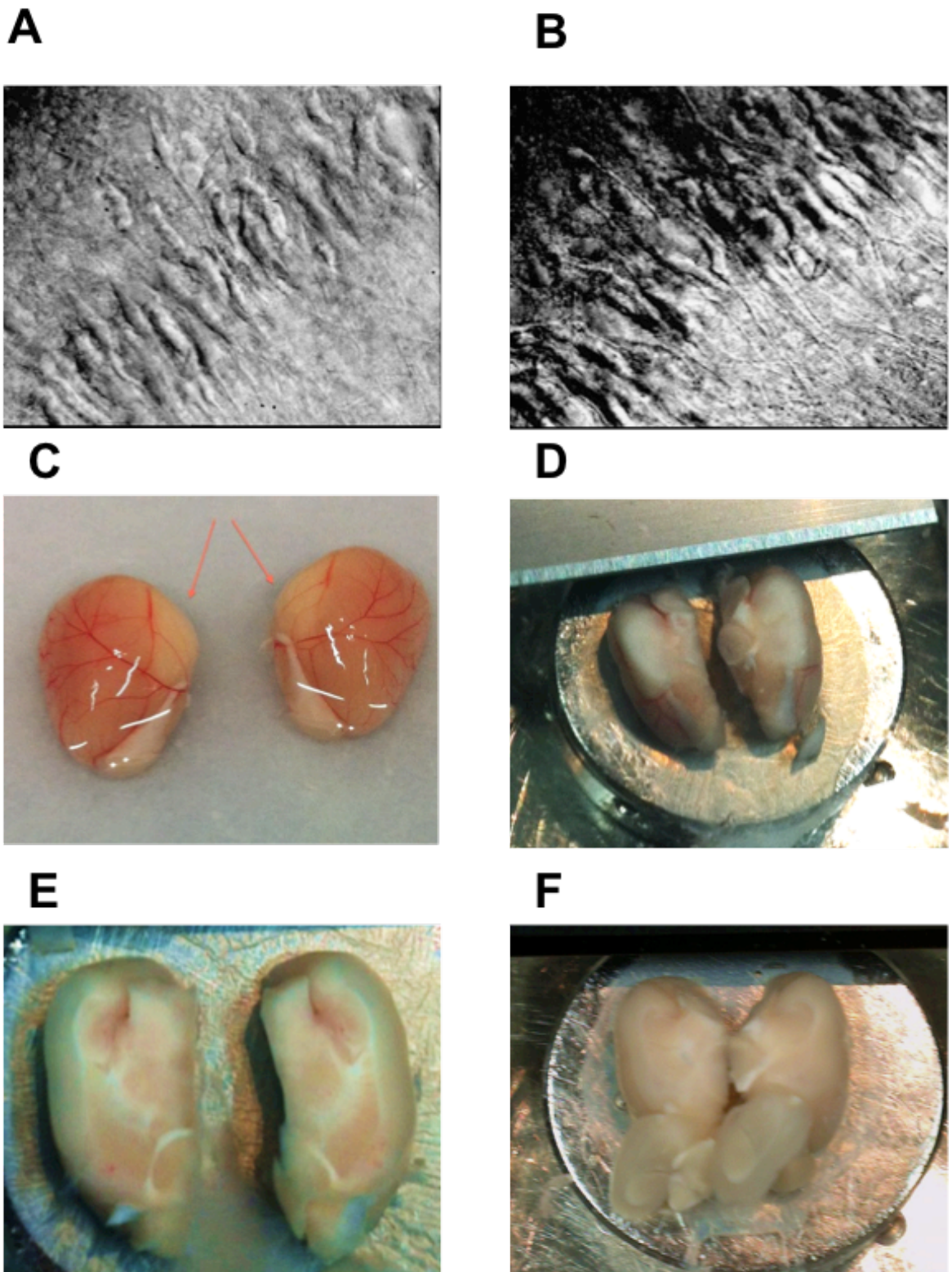


Figure 4.4. Morphology of epileptic brains. A. and B. Images of control and PSE 24h hippocampal CA3 region. C. and D. PSE 24h brain of an animal that had undergone severe SE (signs of sclerosis). E. and F. Sections of PSE 24h brain after a severe SE (visible microhemorrhages) and a healthy brain, respectively.

4.2.3.2. SyO in healthy and epileptic rats

4.2.3.2.1. 24h post-SE

Earlier in this report I described SyO occurring in the hippocampal CA3 region in the absence of any pharmacological stimulation (see Chapter 3). We investigated whether SyO was altered in the slices of animals that had undergone epilepsy induction or whether spontaneous activity was present. We tested the functional capability of hippocampal network at PSE 24h in rats that were recovering from the initial insult and exhibited breakthrough seizures. In healthy AMC brain slices SyO were routinely recorded from CA3 region and had mean peak frequency 28.0 ± 0.9 Hz and mean peak power $46.1 \pm 10.46 \mu\text{V}^2$ (n=17). When recordings were made from PSE 24h slices, SyO were also routinely observed and has mean frequency 30.5 ± 1.1 Hz and mean peak power $36.6 \pm 10 \mu\text{V}^2$ (n=18). Typical SyO data from PSE 24h and AMC are shown in Fig. 4.5A,B. The time-frequency characteristics were assessed by constructing Morlet-wavelet spectrograms and comparing them for PSE 24h and AMC (Fig. 4.5C,D). The results showed a similar profile of gamma oscillatory activity in both conditions, however, in PSE 24h a richer mix of low and high frequency rhythmic activity was observed in CA3 region. When pooled data from 17 AMC and 18 PSE 24h recordings were compared (Fig. 4.5G,H), no significant differences were found in mean peak power or mean peak frequency values ($p > 0.05$, Mann-Whitney test). In order to determine the stability of periodic spontaneous network activity over time, we computed the autocorrelation function for short (1.6 s) epochs of gamma activity in CA3. Under control conditions, the mean peak autocorrelation function was 0.23 ± 0.04 , and this was significantly higher than that determined at PSE 24h (0.15 ± 0.04 ; $p < 0.05$, unpaired t-test, n=20).

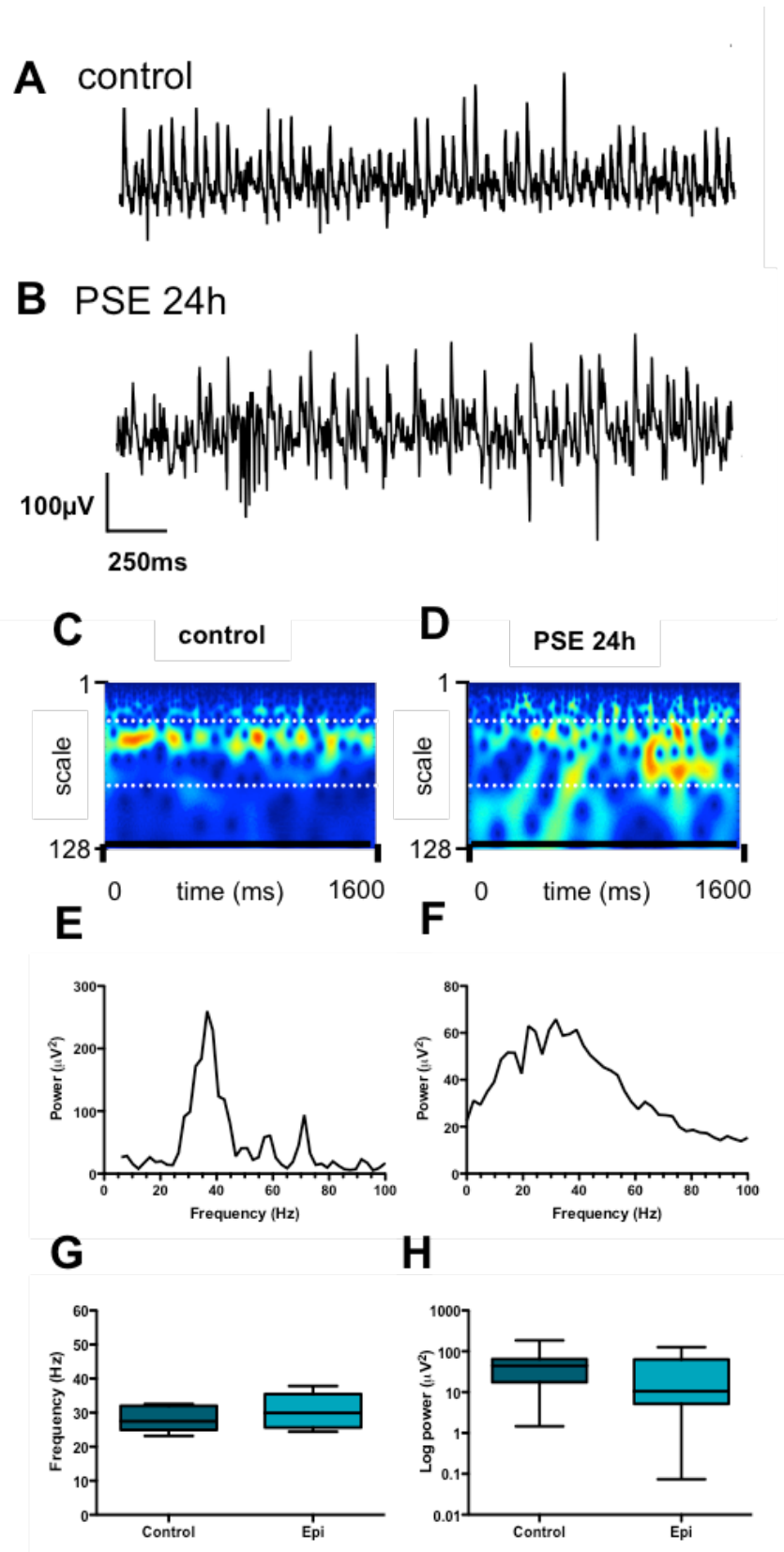


Figure 4.5. At PSE 24h LFP recordings show SyO and fast bursts in CA3. **A.** and **B.** Examples of unfiltered raw traces from AMC and PSE 24h, respectively. **C.** and **D.** Example Morlet wavelet spectra and power spectral density plots of the same traces, white dotted lines on spectra indicate 20-60 Hz pseudofrequency band. **E.** and **F.** Representative power spectra for AMC and PSE 24h, respectively. **G.** and **H.** Pooled peak frequency (**G**) and peak power (**H**) for AMC and PSE 24.

4.2.3.2.2. 7d post-SE

Together with early post-induction period studies, we performed similar investigations at PSE 7d slices, which corresponded to the early seizure-free latent period. At this stage, SyO could be recorded in slices from both PSE 7d and AMC animals. The power of SyO was similar between groups (mean peak power $44.61 \pm 10.12 \mu\text{V}^2$ [n=12] in AMC vs. $44.39 \pm 7.94 \mu\text{V}^2$ [n=10] in PSE 7d, $p > 0.05$), as was the mean peak frequency ($30.40 \pm 1.19 \text{ Hz}$ [n=12] in control vs. $29.81 \pm 0.80 \mu\text{V}^2$ [n=10] in PSE 7d, $p > 0.05$), which is illustrated in Fig. 4.6. Despite the similarities in the static power-frequency parameters, more dynamic data representations involving the time component (raw traces and Morlet-wavelet spectrograms) still demonstrated a tendency towards less stable network oscillatory activity (Fig. 4.6C,D), although comparison of the mean peak autocorrelation function did not quite reach significance (AMC 0.19 ± 0.02 [n=12] vs. PSE 7d 0.13 ± 0.02 [n=10]; $p > 0.05$). Analysis of SyO in PSE 7d slices showed partial recovery of the hippocampal network from the altered state seen at PSE 24h. These results again indicated that CA3 remained functional at this point of epileptogenesis.

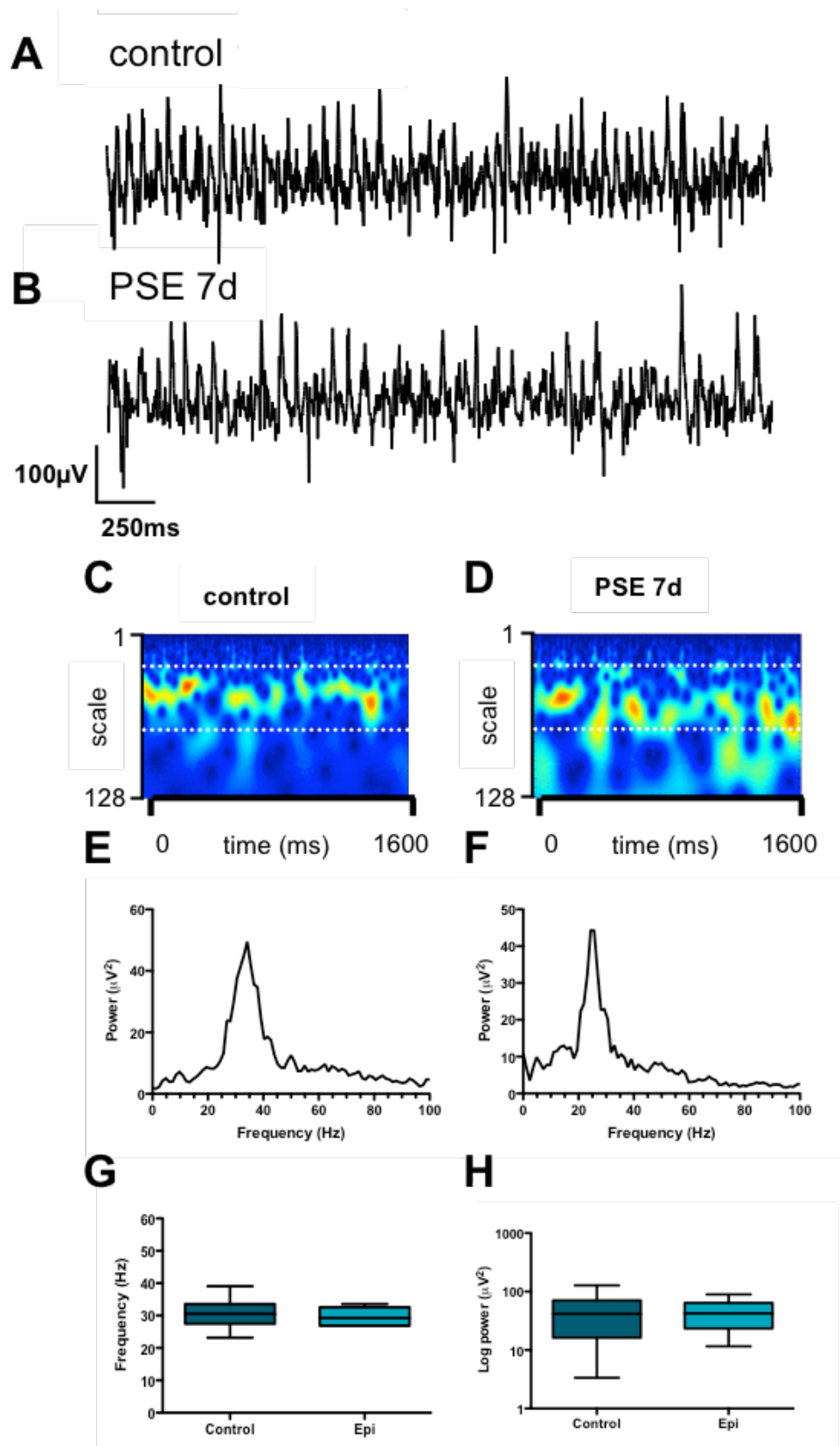


Figure 4.6. SyO in CA3 at PSE 7d. **A. and B.** Examples of unfiltered raw traces from AMC and PSE 7d, respectively. **C. and D.** Example Morlet wavelet spectra and power spectral density plots of the same traces, white dotted lines on spectra indicate 20–60 Hz pseudofrequency band. **E. and F.** Representative power spectra for AMC and PSE 7d, respectively. **G. and H.** Pooled peak frequency (**G**) and peak power (**H**) for AMC and PSE 7d.

4.2.3.2.3. 6-8 wks post-SE

As mentioned before, the length of the latent period varies significantly between animals, and this was also observed between laboratories using the same protocol. Thus, rats in Reading were mostly epileptic by 4-5 weeks, whereas it took around 6-8 weeks for the rats to develop SRS in Birmingham. In both cases, however, the majority of rats exhibited SRS at PSE 90d, as assessed by PSBB and/or behavioural monitoring. Following the plan of comparing epileptic animals at various points of epileptogenesis to AMC, we examined CA3 activity *in vitro* during the 6-8 weeks post-induction (PSE 6wks), which corresponded to the latent period. Our results showed that SyO could be routinely observed in hippocampal CA3 in both PSE 6wks and AMC animals, demonstrating that oscillatory activity remained intact at this stage of epileptogenesis. Fig. 4.7A,B shows typical recordings from PSE 6 wks and AMC slices. SyO recorded under these conditions had a mean peak power of $25.2 \pm 9.9 \mu\text{V}^2$ (n=14) in control slices, as compared to $12.5 \pm 6.2 \mu\text{V}^2$ (n=13) in PSE 6wks slices. Statistical analysis revealed significant differences in the mean peak power of SyO between the two conditions ($p < 0.05$), demonstrated in Fig. 4.7G,H. The mean peak frequency values were very similar in both conditions ($34.7 \pm 0.9 \text{ Hz}$ [n=14] in control vs. $34.7 \pm 1.8 \text{ Hz}$ [n=13] in PSE 6wks, $p > 0.05$). Interestingly, when the peak autocorrelation function was analysed, the mean value for SyO autocorrelation at PSE 6wks appeared to be significantly higher than control values, despite its low oscillatory power (0.19 ± 0.02 [n=14] vs. 0.10 ± 0.02 [n=13], respectively; $p < 0.01$). No spontaneous epileptiform activity was found in recordings during this period, indicating that CA3 remained functionally intact and further suggesting that the model did not grossly damage circuits in this region.

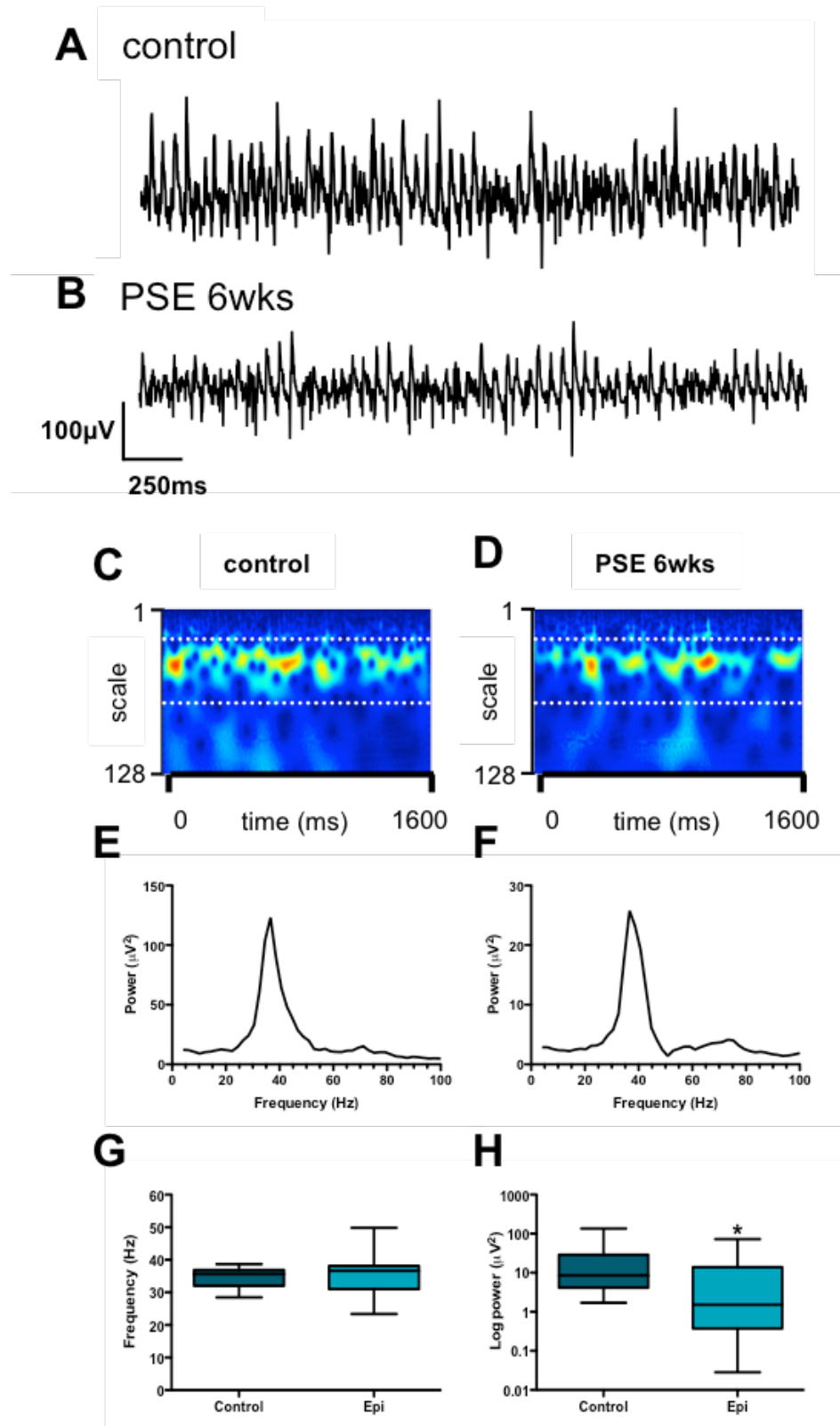


Figure 4.7. SyO in CA3 during PSE 6wks. **A.** and **B.** Examples of unfiltered raw traces from AMC and PSE 6wks, respectively. **C.** and **D.** Example Morlet wavelet spectra and power spectral density plots of the same traces, white dotted lines on spectra indicate 20-60 Hz pseudofrequency band. **E.** and **F.** Representative power spectra for AMC and PSE 6wks, respectively. **G.** and **H.** Pooled peak frequency (**G**) and peak power (**H**) for AMC and PSE 6wks.

4.2.3.2.4. 90+d post-SE

We further investigated the properties of hippocampal networks in epileptic rats by comparing recorded SyO from hippocampal CA3 of PSE 90d and AMC. At this point, the rats exhibited SRS and were considered fully epileptic. In rats now weighing 400-500g, CA3 was again spontaneously active generating similar SyO (mean peak power $65.7 \pm 11 \mu\text{V}^2$ at $36.7 \pm 0.9 \text{ Hz}$, $n=18$) to those observed in controls (mean peak power $84.3 \pm 23.8 \mu\text{V}^2$ at $36.3 \pm 0.9 \text{ Hz}$, $n=14$). The differences in frequency and power between PSE 90d and AMC were statistically non-significant. The results suggested that in epileptic rats CA3 again remained functionally intact. Fig. 4.8 shows typical spontaneous gamma activity in CA3 recorded in PSE 90d and AMC slices. The time-frequency analysis also revealed strong similarity between activity recorded in control and epileptic animals (Fig. 4.8C,D). Neither of the recordings from epileptic rats demonstrated spontaneous ictal activity. Many slices, however, showed SyO with superimposed high frequency activity (Fig. 4.8B).

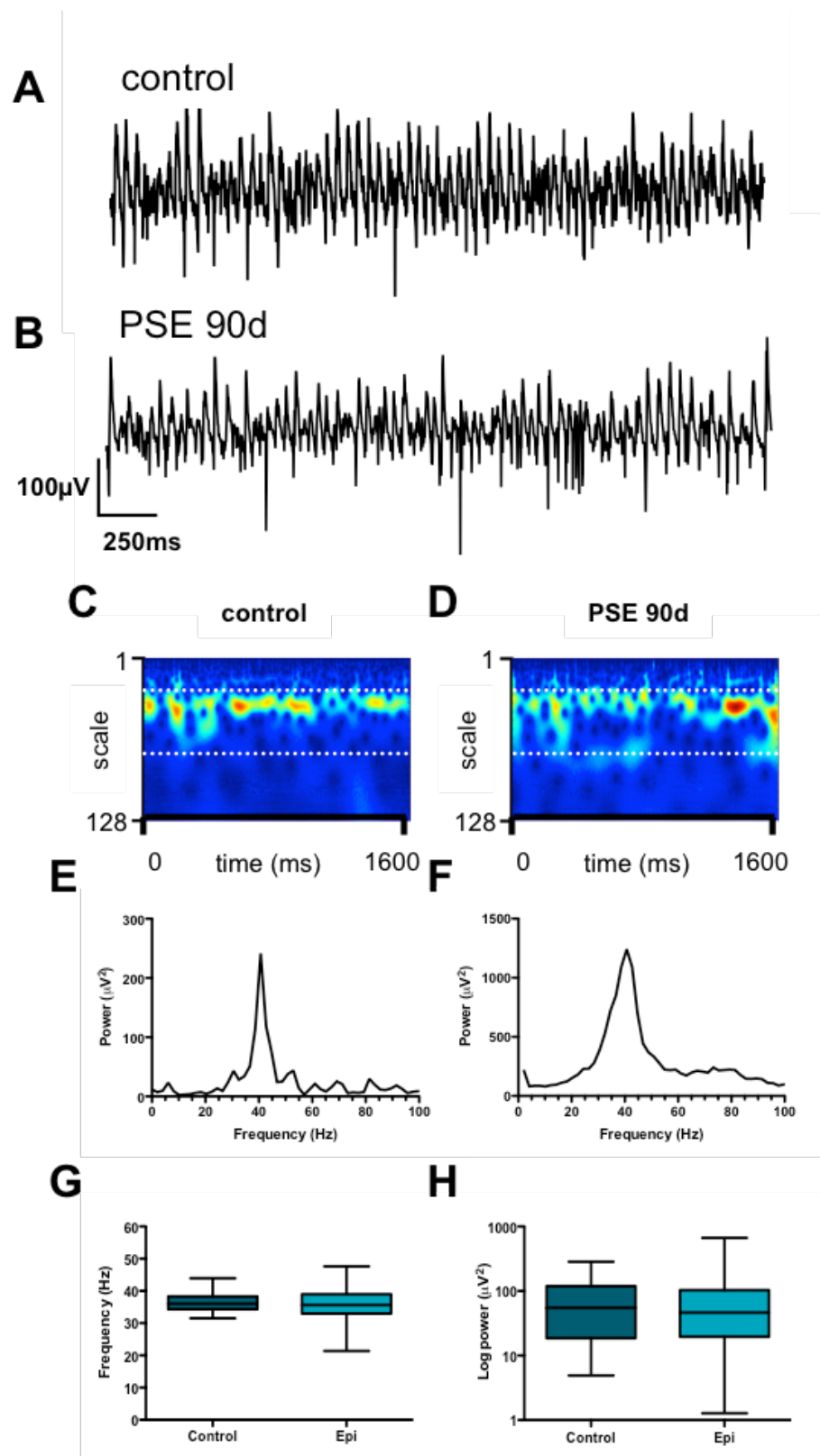


Figure 4.8. SyO in CA3 during PSE 90d. **A. and B.** Examples of unfiltered raw traces from AMC and PSE 90d, respectively. **C. and D.** Example Morlet wavelet spectra and power spectral density plots of the same traces, white dotted lines on spectra indicate 20-60 Hz pseudofrequency band. **E. and F.** Representative power spectra for AMC and PSE 90d, respectively. **G. and H.** Show pooled peak frequency (**G**) and peak power (**H**) for AMC and PSE 90d.

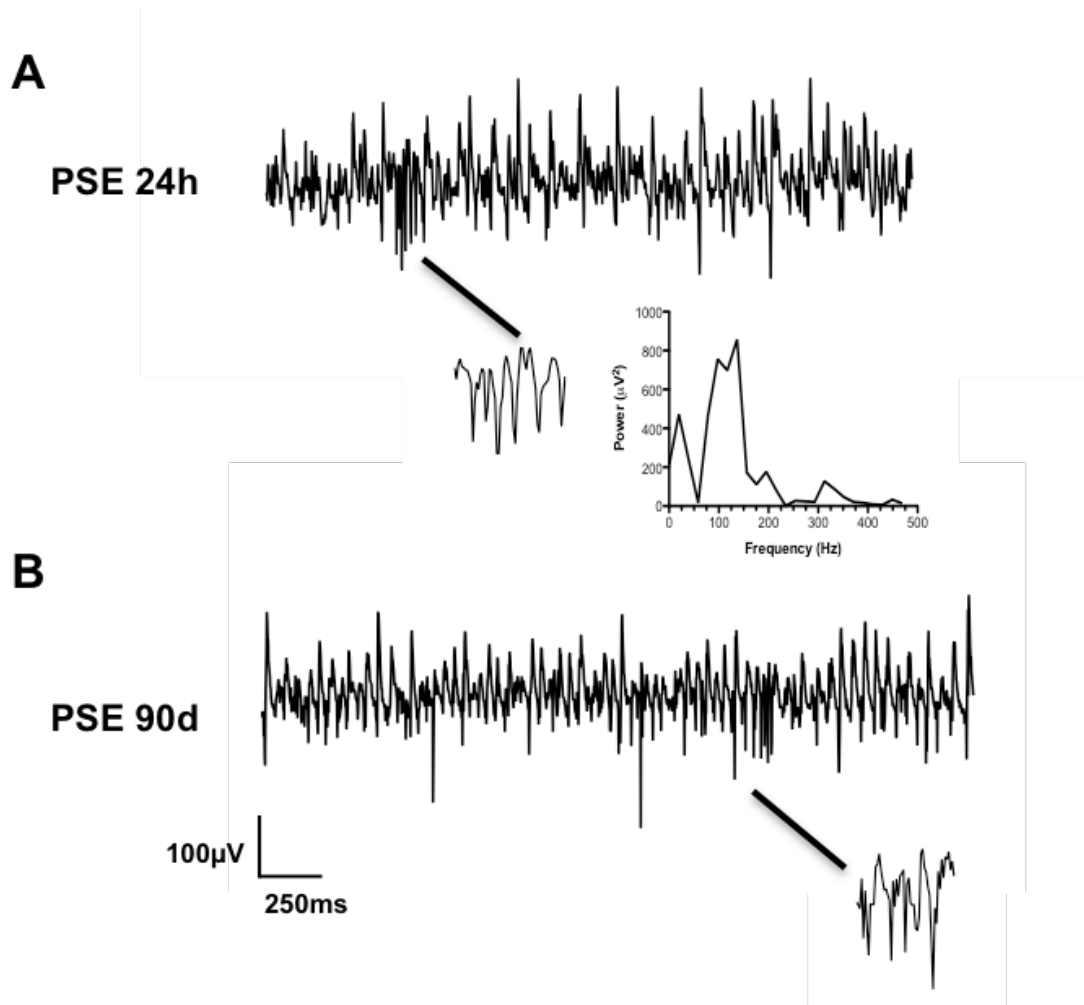


Figure 4.9. VFO as a biomarker of increased excitability in PSE 24h and PSE 90d.

A. Unfiltered raw trace from PSE 24h with an episode of VFO of 120 Hz and the power spectrum of VFO. **B.** Unfiltered raw trace from PSE 90d with an episode of VFO.

4.2.3.3. VFO as a biomarker of epilepsy

VFOs have been implicated in epilepsy, as they have been found to appear at the onset of seizures and during the interictal period (Fisher *et al.*, 1992; Bragin *et al.*, 1999a,b; Traub *et al.*, 2001b; Grenier *et al.*, 2003). In our experiments, when PSE 24h slices were studied for spontaneous hippocampal activity, together with SyO episodes of transient VFO were recorded. The bursts of fast oscillations (range 136–670 Hz, $n=13$) were notable at intervals ranging from 0.6–8.8 seconds. An example of VFO superimposed on SyO is shown in Fig. 4.9. Occasionally, VFO could be observed on top of gamma frequency oscillations (both spontaneous and pharmacologically-induced gamma) in control animals, however this feature was

more prominent in slices from animals that had undergone epilepsy induction. VFO were also observed along with SyO in slices from epileptic rats (PSE 90d), suggesting a correlation between VFO occurrence and seizure manifestations. Example traces from PSE 90d are presented in Fig. 4.9.

4.2.3.4. Ictal and interictal activity in CA3

During the observation of rhythmic activity in the hippocampus throughout different stages of epileptogenesis, ictal activity has been infrequently recorded from both CA3 and EC, although at different time points post-SE. Hippocampal seizures were observed spontaneously during PSE 24h, while PSE 90d exhibited large interictal events in the presence of 100 nM KA. The early period seizure occurred in one slice during a simultaneous recording of SyO with 4 electrodes (Fig. 4.10). An ictal episode consisted of high amplitude sharp rhythmic activity in the high gamma frequency range superimposed on a slow wave, followed by a transient abolition of synaptic activity followed by afterdischarges, after which the normal, pre-ictal gamma returned. Despite the poor quality of the recording, the lag between the 4 sites was obvious. The results suggest that seizure activity was initiated in one site and then propagated further across the area (4->1).

The duration of the episode was around 70 s, it started with a high-amplitude high frequency (~50 Hz) discharge with a large slow wave followed by a period of quiescence for approximately 30 s, after which large-amplitude afterdischarges appeared (Fig. 4.10). A type of interictal events emerged in the CA3 of PSE 90d slice, however, it occurred in the presence of 100 nM KA (Fig. 4.11). The events consisted of a slow wave with superimposed highly-synchronous discharges (100 Hz). Although the occurrence of epileptiform activity during PSE 24h and PSE 90d was in line with the stages of epileptogenesis, their scarcity did not allow us to make any valid conclusions on this matter.

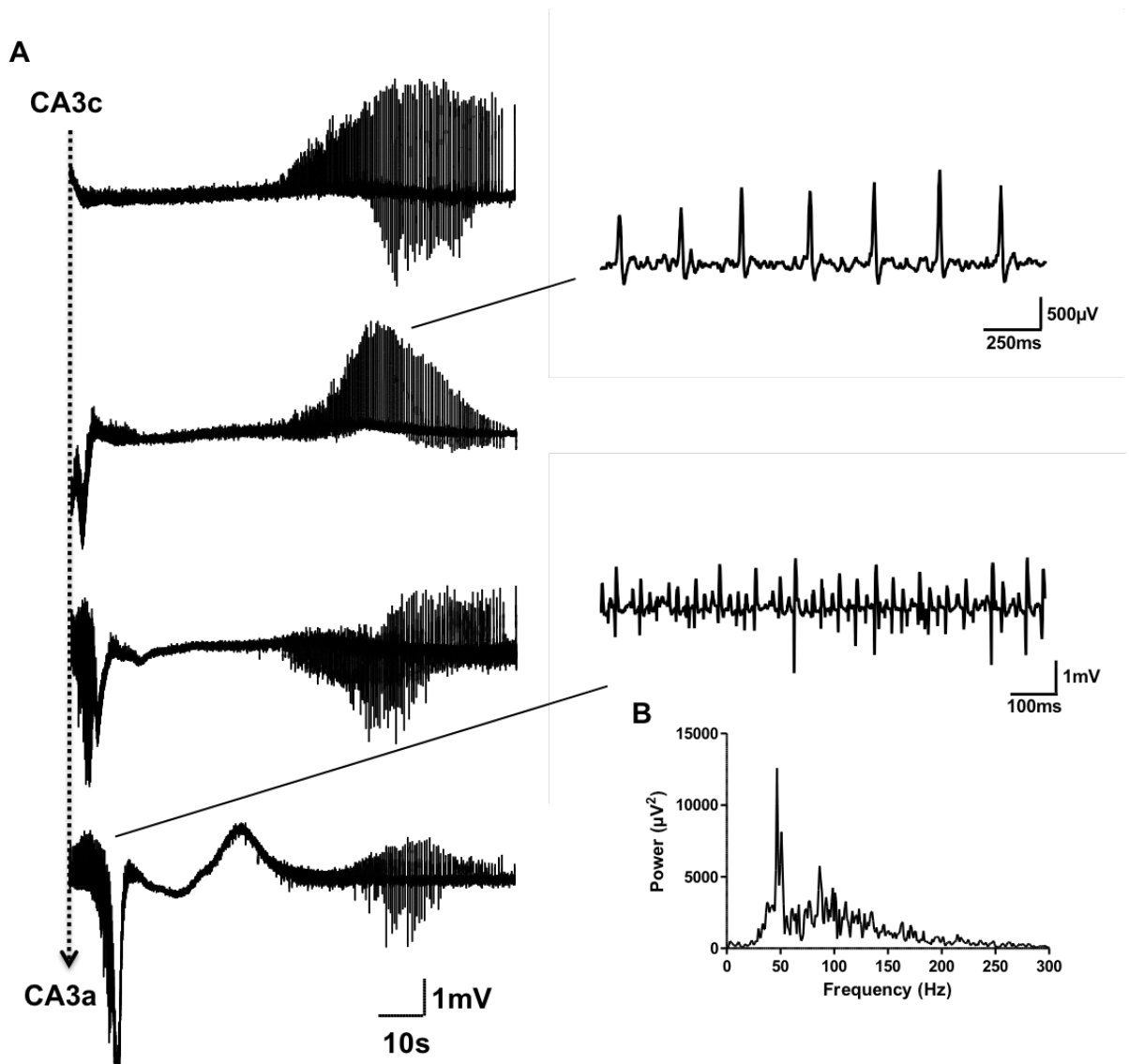


Figure 4.10. Spontaneous ictal activity in the hippocampal CA3 region in PSE 24h.

A. Raw traces from 4 recording electrodes positioned in CA3 (CA3c->CA3a top to bottom trace) of one PSE 24h slice. Clear seizure propagation through CA3 is demonstrated. Enlarged traces show slow high-amplitude afterdischarges at the end of an ictal event and an episode of high-amplitude high-frequency rhythmic discharge at the onset of a seizure (representative power spectrum presented in B).

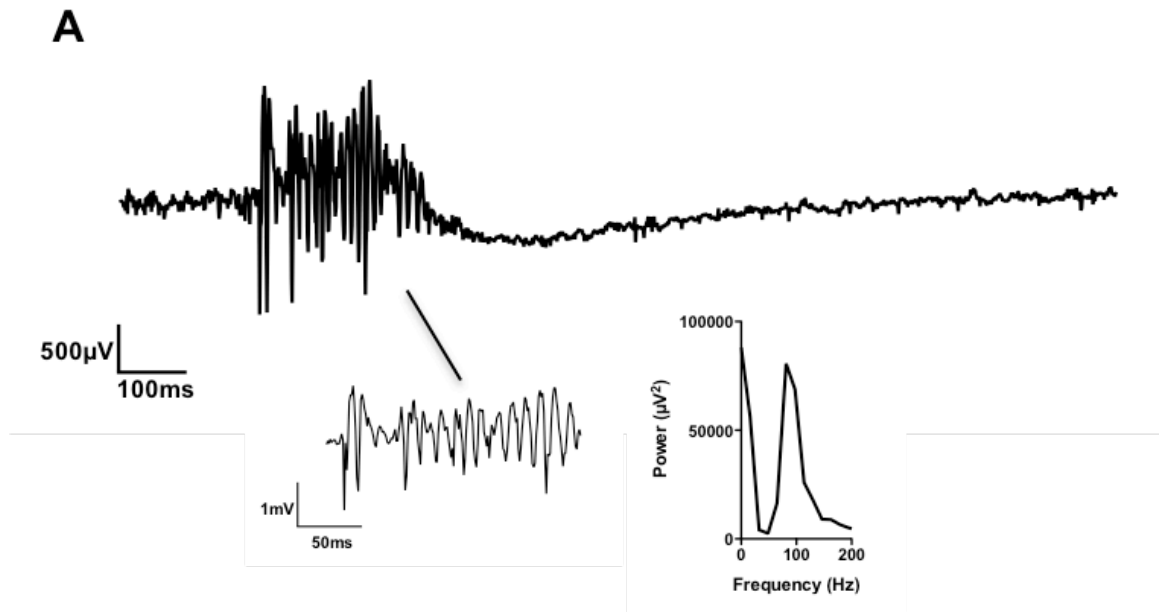


Figure 4.11. Interictal activity in the hippocampal CA3 region in PSE 24h. A. Raw trace from PSE 90d slice in the presence of 100 nM KA and a high-amplitude high-frequency gamma discharge (representative power spectrum presented in B).

4.2.3.5. Spontaneous ictal activity in the mEC in PSE 7d

PSE 7d slices spontaneously exhibited episodes of ictal activity, suggesting the involvement of mEC in the process of epileptogenesis. Seizures consisted of a high gamma frequency (multiple 70–100 Hz) sharp discharge superimposed on a slow wave followed by large amplitude afterdischarges, as illustrated in Fig. 6.16. SWO reappeared 10 mins after the seizure.

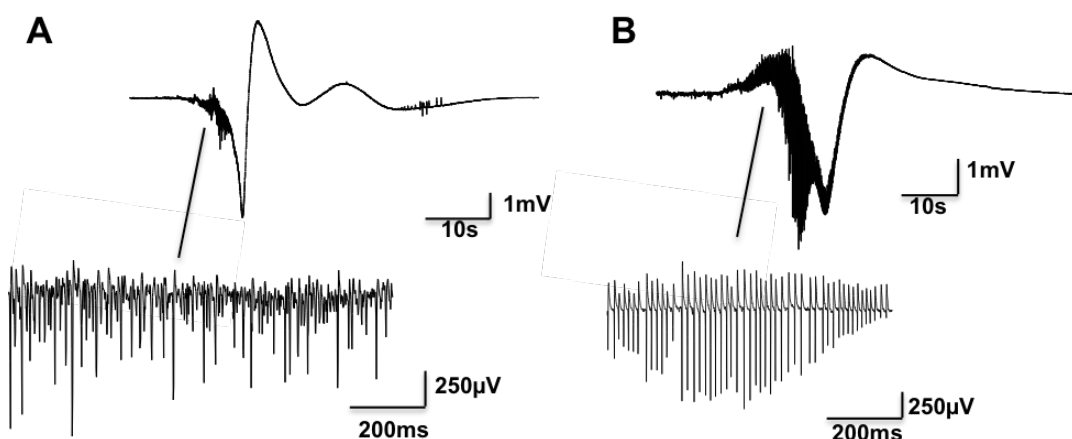


Figure 4.12. Spontaneous ictal events in layers II/III mEC in PSE 7d slices. A. and B. Raw traces showing spontaneous ictal events in PSE 7d slices. Below high-pass filtered (>5 Hz) raw traces showing high-frequency rhythmic activity.

4.3. Discussion

4.3.1. Model refinement

The current model of chronic epilepsy is a modified version of low-dose Li-pilocarpine model described by Glien *et al.* (2001). Model refinement reduced mortality from uncontrollable seizures during the initial insult and minimised the exhausting effects of prolonged seizures, which further reduced mortality during the recovery period. Together with low mortality, the model maintained high morbidity, as the majority of rats undergoing epilepsy induction developed SRS within 3 months.

One of the main refinements employed in RISE was the use of central muscle relaxant xylazine, which has been reported previously by Yang *et al.* (2006), Thompson *et al.* (2007). The effects of xylazine were most likely associated with its action at the central alpha-adrenergic receptors. Joy and colleagues (1983) described the effects of xylazine in seizures as dose-dependent pro- and anticonvulsant (0.3 mg/kg and 3–20 mg/kg, respectively). In addition to any direct effects of xylazine on seizure threshold or ongoing activity in vulnerable neuronal networks, xylazine also exerted sedative and muscle relaxant effects, which seemed to work effectively in reducing the intensity. At the dose used during RISE, xylazine produced sedation, locomotor hypoactivity and ataxia, successfully curtailing behavioural manifestations of SE. In humans, non-convulsive SE has been associated with lower mortality, in comparison to clinically manifested SE (Tatum *et al.*, 2001). Eliminating the convulsive component with xylazine injection may be an important factor in reducing mortality by preventing running/bouncing seizures and decreasing the chance of secondary generalisation involving subcortical structures such as the brainstem (Samoriski and Applegate, 1997).

Another refinement introduced into RISE was administration of the anticonvulsant cocktail in order to terminate SE 1 h after induction. The cocktail contained an mGluR5 antagonist, MPEP, a non-competitive NMDAr antagonist, MK-801 and diazepam, a benzodiazepine. This combination of drugs has previously been used in high-dose pilocarpine studies by Tang and colleagues (2007). The authors demonstrated that MPEP, MK801 and diazepam caused an effective cessation of SE and subsequent neuronal loss in the hippocampus. We used the same combination

of drugs, although a smaller dose of MPEP and a higher dose of diazepam, and observed the same effects in low-dose Li-pilocarpine model. The cocktail successfully terminated RISE, and, furthermore, little damage was observed in the temporal lobe. Together, the reduction of convulsive effects induced by xylazine, and the rapid termination of SE radically reduced mortality associated with epileptogenesis using the pilocarpine model.

4.3.2. Reduced mortality in RISE

High animal mortality of SE epilepsy models is an issue in modern epilepsy research, not only due to the ethical element of the problem, but also the aspect of translational animal research. Mortality rates are often omitted in the scientific literature, and when reported, vary greatly and are usually high (sometimes >90%), even in low dose pilocarpine protocols (see Curia *et al.*, 2008). High mortality in traditional models of acquired epilepsy has to some extent been associated with prolonged period of SE. Sloviter (2005) argued that *continuous* SE resulted in gross neuropathological changes in cortical regions, inflammatory and cerebrovascular lesions, and therefore aggressive models failed to mimic the natural history of epilepsy in humans. In the RISE model mortality was reduced to a minimum (~1%), yet it did not affect the development of epilepsy in lesioned animals (although the progress was relatively slow). Moreover, as mentioned before, administration of xylazine decreased seizure intensity due to reducing highly metabolically demanding continuous convulsive activity during SE. Regarding the animal project licensing and animal welfare, previous models of acquired chronic epilepsy have always been categorized by the Home Office (UK) as being of 'substantial' severity due to the stressful effects of the acute induction and the associated mortality. The RISE model has now been classified as 'moderate' severity. An important point of model improvement is the fact that low mortality rate resulted in fewer animals being used overall, thus the RISE model clearly fulfilled at least two (refinement and reduction) of the 3Rs.

4.3.3. Behavioural studies

Introduction of behavioural assessment methods into the model is a great advancement, as it allows determining the progression of epileptogenesis in a quick and effective manner, avoiding the laborious long-term video or electrophysiological monitoring for seizure onset. Studies carried out by our collaborators in Reading

University showed that PSBB scoring system was sufficient in identifying animals that had developed SRS. With a large variability in the latent period duration, behavioural assessment presents a valuable tool for epilepsy model research and makes the study of SRS in this model more feasible and approachable.

4.3.4. *In vitro* studies of neuronal networks

For *in vitro* investigations, animals were sacrificed for experimental purposes at different time points following SE induction, such that we could study the dynamic changes of neuronal network function throughout the different stages of epileptogenesis. Together with functional studies (LFP), we looked at a general survival of cells in epileptic vs. AMC slices. Our findings indicated that the current RISE model produced more subtle effects, devoid of neuronal damage, in the temporal lobe regions throughout the whole process of epileptogenesis, implying that cell loss and damage were not prerequisite for epilepsy development. The results of haematoxylin and eosin staining showed that even at later stages of epilepsy development the hippocampus was still a viable healthy-looking structure, which again demonstrated that hippocampal lesion was not necessarily a characteristic feature of epilepsy. These findings were in line with the study conducted in humans, where postmortem histological analysis showed normal looking hippocampus in **48%** of patients with epilepsy (Margerison and Corsellis, 1966). Other reports also revealed that the majority of newly diagnosed epilepsy patients only had minimal brain abnormalities and did not show signs of hippocampal sclerosis (Lehericy *et al.*, 1997; Liu *et al.*, 2002 Jackson *et al.*, 2004 and other). It seems plausible that the RISE model in animals is better in reflecting the natural course of human epilepsy. As we have observed, slight increase in pilocarpine dose or individual cases with severe SE stage caused a remarkable damage to the brain. The severe tissue sclerosis and vascular pathologies that we observed showed that the unrefined models were too intense/severe to mimic human condition, supporting the views previously expressed by Sloviter (2005, 2008).

4.3.4.1. Early post-insult alterations in network function

Together with morphological/histological examination, we also measured the functional state of the neuronal networks using LFP recording and found that the vulnerable CA3 region of hippocampus remained spontaneously active *in vitro*

throughout the development of chronic epilepsy, suggesting strongly that our model did not result in wholesale excitotoxic damage to this region. During the early post-insult stage, although the basic characteristics of SyO were similar in both groups, the activity appeared altered compared to AMC, with periodic bursts of VFOs and less stable gamma activity. Despite that, the inhibition required to generate coherent, SyO activity remained generally intact. VFOs, on the other hand, are known to be involved in abnormal epileptogenic mechanisms, as they have been observed during the interictal EEG spikes and are thought to be associated with regions spontaneously generating seizures (Bragin *et al.*, 1999b; Jacobs *et al.*, 2008). Although VFO also appear in healthy controls and relate to normal function of the brain, it is believed that high frequency activity is strongly enhanced in epileptic brains (Buzsaki *et al.*, 1992; Ylien *et al.*, 1995; Draguhn *et al.*, 1998; Bragin *et al.*, 1999b; Engel *et al.*, 2009). In our experiments VFO were sometimes observed together with gamma oscillations in control rats (both spontaneously and in the presence of KA), however, it was more prominent in lesioned rats during early post-insult stages. The findings could indicate that the hippocampal network was still under the effects of SE or breakthrough seizures, suggesting a link between VFO and epileptic/ictal activity.

Throughout the process of epileptogenesis it was extremely difficult to induce any epileptiform activity *in vitro*, let alone to observe it spontaneously. One of the few occasions the ictal activity was detected, was in a PSE 24h slice when 4 electrodes simultaneously recorded a seizure in CA3 region. Different electrographic seizure patterns have been reported in literature, from LFP population spike with associated slow wave to low voltage high-frequency activity (Bragin *et al.*, 2005; Kobayashi *et al.*, 2005; Bragin *et al.*, 2007). Together with a general examination of an ictal episode, these data allowed us a glimpse of seizure propagation phenomenon within the CA3. It appeared that hippocampal cells did not discharge synchronously across the whole area, but a clear order of firing was present instead. Seizure activity propagated from CA3b to CA3a region and was possibly driven by EC/DG inputs or originated independently in the CA3 region (Ben-Ari, 1981; Rafiq *et al.*, 1993; Barbarosie and Avoli, 1997, Bragin *et al.*, 1997, 1999a; Dzhala and Staley, 2003). Although the propagation was clear, we can only hypothesize where the epileptogenic focus was and how the activity spread outside the area covered by our 4 electrodes. It is possible that ictal activity originated in CA3c region and propagated

to CA3a, as demonstrated by several seizure models (Colom and Saggau, 1994; Dzhala and Staley, 2003). Shi and colleagues (2014) showed the following propagation sequence using a multi-electrode array (MEA): EC->DG->CA3c-a->CA1. Another study suggested that sharp-wave seizure type emerged in CA3a-b regions and spread to CA3c before propagating to CA1 (Csicsvari *et al.*, 2000). Only more experiments would shed light on spatiotemporal properties of ictal activity; however, it is extremely challenging to record spontaneous seizures in an SE model *in vitro* in the absence of necessary equipment such as MEA. Possibly, like the VFO observed in PSE 24h slices, the occurrence of a seizure during the same period could characterize enhanced hyperexcitability of the hippocampal network and its susceptibility to seizures, as residual effects of the SE experienced by the animal. The variability in sensitivity towards seizures among animals could also explain why ictal activity was observed only in the minority of slices. Contributing to this might be a different way of brain slice preparation, which preserves more cells, in particular the PV-positive interneurons, which might reflect the situation in an intact brain. As mentioned above, it is difficult to detect spontaneous epileptiform activity even in the truly epileptic material, such as human tissue (Gabriel *et al.*, 2004; Huberfeld *et al.*, 2011). Reduced network connectivity in a brain slice and an increased endogenous anticonvulsant effects have been proposed (Heinemann and Staley, 2014).

4.3.4.2. Neuronal network function during the latent period

Whilst abnormal neuronal activity can be demonstrated in CA3 as early as 24 hours after the initial insult, this activity appears to resolve during the latent period, with the area showing relatively normal spontaneous activity. Indeed, SyO recorded from PSE 7d slices has very similar power-frequency characteristics compared to control slices, which shows that the network remains intact and fully functional. One week after SE would correspond to the early latent period, when seizures subside, animals are fully recovered from initial insult and their behaviour appears normal, which is reflected by electrophysiological recordings. As the hippocampus returns to its normal state, some undefined changes seem to take place in the EC during this period. Two ictal events have been recorded in PSE 7d layers II/III of the mEC in the absence of any pharmacological agents, suggesting imbalance between inhibition and excitation allowing for a simultaneous discharge of cortical neurons.

Further investigation of hippocampal neuronal network function during later stages of latent period revealed robust SyO, suggesting the presence of sufficient inhibitory and excitatory components to generate spontaneous activity. Of particular interest is a significantly lower power of SyO in PSE 6 wks, yet a higher stability of gamma oscillation cycle length compared to control slices. A plausible mechanism could be a large CA3 network breaking up into small internally synchronised local networks of neurons, which could explain a decrease in power and a high degree of oscillation stability. Rhythmic hippocampal activity appears normal in the latent period; however, this possible fragmentation into smaller networks could play a role in reorganisational changes that take place during this period. In the absence of robust global connectivity, it is possible that initiated seizures remain focal. Or the fragmentation of the network could prevent seizure initiation, as, according to Kramer and colleagues (2010), the network shows highest synchronisation at the onset and before the termination of a seizure. Therefore, network compartmentalisation could disrupt seizure initiation or propagation mechanisms, preventing it from generalisation. Determining role of latent period changes in epilepsy development and how they link to the absence of seizure activity in this period is yet to be elucidated. Some of the further work would include exploring the spatial distribution and phase coupling of SyO during the latent period, as a way of evaluating network integrity.

4.3.4.3. Neuronal network function during SRS period

Following the development of SRS three months after initial insult, we compared spontaneous hippocampal activity to AMC. Strong SyO were again present in both groups, demonstrating that even during this period the network remains functional. The rhythmic activity regained its power, in comparison to the late latent period. Interestingly, concurrent bursts of high frequency activity and gamma rhythm were again observed in CA3, resembling the ones observed in PSE 24h slices. These findings indicate some similarities between the two periods. Furthermore, ictal-like events were observed in CA3 in the presence of KA, suggesting higher seizure susceptibility of the tissue. It is debatable whether the observed activity can be considered ictal or interictal preceding a seizure, as it consist of a ripple with a slow wave and has an element of post-ictal synaptic depression. Previous literature described an abruptly occurring population burst as a typical feature of interictal epileptiform discharges (Dzhala and Staley, 2003; Dzhala and Staley, 2004). Another

study reported this type of activity as a seizure-like event (Gong *et al.*, 2010). Recently, the mechanistic differences in the generation of interictal spikes and sharp-wave ripples have been explored (Karlocai *et al.*, 2014; Gulyas and Freund, 2014). In the context of current project, whether the events were ictal or interictal, was not of great importance, since they reflected alterations in the network operation and excitability regardless of their nature. The change of oscillatory power and the occurrence of VFO, as well as ictal-interictal activity, indicate increase in network excitability and possibly connectivity that was undermined during the latent period. These changes coincide with the appearance of behavioural SRS in animals, whether these are linked will have to be determined in the future. Overall, these data strongly suggest that processes underlying epileptogenesis can be readily explored within the model, and hint that a stepwise process involving multiple neuronal regions in the temporal lobe (and beyond) may be involved in the development of SRS.

4.3.4.4. Ictal activity in the mEC

Investigation of neuronal network activity in the mEC has revealed two episodes of spontaneous ictal activity in PSE 7d slices, demonstrating that EC is implicated in the development of chronic TLE, which has been shown in literature (Du *et al.*, 1993; Spencer and Spencer, 1994; Du *et al.*, 1995; Schwarcz *et al.*, 2000). The occurrence of spontaneous seizures coinciding with the possible upregulation of AMPAR in the mEC could indicate that the two are related (see Chapter 6). Of a particular interest is the relationship between the EC and the hippocampus in epilepsy and during epileptogenesis, as these regions are highly interconnected. Spencer and Spencer (1994) showed that the EC and hippocampus interact to produce and propagate seizures. Several paths can be explored in this regard. What is the link between AMPAR and KAr function alterations? Why receptor changes occur at different points of epileptogenesis? Do brain regions undergo epileptogenesis independently or differently?

4.4. Conclusion

Together, the use of the low-dose lithium protocol, minimisation of time spent in SE, administration of xylazine and the use of the multi-drug cocktail provide a highly reliable and repeatable method for induction of epilepsy which reduces mortality

whilst maintaining a high degree of epileptogenicity. A criticism often leveled at animal models of chronic epilepsy by clinical colleagues is that patients almost never present with epilepsy that has resulted following an episode of SE, and, as such, models employing SE during induction are fundamentally unable to mimic human epilepsy (and see Sloviter, 2005). The current model, whilst retaining an element of short-duration, modified SE, goes some way to mitigating this criticism, and shows that prolonged SE is not necessary for the reliable induction of a condition with significant similarities to human epilepsy. In this context, a recent report (Navarro Mora *et al.*, 2009) of slow development of SRS in animals treated with pilocarpine but who did not enter SE suggest it may not be the critical factor in pilocarpine epileptogenesis, and indicates that further development of the current model may be possible. In this regard, refinement of the protocol for administration of lithium, which is an irritant, is both desirable and necessary.

Chapter 5 KAr studies in RISE

5.1. Introduction

Uncovering the mechanisms underlying ictogenesis and epileptogenesis has been one of the main directions pursued by neuroscientists with an interest in epilepsy. It is now clear that epilepsy has a complex, multicomponent mechanism(s). A long-standing opinion among the neuroscience community is the imbalance between inhibition and excitation that underlies this disorder. Researchers have been trying for decades to identify whether it is the excess of excitation or the lack of inhibition or both that is causing seizures to appear. Given the complexity of the problem and the diversity of obtained results so far, it is probably safe to say that changes in both excitation and inhibition may be sufficient, but not necessary to cause epilepsy, and other mechanisms including inflammation and glia-induced hyperexcitability may play important roles (Devisnky *et al.*, 2013). At a more sophisticated level, the 'dormant basket cell' hypothesis was proposed by Sloviter (1983, 1987, 1991), suggesting that hippocampal hyperexcitability emerged due to a selective loss of neurons specifically activating inhibitory basket cells. However, this later proved to be inadequate to explain TLE, with other investigators recording active basket cells in epilepsy and questioning the interpretation of the original papers (Bernard *et al.*, 1998). Indeed, abnormalities in ionic concentrations, receptors, transmitter release/uptake and other factors have all been reported and identified as potentially causal. However, the results so far have been inconsistent, since, for virtually every finding there is a study reporting opposing results. Finally, at the network level, two popular theories have been explored: selective loss of interneurons and axonal sprouting creating recurrent excitatory connections. These mechanisms are not mutually exclusive and can co-exist in an epileptic brain, and some evidence in their support has been evinced (for review see Ben-Ari and Dudek, 2010).

Our previous findings suggested that changes in network excitability occurred throughout the process of epilepsy establishment in RISE model of epilepsy. We intended to investigate what could underlie network excitability decline during the latent period and its return during the SRS stage. We hypothesized that KAr, being one of the major mediators of excitatory glutamatergic transmission and oscillogenesis, could play a key role in the appearance of epileptic activity. Although

KAr studies in epilepsy appear to be rather controversial, a number of reports exist demonstrating abnormal expression of these receptors and, hence, their involvement in epilepsy mechanism. For instance, Graebenitz *et al.* (2011) and Palomero-Gallagher *et al.* (2012) demonstrated an increase in KAr in human epileptic brain tissue, compared to healthy brains. KAr subunit KO studies in animals revealed that GluK2 subunits were associated with low seizure threshold and high KA sensitivity (Fisahn *et al.*, 2004). An overview of KAr expression in epilepsy is presented below, for functional studies see section 1.2.5.

5.1.1. KAr expression in human epilepsy

One of the advantages of obtaining resected epileptic tissue following surgical intervention in refractory epilepsy, is the possibility to perform a variety of techniques to determine changes occurring in epileptic tissue. A number of studies were dedicated to exploring changes in receptor (including KAr) expression in pathological tissue. The findings are often inconsistent, which could be the result of studying different brain regions, progress of epilepsy, types of epilepsy and diversity among patients (adults vs. children). In 1990, Geddes and colleagues reported a decrease in KAr expression in various sclerotic regions of the hippocampus (CA1, CA3 and hilus) in patients with intractable epilepsies. This decrease coincided with an increase in parahippocampal regions, perhaps representing aberrant excitatory connections in these regions. In line with these findings, Brines *et al.* (1997) reported a uniform decrease in KAr expression throughout the whole hippocampal region. Another study was conducted by Zilles and colleagues (1999) on adult temporal cortex from patients with focal epilepsy. They reported no overall change in KAr binding in epileptic tissue compared to control, however it was noticed that KAr density was higher in deeper cortical layers, compared to superficial layers (Zilles *et al.*, 1999; Palomero-Gallagher *et al.*, 2012). In contrast to previously mentioned studies, Graebenitz *et al.* (2011) demonstrated a change in receptor densities and functions, including a significant increase in KAr binding in lateral amygdala nucleus of epilepsy patients. An extensive study characterising receptor alterations was carried out by Palomero-Gallagher and colleagues (2012). The study is an admirable attempt to correlate receptor alterations with different epilepsy subgroups according to clinical and electrophysiological criteria. The results show significant changes in KA, AMPA, M2 and 5HT_{1A} receptors across all subgroups, suggesting these receptors to be the

key players in epilepsy. Focusing on KAr, a positive correlation was found between KAr upregulation and the frequency of seizures in patients with associated brain tumors.

A number of studies have approached KAr function/expression in epilepsy from a subunit-specific point of view, which further complicated already relatively inconsistent findings. On the other hand, considering differential effects of KAr in the brain, systematising according to subunits may be a step forward in understanding the role of KAr in epilepsy. DeFelipe *et al.* (1994) reported patches of reduced GluK1-3 KAr staining in adult epileptic tissue resected from the temporal cortex. They suggested that these foci could be involved in seizure generation and propagation. Another study using the same technique reported an increase in KAr in superficial layers of temporal cortex, yet a decrease in layer VI, which contradicted the results of previously mentioned reports (Gonzalez-Albo *et al.*, 2001). A study focusing on different KAr subunits was conducted by Grigorenko and colleagues (1997), where significant changes were observed in the hippocampal area of epileptic tissue (GluK2 was increased, while GluK4 was decreased). GluK1 KAr were found neither in control nor in epileptic tissue. Using *in situ* hybridisation, Mathern *et al.* (1998) investigated the levels of GluK1-5 in epileptic tissue with and without hippocampal sclerosis and control postmortem tissue. The results demonstrated a decrease in GluK1-2 in different regions of the hippocampus in both groups of epileptic patients. GluK3-5 were also decreased, but only in sclerotic hippocampus (Mathern *et al.*, 1998). Contrary to this report, no change in hippocampal GluK1 and GluK2 was reported by Kortenbruck and colleagues (2001), however, elevated KAr expression was found in the temporal cortex, which was suggested to be a compensatory phenomenon for prevention of excess Ca^{2+} influx during ictal activity. Another study on resected cortical tissue from paediatric patients with epilepsy suggested a reduction in GluK1 while an increase in GluK2 mRNA (Baybis *et al.*, 2004). In line with Mathern *et al.* (1998), Li and colleagues reported a decrease in GluK1 in the hippocampus of patients with complex partial TLE. However, opposite to Mathern report, an increase of GluK4 and GluK5 was found in the hippocampus of epileptic tissue (Das *et al.*, 2012).

5.1.2. KAr expression in animal models of epilepsy

Undoubtedly, animal model studies dedicated to KAr function yield even more diverse results than human data, especially due to such wide variety of models in use. Several studies using kindling by electrical stimulation reported contradictory results, including both increase and decrease in KAr binding in hippocampal CA3 and the dentate gyrus (Savage *et al.*, 1984; Represa *et al.*, 1989). In the model of chemical kindling with PTZ, KAr binding measured 24 h after a seizure revealed reduced binding in limbic structures including EC, hippocampus and amygdala (Cremer *et al.*, 2009). Other kindling studies demonstrated increased GluK4 mRNA in hippocampal CA3 region (Hikiji *et al.*, 1993). Kamphuis *et al.* (1995) reported minor increase in GluK2 and GluK5 in CA1, CA3 and DG, whereas a small reduction in GluK3 in DG, all during early stages of epileptogenesis.

KAr levels were also explored in animals at various timepoints after KA- or pilocarpine-induced SE. Ullal *et al.* (2005) investigated hippocampal protein expression for KAr 72 h, 90 and 180 d post KA-induced SE. Results demonstrated GluK1 expression increase throughout the period of observation, while GluK3 appeared to be decreased only at 90 days, returning to normal levels at 180 days. GluK2 remained unaltered throughout. Porter and colleagues (2006) carried out a study on rats exposed to Li-pilocarpine epilepsy induction and sacrificed 14 days post-induction. Authors report a reduction in GluK2 mRNA and an increase in GluK5, while no change in GluK3 and GluK4 in DG neurons. Although not specified directly, it appears that the study was carried out during the latent period of epileptogenesis. The diversity of reported results in literature does not allow making any conclusions on the precise role of KAr in epilepsy, although it is clear that they have some part in it.

Understanding what changes KAr undergo throughout epileptogenesis may provide an insight into the further role of this class of receptors. The transition from the latent phase to the period of behavioural SRS is a critical point of epileptogenesis when KAr changes may take place. Abnormal KAr function may potentially underlie both hypoexcitability and reduced connectivity of the hippocampal network in seizure-free period and may be responsible for the appearance of epileptic SRS activity later on. To test this, we used the RISE model and attempted an investigation of KAr function

change throughout the epileptogenesis. Both extra- and intracellular techniques were utilised to study KAr on the network and cellular level. Results showed a dramatic reduction in gamma oscillation power during the late stage. Although LFP studies do not provide direct answers in abnormal KAr contribution to epilepsy establishment, experiments with selective KAr agents on SyO, intracellular and immunocytochemical methods could lead to a better understanding of KAr role in this pathological condition.

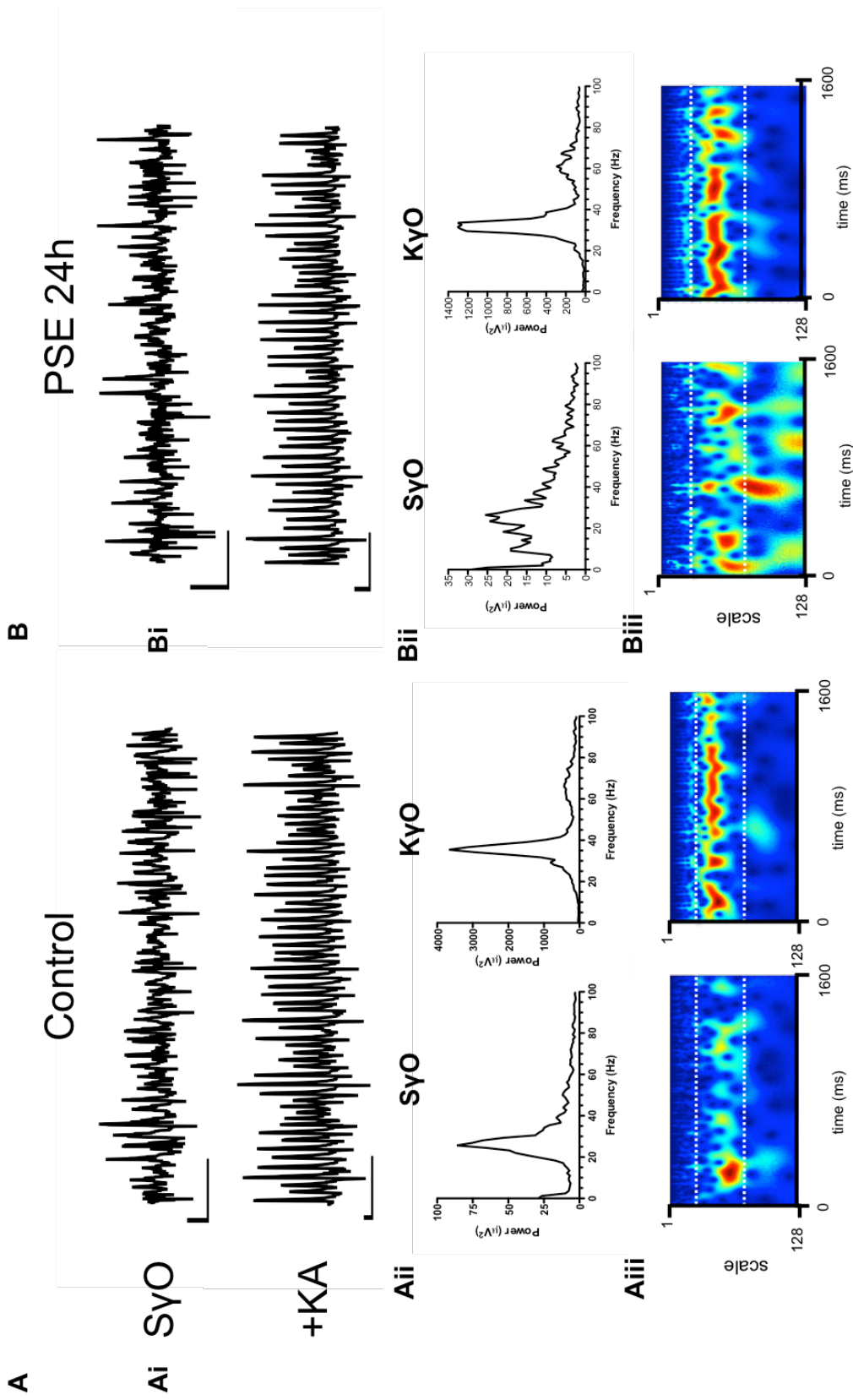
5.2. Results

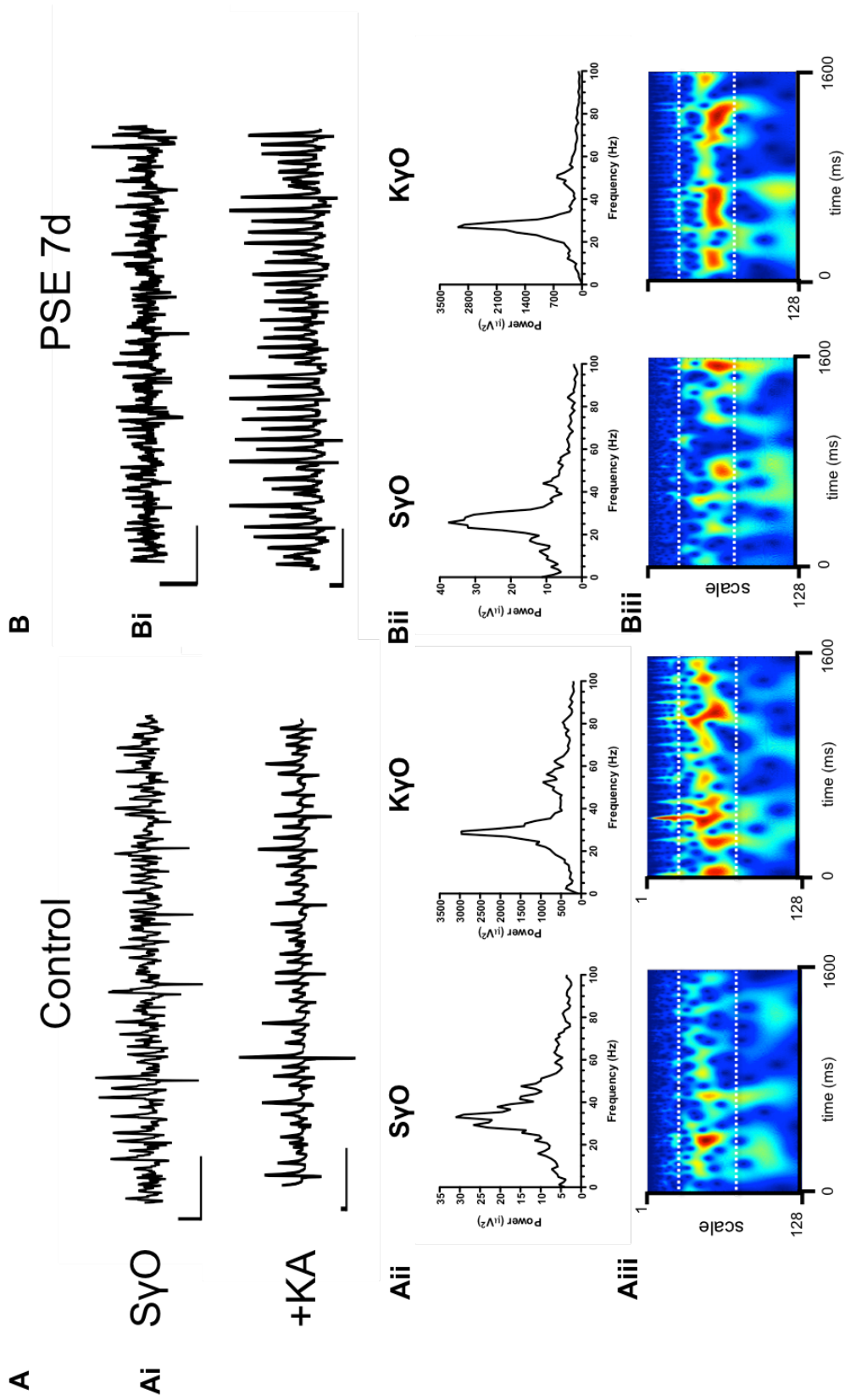
5.2.1. Extracellular recordings

Our previous findings suggested that hippocampal neuronal network exhibited functional changes throughout the process of epileptogenesis in RISE model of epilepsy. The properties of network oscillations were investigated in epileptic vs. AMC rats at various timepoints during epileptogenesis (PSE 24h, PSE 7d, PSE 6wks and PSE 90d). We compared how spontaneous hippocampal activity responded to a challenge with KA in epileptic vs. healthy control brain slices. KA is known to elicit gamma oscillations in hippocampal slices (Hajos *et al.*, 2000; Hormuzdi *et al.*, 2001; Fisahn *et al.*, 2004). Earlier in this report we have demonstrated that hippocampal slices exhibited SyO (see Chapter 3). In this project we first compared the baseline activity (SyO) present in AMC vs. epileptic slices, as well as the activity produced by KA application (KyO) in the same slices. Representative raw traces and power spectra of both oscillation types in PSE 24h and AMC slices are shown in Fig. 5.1. As mentioned previously, SyO in PSE 24h exhibited concurrent high-frequency bursts and gamma rhythm activity, explaining a less defined peak on the FFT, compared to AMC slices where oscillations were more stable and synchronised and appeared to stay within a narrow frequency band (Fig. 5.1). A mix of slow and fast oscillations in PSE 24h came out clearly from Morlet-wavelet spectrogram (Fig. 5.1Aiii,Biii). Although SyO seemed abnormal in PSE 24h, the network was still responsive to 100 nM KA stimulation, causing a large increase in power and producing more coherent synchronised oscillations, comparable to the ones observed in control slices in the presence of KA (Fig 5.1Aii,Bii). Administration of KA suppressed high-frequency activity in epileptic slices. Pooled data demonstrated that SyO PSE 24h had a mean peak power of $36.57 \pm 10.1 \mu V^2$ (n=18) at a mean peak frequency of 30.47 ± 1.1 Hz

(n=18), while in SyO AMC showed a mean peak power $33.74 \pm 6.8 \mu V^2$ (n=13, ns) at a mean peak frequency 26.7 ± 0.8 Hz (n=13, $p < 0.05$) [Fig. 5.5A]. In the presence of 100 nM KA, SyO PSE 24h reached $3235 \pm 1333 \mu V^2$ (n=18) at 36.23 ± 1.4 Hz (n=18), while SyO AMC reached $4024 \pm 2191 \mu V^2$ (n=13, ns) at 29.5 ± 1.4 Hz (n=13, $p < 0.01$).

The analysis of neuronal network oscillations in PSE 7d slices revealed moderate SyO activity in CA3 hippocampus, similar to that observed in AMC slices (Fig. 5.2). SyO in epileptic slices still showed a residual high frequency component, although, compared to PSE 24h, it was less prominent, but the gamma rhythm itself appeared more pronounced (Fig. 5.2Aiii, Biii). When 100 nM KA was bath applied to pre-existing SyO, the activity increased in power dramatically, both in PSE 7d and AMC slices. Representative traces and power spectra are shown in Fig. 5.2A, B. Despite the fact that KyO demonstrated good oscillatory power, as well as sharp and well-defined FFT peaks in both groups, the time-frequency analysis suggested that PSE 7d oscillations were less stable, with patches of low gamma power. Overall, SyO in AMC slices reached the mean peak power of $28.34 \pm 11.38 \mu V^2$ at 32.3 ± 0.9 Hz (n=12), which was comparable to the peak power but not the peak frequency of oscillations observed in PSE 7d ($44.39 \pm 7.9 \mu V^2$ at 29.8 ± 0.8 Hz, n=10, $p > 0.05$ and $p < 0.05$, respectively) [Fig. 5.5B]. Application of 100 nM KA increased SyO to $1666 \pm 554.0 \mu V^2$ at 29.8 ± 1.0 Hz (n=12) in AMC slices and $2039 \pm 585.3 \mu V^2$ at 31.37 ± 2 Hz (n=10) in PSE 7d (both $p > 0.05$).

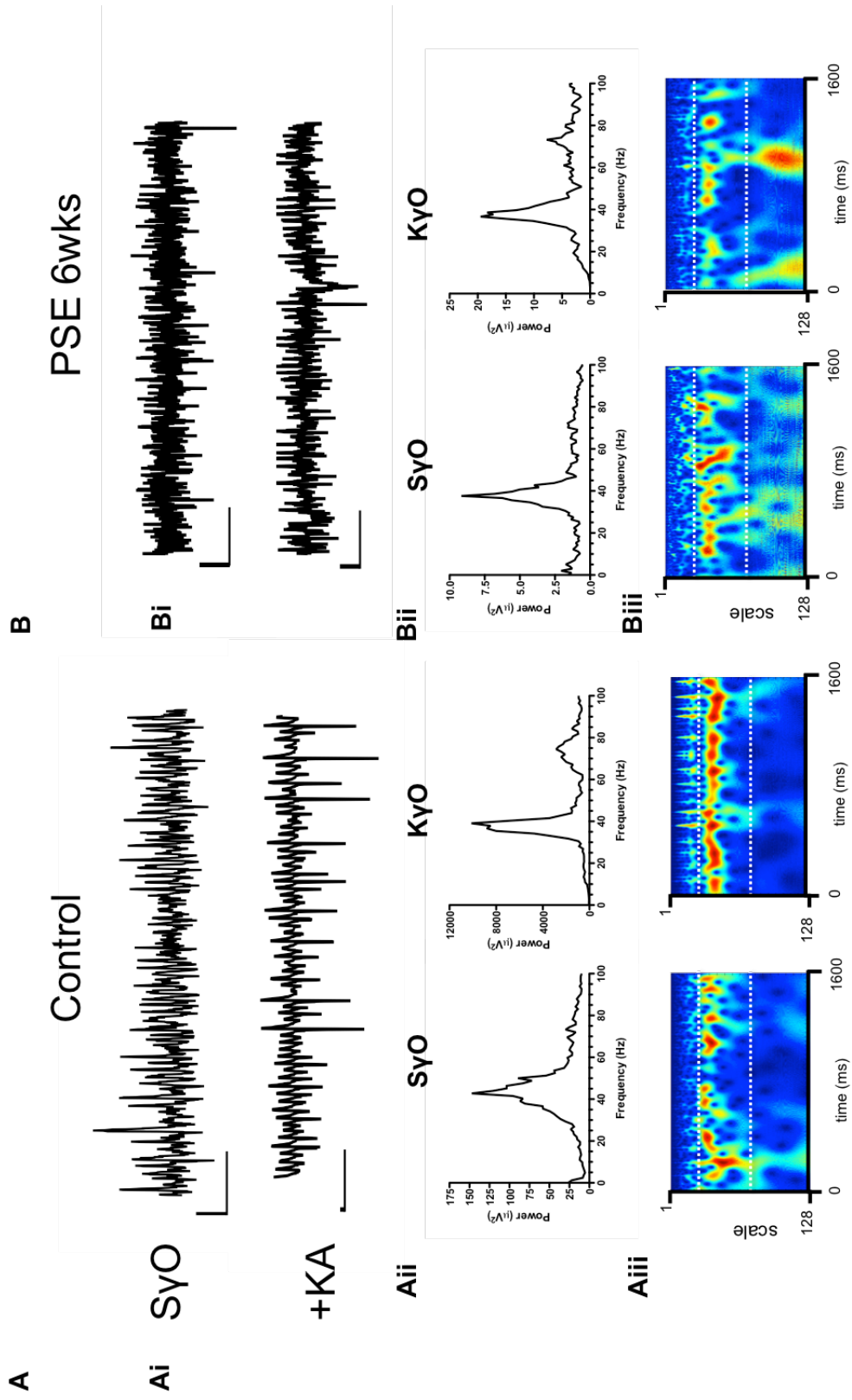


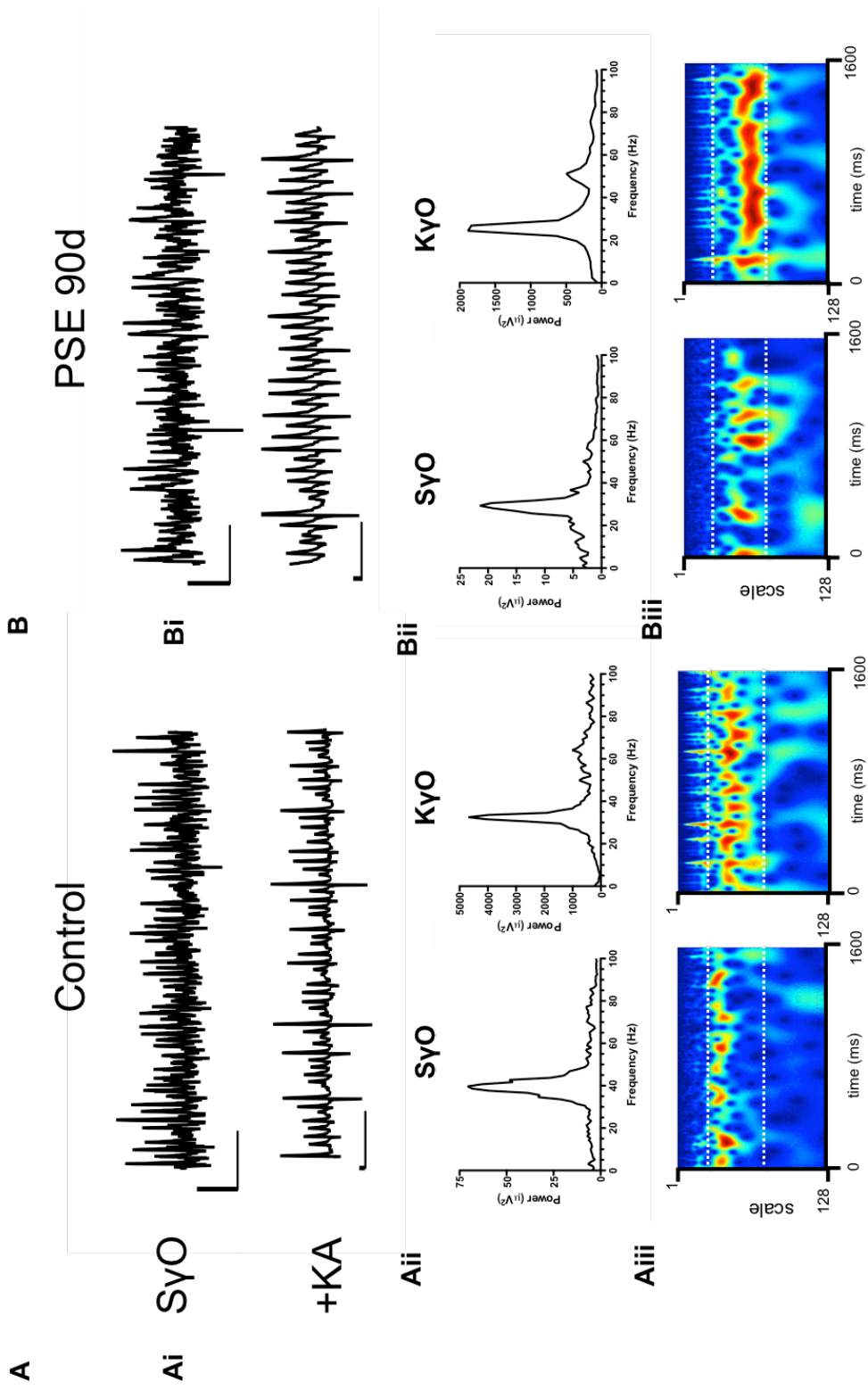


According to our previous findings, SyO exhibited changes during the late latent period (Chapter 4). In this project, we compared both SyO and KyO between PSE 6wks and AMC slices. The results in PSE 6wks demonstrated SyO, which was not observed consistently, indicating underlying abnormalities of the network function (Fig. 5.3). Spontaneous activity was surprisingly small in power, yet highly coherent with a sharp gamma peak on the power spectrum, which is not very characteristic of low-power SyO. These findings may reflect possible involvement of small but synchronous networks (Fig. 5.3Aii,Bii). AMC slices consistently exhibited strong SyO in CA3 region, demonstrating normal operation of the hippocampal neuronal network (Fig. 5.3). 100 nM KA administered to control slices with SyO produced a dramatic increase in the power of oscillations, similar to other AMC slices. In PSE 6wks, application of 100 nM KA, on the contrary, produced only a small change, indicating poor sensitivity to the agent or KAr receptor dysfunction. Stimulation with a double dose of KA (200 nM) resulted in a small increase of oscillatory power, which still was not comparable to control slices (Fig. 5.3Aii,Bii). These findings demonstrated a decrease in network excitability and a disruption of network oscillation mechanism, although the exact involvement of KAr in this case was not clear. Fig. 5.3 presents a recording from an AMC slice challenged with 200 nM KA. Overall, SyO AMC slices was significantly higher in power compared to PSE 6 wks ($41 \pm 11.5 \mu V^2$, $n=18$ vs. $20.59 \pm 6.6 \mu V^2$, $n=20$, $p < 0.05$), although similar in mean peak frequency (35.4 ± 0.9 Hz, $n=18$ vs. 34.87 ± 1.2 Hz, $n=20$, $p > 0.05$). These results showed that network changes/reorganisation in the latent period were already visible from the natural hippocampal activity of the slices. Application of KA revealed further exacerbated the differences between the two groups. The contrast in KyO mean peak power between AMC and PSE 6 wks slices was evident ($1968 \pm 756.8 \mu V^2$, $n=18$ vs. $322.5 \pm 156.7 \mu V^2$, $n=20$, $p < 0.01$), even though no significant difference was observed in mean peak frequency (34.6 ± 0.8 Hz, $n=18$ vs. 36.4 ± 1.3 Hz, $n=20$, $p > 0.05$). Pooled data results are presented in Fig. 5.5C.

To determine whether rhythmic activity in the hippocampus underwent changes during epileptogenesis, we explored SyO and KyO in the slices from fully epileptic rats (PSE 90d) and compared them to AMC. SyO demonstrated strong power in both control and epileptic slices, although concurrently with gamma frequency PSE 90d slices exhibited transient high-frequency activity (Fig. 5.4). Traces demonstrating

multiple frequency components in PSE 90d are shown in Fig. 5.4Bi. These bursts of high-frequency activity may represent increased excitability of the tissue and its susceptibility to seizures. When 100 nM KA was applied to pre-existing SyO, rhythmic activity dramatically increased in power and became regular in both groups (Fig. 5.4Ai,Bi). Moreover, in epileptic slices administration of KA abolished fast activity and introduced a pure gamma frequency rhythm (Fig. 5.4Bi,Bii). The main parameters of SyO were comparable in AMC vs. PSE 90d ($84.29 \pm 23.9 \mu V^2$ at 36.3 ± 0.9 Hz [n=14] vs. $62.65 \pm 9.6 \mu V^2$ at 35.9 ± 0.9 Hz [n=22], $p > 0.05$), as shown in Fig. 5.5D. KyO, on the other hand, were significantly stronger in power in PSE 90d compared to AMC ($3401 \pm 757.4 \mu V^2$ [n=22] vs. $1798 \pm 612.7 \mu V^2$ [n=14], $p < 0.05$). The frequency of KyO did not demonstrate significant differences (29.9 ± 0.8 Hz [n=22] in PSE 90d vs. 31.4 ± 0.4 Hz [n=14] in AMC, $p > 0.05$). Interestingly, it appears that administration of 100 nM KA produced a larger effect in epileptic slices, which is illustrated by Fig. 5.5D. These results could reflect elevated excitability of the tissue, which may be the link to the appearance of behavioural seizures during this period. In addition, ictal/interictal episodes described earlier further support the idea of increased seizure susceptibility of the epileptic tissue/brain.





In this project we used potentiation of baseline oscillatory activity (SyO) upon administration of 100–200 nM KA, as a measure of KAr activity during different stages of epileptogenesis. We compared the changes in power produced by KA application (KyO – SyO) in epileptic and control conditions, as well as between different stages of epileptogenesis. Direct pharmacological stimulation of PSE 24h slices with KA produced similar effects to the ones recorded in AMC ($3198.4 \pm 1333 \mu V^2$, $n=18$ in PSE 24h vs. $3990 \pm 2191 \mu V^2$, $n=13$ in AMC, $p>0.05$). Similar picture was observed in PSE 7d slices, where KA-induced change was comparable to control slices ($1994.6 \pm 585.3 \mu V^2$, $n=10$ in PSE 7d vs. $1647.3 \pm 606.8 \mu V^2$, $n=11$, $p>0.05$). The most dramatic deviation from control values appeared in the late latent period (PSE 6wks). At this time SyO seemed to lose its oscillatory power and even a double concentration of KA failed to produce a response comparable to AMC level ($301.91 \pm 156.8 \mu V^2$, $n=20$ in PSE 6 wks vs. $1926.17 \pm 756.9 \mu V^2$, $n=18$ in AMC, $p<0.05$). Later stages were characterized by robust SyO and KyO in both epileptic and control slices. Development of behavioural seizures seemed to coincide with regained power of SyO and KyO in PSE 90d slices. Although the **change in power** produced by KA in PSE 90d did not reach statistical significance ($3338.35 \pm 757.5 \mu V^2$ in PSE 90d vs. $1713 \pm 613 \mu V^2$, $n=14$, $p>0.05$), it appeared that epileptic slices were more responsive to KA (as the **raw power** of KyO was high), indicating possible increased excitability.

When compared within healthy and lesioned groups, the results demonstrated a similar/consistent level of power change from SyO to KyO throughout all control slices, whereas in epileptic slices the level of power change did not appear stable throughout the epileptogenesis, which indicated underlying network alterations (Fig. 5.6). The figure demonstrates that after the initial insult, KA effect on SyO was gradually declining until reaching the lowest point during the late latent period, when application of KA produced the smallest effect compared to AMC and other stages. Contrary to the latent period, SRS stage was characterized by a rebound of the hippocampal rhythmic activity to the early post, indicating restored mechanisms for synchronisation.

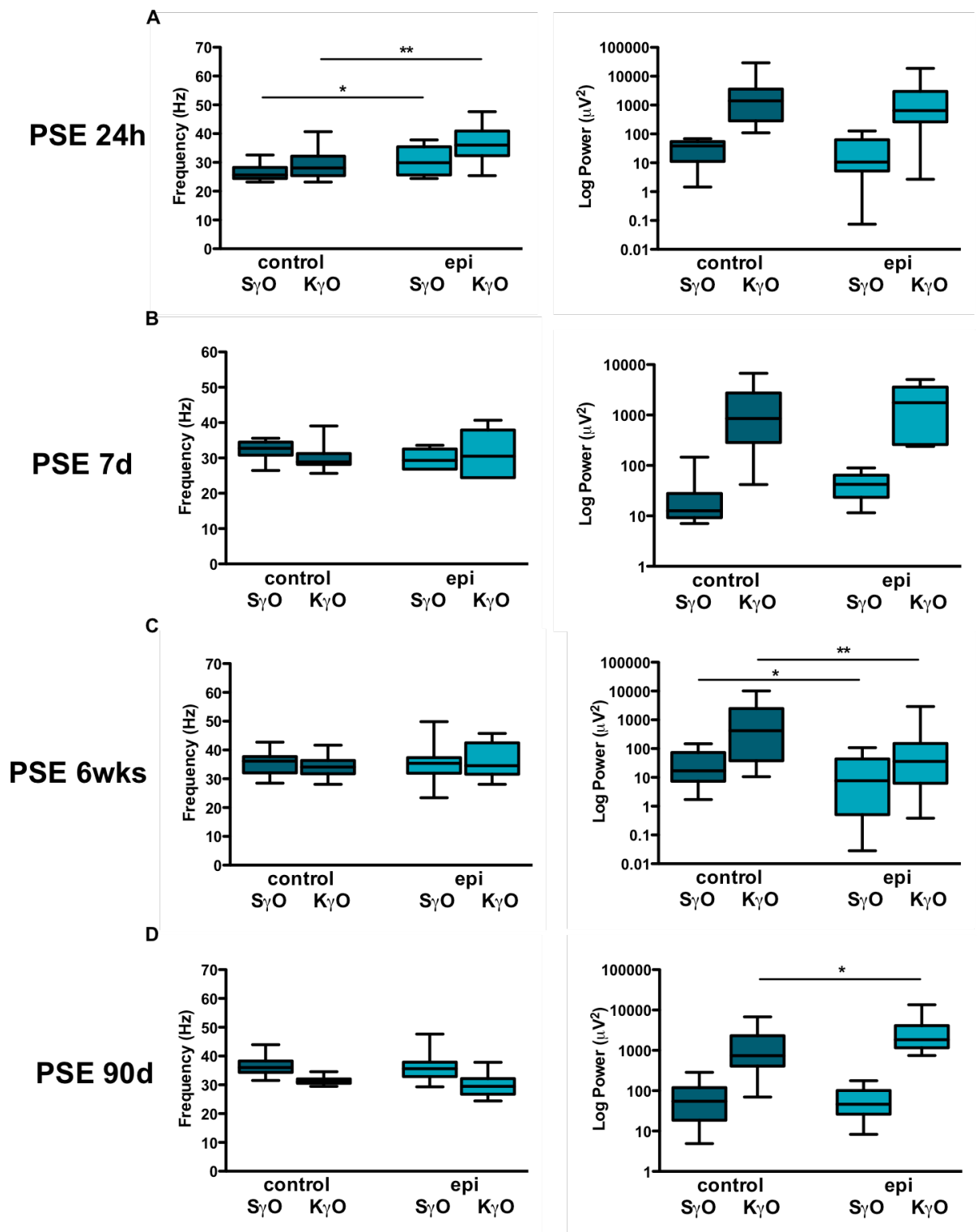


Figure 5.5. Pooled peak frequency and peak power plots for SyO and KyO in control and epileptic conditions. **A.** Pooled peak frequency and peak power plots for PSE 24h and AMC slices. SyO and KyO peak frequency is significantly lower in AMC slices compared to PSE 24h. **B.** Pooled peak frequency and peak power plots for PSE 7d and AMC slices. **C.** Pooled peak frequency and peak power plots for PSE 6wks and AMC slices. A significant reduction in the peak power is observed in SyO and KyO in PSE 6wks compared to AMC. **D.** Pooled peak frequency and peak power plots for PSE 90d and AMC. A significantly higher KyO peak power is demonstrated in PSE 90d compared to AMC slices. ** indicate $p < 0.01$, * indicates $p < 0.05$.

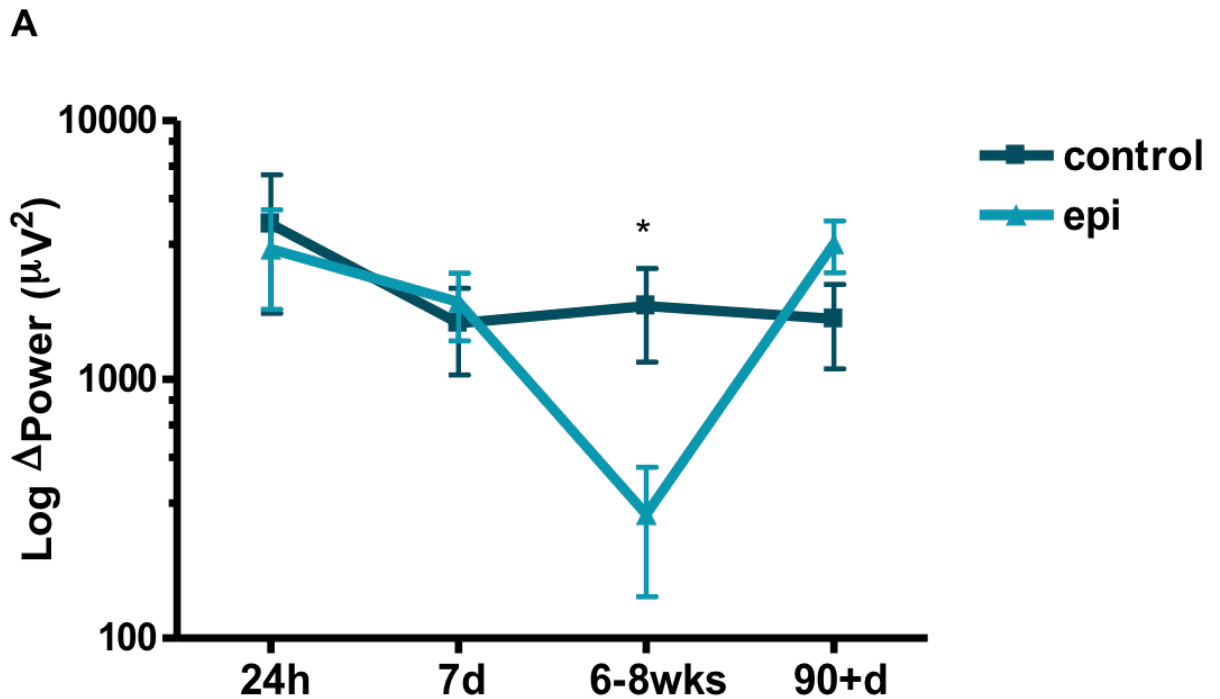


Figure 5.6. KAr response is compromised during PSE 6wks. A. Changes in the peak power of gamma oscillations produced by the application of KA in AMC and epileptic slices at different stages of epileptogenesis.

5.2.2. KAr function in evoked field potential recording

We sought to explore KAr function during the process of epileptogenesis, latent period in particular, using a more direct method. We first attempted to induce and then pharmacologically isolate KAr-mediated effects in CA3 region brain slices from healthy adult rats (~300g, age-matched to PSE 6 wks). The experiments were based on the work of Castillo and colleagues (1997), who used electrical stimulation of mossy fibres to evoke field postsynaptic potentials in CA3 *s. lucidum* of a brain slice. According to experiments described by the authors, application of a single stimulus produced a response that was blocked by selective AMPAr antagonist GYKI 53655. The response, however, was restored by a train of 6 stimuli at 30 Hz in the presence of GYKI 53655, indicating non-involvement of AMPAr. This evoked synaptic potential was blocked by a non-selective KAr/AMPA antagonist CNQX demonstrating that the response was mediated by KAr.

The experiments we repeated in adult rat slices, however, the results were not consistent. A successful experiment is demonstrated in Fig. 5.7A. A response was evoked with a single stimulus (the recording is an average of 10 runs) and was

blocked with 30 μM GYKI 53655. A train of 6 stimuli at 30 Hz every 5 seconds was then applied to initiate glutamate release and hopefully expose KAr-mediated responses. The amplitude of evoked synaptic potential was 1300 μV , which reduced by 60% when 40 μM CNQX was bath-applied. CNQX application produced a significantly smaller effect in comparison to original studies by Castillo *et al.* (1997), which suggested involvement of other receptor types. In other experiments that were conducted, bath application of GYKI 53655 produced either an increase or no change in single stimulus evoked potential amplitude. Administration of another AMPAR antagonist NBQX (2.5 μM) could not block the response either, indicating contribution of other receptors or possible technical issues during the experiment. We also tried co-application of 40 μM MK-801, 20 μM PTX, 5 μM CGP 55845 with 30 μM GYKI 53655. This combination of drugs was administered to pharmacologically isolate KAr-mediated responses. Despite these efforts, synaptic potential evoked by a single stimulus could not be blocked by this cocktail. Application of 40 μM CNQX did not abolish the train-induced potential either (Fig. 5.7B), hence 1 μM tetrodotoxin (TTX) was tested to determine whether the recorded responses were real. TTX produced a small reduction, however could not abolish the activity, suggesting that the signal might reflect volume conduction or directly driven synaptic currents. Overall, the inconsistency of obtained results suggested that this method was not appropriate to characterise KAr function in our brain slices, possibly due to technical limitations.

We also investigated the role of KAr using a different protocol, which at first yielded more consistent results, however, this too eventually proved ineffective. Mossy fibres were stimulated to produce synaptic responses in CA3 hippocampus. A test recording was obtained first, in order to confirm that a single stimulus induced a postsynaptic potential. When this was established, the stimulation protocol was changed to a train of 40 stimuli at 200 Hz, which produced a slow postsynaptic potential, which we believed was mediated by KAr. When a combination of 20 μM PTX, 5 μM CGP 55845, 2.5 μM NBQX, 20 μM SYM2206 and 20 μM MK-801 was bath-applied, the response changed in amplitude and duration, abolishing fast events and retaining the slow component. Application of 40 μM CNQX reduced the slow event (Fig. 5.7C). Pooled data from control slices suggest that mean suppression of

synaptic potential amplitude $46.7 \pm 8.5\%$ ($n=12$), however the results were not consistent. Therefore, we found this protocol inappropriate for investigation of KAr.

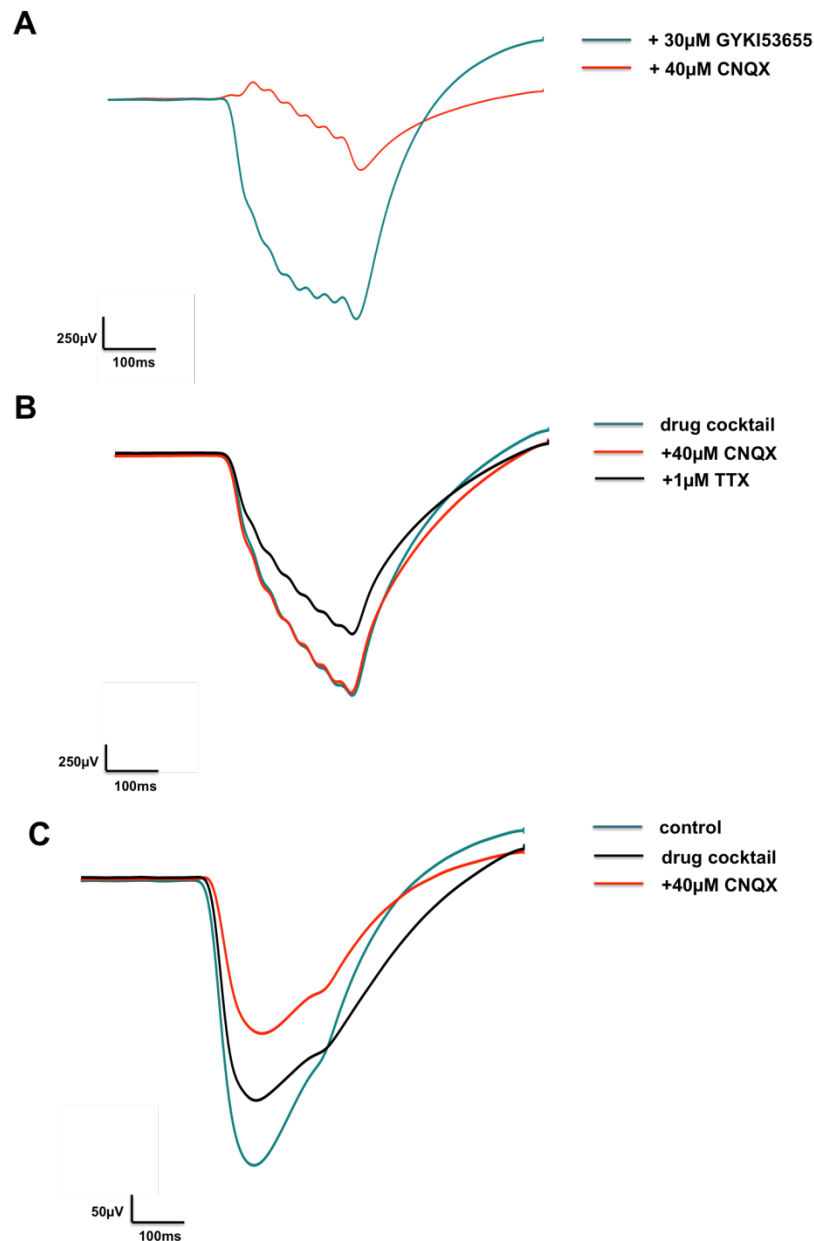


Figure 5.7. Evoked field potential in the hippocampal CA3 region. **A.** Raw trace showing a successfully reproduced experiment by Castillo *et al.* (1997), where AMPAR blockade (teal) exposed a slow postsynaptic potential, which was reduced by CNQX application (red) and was therefore KAr-mediated. **B.** Raw traces showing no change in field postsynaptic potential after blocking all major receptor types. A small effect produced by TTX application (black) raises concerns about the biological nature of observed signals. **C.** Raw traces showing an example of successful experiment, where application of CNQX reduced the amplitude and duration of the evoked field potential. All traces low-pass filtered at 10 Hz.

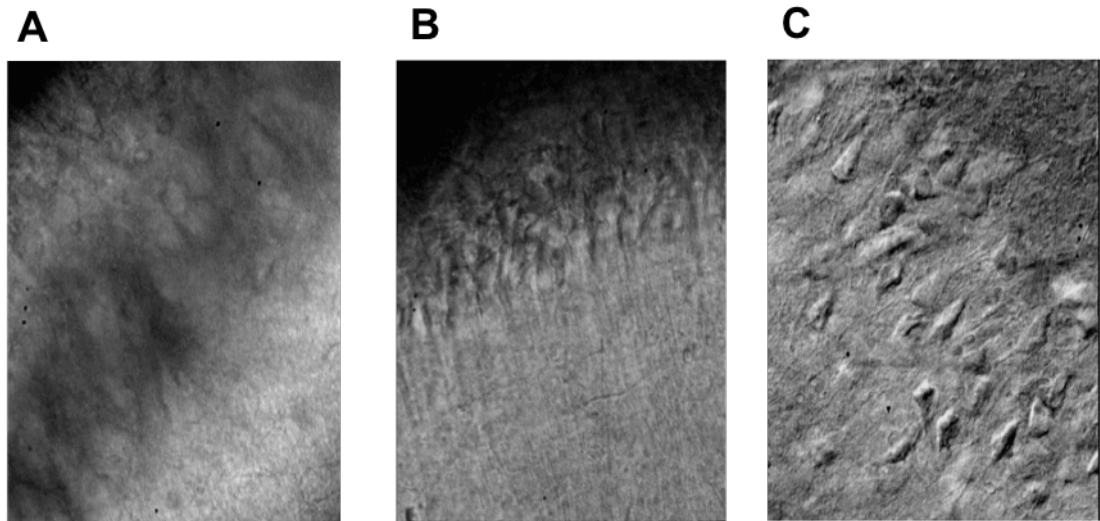


Figure 5.8. Poor survival of the hippocampal CA3 in control adult slices. A., B. and C. images of CA3, CA1 and layer II EC, respectively. Brain slices obtained from 300+g rats.

5.2.3. KAR function in whole-cell patch-clamp recordings

5.2.3.1. Attempts to increase CA3 viability

The whole cell patch-clamp technique was used to determine the change in pre- and post-synaptic contribution of KAR in CA3 throughout epileptogenesis. My initial plan included characterising presynaptic KAR by exploring spontaneous postsynaptic currents (sPSCs) and postsynaptic KAR by exploring evoked EPSCs (eEPSCs). Conclusions drawn from extracellular results suggested close investigation of the latent and SRS stages of epilepsy development. This, however, has proved to be rather challenging, as the survival of CA3 cells decreased dramatically in slices from >300g animals. Despite our best efforts, the hippocampal CA3 region seemed to be extremely vulnerable to manipulations required to make brain slices. In contrast to CA3, CA1 and mEC, for instance, appeared healthy looking (Fig. 5.8). We employed a variety of methods to increase the viability of neurons in the CA3 region. The improved-composition cutting solution routinely used in the lab was not very effective in protecting CA3 neurons, hence we tried using basic cutting solution (see Section 2.1.), which further decreased the quality of slices. Replacing sucrose with an equivalent amount of glycerol resulted in relatively healthy slices, however the cells were very difficult to patch. We then tried different variations of the 'protective recovery method' used by Peca and colleagues (2011), which included preincubation of brain slices in NMDG or choline chloride solution at 32–34°C (for recipes see Appendix 2). Together with protective recovery method, addition of high doses of

NAC to cutting solutions was used to prevent glutathione depletion for better slice preservation. These modifications produced apparent enhanced preservation of CA3 regions, however, cells appeared swollen and when patched were depolarised, suggesting poor viability. We also tried using H₂S donors as an additional component of sucrose cutting solution, in order to suppress oxidative damage through promotion of reductive environment. This did not improve CA3, however. In our attempts to increase morphological preservation of CA3 cells, we tried different cutting blades (ceramic vs. steel), different slicers (Vibroslice HA752 by Campden Instruments vs. HM650V by Microm), different speed (slow vs. fast) and temperature (4–10°C vs. room temperature) of slicing, different brain orientation (slicing back to front vs. side to side) and finally different storing conditions (submerged vs. interface). None of the used method modifications could consistently produce healthy-looking well-preserved CA3 region in slices from 300g and above rats.

5.2.3.2. KAr effects on GABA release

Due to the issues described above, the study of KAr function using intracellular recordings could not be completed, yet some results are still presented in this report. We started investigating KAr activity by recording sIPSCs on CA3 pyramidal cells. Application of 100 nM KA produced a significant decrease in sIPSC inter-event interval (IEI) in 50g control rats (142.6 ± 9.1 ms to 66.9 ± 2.6 ms, $n=3$, KS $p < 0.0001$), as illustrated in Fig. 5.9A,B. In these recordings the frequency of events increased by 53.1%. The amplitude of sIPSCs increased slightly from 40.65 ± 2.4 pA to 46.3 ± 2.8 pA ($n=3$, paired t-test $p > 0.05$), however did not reach significance. In slices from 90–100g animals (AMC to PSE 7d) administration of KA caused a significant reduction in IEI (from 121.0 ± 4.4 ms to 83.4 ± 1.9 ms, $n=5$, KS $p < 0.0001$), thus increasing the frequency by 31.1% (Fig. 5.9C,D). KA also produced a significant increase in sIPSC amplitude (41.7 ± 1.5 pA to 48.5 ± 1.9 , $n=5$, paired t-test, $p < 0.01$). In contrast to control slices, sIPSCs recorded from PSE 7d significantly decreased in amplitude (from 210.6 ± 13.9 pA to 161.3 ± 13 pA, $n=1$, paired t-test, $p < 0.0001$) but exhibited no change in frequency (IEI 105.4 ± 4.5 ms to 114.7 ± 5.1 , $n=1$, $p > 0.05$) [Fig. 5.10A,B]. In adult animals, one recording was obtained from a PSE 6wks slice. Application of KA demonstrated a significant increase in sIPSC amplitude (10.7 ± 0.4 pA to 14.9 ± 0.8 pA, $n=1$, paired t-test, $p < 0.0001$), yet the effect on IEI was not significant (158 ± 8.9 ms to 131.9 ± 7.2 ms, $n=1$, $p > 0.05$) (Fig. 5.10C,D). It appears that pharmacological

stimulation with KA produced presynaptically regulated increase in GABA release. It is yet to determine with more experiments whether the fact that KAr activation in epileptic slices indeed causes no change in sIPSC frequency and, hence GABA release, implying a disrupted function of KAr in epilepsy development. Overall, at this stage it is impossible to draw any conclusions about the changes of either pre- or postsynaptic KAr activity throughout epileptogenesis, as further investigation is required, specifically during latent and SRS stages. These data, however, could contribute to further experiments.

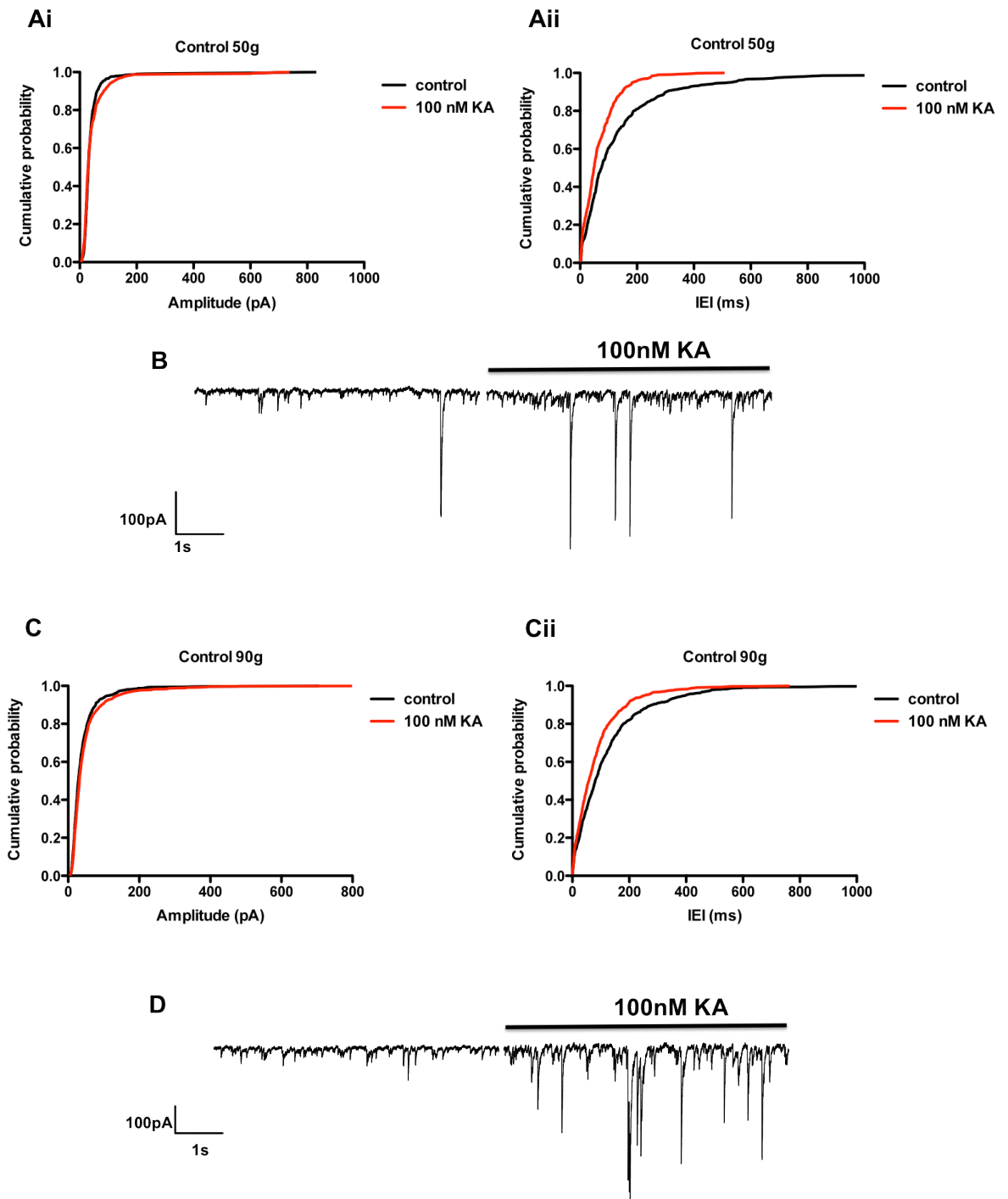


Figure 5.9. KAR effects on GABA release in CA3 of control slices. **Ai.** and **Ci.** Cumulative probability plots showing sIPSC amplitude change upon application of 100 nM KA in 50g and 90g control slices, respectively. **Aii.** and **Cii.** Cumulative probability plots showing sIPSC IEL change upon application of 100 nM KA in 50g and 90g control slices, respectively. **B.** and **D.** Example traces showing control and 100 nM KA condition in 50g and 90g control slices, respectively.

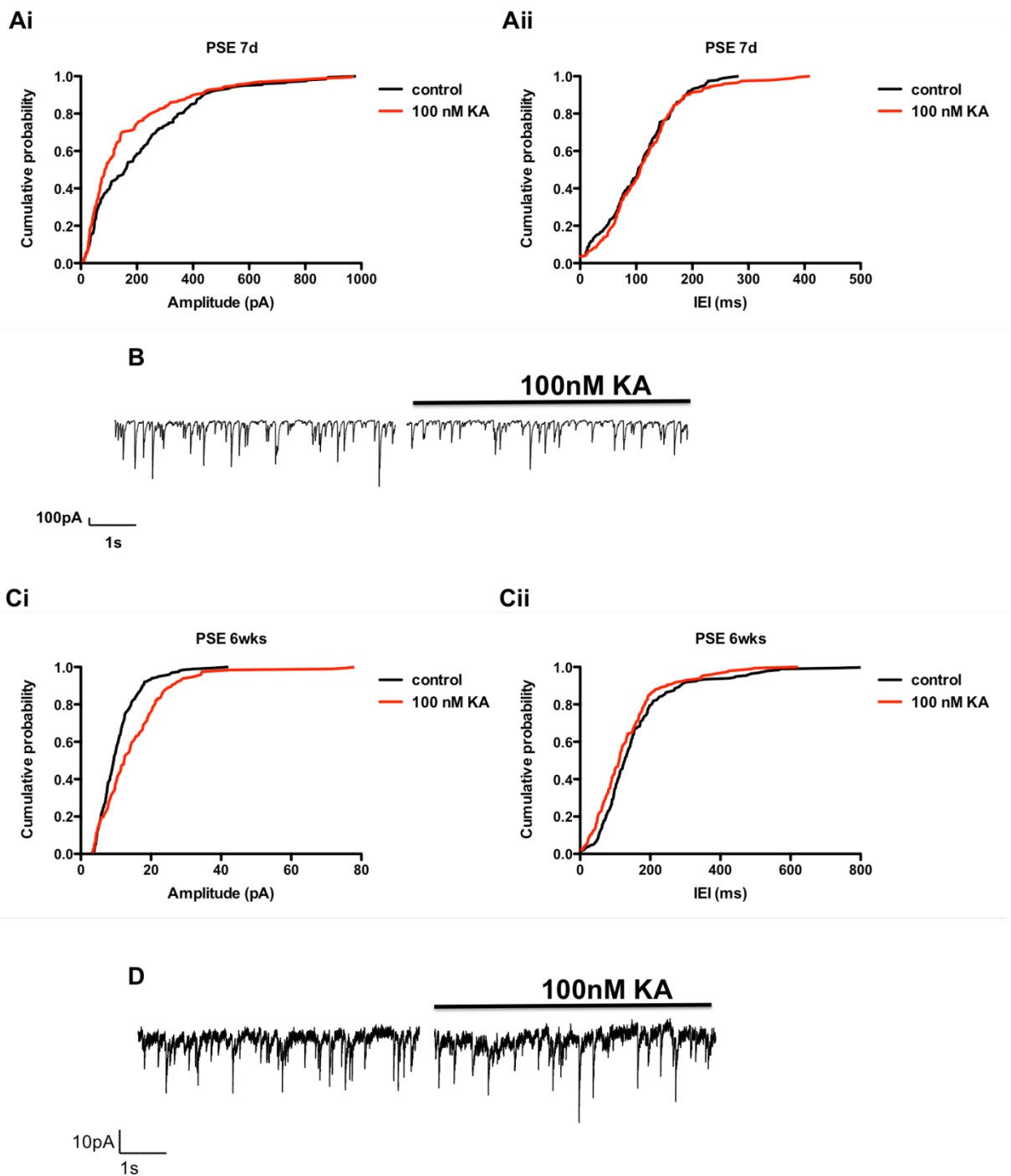


Figure 5.10. KAR effects on GABA release in CA3 of epileptic slices. **Ai.** and **Ci.** Cumulative probability plots showing sIPSC amplitude change upon application of 100 nM KA in PSE 7d and PSE 6wks slices, respectively. **Aii.** and **Cii.** Cumulative probability plots showing sIPSC IEL change upon application of 100 nM KA in PSE 7d and PSE 6wks slices, respectively. **B.** and **D.** Example traces showing control and 100 nM KA condition in PSE7d and PSE 6wks slices, respectively.

5.3 Discussion

There is evidence that KAR play a role in epilepsy and we hypothesise that this class of receptors is involved in crucial network changes underlying the transition from seizure-free latent period to behavioural SRS period. Neuronal network oscillations are a reflection of network activity, therefore we measured the effect produced by KAR stimulation at various stages of epilepsy development. Through results obtained we estimated the contribution of KAR to the network function and how it changed throughout epileptogenesis. During the early post-insult period, although SyO appeared altered, KAR-mediated responses remained intact. A similar picture emerged in PSE 7d slices, as KA application produced comparable effects on gamma oscillations, indicating similar activity of KAR in both PSE 7d and AMC. With the progression of the latent period, epileptic slices exhibited significantly lower SyO and KyO power compared to AMC. Even stronger KA stimulation was not able to produce a response similar to AMC. These results indicated abnormal function of hippocampal network, and although the basic mechanism for rhythmic activity generation was not disrupted, it appeared suppressed. As mentioned in the previous section of this report, changes in the oscillatory activity may reflect fragmentation of entire CA3 network into smaller localised networks due to the loss of interneurons and/or disturbed or limited activity of KAR, which are involved in network synchronisation (Fisahn *et al.*, 2004; Fisahn *et al.*, 2005; Kramer *et al.*, 2010). It is possible that these networks lost means of communication with each other, hence such dramatic change in power was observed. Development of behavioural seizures in animals coincided with a rebound of oscillatory power in both SyO and KyO, indicating restoration and possibly hyperfunction of KAR. The findings suggest that in PSE 90d the network possibly regained synchronisation mechanism and established stronger synaptic connections. The results demonstrated that network/KAR changes do not take place until further into the latent period. Another time point around PSE 3wks might be necessary for future experiments to determine how soon the changes develop.

Results obtained from extracellular recordings let us suggest that KAR underwent certain changes during epileptogenesis, which were reflected by abnormal rhythmogenesis in the epileptic hippocampal slices. KAR are known to mediate a

variety of regulatory effects in neuronal communication and are the key players of glutamatergic transmission in the hippocampus (Cossart *et al.*, 2002). Postsynaptic KAR, due to their slow kinetics, have a role of regulating neuronal excitability and information processing by integrating excitatory synaptic inputs (Frerking and Nicoll, 2000; Frerking and Oligher-Frerking, 2002, Goldin *et al.*, 2007, Pinheiro *et al.*, 2013). Presynaptic KAR, on the other hand, bidirectionally regulate neurotransmitter release at both inhibitory and excitatory synapses (Schmitz *et al.*, 2000; Lauri *et al.*, 2001; Rodriguez-Moreno *et al.*, 1997; Frerking *et al.*, 1999; Cossart *et al.*, 2001). Suppressed oscillatory activity observed during the latent period in response to KA gives an indirect indication of underlying network alterations, however does not identify a clear source of abnormality, considering that rhythmic activity has a complex multi-component network mechanism. Since KAR are heavily involved in synaptic transmission and have means of regulating other network components, without direct intracellular studies exploring the function of KAR during epileptogenesis, it is impossible to make conclusions on the cause of observed changes. KAR may be affected in various ways, which could explain a drop in gamma oscillations during the seizure-free period and its later recovery during the SRS stage. For instance, KAR subunit composition, protein expression, channel gating and other factors influencing KAR kinetics, as well as receptor desensitisation, synaptic plasticity and changes in presynaptic regulation of other neurotransmitters (e.g. GABA) could contribute to or be responsible for an abnormal function of KAR in epilepsy.

To evaluate KAR activity more directly, yet in the network context, we recorded evoked field potentials in CA3 hippocampus. Mimicking glutamate release at mossy fibre terminals by electrical stimulation and subsequent pharmacological decomposition of postsynaptic potentials in an attempt to isolate KAR-mediated responses. Postsynaptic potentials appeared in various shapes and amplitudes, and were neither stable nor consistent. Application of AMPAR, NMDAR, GABA-Ar, GABA-Br, and AMPAR/KAR antagonists did not demonstrate reproducible effects, indicating possible technical faults like artefacts or factors like volume conductance and disruption of electrical activity of cells. Isolation of one neurotransmission element in a population of cells might not be as straightforward as in an individual cells. Replication of the original experimental protocol by Castillo and colleagues (1997)

could not produce reliable results, as GYKI 53655 failed to block AMPAR-mediated component, as did CNQX.

The next step in investigating the functional state of KAr involved intracellular evaluation of pre- and postsynaptic KAr activity at various timepoints of epileptogenesis. The idea of this investigation was to focus on the late latent period of 6-8 wks and the SRS stage when animals exhibit behavioural seizures, as the dramatic changes in network function were observed then. It is known that preservation of neurons in slices from adult/old animals can be challenging, therefore most of the research has been conducted on young animals. We have encountered this problem in the hippocampal brain slices of 300+g animals, where CA3 region exhibited low viability in both epileptic and AMC slices. Interestingly, poor preservation was highly distinctive for CA3, whereas other areas of the slice appeared healthy, which demonstrated a higher age-dependent vulnerability of CA3 cells to mechanical damage. Various brain slice preparation techniques were tested in order to preserve this area (see Appendix 2). Unfortunately, it was not possible to increase survival of CA3 cells and at the same time maintain the morphological and electrophysiological properties of the cells. Due to technical issues and limited time, we gathered little information on KAr properties in AMC and epileptic slices. The results that were obtained were in line with previous reports in literature (Fisahn *et al.*, 2004; Christensen *et al.*, 2004; Chamberlain, 2009). In our experiments application of KA increased the frequency of sIPSCs in CA3 pyramidal cells, indicating positive modulation of GABA release mediated by presynaptic KAr. Conducted experiments are only a first step in characterising KAr function, as more experimental work is needed to investigate both pre- and postsynaptic components. However, the problem of poor CA3 viability in adult brain slices is a serious obstacle, which has to be overcome prior to carrying out intracellular studies.

Having conducted a number of electrophysiological studies exploring functional changes in KAr in epilepsy, we chose to support the findings with immunocytochemical methods to investigate the presence rather than the functional state of KAr during the latent period and the SRS stage (in collaboration with Prof. Elek Molnar, Bristol University). Alterations in KAr subunit expression during the process of epilepsy establishment in the temporal lobe may explain the progression

of epileptogenesis and occurrence of behavioural seizures. Nevertheless, protein expression does not provide a full receptor profile, as a receptor might be expressed but not functionally active, which could be misleading. Therefore it seems reasonable to utilise various characterisation methods to obtain a more detailed picture.

Looking back, it would be beneficial to characterise the role of KAr in SyO during epileptogenesis. Using a variety of subunit-selective KAr antagonists and agonists (e.g. UBP310 and ATPA) would provide insight into the direct contribution of GluK1-containing KAr to the drop of gamma activity during the latent period and gamma power rebound in the SRS stage. Our previous pharmacological findings in control animals demonstrate a difference in GluK1 KAr role in SyO and KyO. Measuring the degree of SyO potentiation upon addition of GluK1 KAr antagonist in epileptic vs. AMC slices would reveal any abnormal function of GluK1 KAr without having to artificially stimulate the receptors with KA.

5.4. Conclusion

Overall, it is clear that the hippocampal CA3 network undergoes certain changes during the latent period of RISE model, when the activity temporarily shrinks and becomes less responsive to KA, as demonstrated by our results. The activity recuperates coincidentally with the appearance of SRS, suggesting a possible restored and augmented function of KAr in epilepsy. One of the limitations in interpreting extracellular data is the fact that the rhythmic activity of a network is a complex process involving multiple interrelated components including KAr. It is known that KAr play a crucial role in the generation and maintenance of the gamma rhythm, but KyO can not be used as a direct measure of KAr activity. Immunocytochemical methods might provide support for our hypothesis. A potentially fruitful approach would also be to test the effects of subunit-selective KAr agents on SyO in epileptic vs. control animals.

Chapter 6 Spontaneous rhythmic activity in layer II mEC

6.1. Introduction

6.1.1. The EC and epilepsy

In the previous chapters we investigated the establishment of epilepsy in the CA3 hippocampus, however, TLE is not restricted to the hippocampal area, but involves other regions like the entorhinal and perirhinal cortices, as well as the amygdala. Some of the work on epilepsy has been dedicated to the role of the EC in the TLE, as various studies have shown that ictal activity can arise independently in this region, in humans (Rutecki *et al.*, 1989; Spencer and Spencer, 1994; Assaf and Ebersole, 1997 and others) and animal models (Ben-Ari *et al.*, 1981; Collins *et al.*, 1983; Stringer *et al.*, 1994). A reduction of the EC volume has been demonstrated in the patients with TLE, suggesting a destructive effect of epilepsy on this area (Bernasconi *et al.*, 1999, 2001; Jutila *et al.*, 2001; Bonilha *et al.*, 2003). Several reports showed a correlation between the size of EC resection and the success rate of the surgery for intractable TLE (Siegel *et al.*, 1990; Fried *et al.*, 1993). EC resections often presented with atrophy and gliosis, while a particular vulnerability was demonstrated for the layer III neurons (Du *et al.*, 1993; Yilmazer-Hanke *et al.*, 2000). Animal studies are in line with human observations, showing neuronal damage in layer III of the EC (Du *et al.*, 1995; Wozny *et al.*, 2005). Opposite views exist on the localisation of seizure focus in the EC. Jones and Lambert (1990) showed that epileptiform activity emerged from the deep layers, while Tolner and colleagues (2005) demonstrated a superficial origin.

Based on the previous knowledge, we set out to investigate the role of EC in the epileptogenesis, using the RISE model. We explored the possibility of differential time scales for epilepsy development in the hippocampus and the EC, as well as a possible migration of a seizure focus. SWO were taken as a measure of network activity in the EC, which were recorded from layers II/III in both AMC and epileptic slices.

6.1.2. The EC and SWO

Slow brain rhythms constitute an important part of neurophysiology, as they appear during sleep and anaesthesia (Steriade *et al.*, 1993a-d). Slow rhythms have been

shown to group and modulate rhythmic activity of higher frequencies, reflecting active processes taking part in the brain during sleep (Steriade and Amzica, 1998). Studies report the occurrence of <1 Hz rhythms in the cortical regions of animals, both *in vivo* and *in vitro* (Steriade *et al.*, 1993a-d; Timofeev and Steriade, 1996; Sanchez-Vives and McCormick, 2000; Shu *et al.*, 2003; Dickson *et al.*, 2003; Cunningham *et al.*, 2006; Sheroziya *et al.*, 2009). The cortex has been shown to exhibit alternating 0.1-0.5 Hz periods of UP (intensive cell firing) and DOWN (periods of quiescence) states. This type of activity has been detected in prefrontal, somatosensory, visual and entorhinal cortices and implications in development, metabolism, as well as information processing have been proposed (Sheroziya *et al.*, 2009; Cunningham *et al.*, 2006; Steriade *et al.*, 1993c; Sanchez-Vives and McCormick, 2000).

A commonly accepted mechanism of slow rhythm generation in the cortex is a combined action of intrinsic and synaptic mechanisms, when activation of $I_{Na(p)}$ and I_{CAN} generate spiking of neurons and together with synaptic mechanisms sustain prolonged bursting, thus forming an UP state (Timofeev *et al.*, 2000; Bazhenov *et al.*, 2002; Sheroziya *et al.*, 2009; Chauvette *et al.*, 2010). DOWN states, on the other hand, reflect periods of hyperpolarisation mediated by K^+ currents and synaptic fatigue (Steriade *et al.*, 1993d; Sanchez-Vives and McCormick, 2000; Bazhenov *et al.*, 2002; Compte *et al.*, 2003; Sheroziya *et al.*, 2009). Moreover, interneurons supposedly govern the synchronised switch from to the DOWN state (Volgushev *et al.*, 2006; Puig *et al.*, 2008).

Of a particular interest to us was spontaneous rhythmic activity of <1 Hz in the EC reported by Dickson *et al.* (2003), Cunningham *et al.* (2006), Gnatkovsky *et al.* (2007) and Sheroziya *et al.* (2009). In these reports, SWO was generated by reducing Mg^{2+} and Ca^{2+} concentrations and/or electrical stimulation of the lateral olfactory tract, by setting the right level of excitation in the slice. While Sheroziya and colleagues (2009) detected slow rhythmic activity only in neonatal rats (P5–P13), others recorded from young adult guinea pig and adult rat brains, which raises a question whether this activity was a truly developmental phenomenon or a result of adjusted experimental conditions. SWO were recorded from layers II/III of the mEC in all studies, and findings from Marco de Curtis' laboratory (Dickson *et al.*, 2003; Gnatkovsky *et al.*, 2007) demonstrated that SWO were generated by the interaction of superficial layer

pyramidal cells and interneurons, although activity could still be recorded layer V mEC.

Although the <1 Hz cortical activity is widely associated with sleep and anaesthesia, the functional relevance might differ between the cortical areas. So far, a common theory has been involvement of SWO in information processing and memory consolidation. For example, Cunningham and colleagues (2006) demonstrated that the activity was driven by the interaction between neuronal network mechanism and metabolism-related mechanism. Sheroziya *et al.* (2009), on the other hand, showed that SWO activity reflected developmental processes and could be important in the maturation of EC and the hippocampus. Future *in vitro* studies combined with *in vivo* research will help uncover the role of alternating states of activity and quiescence.

Searching for network activity in the EC, the presence of spontaneous SWO in control and epileptic slices from young animals was observed. Much like in CA3 hippocampus, these spontaneous oscillations presented an opportunity to explore the differences between slices from healthy animals and from animals that had undergone RISE induction. SWO were a good reflection of the natural network state, therefore any changes in epileptic slices could suggest the effects of epileptogenesis. We, therefore, compared the basic electrophysiological and pharmacological profiles profile pharmacology/mechanism of SWO in both groups of slices.

6.2. Results

6.2.1. Basic profile in control slices

Using the same improved brain slice preparation technique, combined hippocampal-EC brain slices were prepared from healthy 50–100 g rats (n=47 number of animals 12). SWO was recorded from layers II/III of mEC in a traditional aCSF recipe in the absence of driving pharmacological agents. The frequency of SWO varied from 0.1 to 1.8 Hz, with the mean interburst frequency being 0.72 ± 0.1 Hz (n=27). Layers II/III demonstrated a range of electrographic patterns of oscillatory activity, consisting of rhythmic bursts and/or slow waves in various combinations (Fig. 6.1). The bursts lasted for 1.2 ± 0.1 s, while the burst amplitude was $106.9 \pm 13.8 \mu V^2$ with the mean

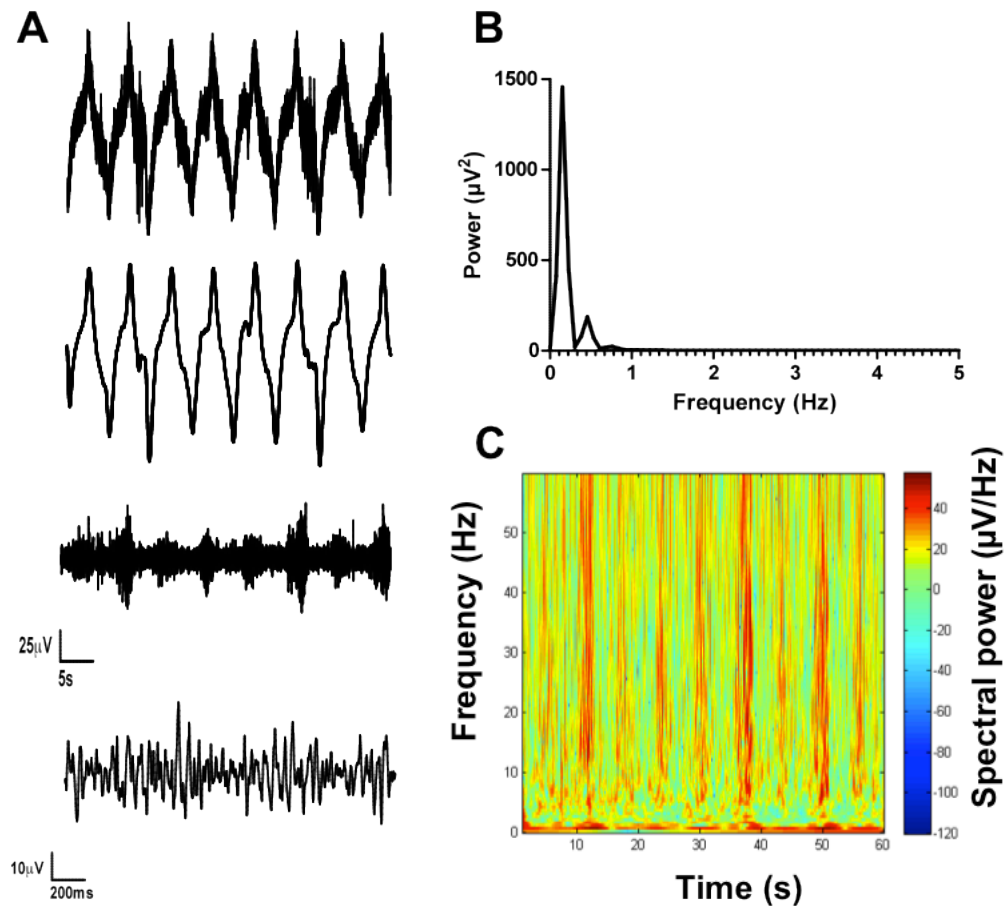


Figure 6.1. Basic profile of SWO in layers II/III of the mEC. **A.** Example unfiltered raw trace showing SWO, low-pass filtered (<1Hz) raw trace showing the slow component of SWO, band-pass filtered (5 – 60 Hz) traces revealing bursts of higher (>5 Hz) frequency activity. **B.** Representative power spectrum of unfiltered data showing a large peak at 0.15 Hz. **C.** Morlet wavelet time-frequency plot of unfiltered SWO data showing very low frequency activity with bursts of 5–40 Hz activity occurring approximately every 5s.

intraburst frequency of 28.97 ± 2.0 Hz ($n=27$). The patterns could be divided into following groups: synchronised bursts/single units with slow wave, synchronised bursts/single units with no slow wave, slow wave no bursts, as well as complex patterns with alternating bursts of higher and lower amplitude (Fig. 6.2). A number of slices exhibited occasional bursts and/or slow waves but no rhythmicity; such recordings were excluded from general characterisation but were included into some pharmacology experiments. The variability of observed oscillatory patterns did not appear to depend on animal age, experimental conditions or layer-specific position of the electrode. The differences in burst/spike patterns could depend on electrode position in relation to individual cells and cell populations. Once established, SWO

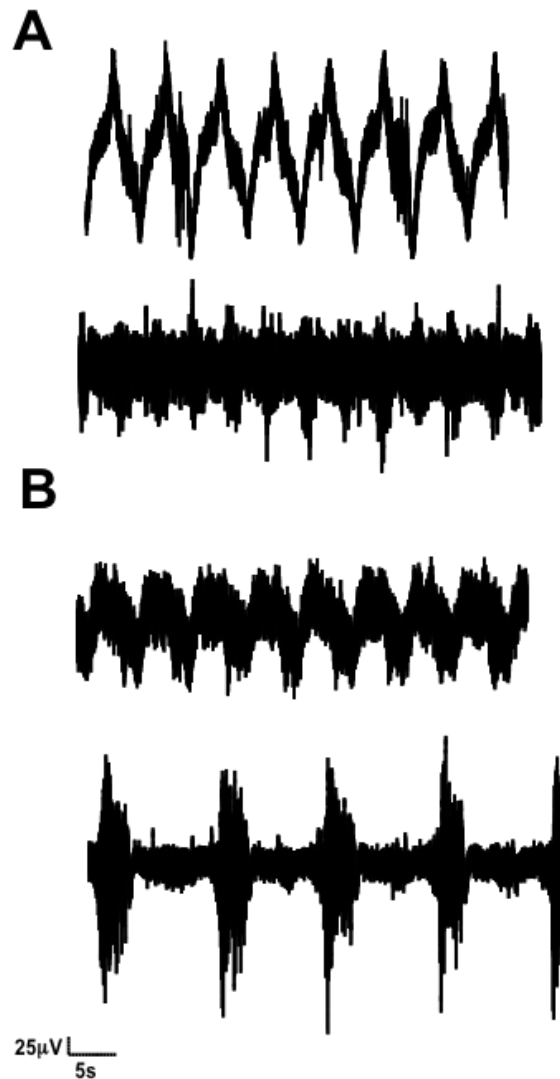


Figure 6.2. Variety of electrographic patterns of SWO in control and PSE 24h/7d slices.
A. Unfiltered raw traces of SWO recorded from layers II/III mEC of AMC slices. **B.** Unfiltered raw traces of SWO recorded from layers II/III mEC of PSE 24h/7d slices.

persisted for several hours, however, in some cases the frequency and the pattern were unstable over time. Apart from layers II/III, SWO could also be recorded from layer V of mEC (Fig. 6.3). Experiments with severed connections between mEC and the hippocampus, as well as between mEC and lateral EC showed that spontaneous SWO were still present in the mEC indicating an intrinsic nature of this activity.

One of the characteristic features of SWO in the mEC in healthy rats was the disappearance of activity in animals older than 100 g when recordings were made in normal aCSF with standard $[Mg^{2+}]$ and using a 30 minute period in which to test for the appearance of SWO activity. A cutoff at 100 g suggested some developmental

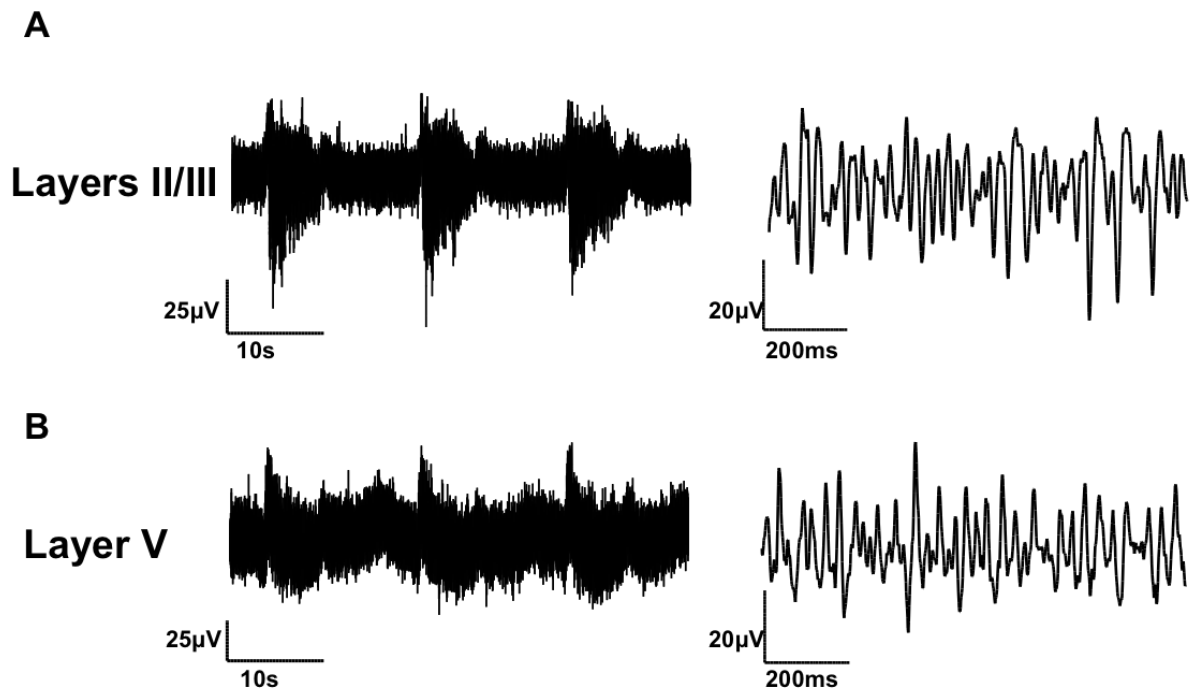


Figure 6.3. SWO in deep and superficial layers of the mEC. **A.** Unfiltered raw trace of SWO (left) recorded from layers II/III mEC of control slices. Band-pass filtered (10 – 60 Hz) raw trace (right) showing a burst of high-frequency component. **B.** Unfiltered raw trace of SWO (left) recorded from layer V mEC of control slices. Band-pass filtered (10 – 60 Hz) raw trace (right) showing a burst of high-frequency component.

changes taking place in the EC at this stage, however, by this age the development should be completed. Fig. 6.4 shows a plot of the percentage of slices exhibiting SWO within 30 minutes of commencing recording. It is clear that slices from chronically epileptic rats show an enhanced tendency towards generation of SWO. A number of brain slices from adult rats exhibited either irregular elements of slow activity (occasional bursts and/or slow waves) or episodes of rhythmic activity, however, these required several hours to develop. A possible explanation for this phenomenon could be a reduction of slice thickness over time and possibly better penetration/diffusion of the perfusate. To determine whether enhanced excitability in the slice would promote spontaneous SWO in slices from adult rats similar to Cunningham *et al.* (2006), we changed traditional aCSF to '*in vivo*-like' aCSF. Increasing the level of excitation in the slice promoted bursting and rhythmic activity, indicating insufficient excitation in adult slices to generate spontaneous rhythmic activity (Fig. 6.5).

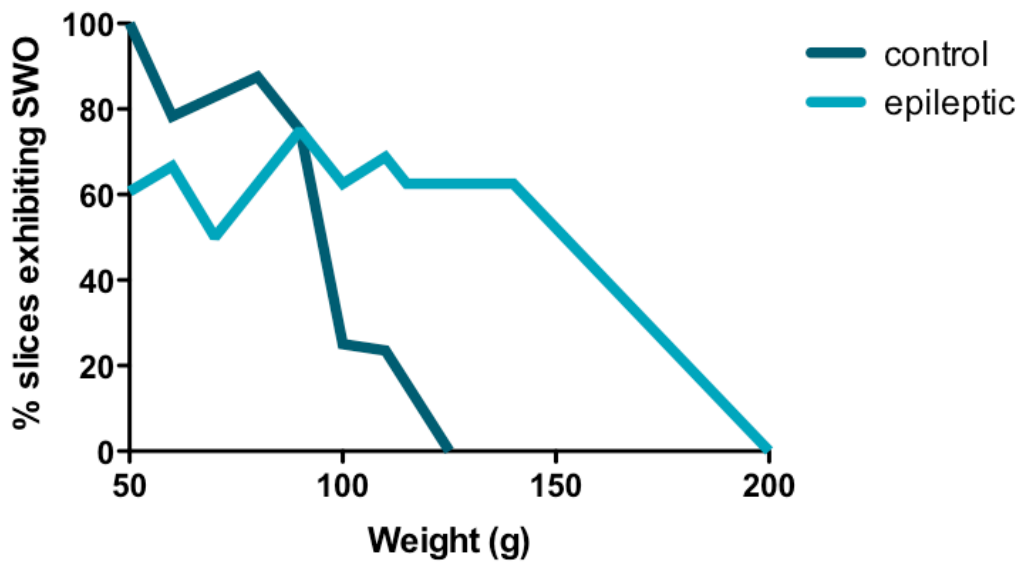


Figure 6.4. Differences in the developmental profile of SWO in control and epileptic slices. The graph shows an earlier decline of SWO occurrence in control compared to epileptic slices.

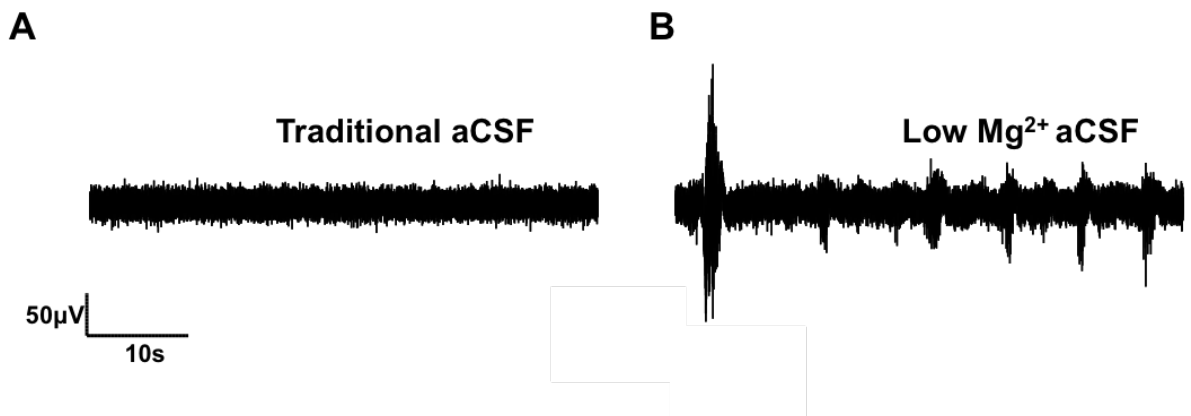


Figure 6.5. Reducing $[Mg^{2+}]_o$ promotes SWO in control adult slices. **A.** Unfiltered raw trace recorded from layers II/III mEC of a control slice in traditional aCSF composition. **B.** Unfiltered raw trace recorded from layers II/III mEC of a control slice in low Mg^{2+} aCSF composition.

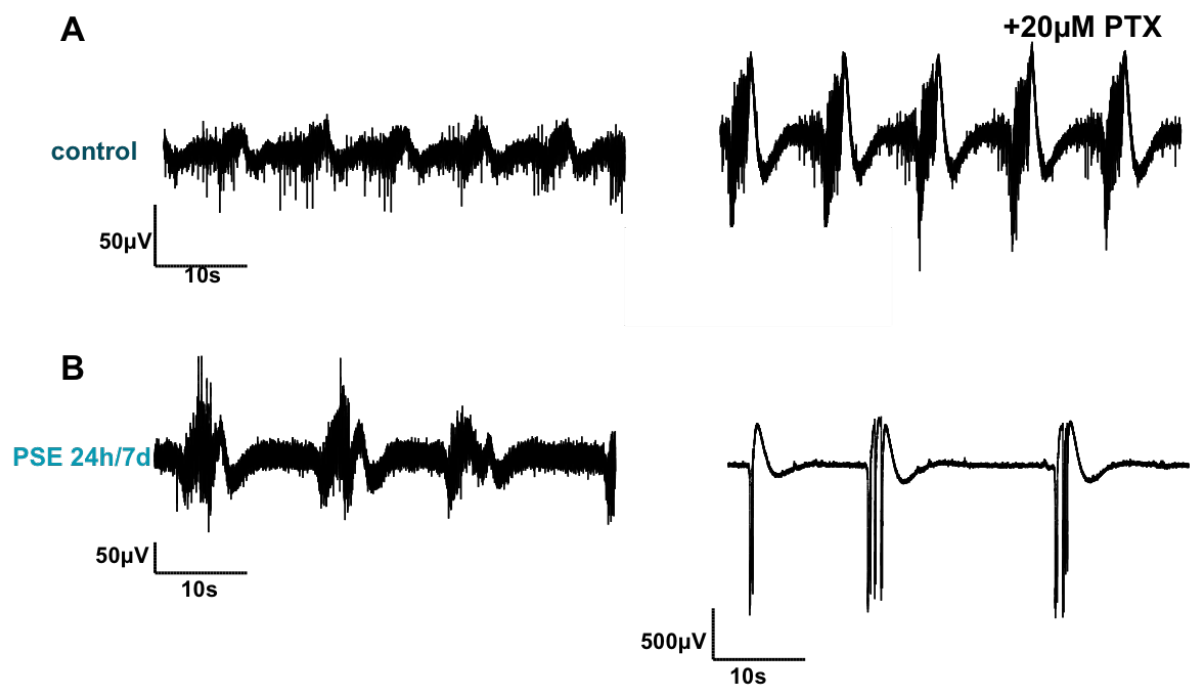


Figure 6.6. Differential effects of GABA-Ar blockade on SWO in control and PSE 24h/7d slices. **A.** Unfiltered raw traces in control (left) and 20 µM PTX (right) conditions in a control slice. PTX enhances SWO. **B.** Unfiltered raw trace in control (left) and 20 µM PTX (right) in a PSE 7d slice. PTX transforms SWO into interictal discharges.

6.2.2. Pharmacological characterisation

We explored the contribution of synaptic component into generation and maintenance of spontaneous SWO activity in the mEC. We started the pharmacological characterisation by looking at GABA-ergic inhibition, as it is known to be involved in network synchronisation. Application of GABA-Ar blocker PTX (20 µM) enhanced slow rhythmic activity, increased burst amplitude by $46 \pm 18\%$ ($p < 0.05$, $n=4$) and the intraburst frequency by $44.73 \pm 12\%$ ($p < 0.05$, $n=4$; Fig. 6.6A). Although blocking GABA-Ar increased the amplitude of bursts, it did not promote synchronisation of cell firing. It should be noted that blocking the inhibition was able to generate SWO in slices with no initial activity. The results suggest that GABA-ergic inhibition does not have the same function in the generation of spontaneous SWO, as compared to gamma rhythm synchronisation. The function of slow GABA-Br-mediated inhibition was explored by administration of receptor antagonist CGP 55845 (5 µM). GABA-Br blockade seemed prolong burst duration in some slices (Fig. 6.7A), however, this was not significant ($p > 0.05$, $n=5$). CGP 55845 promoted SWO in some slices without pre-existing spontaneous activity.

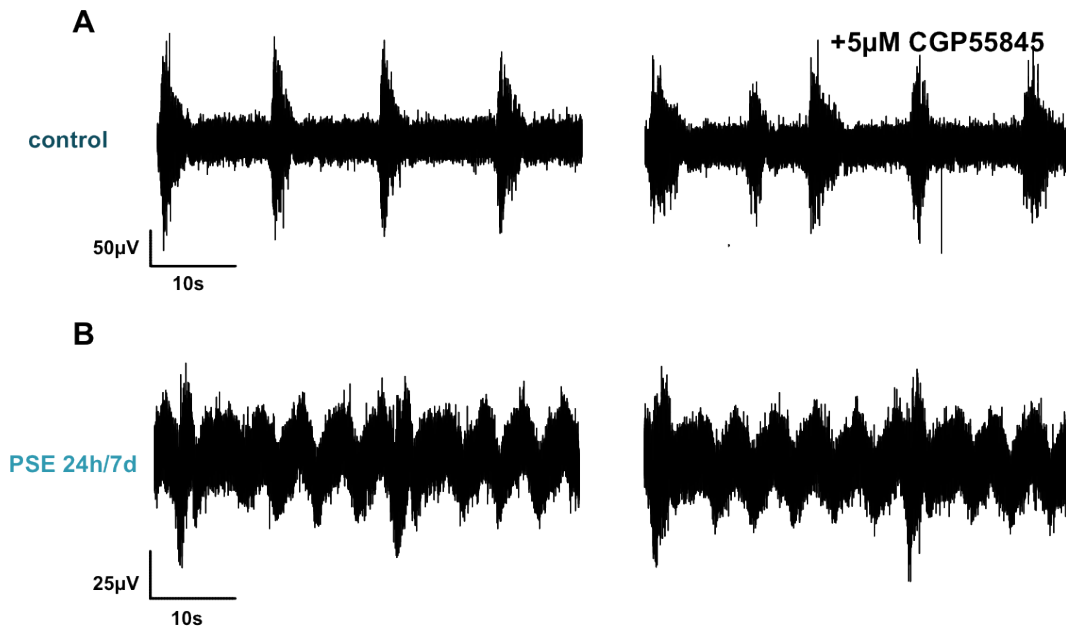


Figure 6.7. The effects of GABA-Br blockade on SWO in control and PSE 24h/7d slices. **A.** Unfiltered raw traces in control (left) and 5 μM CGP55845 (right) conditions in a control slice. **B.** Unfiltered raw trace in control (left) and 5 μM CGP55845 (right) in a PSE 7d slice.

We next investigated the role of ionotropic glutamatergic transmission by blocking NMDAr, AMPAr/KAr, AMPAr, KAr and with 20 μM MK-801, 20 μM CNQX, 2.5 μM NBQX, and 3 μM UBP310, respectively. The contribution of NMDAr was inconclusive, since changes in none of the measured burst parameters reached significance ($p > 0.05$, $n = 4$ for both amplitude and duration); Fig. 6.8A, however, shows there was a tendency for NMDAr antagonist to increase burst amplitude and reduce the frequency of SWO. Application of CNQX abolished all spontaneous activity in layers II/III of the mEC in 10/10 slices, as illustrated in Fig. 6.9A. Administration of UBP310, a selective GluK1 and GluK3-containing KAr antagonist, readily abolished all spontaneous activity in the mEC in 7/7 slices, indicating that KAr-mediated transmission was a crucial part of the generation mechanism (Fig. 6.10A). When 200 nM KA was applied, a cessation of SWO was observed prior to the emergence of persistent gamma oscillations in the mEC (Fig. 6.11). Selective blockade of AMPAr with low concentration NBQX (2.5 μM) produced mixed effects, as it terminated all activity in 2 out of 7 slices, while abolished or reduced only the burst component but kept the rhythmic slow wave in 4 out of 7 slices (Fig. 6.12A). In one slice with a complex oscillatory pattern, NBQX selectively abolished low amplitude bursts, yet retained large bursts and a slow wave. Overall, NBQX reduced SWO power by $14.4 \pm 17.0\%$, however, this was not significant ($p > 0.05$, $n = 7$).

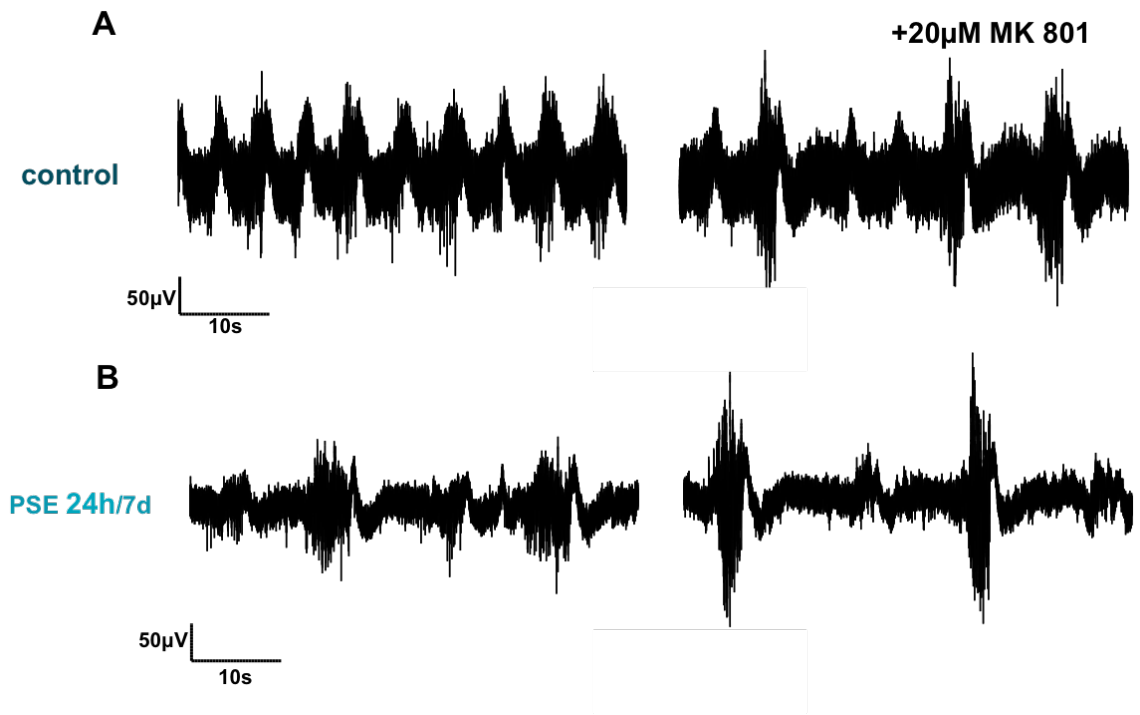


Figure 6.8. NMDA receptor blockade reduces the interburst frequency but increases burst amplitude in control and PSE 24h/7d. **A.** Unfiltered raw traces in control (left) and 20 µM MK801 (right) conditions in a control slice. **B.** Unfiltered raw trace in control (left) and 20 µM MK801 (right) in a PSE 7d slice.

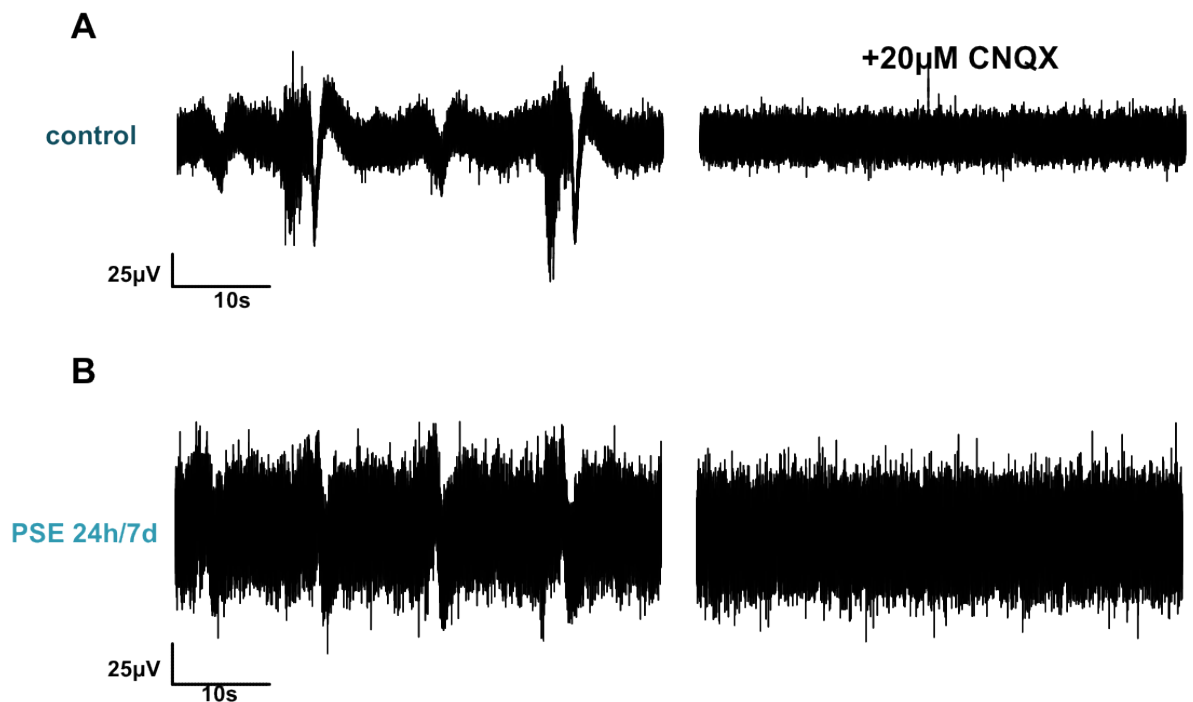


Figure 6.9. AMPA/KAR blockade abolishes SWO in control and PSE 24h/7d slices. **A.** Unfiltered raw traces in control (left) and 20 µM CNQX (right) conditions in a control slice. CNQX abolishes all activity. **B.** Unfiltered raw trace in control (left) and 20 µM CNQX (right) in a PSE 7d slice. CNQX abolishes all activity.

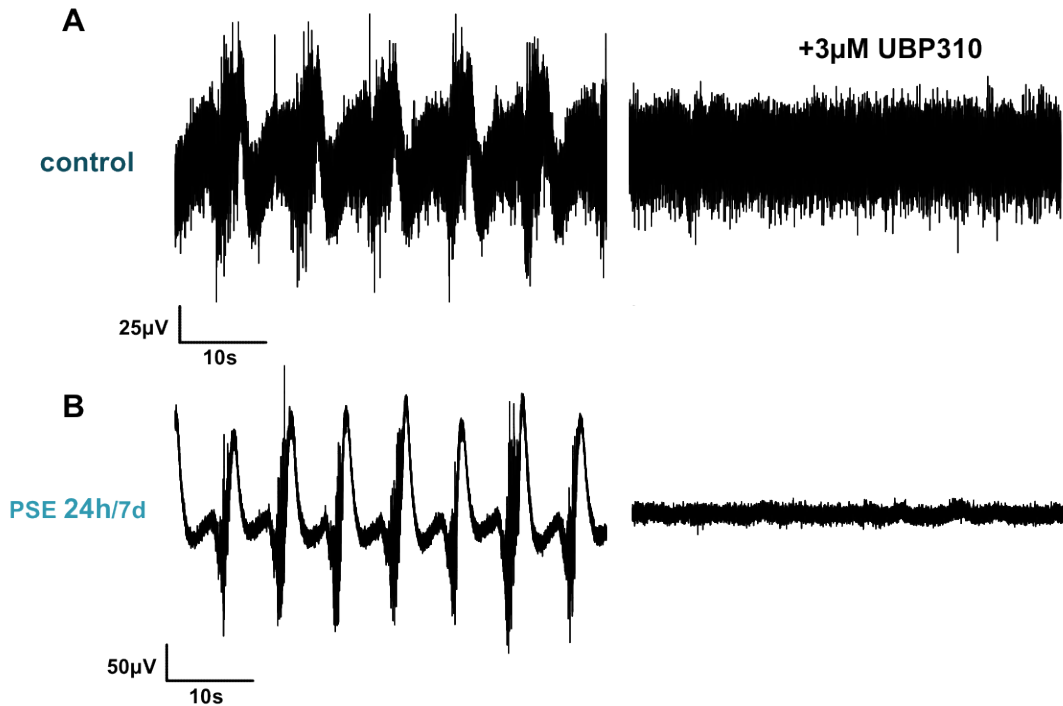


Figure 6.10. GluK1,3 KAr blockade abolishes SWO in control and PSE 24h/7d slices . **A.** Unfiltered raw traces in control (left) and 3 μ M UBP310 (right) conditions in a control slice. UBP310 abolishes all activity. **B.** Unfiltered raw trace in control (left) and 3 μ M UBP310 (right) in a PSE 7d slice. UBP310 abolishes all activity.

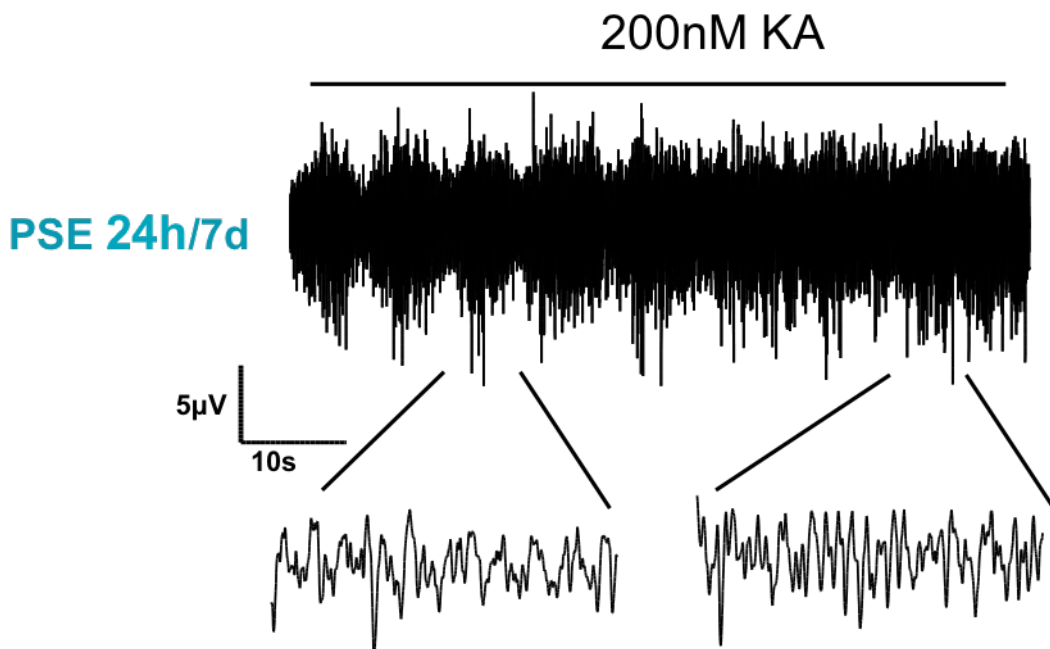


Figure 6.11. The effect of KAr activation on SWO in PSE 24h/7d. Figure shows an unfiltered raw trace of SWO at the onset of KA effect, demonstrating a gradual transformation of SWO into a persistent gamma rhythm. An increase in the frequency of the fast component is observed, while the low-frequency modulation of amplitude (burstiness) disappears.

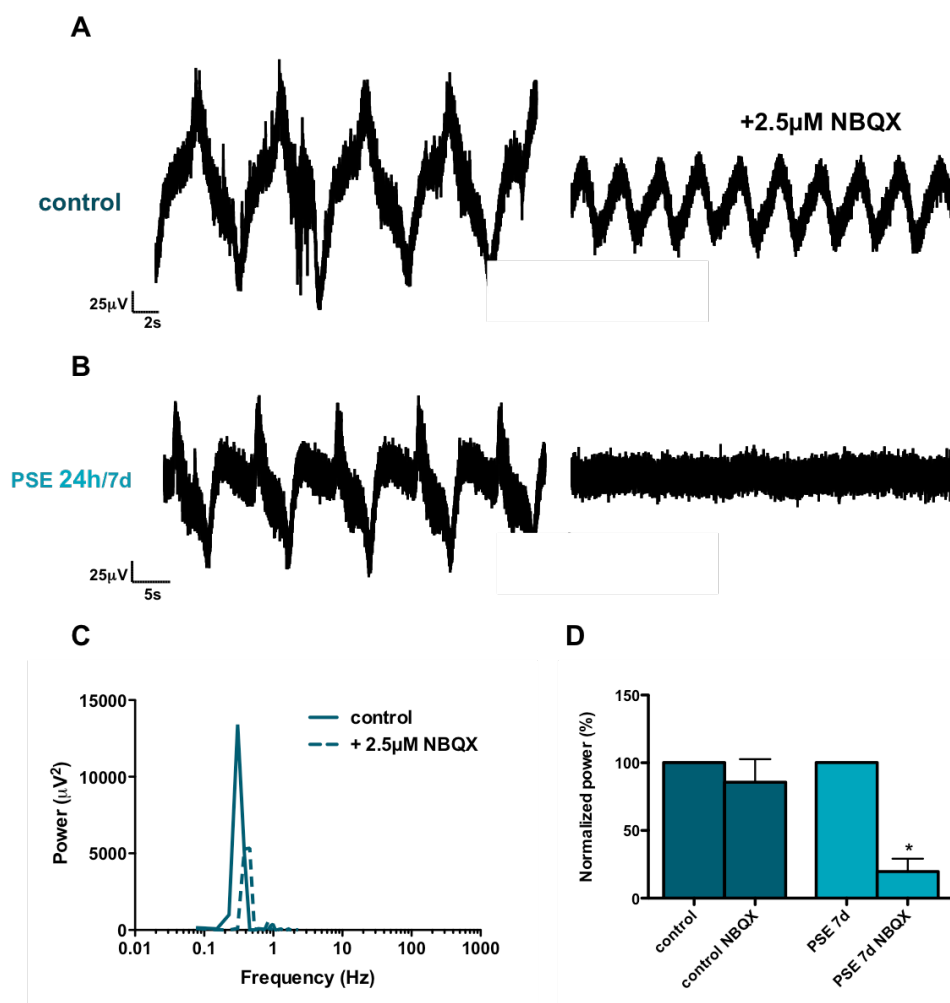


Figure 6.12. AMPA blockade abolishes SWO in PSE 24h/7d but not control slices . **A.** Unfiltered raw traces in control (left) and 2.5 μM NBQX (right) conditions in a control slice. NBQX abolishes bursts of high frequency activity but retains the slow wave. **B.** Unfiltered raw trace in control (left) and 2.5 μM NBQX (right) in a PSE 7d slice. NBQX abolishes all activity. **C.** Power spectra showing the effect of AMPA blockade on SWO in control slices. **D.** Pooled data showing the effect of NBQX on the peak power of SWO in control and PSE 7d slices. * indicates $p < 0.05$.

The contribution of slow glutamatergic transmission mediated by mGluRs was explored using selective antagonists for groups I and II/III (MTEP and LY 341495). The results showed apparent potentiation of spontaneous slow rhythmic activity produced by both antagonists. The effect of MTEP on SWO parameters did not reach significance ($p > 0.05$, $n = 6$). Group II and III antagonist LY 341495 increased the number of events in the bursts by $54.2 \pm 13.2\%$, $p < 0.01$, and the intraburst frequency by $23.4 \pm 6.4\%$, $p < 0.05$ ($n = 8$). Blocking mGluRs appeared to enhance the synchrony of bursting cells, which is visible from the Morlet wavelet time-frequency spectrograms (Figs. 6.13A and 6.14A). These findings might indicate an indirect modulation of GABA release taking part in the network synchronisation.

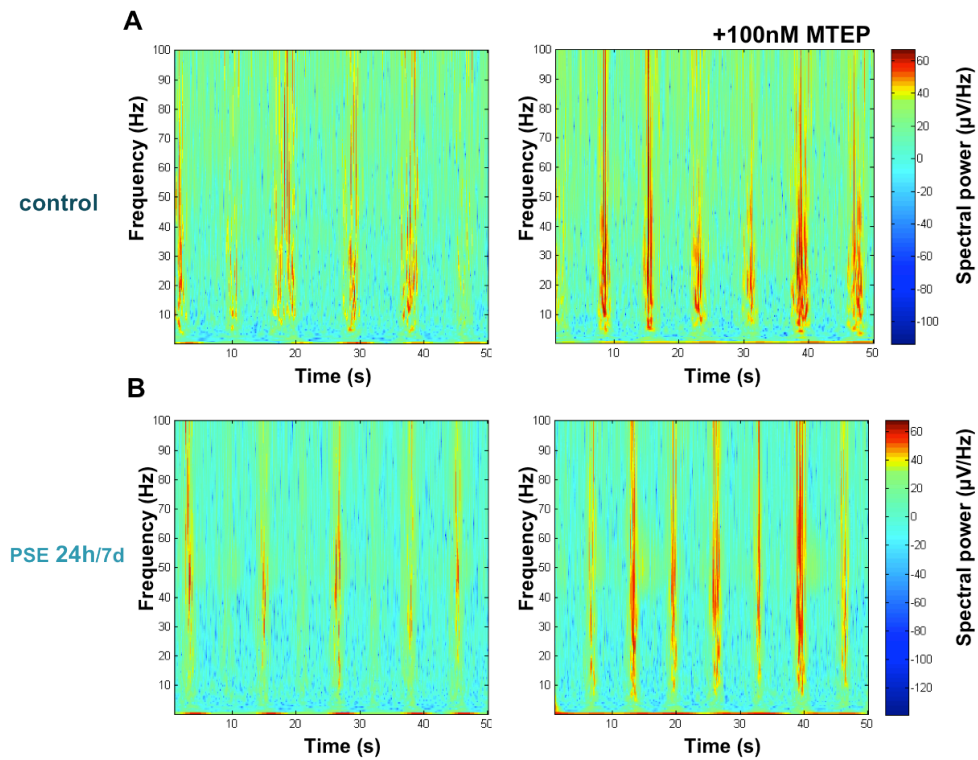


Figure 6.13. mGluR₅ blockade promotes intraburst synchrony in control and PSE 24h/7d. **A.** Morlet wavelet time-frequency plots in control (left) and 100 nM MTEP (right) conditions in a control slice. **B.** Morlet wavelet time-frequency plots in control (left) and 100 nM MTEP (right) in a PSE 7d slice.

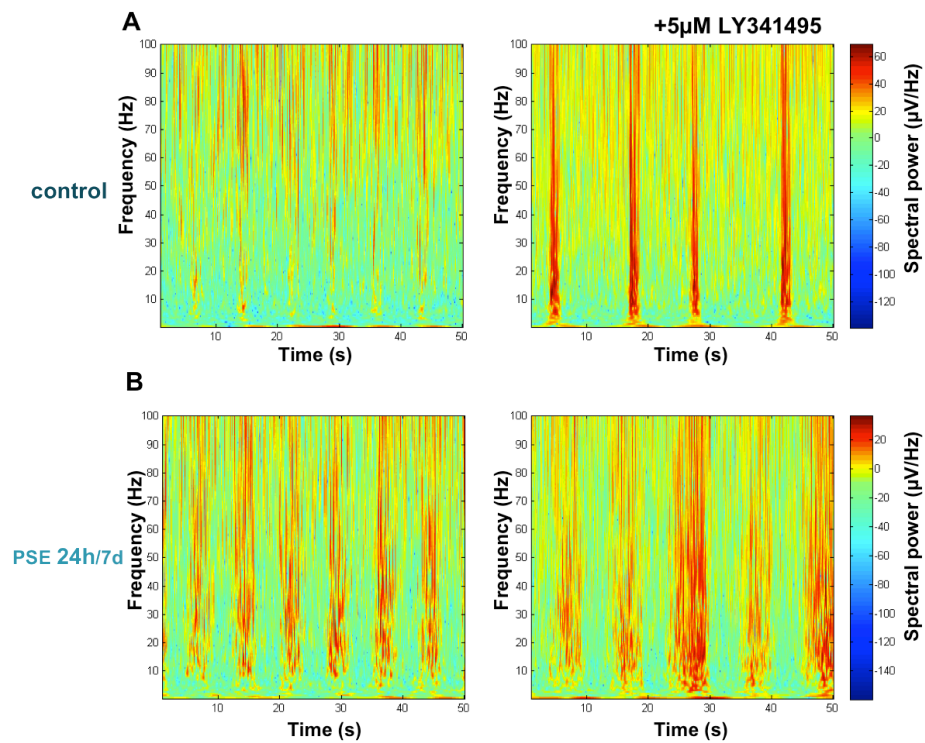


Figure 6.14. mGluR groups II/III blockade promotes intraburst synchrony in control and PSE 24h/7d. **A.** Morlet wavelet time-frequency plots in control (left) and 5 μM LY341495(right) conditions in a control slice. **B.** Morlet wavelet time-frequency plots in control (left) and 5 μM LY341495 (right) in a PSE 7d slice.

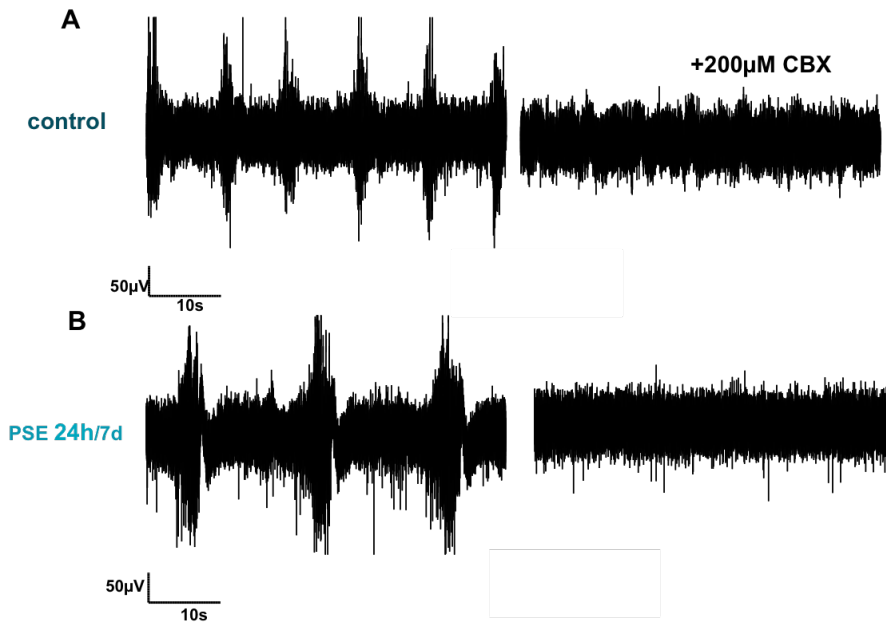


Figure 6.15. Gap junction blockade abolishes SWO in control and PSE 24h/7d. **A.** Unfiltered raw traces in control (left) and 200 μM CBX (right) conditions in a control slice. **B.** Unfiltered raw trace in control (left) and 200 μM CBX (right) in a PSE 7d slice.

Previous studies have shown that gap junctions play an important role in network synchronisation at high and very high frequencies (Hormuzdi *et al.*, 2001; Buhl *et al.*, 2003; Draguhn *et al.*, 1998). Application of gap junction blocker, CBX, at 200 μM abolished all activity in 3 out of 8 slices. In the rest of the slices (5/8), CBX caused a decrease in SWO power (Fig. 6.15A). Overall, CBX application reduced SWO by $50.41 \pm 20.5\%$ ($p < 0.05$, $n=8$). These findings confirm that SWO share the same mechanisms with the persistent high frequency activity such as gamma rhythm oscillations.

6.2.3. Spontaneous SWO in RISE

SWO were observed in combined hippocampal-EC slices from animals that had undergone epilepsy induction (RISE). The activity was most prominent in layers II/III of the mEC in PSE 24h and PSE 7d animals, corresponding to 50-140 g. Overall, spontaneous SWO in epileptic rats were similar in their basic characteristics to the ones observed in control animal with mean burst duration 1.3 ± 0.2 s, inter- and intraburst frequencies being 0.21 ± 0.05 Hz and 27.9 ± 2.2 Hz ($n=31$). The mean peak amplitude, however, was significantly lower compared to control slices (61.14 ± 7.2

μV^2 vs. $106.9 \pm 13.8 \mu V^2$, $p < 0.01$). Epileptic slices also resembled AMC slices in a variety of produced oscillatory patterns of low frequency (Fig. 6.2).

Interestingly, in AMC slices spontaneous SWO disappeared, with rare exceptions, after the animals reached 100g. On the other hand, in animals that had previously undergone SE spontaneous SWO were still prominent between 100-140 g, suggesting underlying differences in brain development or network excitability in epileptic animals. The percentage of spontaneously active slices from the 100 – 140 g weight category was 21.2% (7/33) in control vs. 65% (26/40) in epileptic slices, as illustrated by Fig. 6.4. No evident spontaneous activity was observed in the mEC of adult animals further into epilepsy development, perhaps indicating that similarly to healthy animals, SWO activity undergoes some form of developmental regulation in the epileptic brain.

6.2.4. Pharmacology of SWO in epileptic slices

Taking into account the differences in developmental profile of SWO in control and epileptic slices, we investigated whether SWO in epileptic animals were driven by the same mechanisms. The results demonstrated in Fig. 6.6B showed that GABA-Ar blockade produced similar effects as in AMC by enhancing SWO, however, unlike control slices, PTX quickly transformed SWO into interictal type activity ($n=4$). Blocking GABA-Br-mediated slow inhibition seemed to decrease the frequency of bursts, however the results again did not reach significance ($p > 0.05$, $n=5$). GABA-Br blockade effects are demonstrated in Fig. 6.7B. Overall, it appeared that GABA-ergic inhibition remained in balance with excitation, which allowed generation of SWO in the mEC in both control and epileptic slices.

NMDAr antagonist seemed to increase the amplitude of bursts, which was similar to control slices, however, the results did not reach significance ($p > 0.05$, $n=4$) Fig. 6.8B). We then explored the role of excitation by blocking AMPAr and KAr with $20 \mu M$ CNQX, which abolished all rhythmic activity in 5/5 slices (Fig. 6.9B), suggesting a crucial role of these receptors in SWO generation. In order to separate KAr and AMPAr contributions to SWO mechanism, selective antagonists ($3 \mu M$ UBP 310 and $2.5 \mu M$ NBQX, respectively) were administered. UBP 310 had a similar effect as in AMC, terminating SWO in 5 out of 6 slices (Fig. 6.10B). KA application demonstrated

the same action on SWO, as in AMC, transforming slow activity into a persistent gamma rhythm (Fig. 6.11). The most interesting effect, however, was produced by low dose (i.e. AMPAR selective) NBQX (2.5 μ M), which nearly abolished rhythmic activity in all slices (reduction of SWO power by $80.38 \pm 9.5\%$, $n=7$, $p<0.05$), indicating that, unlike control slices, both slow and fast components of SWO were AMPAR-dependent in epileptic slices (Fig. 6.12). These findings might be the key element underlying the difference between healthy and pathological networks in the EC.

Investigation of mGluR contribution to SWO generation in PSE 24h – PSE 7d slices yielded similar results as in AMC. Although the parameters did not reach statistical significance, blocking mGluR groups I ($n=8$) and II/III ($n=5$) had a positive effect on spontaneous activity, enhancing SWO and promoting synchronisation of the UP states (Figs. 6.13, 6.14). And finally a gap junction blocker, CBX, abolished all activity in 4/7 epileptic slices, overall decreasing SWO power by $73.12 \pm 14.2\%$ ($p<0.01$, $n=7$). CBX effects showed a substantial contribution of electrical coupling in the generation of SWO in both control and epileptic slices (Fig. 6.15).

6.3. Discussion

6.3.1. Basic profile of SWO in control vs. epileptic slices

Improving brain slice preparation technique has resulted in an increased viability of slices and a better preservation of local neuronal networks. This has allowed for the slices to exhibit their natural activity not only in the hippocampus, but also in the EC. Spontaneous SWO observed in the brain slices from young rats were similar to those reported *in vitro* by Dickson *et al.* (2003), Cunningham *et al.* (2006) and Sheroziya *et al.* (2009). SWO in the mEC were detected in control animals younger than 100 g, suggesting late developmental/age-dependent changes such as reduction in cellular excitability, which prevent the activity from appearing spontaneously under normal experimental conditions. It seems plausible that ambient glutamate levels play an important role in spontaneous generation of SWO, hence the developmental upregulation of glutamate transporters (Danbolt, 2001) and an increase of extracellular space could lead to the disappearance of rhythmic activity in slices from older animals (Sykova *et al.*, 2000). Based on the previous studies of spontaneous oscillations in EC, it appears that by adjusting the level of excitability, either by

changing aCSF composition or by electrical stimulation, it is possible to manipulate the appearance of rhythmic activity. Therefore, in our experiments, 'in vivo-like' aCSF was able to generate slow oscillations in the mEC of the adult animal slices. Chamberlain (2009) investigated the changes produced by lowering Mg^{2+} concentration, which allowed for the generation of SWO in adult slices. Reducing $[Mg^{2+}]$ was shown to increase glutamate release, which strongly activated GluK1 KAR, which, in turn, increased GABA release (Chamberlain, 2009).

In contrast to AMC slices, epileptic slices (PSE 24h and PSE 7d) produced evident SWO in animals up to 140 g, suggesting two possible mechanisms: delayed development or increased excitability of epileptic slices. Hence, the stressful insult of SE and associated damage to sensitive neural circuits may result in a delayed neurodevelopment. Another possibility for a prolonged appearance of spontaneous SWO in epileptic slices is tissue hyperexcitability due to such factors as increased levels of ambient glutamate, enhanced sensitivity of receptors and others. These effects may occur as a result of epilepsy establishment in the EC and, indeed, may reflect the early stages of altered balance between excitation and inhibition.

A variety of oscillatory patterns generated by local cortical networks might suggest a multicomponent mechanism of SWO. The patterns clearly showed interchanging periods of high (UP state) and low (DOWN state) activity at ~ 0.7 Hz, resembling that reported by Steriade *et al.* (1993c,d) during sleep and anaesthesia. In both AMC and epileptic slices, UP states were represented by bursts of single-unit spikes, epochs of synchronised 10-40 Hz activity and/or ascending part of the slow wave. Intracellular studies in the literature suggested that UP states were generated by intensive neuronal firing, represented by unit activity or local network oscillations, while DOWN states reflected periods of hyperpolarisation (Dickson *et al.*, 2003; Cunningham *et al.*, 2006; Gnatkovsky *et al.*, 2007; Sheroziya *et al.*, 2009). The complex structure of SWO contains a low frequency component, which reflects the temporally broad cellular excitability, and a fast component, which determines the exact timing when an AP is generated (Hasenstaub *et al.*, 2005). A large number of our slices (both AMC and epileptic) exhibited SWO with superimposed periods of fast (theta/gamma) oscillations, which resembled the ones described by Le Van Quyen *et al.* (2010) in human EC during sleep. Indeed, the authors showed that gamma frequency

episodes appeared at the UP states of slow oscillations during slow-wave sleep and were coherent over a single cortical region. Similar patterns of activity have been reported in animals *in vivo* by Steriade *et al.* (1996), Isomura *et al.* (2006) and *in vitro* by Dickson *et al.* (2003) and Compte *et al.* (2008), indicating a common cortical phenomenon. Cellular studies did not identify rhythmicity in the firing pattern; however, the firing was phase-locked to the gamma rhythm, reflecting sparse neuronal participation in the rhythmogenesis (Compte *et al.*, 2008; Le Van Quyen *et al.*, 2010).

Much research has been conducted on the origin of SWO and its laminar cortical profile. It has been established by several studies that SWO emerged intracortically, which was also confirmed in our experiments with preserved spontaneous rhythmic activity in isolated mEC slices (Steriade *et al.*, 1993e; Timofeev and Steriade, 1996). Previous reports demonstrated that the activity was generated in the superficial layers of the EC, although deep layer origin has also been reported in other areas (Cunningham *et al.*, 2006; Gnatkovsky *et al.*, 2007, Sheroziya *et al.*, 2009; Sanchez-Vives and McCormick, 2000; Chauvette *et al.*, 2010). Contrary to the observations of Cunningham and colleagues (2006), spontaneous SWO recorded by our group persisted in layers II/III and V of the mEC, suggesting the propagation of activity from superficial to deep layers.

6.3.2. Pharmacology of SWO in control vs. epileptic slices

The presence of spontaneous SWO in the EC can be used as a measure of neuronal network activity, which is important in the context of TLE. We, therefore, explored pharmacological properties of SWO in both epileptic and AMC slices to determine the nature of spontaneously occurring activity, as well as to compare it between healthy and pathological conditions. Pharmacological characterisation revealed that SWO in the EC shared similar elements of generation mechanism with higher frequency rhythmic activity, such as earlier described SyO. Related to this point is the fact that gamma oscillations appeared as a part of slow activity. According to previous studies, SWO in the cortex emerged from the balance between recurrent excitation and inhibition with contributing intrinsic mechanisms (Shu *et al.*, 2003; Compte *et al.*, 2003, 2008; Haider *et al.*, 2006). We investigated the role of synaptic component by

application of selective agonists and antagonists for the main types of receptors known to be involved in rhythmogenesis. The findings showed that glutamatergic transmission, especially mediated by KAr and AMPAr, was the key player in the generation of SWO in the mEC. It appeared that ambient levels of glutamate were sufficient to spontaneously produce SWO, which were readily blocked by CNQX both in our experiments and in literature (Cunningham *et al.*, 2006 in EC; Sanchez-Vives and McCormick, 2000; Shu *et al.*, 2003 in other regions). Reliable abolition of SWO with GluK1,3-containing KAr antagonist (in line with Cunningham *et al.*, 2006) and high doses of agonist (KA) suggested a window of receptor activation allowing for the generation of rhythmic activity in both control and epileptic slices.

Interestingly, the role of AMPAr and its change in epileptic animals was fundamentally different to controls. As might be expected, blockade of AMPAr reduced the general level of excitation and decreased SWO bursts in control slices, however, the slow component of SWO often remained and abolition of all activity was only ever achieved in the presence of KAr blockade. These findings indicate that both fast excitation through AMPAr and slower excitation via KAr is required for full expression of SWO activity under control conditions. Interestingly, observations by the Cunningham group (Cunningham *et al.*, 2006) showed increased cell firing produced by an AMPAr antagonist, which might seem to be at odds with our data, although we did not conduct any intracellular recordings with which to make direct comparisons. Taking into account the fact that KAr blocker abolished all activity, while AMPAr blockers only reduced it, control SWO appear to rely more on KAr-mediated excitation. A different picture was observed in PSE 24h and PSE 7d slices, where all rhythmic activity (both fast and slow) was abolished by AMPAr blockade, suggesting greater participation of these receptors in SWO. These results suggest an increase in the function of AMPAr in the early stages of epileptogenesis, which might reflect neuronal network alterations due to either an initial insult (SE) or a progressing establishment of epilepsy. Several factors could account for that, including altered expression with insertion of AMPAr caused by the SE and abnormal receptor function due to delayed development. Previous reports in literature have demonstrated AMPAr plasticity taking place after SE. Rajasekaran and colleagues (2012) showed a loss of GluA2 and an increase in GluA1 subunits of AMPAr following the SE, which resulted in another source of Ca^{2+} entry into the neurons (as GluA2-lacking AMPAr

flux Ca^{2+}), thus increasing excitability and possibly susceptibility to seizures, which we have observed spontaneously in PSE 7d slices in the EC. Ca^{2+} -permeable AMPAR are not only a pathological, but also a developmental feature, as GluA2-lacking AMPAR are replaced by Na^+ and K^+ -permeable GluA2-containing AMPAR during development, which has been shown in CA1 (Stubblefield and Benke, 2010). Therefore, taking into account delayed development in our PSE 24h/7d slices, it is plausible that AMPAR remained in their developmental state. Furthermore, Abegg *et al.* (2004) have shown that in the hippocampus epileptiform activity strengthens excitatory synapses by increasing the number of functional AMPAR. By contrast, Hu and colleagues (2012) demonstrated a reduction of AMPAR following the SE, however they also observed changes in the subunit composition of the receptors, which might suggest that in our model it is not the quantity, but the “quality” (perhaps efficacy) of AMPAR that may alter network activity and play a role in epileptogenesis.

In agreement with Cunningham *et al.* (2006), but contrary to other reports (Sanchez-Vives and McCormick, 2000; Shu *et al.*, 2003; Sheroziya *et al.*, 2009), NMDAR did not appear to play a crucial role in the mechanism of SWO neither in AMC nor in epileptic slices. By contrast, recorded rhythmic activity, especially its burst component, was significantly affected by mGluR groups I-III antagonists, which enhanced theta/gamma oscillations nested on the slow wave by modulating the levels of glutamate and GABA via different mechanisms. Errington and colleagues (2011) demonstrated an increase in tonic inhibition by activation of the group I mGluR. Activation of mGluR group II is known to presynaptically reduce glutamate release in the EC (Bandrowski *et al.*, 2003; Wang *et al.*, 2012). Woodhall *et al.* (2001) demonstrated that mGluR group III were not tonically activated in the EC, hence are probably not involved in the generation of SWO. Overall, the findings suggested that tonically activated mGluR contributed to the balance of excitation and inhibition, which gave rise to SWO. Sheroziya and colleagues (2009) also demonstrated that application of a group I/II antagonist E4CPG did not abolish intrinsic bursting of layer III neurons.

The disinhibition of control and epileptic slices with a GABA-Ar blocker produced differential effects on spontaneous SWO. Previous studies have demonstrated that blocking GABA-Ar transformed SWO into epileptiform activity (Sanchez-Vives and

McCormick, 2000; Shu *et al.*, 2003; Sheroziya *et al.*, 2009). Our experiments, on the other hand, showed interictal-type activity in PSE 24h and PSE 7d, but not in control slices, where merely a potentiation of SWO was observed. In control slices, PTX appeared to create favourable conditions for the SWO development. However, the disinhibition of epileptic slices revealed a somewhat augmented excitatory component, which could be associated with the change in AMPAr function. Blocking slow GABA-Br resulted in what seemed like an enhancement of rhythmic activity, suggesting GABA-Br acted to suppress slow activity and kept it at a slow pace, although the effect was not consistent. The role of inhibition in control over UP and DOWN states has previously been explored in the EC by Mann and colleagues (2009). They demonstrated that increasing concentrations of gabazine (GBZ) shortened the duration of the UP state and increased the spiking frequency, eventually transforming it into epileptiform activity. GABA-Br, on the other hand, were involved in the UP state termination, as GABA-Br blockade resulted in a prolongation of UP states, which is generally in line with some of our findings. It has been demonstrated that DOWN states appeared synchronously (Volgushev *et al.*, 2006), hence Mann and colleagues (2009) suggested that it was GABA-Br that determined the transition from active to silent state, together with GABA-Ar controlling spike rate and synchrony.

Application of a gap junction blocker produced a marked overall reduction of SWO power, suggesting the involvement of gap junctions in the both slow and fast network synchronisation, which has been previously established in gamma oscillations (Hormuzdi *et al.*, 2001; Buhl *et al.*, 2003). By contrast, Sheroziya *et al.* (2009) showed that SWO were not affected by a gap junction blocker.

Despite a substantial body of literature on slow sleep oscillations observed in various cortical regions, pharmacological studies are limited to the effects of GABA and iGluR antagonists. Considering the importance of synaptic transmission in the generation of SWO, it is necessary to carry out a more in depth analysis to determine more contributing elements. We, therefore, investigated the roles of mGluRs and gap junctions, together with the basic pharmacology, which we compared to previous literature. It would also be interesting to explore cholinergic and histaminergic effects

on SWO, as these systems are known to be involved in sleep/wakefulness processes.

6.3.3. Functional significance and relation to *in vivo* studies

To understand the functional relevance of *in vitro* findings, the results need to be considered in the context of *in vivo* animal and human research. Spontaneous SWO have been initially observed in animals *in vivo* during sleep and anaesthesia by the group of M. Steriade (Steriade *et al.*, 1993a-e). Since then SWO have been recorded and explored in different cortical areas in both animals and humans (e.g. Timofeev *et al.*, 2000; Hasenstaub *et al.*, 2005; Isomura *et al.*, 2006; Volgushev *et al.*, 2006; Luczak *et al.*, 2007; Csercsa *et al.*, 2010; Le Van Quyen *et al.*, 2010 and other). Different functions of slow rhythmic activity have been proposed, some of the most popular being memory consolidation, information processing, homeostatic and developmental (Steriade and Timofeev, 2003; Huber *et al.*, 2004; Luczak *et al.*, 2007; Tononi and Cirelli, 2006; Cunningham *et al.*, 2006; Sheroziya *et al.*, 2009).

Interestingly, Le Van Quyen *et al.* (2010) reported episodes of gamma oscillations appearing on the UP states of SWO in the EC of sleeping humans during slow-wave sleep (non-REM). This activity closely resembled our observations in the rat EC. Le Van Quyen and colleagues suggested that, since fast rhythmic activity was similar to that appearing in wakefulness, these ‘microwakes’ reflected or ‘replayed’ previously experienced events in a form of synchronisations incorporated into slow wave sleep activity (Ji and Wilson, 2006). Authors also pointed out that synchronised gamma activity might represent means of local cortical communication (Le Van Quyen *et al.*, 2010).

Another aspect of spontaneous SWO is their disappearance in adult brain slices, whether this phenomenon is limited to brain slices and experimental set up or whether the activity in mEC is indeed age-dependent. Previous *in vitro* studies in this brain region suggested that experimental conditions greatly affected spontaneous activity in mEC (Dickson *et al.*, 2003; Cunningham *et al.*, 2006; Sheroziya *et al.*, 2009). On the other hand, human sleep studies demonstrated that throughout childhood and adolescence SWO shifted from posterior to anterior regions of the brain, which followed the same time course as cortical maturation (Shaw *et al.*, 2008;

Kurth *et al.*, 2010). These authors suggested that, apart from regional development of the cortex, SWO alterations reflected changes in synaptic density (synaptic pruning), which affected network synchronisation (Sowell *et al.*, 2004; Vyazovskiy *et al.*, 2009). It has been shown that slow activity strongly correlated with grey matter thickness, both decreasing with age (Buchman *et al.*, 2011). These findings indicated a clear developmental component in the operation of slow rhythmic activity associated with sleep in the human brain, however, *in vivo* studies might help determine the role of development in animals.

The possible involvement of slow rhythmic activity in memory consolidation raises an interesting question regarding cortico-hippocampal interactions during sleep and whether cortical SWO are correlated with hippocampal activity. Several studies have explored these relationships *in vivo*, including Isomura *et al.* (2006), Ji and Wilson (2006), Le Van Quyen *et al.* (2010). In a study carried out by Isomura and colleagues (2006) *in vivo* recordings were taken from the hippocampus, neo- and paleocortex. The results showed that while EC neurons dwelled in a bimodal (UP-DOWN) state associated with slow oscillations, hippocampal neurons exhibited independent firing patterns. Nevertheless, these authors showed that excitatory component of SWO did spread from the neocortex to the hippocampus via EC, although hippocampal neurons still remained active during cortical DOWN states. Overall, it was concluded that hippocampal neurons operated via both neo-/paleocortex-dependent and independent mechanisms, suggesting some degree of cortico-hippocampal interaction during sleep. It would be interesting to explore the relationship between the EC and hippocampus in both healthy and epileptic animals, as we have an opportunity to simultaneously observe SWO and SyO in a slice.

Finally, as is clear from the results above, from a methodological point of view these studies were difficult to analyse and interpret and, in particular, statistical validation of observations was problematic. This was due in no small part to the variability between recordings of SWO, which are difficult to quantify in a manner that is both rigorous and repeatable. Further work in this area is ongoing in the laboratory, and we hope to develop more reliable indices of SWO 'power', perhaps by including both slow-wave amplitude and intraburst power in a combined metric.

6.4. Conclusions

Our investigations into how the EC network operation changed during epilepsy development revealed that spontaneous SWO employed a different mechanism of oscillogenesis, which relied more on AMPAr activation, as compared to control slices. It is yet to determine the exact role that AMPAr take over and its significance in the context of epileptogenesis. We can also conclude that epilepsy development or the initial insult (SE) acted to delay network maturation in animals that had experienced RISE.

Chapter 7 Electrophysiology of paediatric brain tissue resected from patients with intractable epilepsy

7.1. Introduction

Despite the existence of a large variety of AEDs, 30–40% of patients with epilepsy exhibit seizures that are poorly controlled by medication (Kwan and Brodie, 2000). TLE is generally one of the most common types of epilepsy, however, it also constitutes 50–70% of intractable epilepsy cases (Semah *et al.*, 1998; Wass *et al.*, 1985; Guldvog *et al.*, 1994; Keene *et al.*, 1997). Characteristic changes such as hippocampal sclerosis with excessive gliosis and cell death, neuronal circuit reorganisation with axonal sprouting and synaptogenesis are normally associated with TLE (Sutula *et al.*, 1988, 1989; Mikkonen *et al.*, 1998). Studies suggest that 50% of epilepsy cases begin before the age of 5 (Hauser, 1992). Although TLE is not the most common type of epilepsy in paediatric patients, it forms a large part of drug-resistant cases requiring surgical intervention. Manifestations of temporal lobe seizures include the onset of aura (e.g. olfactory, gustatory, auditory) indicating a simple partial seizure, followed by a complex partial seizure (automatisms, psychomotor seizures) with impaired consciousness and possibly culminating in generalised tonic-clonic seizures (Adelson, 2008). The most common pathological substrates in paediatric drug-resistant epilepsy are cortical dysplasia, tumors, mesial temporal lobe sclerosis and vascular lesions (review by Cataltepe and Cosgrove, 2011). Nowadays, advanced surgical expertise allows good outcomes with low morbidity and mortality (Benifla *et al.*, 2006; Kan *et al.*, 2008). Reviews published by Engel *et al.* (2003) and Schmidt and Stavem (2009) point out that surgical resection produces a seizure-free outcome in 40–60% of cases, which is 4–5 times higher compared to prolonged medication. A more recent report by Muhlebner *et al.* (2014) demonstrated that 80% of the patients were seizure-free (56.7% stopped receiving AEDs). It appears that similar surgical outcomes were observed in children regardless of age (Chugani *et al.*, 1993; Wyllie *et al.*, 1998; Maton *et al.*, 2008).

Epileptic brain tissues surgically resected from patients with pharmacoresistant epilepsies present extremely valuable material for studying cellular and network changes. A direct relation to human pathology is one of the obvious advantages that human tissue possesses compared to animal research. A limited number of laboratories around the world use various techniques to characterise human brain

tissue. Over the years, information has been accumulated on electrophysiological properties of human cortical neurons (Avoli and Olivier, 1989; McCormick, 1989; Foehring *et al.*, 1991; de la Prida, 2002; Molnar *et al.*, 2008; Florez *et al.*, 2013) and the role and mechanism of VFOs in epileptic human tissue (Roopun *et al.*, 2010; Cunningham *et al.*, 2012; Simon *et al.*, 2014). However, only one report described physiological network function has recently appeared in literature (Florez *et al.*, 2013). The lack of studies characterising neuronal network synchronisation in human brain tissue indicates a clear gap in our knowledge. Abnormal network function constitutes the basis of epileptic disorder, therefore investigation and establishment of physiological/baseline human network profile seems of major importance. One of the main limitations is the paucity of control human brain tissue. However certain surgeries require resection of healthy tissue to gain access to remote epileptic regions. In addition, brain resections of non-epileptic pathologies such as brain tumors could also be utilised as a control tissue. Despite the fact that extensive animal research characterising healthy and epileptic networks has been conducted for decades, similar investigations in the human brain are required to establish differences and similarities. Therefore, we started a pharmacological characterisation of neuronal network oscillations recorded from resected cortical brain tissue from paediatric patients with drug-resistant epilepsy.

7.2. Results

7.2.1. Basic profile of neuronal network oscillations

Human brain tissue was resected from the brains of paediatric patients suffering from intractable epilepsy. We received brain tissue samples of 5 patients with cortical dysplasia, the specimens were mostly taken from the temporal cortex and were either normal or dysplastic (see Section 2.3.).

As a collective effort from all members of the lab (Jane Pennifold, Darshna Shah, Swetha Kalyanapu, Dr. Emma Prokic, and Nicholas Johnson), brain slices were prepared the same way as described for animal slices (see Section 2.1.). LFP recordings were made from human cortical tissue under control drug-free conditions, as well as during pharmacological stimulation with various doses of KA and CCh. Electrodes were placed in both deep and superficial cortical layers, although in some

cases it was impossible to distinguish between them. Slices did not exhibit any spontaneous activity, apart from occasional single-unit spikes. When a human cortical slice was washed with '*in vivo*-like' aCSF, which enhanced tissue excitability, slow baseline fluctuations (~0.1 Hz) appeared, but no stable rhythmicity or ictal/interictal events were detected.

Different concentrations of KA (150 nM, 300-400 nM, 800 nM and 1-1.2 μ M) were bath-applied in order to elicit rhythmic activity in the slices. Induced oscillations emerged 10-15 mins after drug application and were persistent for several hours. Lower doses of KA generated low power low frequency oscillations as demonstrated by raw traces and power spectra in Fig. 7.1B-D. Application of 150 nM KA produced oscillations with the mean peak frequency 5.6 ± 0.5 Hz and mean peak power $1.95\pm 0.6 \mu\text{V}^2$ (n=2). In a different set of slices administration of 300 – 400 nM KA resulted in rhythmic activity with higher mean peak frequency 10.17 ± 2.2 Hz and similar mean peak power of $1.85\pm 0.5 \mu\text{V}^2$ (n=6). A higher concentration of 800 nM KA produced beta frequency rhythmic activity (mean peak frequency 21.57 ± 1.1 Hz) with higher mean peak power of 11.49 ± 9.7 (n=3). Gamma frequency oscillations were observed upon application of 1-1.2 μ M KA. An increased dose produced faster but not larger oscillations (mean peak frequency 27.47 ± 6.2 Hz and mean peak power $7.37\pm 2.7 \mu\text{V}^2$, n=4). We also tested the effects of KA and CCh co-application in 7 cortical slices, which resulted in generation of beta frequency activity (mean peak frequency 17.38 ± 2.3 Hz) with consistently higher power compared to KA-induced oscillations (mean peak power $20.97\pm 7.2 \mu\text{V}^2$). Frequency-power characteristics of recorded neuronal network oscillations are summarised in Fig. 7.2C, where a positive correlation could be observed between KA dose and the frequency of induced oscillations. Using Morlet wavelet method, the time-frequency characteristics were analysed for different types of induced oscillations and showed stable oscillatory activity over time (Fig. 7.2A,B).

Simultaneous recording of field potential from deep and superficial layers of the human cortex revealed a more prominent rhythmic activity in superficial layers upon application of 400-800 nM KA. Increasing the dose of KA from 400 nM to 800 nM resulted in the oscillation frequency shift from 15 Hz to 35 Hz in the superficial layers, while no network synchronisation was observed in the deep cortical layers (n=1).

These findings could indicate disruption of laminar connectivity, independent rhythm generators within the cortex or poor survival of deep layer neurons. Florez and colleagues (2013) have previously pointed out the differences in the laminar profile of network oscillations in the human cortex. In that study, superficial layers generated higher power rhythmic activity compared to deep layers in response to cholinergic activation, which was explained by histological differences and a higher density of muscarinic receptors in superficial layers (Florez *et al.*, 2013).

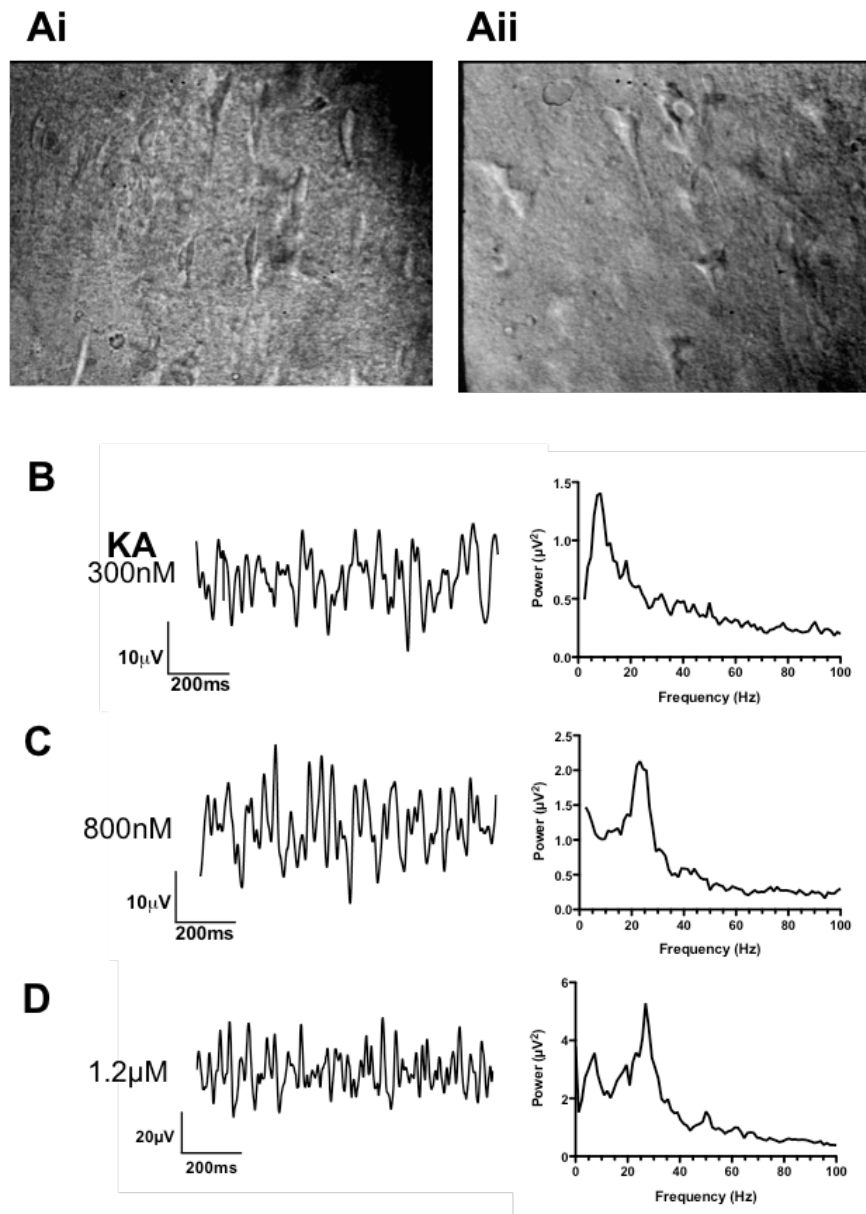


Figure 7.1. Human brain tissue slice morphology and KA-induced rhythmic activity. **Ai** and **Aii**. Images of normal and dysplastic human cortical brain tissue, respectively. **B.**, **C.** and **D.** Band-pass filtered (2 – 50 Hz) raw traces and representative power spectra for oscillations induced by 300 nM, 800 nM and 1.2 μM KA, respectively.

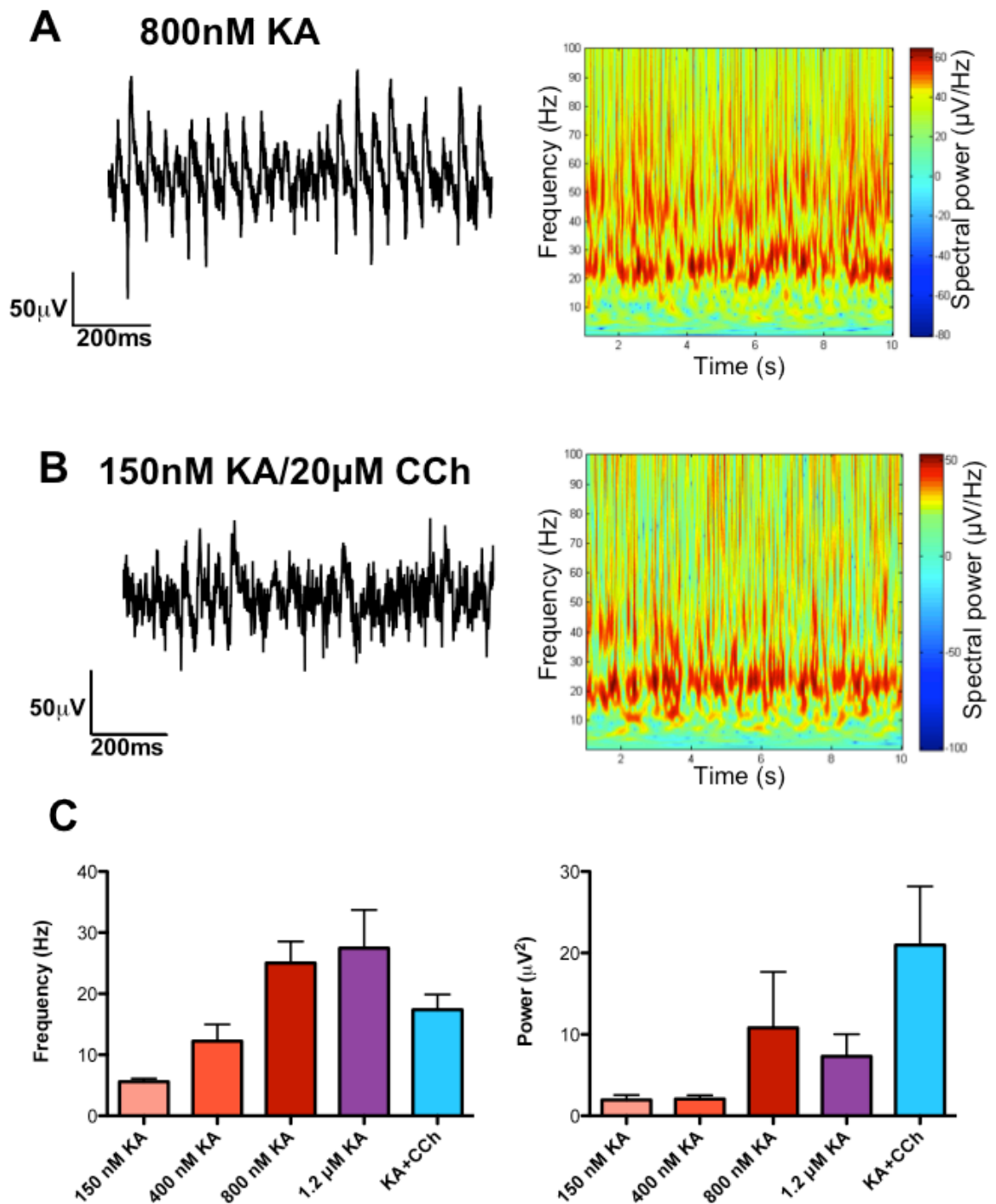


Figure 7.2. KA- and CCh-induced rhythmic activity in human cortical brain tissue. **A.** Unfiltered raw trace of KA-induced oscillations and representative Morlet wavelet time-frequency plot. **B.** Unfiltered raw trace of KA+CCh-induced oscillations and representative Morlet wavelet time-frequency plot. **C.** Bar charts showing peak frequency and peak power of rhythmic activity induced by different concentrations of driving agents (recordings not paired). A positive correlation is observed between the dose of KA and the peak frequency of induced oscillations.

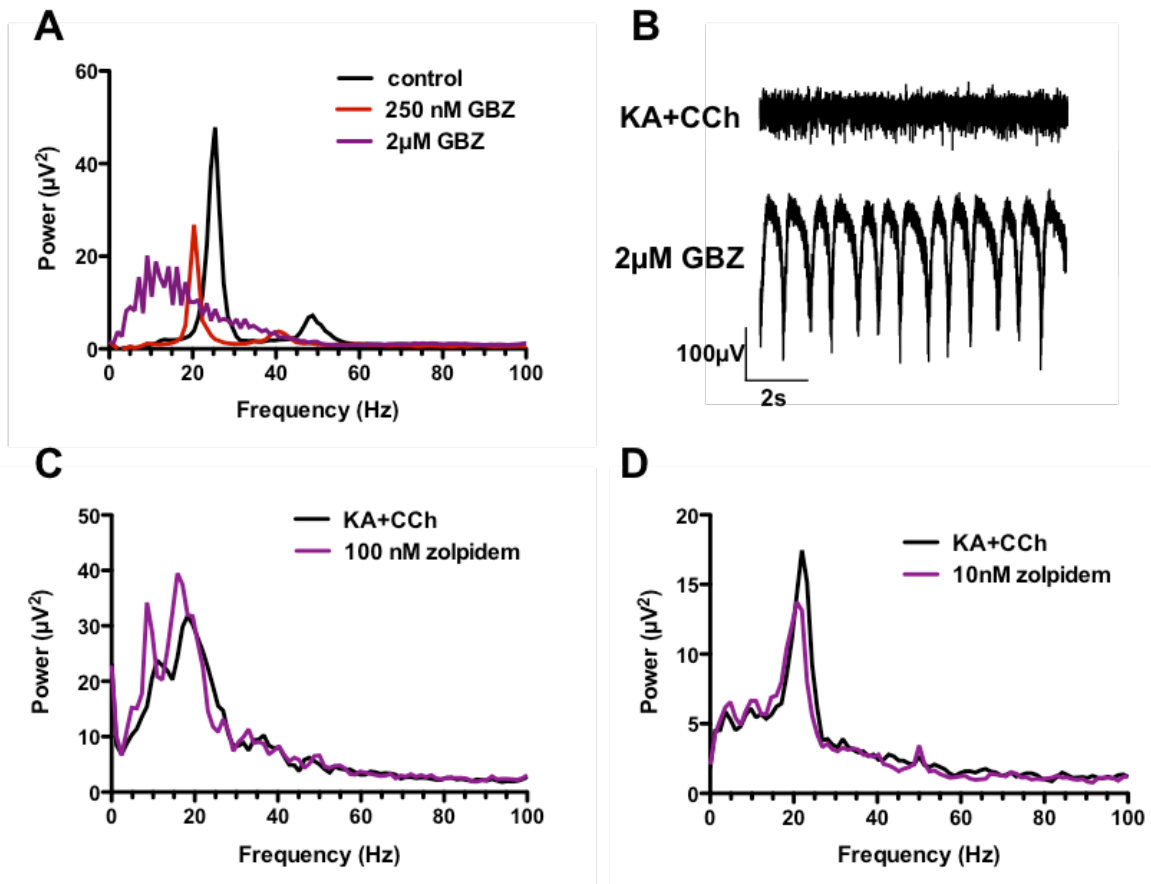


Figure 7.3. Rhythmic activity in the human cortex is mediated by GABA-Ar. **A.** Power spectra showing a reduction in the peak power of oscillations produced by low concentration GBZ (250 nM) and a desynchronisation produced by 2 μM GBZ. **B.** Unfiltered raw traces showing large delta-type oscillations produced by 2 μM GBZ. **C.** and **D.** Power spectra showing differential dose-dependent effects of 100 nM and 10 nM zolpidem, respectively.

7.2.2. Pharmacological characterisation

Together with basic characterisation, we started pharmacological analysis of the rhythmic activity to determine whether it shared the same mechanism with oscillations in animal brain slices. Original studies established that synchronous activity in animal slices crucially depended on GABA-mediated inhibition (Whittington *et al.*, 1995; Buhl *et al.*, 1998), hence the effect of GABA-Ar antagonist GBZ was tested on pharmacologically-induced oscillations in human cortical slices. At 250 nM GBZ produced a decrease in the peak power of oscillations by $32.04 \pm 11.1\%$ and a small reduction in the peak frequency from 22.5 ± 6.8 Hz to 18.8 ± 0.5 Hz, $n=2$ (Fig. 7.3A). As illustrated by Fig. 7.3B, high concentration (2 μM) of the antagonist abolished oscillations and introduced a low-frequency high-power rhythmic activity of delta frequency range, which was possibly mediated by excitatory transmission. The

mean peak frequency decreased from 22.5 ± 6.8 Hz to 5.03 ± 1.7 Hz ($n=4$), whereas power increased >10000 -fold (%). These results indicate that beta-gamma synchronous activity generated by human tissue networks is dependent on GABA inhibition. These findings were further supported by the effect of a GABA-Ar blocker, PTX ($20 \mu\text{M}$), which also abolished network oscillations. The activity was also affected by a benzodiazepine site agonist, zolpidem, which produced differential effects at 10 nM and 100 nM concentrations. High concentration of zolpidem produced an increase in the peak power of beta band rhythmic activity by 24.2% , while a reduction in the peak frequency from 18.3 Hz to 15.9 Hz ($n=1$), as demonstrated by Fig. 7.3C. Low dose of zolpidem, on the other hand, resulted in a slight reduction of beta oscillation power by 21.3% and a minor decrease in the peak frequency from 22.0 Hz to 20.8 Hz , $n=1$ (Fig. 7.3D). It is not possible to make conclusions about the effects of zolpidem, however, the results already suggest a certain level of modulation.

The second main component of rhythm generation in animals is AMPAr-mediated excitation (Whittington *et al.*, 1995). We, therefore, explored the effects of an AMPAr antagonist, NBQX ($2.5 \mu\text{M}$), on KA+CCh-induced oscillations in the human cortical slices. Blockade AMPAr resulted in the abolition of gamma activity and appearance of a slow rhythm with a lower peak power instead (the peak shifted from 30.5 Hz to 6.1 Hz and decreased in power by 52% , $n=1$), indicating involvement of glutamatergic transmission in the generation and maintenance of rhythmic activity in human neuronal networks (Fig. 7.4A). The role of NMDAr in the generation and maintenance of rhythmic activity was explored by application of $50 \mu\text{M}$ DL-AP-5. NMDAr blocked reduced gamma peak by 54.4% ($n=1$), while retained the slow rhythm (Fig. 7.4B). To investigate the contribution of KAr, a selective GluK1,3 subunit agonist UBP310 ($3 \mu\text{M}$) was bath-applied to KA- and KA+CCh-induced oscillations. The results demonstrated similar effects to non-selective AMPAr/KAr blockade, as UBP310 caused a significant reduction in beta band power, yet an increase in lower frequencies (Fi. 7.4C,D). The peak frequency shifted from 15.9 Hz to 7.3 Hz , whereas the peak power decreased by 47.2% ($n=1$). These findings suggest a role of KAr in beta/gamma frequency network synchronisation, similarly to findings in animal slices.

Cholinergic involvement in the generation of rhythmic activity was explored by addition of 5 μM atropine, an mAChR antagonist. Cholinergic blockade produced different effects in KA- and KA+CCh-induced oscillations, similar to our previous findings in rodent hippocampus (Chapter 3). KA-induced oscillations persisted in the

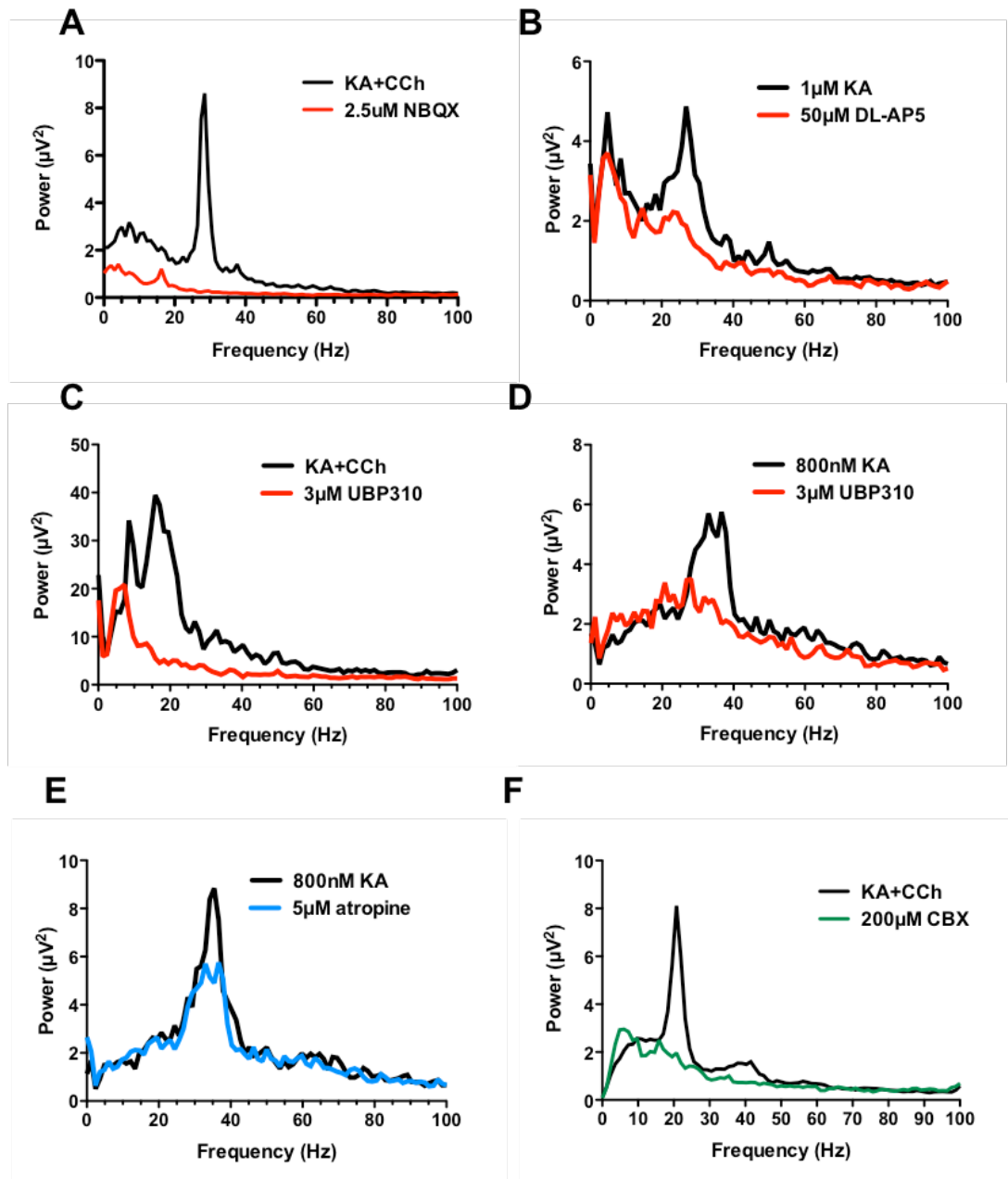


Figure 7.7.4. Pharmacological profile of pharmacologically-induced rhythmic activity in the human cortical tissue. **A.** Power spectra showing a dramatic reduction in the peak frequency and peak power of oscillations produced by 2.5 μM NBQX. **B.** Power spectra showing the NMDAR blockade with 25 μM AP-5 causes a marked desynchronisation in the gamma frequency band, yet maintains the low-frequency peak. **C.** and **D.** Power spectra showing a reduction in the peak frequency and peak power of KA+CCh- (**C.**) and KA- (**D.**) induced oscillations produced by 3 μM UBP310. **E.** Power spectra showing a reduction in the peak power of KA-induced oscillations produced by 5 μM atropine. **F.** Power spectra showing gamma frequency desynchronisation produced by a gap junction blocker, CBX (200 μM).

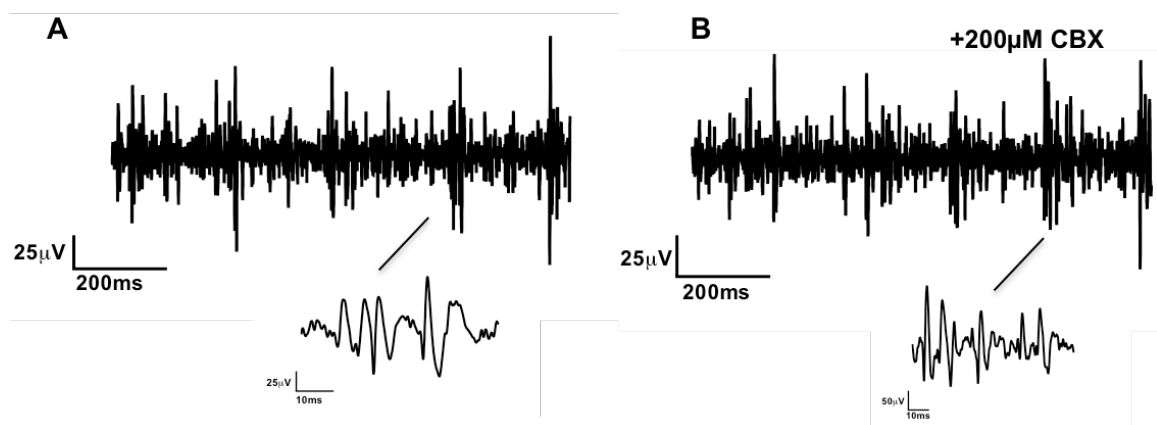


Figure 7.5. VFOs are not mediated via gap junctions. **A.** High-pass filtered (at 100 Hz) raw trace in control conditions showing high-frequency episodes. **B.** High-pass filtered (at 100 Hz) raw trace showing that application of a gap junction blocker did not abolish VFOs.

presence of atropine with the peak power reduction by 34.9% ($n=1$), whereas KA+CCh-induced activity was rapidly abolished ($n=1$), indicating that cholinergic activation is not essential for oscillation generation and maintenance and that the two oscillation models rely on different mechanisms (Fig. 7.4E). Similar results were reported by Florez and colleagues (2013), where KA+CCh-induced oscillations were abolished by atropine application in the human tissue.

Electrical coupling between neurons is a potent facilitatory mechanism of rhythmic network activity in rodent brain (Traub *et al.*, 2000, 2003; Hormuzdi *et al.*, 2001; Buhl *et al.*, 2003; Pietersen *et al.*, 2009). Gap junctions have been linked to VFOs in human epileptic brain (Cunningham *et al.*, 2012). Taking these findings into consideration, 200 μM CBX was bath-applied to existing beta frequency oscillations. The gap junction blocker readily curtailed rhythmic activity in the beta range, however augmented the power level in the delta frequency band (peak frequency changed from 20.8 Hz to 6.1 Hz, while delta-peak power was 63.6% lower than beta peak, $n=1$), as illustrated by Fig. 7.4F. Several human tissue recordings presented with episodes of high frequency activity (Fig. 7.5). We, therefore, applied 200 μM CBX to determine whether the observed fast component was mediated via gap junctions. In a single recording, gap junction blocker did not appear to produce any effect on fast oscillations (Fig. 7.5). In an attempt to promote high frequency oscillations, a gap junction opener, 10mM trimethylamine, was bath applied. Stimulation of gap junction conductance reduced beta oscillation power, which was counterintuitive, considering similar effects produced by a gap junction blocker, and did not enhance high frequency activity.

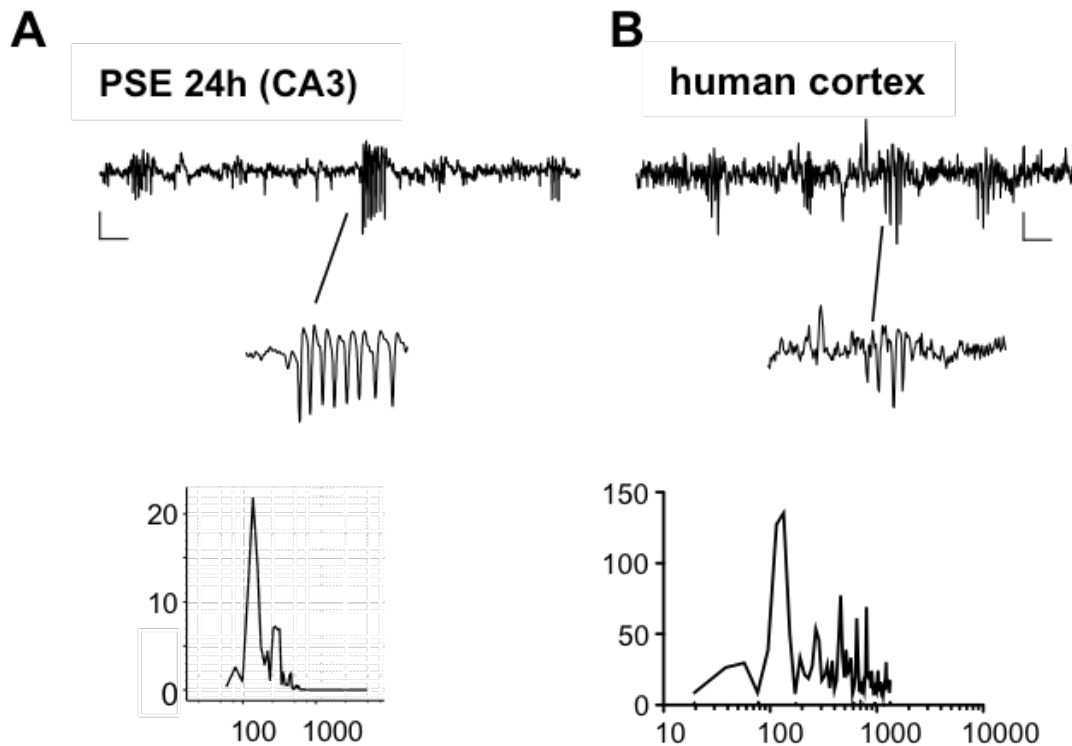


Figure 7.6. Similarities between VFO in PSE 24h slices and epileptic human tissue. A. Unfiltered raw traces showing episodes of VFO recorded from PSE 24h slices. Power spectrum of the VFO showing a peak at 150 Hz. **B.** Unfiltered raw traces showing episodes of VFO recorded from epileptic human brain slices. Power spectrum of the VFO showing a peak at around 150 Hz. Scale bars 200ms \times 50 μ V.

7.2.3. VFO and ictal activity

As mentioned earlier, human cortical slices occasionally exhibited bursts of high frequency activity, similar to the ones observed in brain slices from epileptic rats (Fig. 7.6). The epochs of fast activity were of 200 – 600 Hz frequency range. Since enhanced VFOs have been associated with epilepsy, it would be reasonable to assume that high frequency oscillations observed in our human and rat slices are a characteristic feature of epileptogenicity. An episode of ictal activity was also recorded from the human cortical tissue. The seizure consisted of a high-amplitude relatively slow wave followed by a period of rhythmic activity with multiple frequency components (Fig. 7.7A). The episode exhibited a changing frequency pattern, which is illustrated by the Morlet-wavelet spectrogram (Fig. 7.7B).

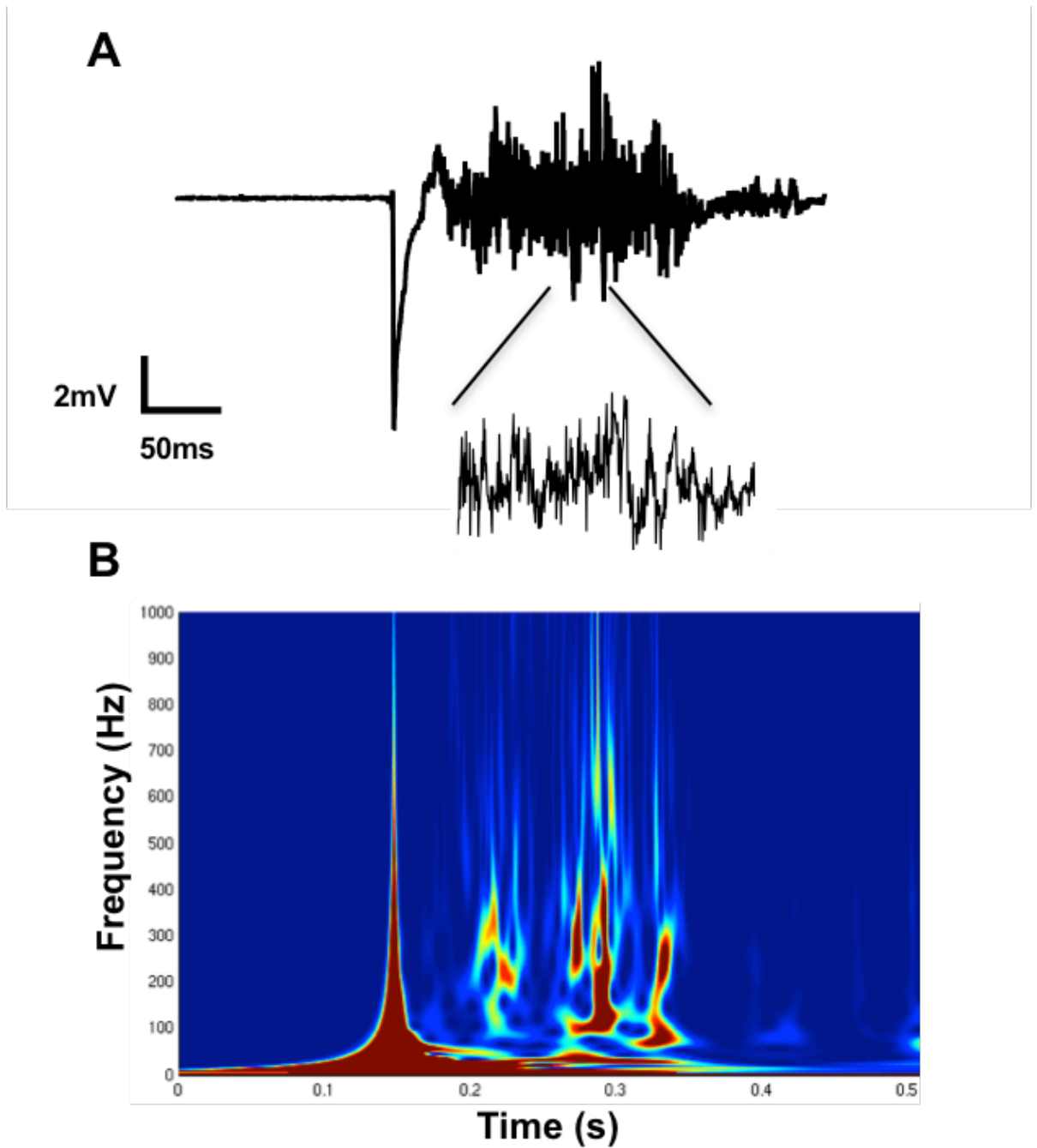


Figure 7.7. Ictal event in epileptic cortical tissue from a human brain. A. Unfiltered raw trace recorded from the epileptic human tissue. **B.** Representative Morlet wavelet time-frequency spectrogram.

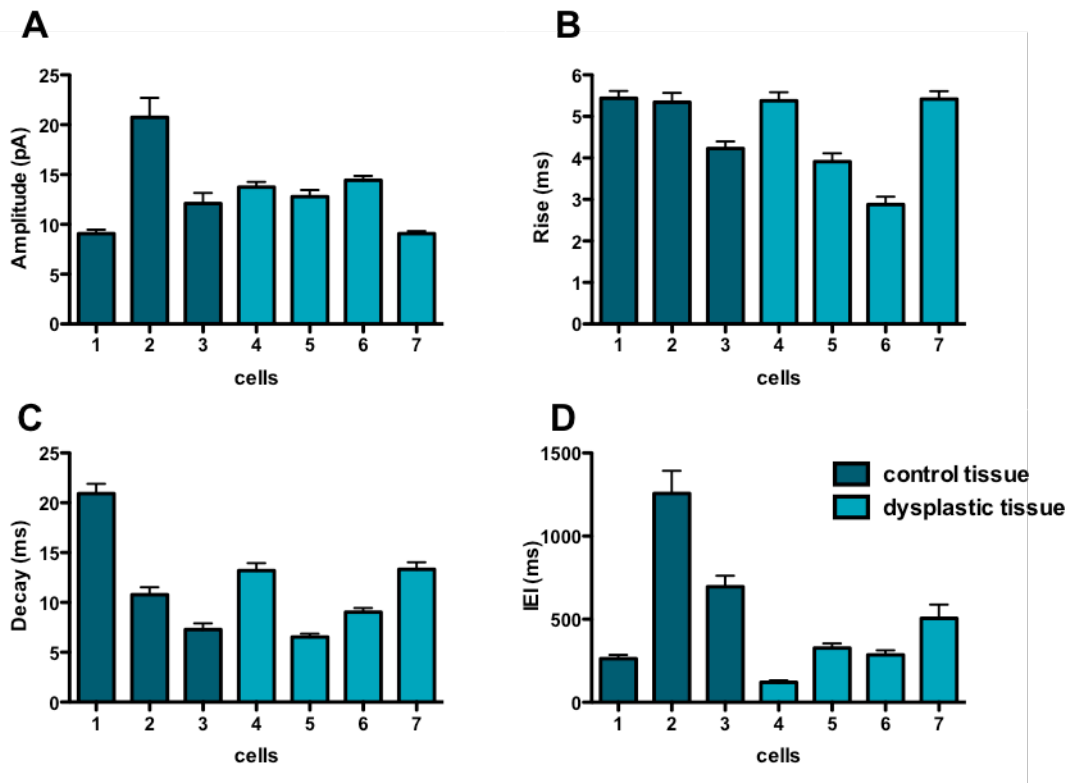


Figure 7.8. GABA sIPSC kinetic properties of the individual cells in normal and dysplastic human tissues. **A.** Bar chart showing sIPSC amplitude across 7 cells. **B.** Bar chart showing sIPSC rise time across 7 cells. **C.** Bar chart showing sIPSC decay time across 7 cells. **D.** Bar chart showing sIPSC IEI across 7 cells.

7.2.4. IPSC kinetics in human cortical slices

Intracellular patch-clamp recordings were taken from the human cortical neurons. We recorded sIPSCs in 7 pyramidal-looking cells from control and dysplastic tissues and summarised their kinetic properties under control (drug-free) conditions. The events had the mean amplitude of 12.8 ± 0.4 pA, a mean rise time of 4.75 ± 0.1 ms and mean decay time 11.75 ± 0.3 ms, while the IEI was 445.3 ± 29.1 ms ($n=7$). The parameters across individual cells are presented in Fig. 7.8. The amplitude and the rise time appeared to be more consistent from cell to cell in comparison to the decay time and IEI. Cells from supposedly dysplastic regions did not appear to show significant differences, as some of the kinetic parameters were rather variable. At this stage of investigations it is too early to draw conclusions.

To investigate the effects of KA on GABA release in human brain slices, 100 nM KA was bath-applied. In one cell recording in control tissue, KA administration caused a significant decrease in the frequency of sIPSCs, indicating negative modulation by

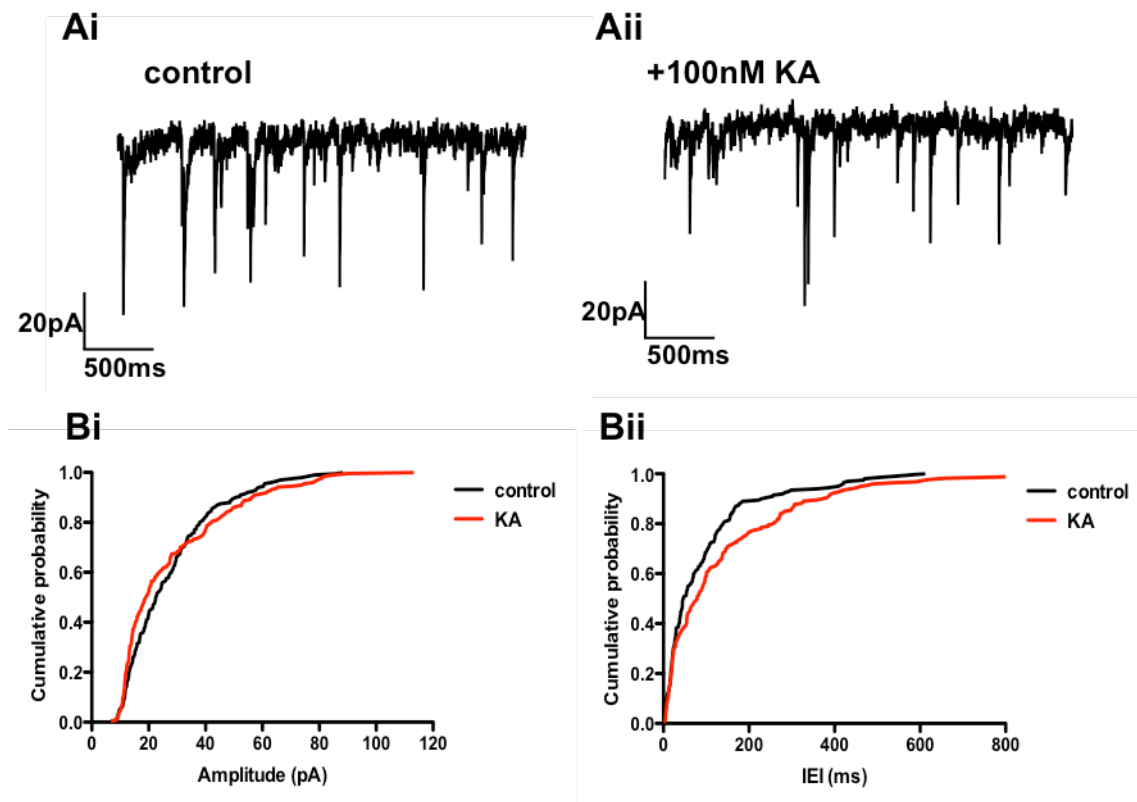


Figure 7.9. KAR modulated GABA release. Ai. and Aii. Raw traces of sIPSCs in control and 100 nM KA conditions. **Bi. And Bii.** Cumulative probability plots showing changes in sIPSCs amplitude and IELI upon the application of 100 nM KA.

presynaptic KAR ($p < 0.05$), as illustrated by Fig. 7.9Bii. No significant changes in amplitude, rise and decay times were observed upon addition of KA. It is obvious that more experiments are required to make conclusions on the modulatory presynaptic functions of KAR in human cortical neurons.

7.3. Discussion

7.3.1. Basic profile of human tissue oscillations

The ultimate goal of animal research is understanding neurophysiological and neuropathological processes taking part in the human brain and finding ways of altering these conditions. Although animal research has yielded a substantial part of our knowledge of human physiology, the question of species differences is always open for discussion. Therefore exploring electrophysiological properties of neurons and neuronal networks in human brain tissue constitutes a valuable section of brain research. Brain tissue resection is common for surgical treatment of intractable epilepsy in humans, and this fact presents an opportunity to study pathological

changes occurring in epilepsy. We explored neuronal network properties in human brain slices by eliciting rhythmic activity in the temporal cortex. Previous human tissue studies mostly focused on the electrophysiology of individual cells, however several reports demonstrated the existence of transient oscillations of mostly theta and high gamma frequencies (Cunningham *et al.*, 2012; Florez *et al.*, 2013). Here, we report persistent neuronal network oscillations of different frequencies induced in the human cortical tissue, which, to our knowledge, has not been reported in the literature to date. Similar to animal models of brain rhythms, oscillations in the human cortex could be generated by application of KA or KA+CCh (Buhl *et al.*, 1998; Cunningham *et al.*, 2003; Roopun *et al.*, 2006; Yamawaki *et al.*, 2008). Florez and colleagues (2013) used a combination of KA and CCh to induce theta oscillations that lasted for approximately three minutes. The differences between oscillations could be determined by different experimental conditions (Mg^{2+} concentration in aCSF, submerged recording and temperature) and doses of driving agents.

The aim of initial experiments was to establish an induction protocol, which would reliably generate rhythmic activity in human brain slices. The starting concentrations of KA and CCh were chosen based on the protocol of gamma oscillation induction in cortical rat brain slices (entorhinal, motor and piriform cortices). Established doses in human slices roughly corresponded to those used in rodent slices. Despite this fact, human rhythmic activity was much lower in power compared to that induced in animals. Several factors could account for that: higher cell survival rate and preservation of local circuits in animal slices. Interestingly, in rodents application of a driving agent resulted in a dose-dependent increase in oscillatory power, yet in little change in the frequency of oscillations. In human brain slices, on the other hand, a positive correlation was observed between the dose KA and produced frequency of oscillations, while the power did not seem to consistently depend on the strength of the drive. The power of oscillations, however, could be limited by the size of the network (the number of survived neurons) or a more sparse location of cells in the human brain. It appeared that cortical neurons in the human brain were more sensitive to a gain in the input drive, increasing the firing rate or changing the kinetics of GABA IPSCs, as it is known to determine the frequency of oscillations.

Application of KA in the human cortex was able to produce network oscillations of various frequency bands (5 – 30 Hz), which means that the level of excitatory drive could be matched to induce rhythmic activity observed in the intact human brain. However, the fact that the same area could generate multiple oscillation frequencies depending on the excitation suggests similar underlying mechanism, which does not seem to be the case in rodent slices. Another question is whether the induction method is important, as we know application of KA alone and KA+CCh are able to induce various types of rhythmic activity, whereas pure cholinergic activation was insufficient to generate oscillations (Florez *et al.*, 2013). In our human tissue experiments, co-administration of CCh and KA consistently produced higher power of oscillations, compared to KA alone, however, had a less pronounced effect on the frequency. These results together with pharmacological data suggest that cholinergic input indeed modulates the generation of rhythmic activity, but is not a prerequisite. Hence, it is not clear whether the cholinergic activation participates in the generation of neuronal network oscillations in an intact human brain. Our previous findings demonstrated that in the rodent hippocampus the naturally occurring spontaneous rhythmic activity is different from both KA- and CCh-induced oscillations (Chapter 3). However, in the absence of spontaneous cortical activity in human slices, which model of oscillations is more physiologically relevant? Given the existence of different oscillation induction mechanisms, it is an important question, whether cholinergic activation is involved in rhythm generation *in vivo*. Previous reports suggest that KA-induced oscillations persist in the absence of cholinergic input, whereas CCh-induced activity is abolished with blocked glutamatergic transmission. In a complex system such as intact brain, it is plausible that both systems act separately or together to generate different rhythms in various parts of the brain. However, when working with a simpler model like a brain slice, unless spontaneous rhythmic activity presents itself, researchers have to choose among several ways of induction. Personal preferences for a particular model and the diversity of available models may complicate the generalisation of accumulated knowledge.

Stimulation of cortical network with different doses of KA elicited oscillations ranging from 4 to 45 Hz. Generation of different oscillation frequencies could either indicate a similar underlying mechanism with altered neuronal firing or employment of different network mechanisms depending on the level of excitatory drive. A substantial amount

of intra- and extracellular studies are required to determine the origin of observed frequency change. It can still be speculated that KA application is able to induce rhythmic activity with different mechanisms and properties. For instance, a relatively low concentration of KA produced slow theta frequency rhythm. Although theta oscillations have been widely reported in the hippocampus of rodents, in humans theta frequencies have been observed in cortical structures, but several studies suggest that these rhythms are not coherent with theta in the hippocampus and represent different states in each region (Kahana, 1999; Raghavachari *et al.*, 2001). Theta rhythm has been linked to various behavioural states, in particular associated with voluntary movement (Vanderwolf, 1969; Whishaw and Vanderwolf, 1973; Bland and Oddie, 2001). However, theta waves were also observed in animals during immobility associated with fear conditioning and attention to predators (Whishaw, 1972; Sainsbury *et al.*, 1987a,b). Some findings also suggest that theta rhythm is involved in the processes of memory and learning (Berry and Thompson, 1978; Winson, 1978; Givens and Olton, 1990; Vertes and Kocsis, 1997; Berry and Seager, 2001).

Increased KA concentration caused a significant shift in oscillation frequency producing a 10 Hz oscillation, which corresponded to alpha frequency band in the human brain. In literature alpha oscillations are categorised into three types. The first type is the “occipital alpha”, which prevails during quiet wakefulness and is decreases by eye opening. Occipital alpha is a major contributor to the alpha band magnitude during this behavioural state. Another type of alpha frequency rhythm is known as the mu rhythm, these waves are present in the central cortical areas and can be observed only in a small number of individuals (< 15%) during relaxed wakefulness (Jasper and Andrews, 1938; Maddochs *et al.*, 1951; Schutz and Muller, 1951). Studies demonstrate the attenuation of this rhythm by motor movements or somatosensory stimuli (Pfurtscheller *et al.*, 1998). The third type of alpha rhythm is the “third rhythm” (independent temporal alphoid rhythm) observed in the temporal region and described by Niedermeyer (1990; 1991). However, these waves are visible on the EEG only in subjects with skull defects (Niedermeyer, 1997). A distinctive feature of the third rhythm is the absence of a specific blocking process or stimulus, unlike with occipital alpha or mu rhythm (Niedermeyer, 1997). It seems plausible that the third rhythm analogue could be generated in the temporal cortex

slices, although it should be noted that a brain slice is a reduced system with limited connectivity.

A further increase in the glutamatergic drive resulted in alpha oscillations developing into a beta frequency (~15-20 Hz) rhythm. In humans beta rhythm is associated with sensorimotor functions and cognitive processing related to stimulus assessment and decision-making. Beta activity is prominent during steady contractions and holding periods following movements, and is blocked by voluntary movement (Sanes and Donoghue, 1993; Baker *et al.*, 1997; Kilner *et al.*, 1999; Klostermann *et al.*, 2007). Apart from sensory-motor area, beta frequencies have been recorded from more frontal, as well as posterior and temporal regions (for review see Niedemeyer and Lopes da Silva, 2005). There is a possibility that beta oscillations represent pathological states and are enhanced in such conditions as Parkinson's and epilepsy. *In vitro* experiments might support this idea. It is yet to determine whether beta oscillations recorded from the epileptic human brain slices are physiological or emerge as a consequence of a pathological condition. Another possibility is that what appears to be a beta type activity could in fact be a slow gamma rhythm, indicating the same underlying mechanism. Therefore, more studies will help identify the nature of recorded activity.

Acceleration of rhythmic activity at high doses of KA in human slices demonstrated capability of the human cortex to generate gamma oscillations *in vitro*. The gamma rhythm in human slices was similar to that recorded from rodents, although in an intact human brain gamma oscillations tend to be of a higher frequency. This, however, could be explained by reduced connectivity in a slice, as well as artificial experimental conditions. It is believed that the functional role of gamma oscillations is involvement in temporal encoding, sensory binding of features, learning and memory processes (Hopfield *et al.*, 1995; Buzsaki and Chrobak, 1995; Lisman and Idiart, 1995; Lisman, 1999, Jensen *et al.*, 2007). Gamma oscillations are observed during attentive state, focused wakefulness, sensory perception, object recognition, and language perception (Bouyer *et al.*, 1981; Sheer *et al.*, 1989; Murthy and Fetz, 1992; Pfurtscheller and Neuper, 1992, Bragin *et al.*, 1995; Jensen *et al.*, 2007). On a global scale, gamma frequency oscillations are thought to reflect integration mechanisms in the brain (Herrmann *et al.*, 2004).

7.3.2. Pharmacology of human tissue oscillations

Pharmacological investigation of synchronous activity in the human cortical tissue revealed similar findings to rodent pharmacology, implying similar underlying mechanism. Crucial role of GABA-ergic inhibition and glutamatergic excitation in the generation of beta/gamma oscillations suggests that the species share basic mechanisms of neuronal communication and information processing/transmission (Buhl *et al.*, 1998; Cunningham *et al.*, 2003; Yamawaki *et al.*, 2008). Initial results demonstrated that a benzodiazepine site agonist, zolpidem, produced a dual dose-dependent modulation of rhythmic activity, which again supported the role of GABA-Ar and was in line with the effects reported in rat M1 (Yamawaki *et al.*, 2008; Prokic, 2012). KAr are known to take part in the generation and maintenance of neuronal network activity (Stanger *et al.*, 2008), and our results showed that GluK1 subunit-containing KAr were also involved in the network synchronisation in the human tissue. Our findings demonstrated that human oscillations relied heavily on gap junction transmission, similar to animal findings *in vitro*. Together with the similarities, several differences occurred when human pharmacology was compared to rodent oscillations. It appeared that NMDAr and mAChr were more involved in the generation and maintenance of gamma activity in the human cortex, compared to KA-induced oscillations in rodents. At the moment, our dataset is limited; therefore it is too early to make conclusions on the mechanism of human oscillations *in vitro*.

7.3.3. VFO and ictal activity

Several experiments revealed episodes of high frequency activity recorded from human brain slices taken from paediatric patients suffering from intractable epilepsy. The burst of fast oscillations resembled those recorded from PSE 24h and PSE 90d slices, indicating that RISE model bears at least a superficial similarity to the human condition. As mentioned earlier, fast oscillations are significantly enhanced in epilepsy and are known to precede and superimpose upon seizure activity. High frequency oscillations have been observed both *in vivo* and *in vitro*, in humans and animals (for review see Traub *et al.*, 2012). Studies suggest that high frequency activity can be generated in the absence of chemical neurotransmission by non-synaptic mechanisms relying on axonal gap junctions. In our experiments, however, gap junction blocker did not produce the expected effect suggesting a different

physiological mechanism or a non-biological nature of the events. Gap junction activation with TMA could not promote high frequency activity in human slices, although more experiments are needed to draw conclusions on the origins of fast oscillations.

An ictal episode observed in one of the human brain slices confirmed the epileptogenic nature of the tissue. As previously mentioned, human tissue *in vitro* appears to be relatively seizure-resistant, making epilepsy research *in vitro* rather difficult (Heinemann and Staley, 2014). Various methods have been used to promote ictogenesis in the brain slice, including 4-AP, bicuculline, elevated K^+ and reduced Mg^{2+} , however whether these models are physiologically relevant is still a question open for discussion (Avoli *et al.*, 2003; Gabriel *et al.*, 2004; Huberfeld *et al.*, 2011). Recent advances in the clinical field demonstrate the use of a single pulse electrical stimulation as a new diagnostic tool for epileptogenic focus detection (Valentin *et al.*, 2008). It has been shown that a single pulse of electrical stimulation produces a different response in the regions of spontaneous seizure occurrence, compared to normal brain regions. This method could be implemented *in vitro* to facilitate epilepsy research and is now being piloted in the laboratory.

7.4. Conclusion

Overall, we are starting to uncover electrophysiological properties and neuronal network dynamics of the human brain tissue. We are still in the early stages of understanding cellular and network mechanisms of synchronised activity in the human brain. Nevertheless, the findings we have so far show a striking similarity between the human and animal brain tissue. We have demonstrated the possibility of recording oscillations of various frequencies in reduced cortical networks of the human brain, much like in rat brain slices. The mechanism of human oscillations is also similar in its dependence on both synaptic inhibition and excitation, as well as non-synaptic mechanisms. Completing pharmacological and electrophysiological characterisation of rhythmic activity and supporting LFP findings with intracellular data would set a solid foundation for *in vitro* human brain research, which could be built on and compared to in pathological conditions. Once the electrophysiological properties of human brain tissue are established, it would present an opportunity to explore KAr and AMPAr changes, as well as other alterations in the human epilepsy.

Chapter 8 General discussion and future work

The ultimate goal of this project was to explore the process of epileptogenesis in the temporal lobe, since TLE, intractable forms in particular, constitute a large clinical problem. As the hippocampus and the EC are known to be implicated in the development of TLE, these were the areas of our focus.

To understand the course of epileptogenesis, it is important to approach it at the right organisational level, as epilepsy is a network disorder. Dynamic changes in the network operation could well reflect the progression of epileptogenesis. We therefore chose spontaneous rhythmic activity of neuronal populations to characterize the state of hippocampal and EC networks throughout the development of epilepsy. Spontaneous oscillations seem to represent well the natural (free of external intervention) state of the network and do not raise questions about the validity of induction models of rhythmic activity *in vitro*.

Having this in mind, we established a model of SyO in the hippocampal CA3 region. SyO had been previously observed by Pietersen *et al.* (2009), however, on a less regular and reliable basis than our own observations. We determined the nature of this activity and carried out a pharmacological comparison to other gamma oscillation models existing in literature (KyO and CChyO). The results showed that SyO represented a separate class of rhythmic activity, as they were pharmacologically different from previously described KyO and CChyO. These findings were further confirmed by phase analysis of the models. Nevertheless, having routinely observed stable SyO in the hippocampus was a reliable way of assessing network function in healthy and pathological conditions. Despite the fact that spontaneous activity in the hippocampus has been reported by a number of studies, the transient nature and sporadic occurrence of spontaneous oscillations present serious limitations for the utilisation of this model in hippocampal studies. By contrast, our slices routinely exhibited a persistent activity of high frequency and power, which was stable for hours, thus allowing the use of this activity to characterise network function in various physiological and pathological states, epilepsy in particular. Together with the hippocampus, we explored the EC and detected spontaneous rhythmic activity of low frequency in layers II/III (SWO). SWO were pharmacologically characterised to establish basic synaptic mechanism of these oscillations, which were used to study epilepsy development in the EC. Overall, established and characterised spontaneous

activity in the major regions of the temporal lobe set a solid foundation for exploring network changes occurring during epileptogenesis and leading to the development of behavioural seizures.

To study chronic TLE, we developed Li-pilocarpine-based RISE model, which proved to have reduced severity, yet high morbidity. The use of the Li-low-dose pilocarpine protocol, reduction of SE duration, administration of xylazine and the use of the multi-drug cocktail altogether provide a highly reliable and repeatable method for induction of epilepsy which reduces mortality whilst maintaining a high degree of epileptogenicity. Unlike other, more aggressive models, the subtle nature of this model does not allow gross neuropathological changes, thus mimicking the natural course of epilepsy. We assessed the progression of epileptogenesis in this model based on the changes in hippocampal $S\gamma O$ and EC SWO. Recordings were conducted at 4 timepoints following the initial insult (SE): PSE 24h (recovery from SE), PSE 7d and PSE 6wks (early and late latent period, respectively), PSE 90d (occurrence of SRS). Observations, supposedly, covered the main stages of epileptogenesis, such as SE, followed by a seizure-free latent period, culminating in the appearance of behavioural seizures (SRS). The hippocampal network demonstrated signs of hyperactivity with elements of high frequency oscillations shortly after the SE and during the SRS stage, when ictal and interictal activities were also detected. The late latent period (seizure-free stage), on the other hand, showed reduced network activity, which was reflected by reduced power of $S\gamma O$ in CA3. These findings suggested that certain changes occurred in the network during epileptogenesis, in particular during latent and SRS stages, when a period of quiescence was associated with reduced neuronal synchronisation, while the appearance of behavioural seizure coincided with the network activity bouncing back. We hypothesised that network fragmentation during the latent period (possibly due to the loss of interneurons) and its reconnection during the SRS stage might underlie the transition from no-seizure to seizure period. A substantial body of literature is still focused on the role of GABA inhibition in epilepsy, while changes in the excitatory component are sometimes overlooked. Nevertheless, several studies have pointed out the role of KAr in the epileptic condition (Mulle *et al.*, 1998; Mathern *et al.*, 1998; Smolders *et al.*, 2002; Fisahn *et al.*, 2004). We, therefore, explored KAr function and their possible role in the network alterations throughout epileptogenesis, including

network fragmentation. SyO, in this light, presented a useful tool for exploring network properties.

We set out to test this hypothesis by challenging hippocampal SyO with KA, to evaluate the response/network excitability at different stages of epileptogenesis. The results showed a striking difference in the latent period, when KAr stimulation produced a minimal effect. By contrast, the response was restored when epilepsy was established and behavioural seizures occurred, which guided us to further investigate KAr function directly via intracellular recordings. Unfortunately, due to poor survival of CA3 region in older animals, this has proved to be rather challenging. Therefore, at this point it is not clear whether the effect was mediated by direct activation of KAr or presynaptic modulation via KAr. Nevertheless, it is clear that the latent period deserves attention, as the occurring changes might play a key role in the establishment of epilepsy in the hippocampus. We also investigated neuronal network changes appearing in the EC and used spontaneous SWO for their evaluation. It should be noted that SWO were present in the slices only up to a certain animal age, therefore EC network function was explored during the early stages post-SE. Generally, spontaneous activity was fairly similar between epileptic and AMC slices. However, shortly after the SE, the system showed a greater dependence on AMPAr activation compared to control slices. Possible mechanisms could include upregulation or abnormal function/subunit composition of AMPAr following the SE. Overall, alterations in the function of KAr and AMPAr might be a part of the complex changes associated with epileptogenesis.

The role of excitatory glutamatergic transmission in epilepsy has been in the shadow of GABA research. However, both AMPAr and KAr appear to be involved in the complex mechanism of epileptogenesis and might contribute to/be responsible for the development of behavioural seizures. As our findings demonstrated, both the hippocampus and the EC neuronal networks undergo changes associated with glutamatergic receptors. Considering the complexity of epilepsy mechanism, it is worth exploring multiple receptor types, as has been done by Graebenitz and colleagues (2011) and Palomero-Gallagher *et al.* (2012) who have shown altered expression of glutamatergic, cholinergic and adrenergic receptors in human epilepsy. It is worth asking: what are the differences in epileptogenesis between the

hippocampus and the EC, does it develop on a different time scale in these regions, what are the roles of KAr and AMPAr, as well as what happens in the EC later into the epileptogenesis. Hence, there is plenty of room for further research:

- .: Explore the role of KAr in the hippocampus during epileptogenesis using intracellular techniques. Investigate possible involvement of AMPAr in the hippocampus.
- .: Explore the role of AMPAr and KAr in the EC during all stages of epileptogenesis.
- .: Correlate findings from RISE model in animals with the epileptic human tissue data.

References

- Abegg, M. H., Savic, N., Ehrenguber, M.U., McKinney, R.A. and Gähwiler, B.H. (2004). Epileptiform activity in rat hippocampus strengthens excitatory synapses. *J Physiol*, 554(2), p.439-448.
- Achermann, P. and Borbely, A. A. (1997). Low-frequency (< 1 Hz) oscillations in the human sleep electroencephalogram. *Neuroscience*, 81, p.213-222.
- Acsady, L., Gorcs, T.J. and Freund, T.F. (1996). Different populations of vasoactive intestinal olpeptide-immunoreactive interneurons are specialized to control pyramidal cells or interneurons in the hippocampus. *Neuroscience*, 73, p.317-334.
- Adelson, P.D. (2008). The surgical treatment of temporal lobe epilepsy in children. *Progress in Clinical Neurosciences*, 23, p.201.
- Aghajanian, G. K. and Rasmussen, K. (1989). Intracellular studies in the facial nucleus illustrating a simple new method for obtaining viable motoneurons in adult rat brain slices. *Synapse*, 3(4), p.331-338.
- Alger, B. E. (1984). Characteristics of A Slow Hyperpolarizing Synaptic Potential in Rat Hippocampal Pyramidal Cells-Invitro. *J. Neurophysiol.*, 52(5), p.892-910.
- Allene, C., Cattani, A., Ackman, J.B., Bonifazi, P., Aniksztejn, L., Ben-Ari, Y. and Cossart, R. (2008). Sequential generation of two distinct synapse-driven network patterns in developing neocortex. *J. Neurosci.*, 28, p.12851-12863.
- Allen, P.J., Fish, D.R. and Smith, S.J. (1992). Very high-frequency rhythmic activity during SEEG suppression in frontal lobe epilepsy. *Electroen. Clin. Neuro.*, 82, p.155-159.
- Alt, A., Weiss, B., Ogden, A.M., Knauss, J.L., Oler, J., Ho, K., Large, T.H. and Bleakman, D. (2004). Pharmacological characterization of glutamatergic agonists and antagonists at recombinant human homomeric and heteromeric kainate receptors *in vitro*. *Neuropharmacol.*, 46, p.793-806.
- Amzica, F. and Steriade, M. (1998). Electrophysiological correlates of sleep delta waves. *Electroen. Clin. Neuro.*, 107(2), p.69-83.
- Andersen, P., Bland, B., Skrede, K., Sveen, O. and Westgaard. R. (1972). Single unit discharge in brain slices maintained *in vitro*. *Acta Physiol Scand*, 84, p.1-2.
- André, V., Dubé, C., François, J., Leroy, C., Rigoulot, M.A. and Roch, C. (2007). Pathogenesis and pharmacology of epilepsy in the lithium–pilocarpine model. *Epilepsia*, 48(Suppl 5), p.41-47.
- Apland, J.P., Aroniadou-Anderjaska, V. and Braga, M.F. (2009). Soman induces ictogenesis in the amygdala and interictal activity in the hippocampus that are blocked by a GluR5 kainate receptor antagonist *in vitro*. *Neuroscience*, 159, p.380-389.
- Apland, J.P., Aroniadou-Anderjaska, V., Figueiredo, T.H., *et al.* (2013). Efficacy of the GluK1/AMPA receptor antagonist LY293558 against seizures and

- neuropathology in a soman-exposure model without pretreatment and its pharmacokinetics after intramuscular administration. *J Pharmacol Exp Ther*, 344, p.133-140.
- Assaf, B.A. and Ebersole, J.S. (1997). Continuous source imaging of scalp ictal rhythms in temporal lobe epilepsy. *Epilepsia*, 38(10), p.1114-1123.
- Avoli, M. and Olivier, A. (1989). Electrophysiological properties and synaptic responses in the deep layers of the human epileptogenic neocortex *in vitro*. *J. Neurophysiol.*, 61(3), p.589-606.
- Avoli, M., Drapeau, C., Louvel, J., Pumain, R., Olivier, A. and Villemure, J.G. (1991). Epileptiform activity induced by low extracellular magnesium in the human cortex maintained *in vitro*. *Ann. Neurol.*, 30, p.589-596.
- Avoli, M., Mattia, D., Siniscalchi, A., Perreault, P. and Tomaiuolo, F. (1994). Pharmacology and electrophysiology of a synchronous GABA-mediated potential in the human neocortex. *Neuroscience*, 62, p.655-666.
- Avoli, M., Louvel, J., Kurcewicz, I., Pumain, R. and Barbarosie, M. (1996). Extracellular free potassium and calcium during synchronous activity induced by 4-aminopyridine in the juvenile rat hippocampus. *J. Physiol (Lond.)*, 493, p.707-717.
- Babiloni, C., Ferri, R., Moretti, D.V., Strambi, A., Binetti, G., Dal Forno, G., Ferreri, F., Lanuzza, B., Bonato, C., Nobili, F., *et al.* (2004). Abnormal fronto-parietal coupling of brain rhythms in mild Alzheimer's disease: a multicentric EEG study. *Eur. J. Neurosci.*, 19, p.2583-2590.
- Baker, S.N., Olivier, E. and Lemon, R.N. (1997). Coherent oscillations in monkey motor cortex and hand muscle EMG show task-dependent modulation. *J. Physiol.*, 501(Pt 1), p.225-241.
- Bandrowski, A.E., Huguenard, J.R. and Prince, D.A. (2003). Baseline glutamate levels affect group I and II mGluRs in layer V pyramidal neurons of rat sensorimotor cortex. *J. Neurophysiol.*, 89(3), p.1308-1316.
- Barbarosie, M. and Avoli, M. (1997). CA3-driven hippocampal-entorhinal loop controls rather than sustains *in vitro* limbic seizures. *J. Neurosci.*, 17, p.9308-9314.
- Bartolomei, F., Khalil, M., Wendling, F., Sontheimer, A., Regis, J. and Ranjeva, J.P. (2005). Entorhinal cortex involvement in human mesial temporal lobe epilepsy: an electrophysiologic and volumetric study. *Epilepsia*, 46, p.677-687.
- Barton, M.E., Klein, B.D., Wolf, H.H. and White, H.S. (2001). Pharmacological characterization of the 6 Hz psychomotor seizure model of partial epilepsy. *Epilepsy Res.*, 47, p.217-227.
- Baybis, M., Lynch, D., Lee, A., Patel, A., McKhann, G., Chugani, D., . and Crino, P. B. (2004). Altered Expression of Neurotransmitter-receptor Subunit and Uptake Site mRNAs in Hemimegalencephaly. *Epilepsia*, 45(12), p.1517-1524.

- Bazhenov, M., Timofeev, I., Steriade, M. and Sejnowski, T.J. (2002). Model of thalamocortical slow-wave sleep oscillations and transitions to activated states. *J. Neurosci.*, 22(8), p.691-704
- Beck, H., & Yaari, Y. (2008). Plasticity of intrinsic neuronal properties in CNS disorders. *Nat. Rev. Neurosci.*, 9(5), 357-369.
- Beed, P.S., Salmen, B. and Schmitz, D. (2009). GluK2-mediated excitability within the superficial layers of the entorhinal cortex. *PLoS One* 4, e5576.
- Behr, J., Gebhardt, C., Heinemann, U. and Mody, I. (2002). Kindling enhances kainate receptor-mediated depression of GABAergic inhibition in rat granule cells. *Eur. J. Neurosci.*, 16, p.861-867.
- Belluscio, M.A., Mizuseki, K., Schmidt, R., Kempter, R. and Buzsaki, G. (2012). Cross-frequency phase-phase coupling between theta and gamma oscillations in the hippocampus. *J. Neurosci.*, 32(2), p.423-35.
- Ben-Ari, Y. (1985). Limbic seizure and brain damage produced by kainic acid: mechanisms and relevance to human temporal lobe epilepsy. *Neuroscience*, 14(2), p.375-403.
- Ben-Ari, Y. and Cossart, R. (2000). Kainate, a double agent that generates seizures: two decades of progress. *Trends Neurosci.*, 23, p.580-587.
- Ben-Ari, Y. (2004). History of Neuroscience: Kainic Acid and Temporal Lobe Epilepsy. *IBRO History of Neuroscience*.
- Benifla, M., Otsubo, H., Ochi, A., Weiss, S.K., Donner, E.J., Shroff, M. and Rutka, J.T. (2006). Temporal Lobe Surgery for Intractable Epilepsy in Children: An Analysis Of outcomes in 126 Children. *Neurosurgery*, 59(6), p.1203-1214.
- Bernard, C., Esclapez, M., Hirsch, J. C. and Ben-Ari, Y. (1998). Interneurons are not so dormant in temporal lobe epilepsy: a critical reappraisal of the dormant basket cell hypothesis. *Epilepsy Res.*, 32(1), p.93-103.
- Bernard, C., Cossart, R., Hirsch, J.C., Esclapez, M. and Ben-Ari, Y. (2000). What is GABAergic inhibition? How is it modified in epilepsy? *Epilepsia*, 41, p.90-95.
- Bernasconi, N., Bernasconi, A. and Andermann, F., Dubeau, F., Feindel, W. and Reutens, D.C. (1999). Entorhinal cortex in temporal lobe epilepsy A quantitative MRI study. *Neurology*, 52(9), p.1870-1870.
- Berry, S.D. and Thompson, R.F. (1978). Prediction of learning rate from the hippocampal electroencephalogram. *Science*, 200, p.1298-1300.
- Berry, S.D. and Seager, M.A. (2001). Hippocampal theta oscillations and classical conditioning. *Neurobiol Learn Mem*, 76, p.298-313.
- Best, N., Mitchell, J. and Wheal, H.V. (1994). Ultrastructure of parvalbumin-immunoreactive neurons in the CA1 area of the rat hippocampus following a kainic acid injection. *Acta neuropathologica*, 87(2), p.187-195.

Bettler, B. and Mulle, C. (1995). Review: neurotransmitter receptors. II. AMPA and kainate receptors. *Neuropharmacol.*, 34, p.123-139.

Bialer, M., Johannessen, S.I., Levy, R.H., Perucca, E., Tomson, T. and White, H.S. (2009). Progress report on new antiepileptic drugs: a summary of the Ninth Eilat Conference (EILAT IX). *Epilepsy Res.*, 83, p.1-43.

Bland, B.H. and Oddie, S.D. (2001). Theta band oscillation and synchrony in the hippocampal formation and associated structures: the case for its role in sensorimotor integration. *Behav. Brain. Res.*, 127(1), p.119-136.

Boddeke, H.W., Best, R. and Boeijinga, P.H. (1997). Synchronous 20 Hz rhythmic activity in hippocampal networks induced by activation of metabotropic glutamate receptors *in vitro*. *Neuroscience*, 76, p.653-658.

Bonilha, L., Kobayashi, E., Rorden, C., Cendes, F. and Li, L.M. (2003). Medial temporal lobe atrophy in patients with refractory temporal lobe epilepsy. *J Neurol Neurosurg Psychiatry*, 74(12), p.1627-1630.

Bouyer, J.J., Montaron, M.F. and Rougeul, A. (1981). Fast fronto-parietal rhythms during combined focused attentive behavior and immobility in cat: cortical and thalamic localizations. *Electroencephal Clin Neurophysiol*, 51, p.244-252.

Bragin, A., Jando, G., Nadasdy, Z., Hetke, J., Wise, K. and Buzsaki, G. (1995). Gamma frequency (40-100 Hz) patterns in the hippocampus of the behaving rat. *J. Neurosci.*, 15, p.47-60.

Bragin, A., Csicsvari, J., Penttonen, M. and Buzsaki, G. (1997). Epileptic afterdischarge in the hippocampal-entorhinal system: current source density and unit studies. *Neuroscience*, 76, p.1187-1203.

Bragin, A., Engel, J. Jr, Wilson, C.L., *et al.* (1999a). Hippocampal and entorhinal cortex high-frequency oscillations (100–500 Hz) in human epileptic brain and in kainic acid-treated rats with chronic seizures. *Epilepsia*, 40, p.127-37.

Bragin, A., Engel, J. Jr, Wilson, C.L., Fried, I. and Buzski, G. (1999b). High-frequency oscillations in the human brain. *Hippocampus*, 9, p.137-142.

Bragin, A., Azizyan, A., Almajano, J., Wilson, C. L. and Engel, J. (2005). Analysis of chronic seizure onsets after intrahippocampal kainic acid injection in freely moving rats. *Epilepsia*, 46(10), p.1592-1598.

BrainSliceMethods, accessed on 01 August 2014, <http://www.brainslicemethods.com/#!/recipes/czv4>.

Brines, M.L., Sundaresan, S., Spencer, D.D. and Lanerolle, N. C. (1997). Quantitative Autoradiographic Analysis of Ionotropic Glutamate Receptor Subtypes in Human Temporal Lobe Epilepsy: Up-regulation in Reorganized Epileptogenic Hippocampus. *Eur. J. Neurosci.*, 9(10), p.2035-2044.

Brock, J., Brown, C.C., Boucher, J. and Rippon, G. (2002). The temporal binding deficit hypothesis of autism. *Dev. Psychopathol.*, 14, p.209-224.

- Brown, J.T., Teriakidis, A. and Randall, AD. (2006). A pharmacological investigation of the role of GLUK5-containing receptors in kainate-driven hippocampal gamma band oscillations. *Neuropharmacol.*, 50. P.47-56.
- Bruckner, C. and Heinemann, U. (2000). Effects of standard anticonvulsant drugs on different patterns of epileptiform discharges induced by 4-aminopyridine in combined entorhinal cortex-hippocampal slices. *Brain Res.*, 859, p.15-20.
- Buchheim, K., Schuchmann, S., Siegmund, H., Weissinger, F., Heinemann, U. And Meierkord, H. (2000). Comparison of intrinsic optical signals associated with low Mg^{2+} -4-aminopyridine-induced seizure-like events reveals characteristic features in adult rat limbic system. *Epilepsia*, 41, p.635-641.
- Buchmann, A., Kurth, S., Ringli, M., Geiger, A., Jenni, O.G. and Huber, R. (2011). Anatomical markers of sleep slow wave activity derived from structural magnetic resonance images. *J. Sleep Res.*, 20(4), p.506-513.
- Buckmaster, P.S. and Jongen-Relo, A.L.(1999). Highly specific neuron loss preserves lateral inhibitory circuits in the dentate gyrus of kainate-induced epileptic rats. *J. Neurosci.* 19, p.9519-9529.
- Buhl, E.H., Halasy, K. and Somogyi. P. (1994). Diverse sources of hippocampal unitary inhibitory postsynaptic potentials and the number of synaptic release sites. *Nature*, 368, p.823-828.
- Buhl, E.H., Tamas, G. and Fisahn, A. (1998). Cholinergic activation and tonic excitation induce persistent gamma oscillations in mouse somatosensory cortex *in vitro*. *J Physiol (Lond)*, 513, p.117-126.
- Buhl, D.L., Harris, K.D., Hormuzdi, S.G., Monyer, H. and Buzsaki, G. (2003). Selective impairment of hippocampal gamma oscillations in connexin-36 knock-out mouse *in vivo*. *J. Neurosci.*, 23, p.1013-1018.
- Buzsaki, G., Leung, L. and Vanderwolf, C.H. (1983). Cellular bases of hippocampal EEG in the behaving rat. *Brain Res. Rev*, 6, p.139-171.
- Buzsaki, G., Horvath, Z., Urioste, R., Hetke, J. and Wise, K. (1992). High-frequency network oscillation in the hippocampus. *Science*, 256, p.1025-1027.
- Buzsáki, G. and Chrobak, J.J. (1995). Temporal structure in spatially organized neuronal ensembles: a role for interneuron networks. *Curr Opin Neurobiol*, 5, p.504-510.
- Buzsáki, G., Buhl, D.L., Harris, K.D., Csicsvari, J., Czeh, B. and Morozov, A. (2003). Hippocampal network patterns of activity in the mouse. *Neuroscience*, 116, p.201-211.
- Buzsaki, G. and Draguhn, A. (2004) Neuronal oscillations in cortical networks. *Science*, 304 (00:00), p.1926 -1929.
- Buzsaki, G. (2006). *Rhythms of the Brain*. Oxford University Press.

- Buzsáki, G. and Wang, X.J. (2012). Mechanisms of gamma oscillations. *Annu. Rev. Neurosci.*, 35, p.203–225.
- Castillo, P.E., Malenka, R.C. and Nicoll, R.A. (1997). Kainate receptors mediate a slow postsynaptic current in hippocampal CA3 neurons. *Nature*, 388, p.182-186.
- Case, L. and Broberger, C. (2013). A method for visually guided whole-cell recordings in brain slices exhibiting spontaneous rhythmic activity. *J. Neurosci. Methods*, 212(1), p.64-71.
- Cataltepe, O. and Cosgrove, G.R. (2011). Surgical Management of Lesional Temporal Lobe Epilepsy. In: Cataltepe, O. and Jallo, G.I. (eds.) *Pediatric Epilepsy Surgery: Preoperative Assessment and Surgical Treatment*. p.161-174.
- Cavalheiro, E.A., Leite, J.P., Bortolotto, Z.A., Turski, W.A., Ikonomidou, C. and Turski, L. (1991). Long-term effects of pilocarpine in rats: structural damage of the brain triggers kindling and spontaneous recurrent seizures. *Epilepsia*, 32, p.778-782.
- Cavalheiro, E.A., Naffah-Mazzacoratti, M.G., Mello, L.E. and Leite, J.P. (2006). The Pilocarpine Model of Seizures. In: Pitkänen, A., Schwartzkroin, P.A. and Moshé, S.L. (eds.) *Models of Seizures and Epilepsy*. Burlington, MA: Elsevier Academic, p.433-449.
- Cendes, F., andermann, F., Carpenter, S., Zatorre, R.J. and Cashman, N.R. (1995). Temporal lobe epilepsy caused by domoic acid intoxication: evidence for glutamate receptor-mediated excitotoxicity in humans. *Ann. Neurol.*, 37, p.123-126.
- Chakir, A., Fabene, P.F., Ouazzani, R. and Bentivoglio, M. (2006). Drug resistance and hippocampal damage after delayed treatment of pilocarpine-induced epilepsy in the rat. *Brain Res Bull.*, 71, p.127-138.
- Chamberlain, S. (2009). *Functional role of kainate receptors in the rat entorhinal cortex* (Doctoral dissertation, University of Bath).
- Chamberlain, S.E., Jane, D.E. and Jones, R.S. (2012). Pre- and post-synaptic functions of kainate receptors at glutamate and GABA synapses in the rat entorhinal cortex. *Hippocampus* 22, p.555-576.
- Chauvette, S., Volgushev, M. and Timofeev, I. (2010). Origin of active states in local neocortical networks during slow sleep oscillation. *Cereb Cortex*, 20, p.2660-2674.
- Chittajallu, R., Vignes, M., Dev, K.K., Barnes, J.M., Collingridge, G.L. and Henley, J.M. (1996). Regulation of glutamate release by presynaptic kainite receptors in the hippocampus. *Nature*, 379, p.78-81.
- Christensen, J.K., Paternain, A.V., Selak, S., Ahring, P.K. and Lerma, J. (2004). A mosaic of functional kainate receptors in hippocampal interneurons. *J. Neurosci.*, 24(41), p.8986-8993.
- Chugani, H.T., Shewmon, D.A., Shields, W.D., Sankar, R., Comair, Y., Vinters, H.V. and Peacock, W.J. (1993). Surgery for intractable infantile spasms: neuroimaging perspectives. *Epilepsia*, 34(4), p.764-771.

- Clarke, V.R.J., Ballyk, B.A., Hoo, K.H., Mandelzys, A., Pellizzari, A., Bath, C.P., Thomas, J., Sharpe, E.F., Davies, C.H., Ornstein, P.L., Schoepp, D.D., Kamboj, R.K., Collingridge, G.L., Lodge, D. and Bleakman, D. (1997). A hippocampal GluR5 kainate receptor regulating inhibitory synaptic transmission. *Nature*, 389, p.599-603.
- Clifford, D.B., Olney, J.W., Maniotis, A., Collins, R.C. and Zorumski, C.F. (1987). The functional anatomy and pathology of lithium-pilocarpine and high-dose pilocarpine seizures. *Neuroscience*, 23, p.953-968.
- Cobb, S.R., Halasy, K., Vida, I., Nyiri, G., Tamas, G., Buhl, E.H. and Somogyi, P. (1997). Synaptic effects of identified interneurons innervating both interneurons and pyramidal cells in the rat hippocampus. *Neuroscience*, 79, p.629-648.
- Colgin, L.L., Denninger, T., Fyhn, M., Hafting, T., Bonnevie, T., Jensen, O., Moser, M.B. and Moser, E.I. (2009). Frequency of gamma oscillations routes flow of information in the hippocampus. *Nature*, 462(7271), p.353-357.
- Colgin, L.L. and Moser, E.I. (2010). Gamma oscillations in the hippocampus. *Physiol (Bethesda)*, 25, p.319-329.
- Collins, R.C., Tearse, R.G. and Lothman, E.W. (1983). Functional anatomy of limbic seizures: focal discharges from medial entorhinal cortex in rat. *Brain Res.*, 280(1), p.25-40.
- Colom, L.V. and Saggau, P. (1994). Spontaneous interictal-like activity originates in multiple areas of the CA2-CA3 region of hippocampal slices. *J Neurophysiol*, 71, p.1574-1585.
- Compte, A., Sanchez-Vives, M.V., McCormick, D.A. and Wang, X.J. (2003). Cellular and network mechanisms of slow oscillatory activity (<1 Hz) and wave propagations in a cortical network model. *J Neurophysiol*, 89, p.2707-2725.
- Compte, A., Reig, R., Descalzo, V.F., Harvey, M.A., Puccini, G.D. and Sanchez-Vives, M.V. (2008). Spontaneous high-frequency (10–80 Hz) oscillations during up states in the cerebral cortex *in vitro*. *J. Neurosci.*, 28(51), p.13828-13844.
- Contractor, A., Swanson, G. & Heinemann, S.F. (2001). Kainate receptors are involved in short- and long-term plasticity at mossy fiber synapses in the hippocampus. *Neuron*, 29, p.209-216.
- Contractor, A., Mulle, C. and Swanson, G.T. (2011). Kainate receptors coming of age: milestones of two decades of research. *Trends Neurosci.*, 34, p.154-163.
- Cossart, R., Esclapez, M., Hirsch, J.C., Bernard, C. and Ben-Ari, Y. (1998). GluR5 kainate receptor activation in interneurons increases tonic inhibition of pyramidal cells 41. *Nat. Neurosci.*, 1, p.470-478.
- Cossart, R., Tyzio, R., Dinocourt, C., Esclapez, M., Hirsch, J.C., Ben-Ari, Y. and Bernard, C. (2001). Presynaptic kainate receptors that enhance the release of GABA on CA1 hippocampal interneurons. *Neuron*, 29, p.497-508.

- Cossart, R., Epsztein, J., Tyzio, R., Becq, H., Hirsch, J., Ben-Ari, Y. and Crépel, V. (2002). Quantal release of glutamate generates pure kainate and mixed AMPA/kainate EPSCs in hippocampal neurons. *Neuron*, 35, p.147-159.
- Cremer, C. M., Palomero-Gallagher, N., Bidmon, H. J., Schleicher, A., Speckmann, E. J., and Zilles, K. (2009). Pentylentetrazole-induced seizures affect binding site densities for GABA, glutamate and adenosine receptors in the rat brain. *Neuroscience*, 163(1), p.490-499.
- Csicsvari, J., Hirase, H., Mamiya, A. and Buzsáki, G. (2000). Ensemble patterns of hippocampal CA3-CA1 neurons during sharp wave-associated population events. *Neuron*, 28(2), p.585-594.
- Csicsvari, J., Jamieson, B., Wise, K.D. and Buzsaki, G. (2003). Mechanisms of gamma oscillations in the hippocampus of the behaving rat. *Neuron*, 37, p.311-322.
- Csercsa, R., Dombovari, B., Fabo, D., Wittner, L., Eross, L., Entz, L., Solyom, A., Rasonyi, G., Szucs, A., Kelemen, A., *et al.* (2010). Laminar analysis of slow wave activity in humans. *Brain*, 133, p.2814-2829.
- Cunningham, M.O., Davies, C.H., Buhl, E.H. and Whittington, M.A. (2003). Gamma oscillations induced by kainate receptor activation in the entorhinal cortex *in vitro*. *J. Neurosci.* 23(30), p.9761-9769.
- Cunningham, M.O., Halliday, D.M., Davies, C.H., Traub, R.D., Buhl, E.H. and Whittington, M.A. (2004). Coexistence of gamma and high frequency oscillations in rat medial entorhinal cortex *in vitro*. *J Physiol.*, 559(2), p.347-353.
- Cunningham, M.O., Pervouchine, D.D., Racca, C., Kopell, N.J., Davies, C.H., Jones, R.S., Traub, R.D. and Whittington, M.A. (2006). Neuronal metabolism governs cortical network response state. *Proc Natl Acad Sci USA*, 103, p.5597-5601.
- Cunningham, M.O., Roopun, A., Schofield, I.S., Whittaker, R.G., Duncan, R., Russell, A. and Traub, R.D. (2012). Glissandi: transient fast electrocorticographic oscillations of steadily increasing frequency, explained by temporally increasing gap junction conductance. *Epilepsia*, 53(7), p.1205-1214.
- Curia, G.L., Biagini, G., Jones, R.S.G. and Avoli, M. (2008). The pilocarpine model of temporal lobe epilepsy. *J. Neurosci. Meth.*, 172, p.143-157.
- Curio, G., Mackert, B.M., Burghoff, M., Koetitz, R., Abraham-Fuchs, K. and Harer, W. (1994). Localization of evoked neuromagnetic 600 Hz activity in the cerebral somatosensory system. *Electroen. Clin. Neuro.*, 91, p.483- 487.
- Danbolt, N.C. (2001). Glutamate uptake. *Progress in neurobiology*, 65(1), p.1-105.
- Darstein, M., Petralia, R.S., Swanson, G.T., Wenthold, R.J. and Heinemann, S.F. (2003). Distribution of kainate receptor subunits at hippocampal mossy fiber synapses. *J. Neurosci.*, 23, p.8013-8019.
- Das, A., Wallace Iv, G. C., Holmes, C., McDowell, M. L., Smith, J. A., Marshall, J. D. and Banik, N. L. (2012). Hippocampal tissue of patients with refractory temporal lobe

epilepsy is associated with astrocyte activation, inflammation, and altered expression of channels and receptors. *Neuroscience*, 220, p.237-246.

de Almeida, L., Idiart, M. and Lisman, J.E. (2009). A second function of gamma frequency oscillations: an E%-max winner-take-all mechanism selects which cells fire. *J. Neurosci.*, 29, p.7497-7503.

DeFelipe, J., Huntley, G. W., del Río, M. R., Sola, R. G. and Morrison, J. H. (1994). Microzonal decreases in the immunostaining for non-NMDA ionotropic excitatory amino acid receptor subunits GluR 2/3 and GluR 5/6/7 in the human epileptogenic neocortex. *Brain Res.*, 657(1), p.150-158.

de la Prida, L.M., Benavides-Piccione, R., Sola, R. and Pozo, M.A. (2002). Electrophysiological properties of interneurons from intraoperative spiking areas of epileptic human temporal neocortex. *Neuroreport*, 13(11), p.1421-1425.

Desai, M.A., McBain, C.J., Kauer, J.A. and Conn, P.J. (1994). Metabotropic glutamate receptor-induced disinhibition is mediated by reduced transmission at excitatory synapses onto interneurons and inhibitory synapses onto pyramidal cells. *Neurosci Lett*, 181, p.78-82.

Devinsky, O., Vezzani, A., Najjar, S., De Lanerolle, N.C. and Rogawski, M.A. (2013). Glia and epilepsy: excitability and inflammation. *Trends Neurosci.*, 36(3), p.178-184.

Dickson, C.T., Biella, G., de Curtis, M. (2003). Slow periodic events and their transition to gamma oscillations in the entorhinal cortex of the isolated guinea pig brain. *J Neurophysiol*, 90, 39-46.

Doischer, D., Hosp, J.A., Yanagawa, Y., Obata, K., Jonas, P., Vida, I. and Bartos, M. (2008). Postnatal differentiation of basket cells from slow to fast signaling devices. *J. Neurosci.*, 28(48), p.12956-12968.

Dolman, N.P., More, J.C.A., Alt, A., Ogden, A.M., Troop, H.M., Bleakman, D., Collingridge, G.L. and Jane, D.E. (2006). Structure–activity relationship studies on N3 -substituted willardiine derivatives acting as AMPA or kainate receptor antagonists. *J. Med. Chem.*, 49, p.2579-2592.

Dolman, N.P., More, J.C.A., Alt, A., Knauss, J.L., Pentikäinen, O.T., Glasser, C.R., Bleakman, D., Mayer, M.L., Collingridge, G.L. and Jane, D.E. (2007). Synthesis and pharmacological characterization of N 3-substituted willardiine derivatives: role of the substituent at the 5-position of the uracil ring in the development of highly potent and selective GLUK5 kainate receptor antagonists. *J. Med. Chem.*, 50, p.1558-1570.

Draguhn, A., Traub, R.D., Schmitz, D., Jefferys, J.G.R. (1998). Electrical coupling underlies high-frequency oscillations in the hippocampus *in vitro*. *Nature*, 394, p.189-192.

Dudek, F.E., Hellier, J.L., Williams, P.A., Ferraro, D.J. and Staley, K.J. (2002). The course of cellular alterations associated with the development of spontaneous seizures after status epilepticus In: Sutula, T. and Pitkanen, A. (eds.) *Do seizures damage the brain?* (Elsevier, Amsterdam), p.53-65.

- Dudek, F. and Shao, L. (2004). Mossy fiber sprouting and recurrent excitation: Direct electrophysiological evidence and potential implications. *Epilepsy Currents*, 4, p.184-187.
- Dudek, F.E., Clark, S., Williams, P.A. and Grabenstatter, H.L. (2006). Kainate-Induced Status Epilepticus: a Chronic Model of Acquired Epilepsy. In: Pitkänen, A., Schwartzkroin, P.A., Moshé, S.L. (eds.) *Models of Seizures and Epilepsy*. Burlington, MA: Elsevier Academic, p.415-433.
- Du, F., Whetsell, W.O. Jr, Abou-Khalil, B., Blumenkopf, B., Lothman, E.W. and Schwarcz, R. (1993). Preferential neuronal loss in layer III of the entorhinal cortex in patients with temporal lobe epilepsy. *Epilepsy Res*, 16, p.223-233.
- Du, F., Eid, T., Lothman, E.W., Köhler, C. and Schwarcz, R. (1995). Preferential neuronal loss in layer III of the medial entorhinal cortex in rat models of temporal lobe epilepsy. *J. Neurosci.*, 15, p.6301-6313.
- Dzhala, V.I. and Staley, K.J. (2003). Transition from interictal to ictal activity in limbic networks *in vitro*. *J. Neurosci.*, 23, p.7873-7880.
- Dzhala, V. I. and Staley, K. J. (2004). Mechanisms of fast ripples in the hippocampus. *J. Neurosci.*, 24(40), p.8896-8906.
- Engel Jr, J. (1996). Introduction to temporal lobe epilepsy. *Epilepsy Res*, 26, p.141-150.
- Engel, A., Fries, P. and Singer, W. (2001). Dynamic predictions: oscillations and synchrony in top-down processing. *Nat. Rev. Neurosci.*, 2, p.704-716.
- Engel Jr, J. (2006). ILAE classification of epilepsy syndromes. *Epilepsy Res.*, 70, p.5-10.
- Engel Jr, J., Bragin, A., Staba, R. and Mody, I. (2009). High-frequency oscillations: what is normal and what is not? *Epilepsia*, 50, p.598-604.
- Epsztein, J., Repressa, A., Jorquera, I., Ben-Ari, Y. and Crépel, V. (2005). Recurrent mossy fibers establish aberrant kainate receptor-operated synapses on granule cells from epileptic rats. *J. Neurosci.*, 25(36), p.8229-8239.
- Epsztein, J., Sola, E., Represa, A., Ben-Ari, Y. and Crepel, V.A. (2010). Selective interplay between aberrant EPSPKA and INaP reduces spike timing precision in dentate granule cells of epileptic rats. *Cereb Cortex*, 20, p.898-911.
- Favero, M., Varghese, G. and Castro-Alamancos, M.A. (2012). The state of somatosensory cortex during neuromodulation. *J Neurophysiol*, 108, p.1010-1024.
- Fellous, J-M., Sejnowski, T. (2000). Cholinergic induction of oscillations in the hippocampal slice in the slow (0.5–2 Hz), theta (5–12 Hz), and gamma (35–70 Hz) bands. *Hippocampus*, 10, p.187-197.
- Figueiredo, T.H., Qashu, F., Apland, J.P., Aroniadou-Anderjaska, V., Souza, A.P. and Braga, M.F. (2011). The GluK1 (GluR5). Kainate/{alpha}-amino-3-hydroxy-5-

- methyl-4-isoxazolepropionic acid receptor antagonist LY293558 reduces soman-induced seizures and neuropathology. *J Pharmacol Exp Ther.*, 336, p.303-312.
- Fisahn, A., Pike, F.G., Buhl, E.H. and Paulsen, O. (1998). Cholinergic induction of network oscillations at 40 Hz in the hippocampus *in vitro*. *Nature*, 394, p.186-189.
- Fisahn, A., Contractor, A., Traub, R.D., Buhl, E.H., Heinemann, S.F. and McBain, C.J. (2004). Distinct roles for the kainate receptor subunits GluR5 and GluR6 in kainate-induced hippocampal gamma oscillations. *J. Neurosci.*, 24, p.9658-9668.
- Fisahn, A. (2005). Kainate receptors and rhythmic activity in neuronal networks: hippocampal gamma oscillations as a tool. *J. Physiol.*, 562(1), p.65-72.
- Fisher, R.S., Alger, B.E. (1984). Electrophysiological mechanisms of kainic acid-induced epileptiform activity in the rat hippocampal slice. *J. Neurosci.*, 4(5), p.1312-1323.
- Fisher, R.S., Webber, W.R., Lesser, R.P., Arroyo, S. and Uematsu, S. (1992). High-frequency EEG activity at the start of seizures. *J Clin Neurophysiol*, 9, p.441-448.
- Florez, C.M., McGinn, R.J., Lukankin, V., Marwa, I., Sugumar, S., Dian, J., and Valiante, T.A. (2013). *In vitro* recordings of human neocortical oscillations. *Cereb. Cortex*, bht235.
- Foehring, R.C., Lorenzon, N.M., Herron, P.A. U. L. and Wilson, C.J. (1991). Correlation of physiologically and morphologically identified neuronal types in human association cortex *in vitro*. *J neurophysiol*, 66(6), p.1825-1837.
- Frerking, M., Petersen, C.C. and Nicoll, R.A. (1999). Mechanisms underlying kainate receptor-mediated disinhibition in the hippocampus. *Proc. Natl. Acad. Sci. USA*, 96, p.12917-12922.
- Frerking, M. and Nicoll, R.A. (2000). Synaptic kainate receptors. *Curr Opin Neurobiol.*, 10(3), p.342-351
- Frerking, M. and Ohliger-Frerking, P. (2002). AMPA receptors and kainite receptors encode different features of afferent activity. *J. Neurosci.*, 22, p.7434-7443.
- Fried I. (1993). Anatomic temporal lobe resections for temporal lobe epilepsy. *Neurosurg Clin N Am.*, 4(2), p.233-42.
- Fuchs, E.C., Zivkovic, A.R., Cunningham, M.O., Middleton, S. and Lebeau, F.E. (2007). Recruitment of parvalbumin-positive interneurons determines hippocampal function and associated behavior. *Neuron*, 53, p.591-604.
- Fukuda, T. and Kosaka, T. (2000). Gap junctions linking the dendritic network of GABAergic interneurons in the hippocampus. *J. Neurosci.*, 20, p.1519-1528.
- Gabriel, S., Njunting, M., Pomper, J.K., Merschhemke, M., Sanabria, E.R.G., Eilers, A., Kivi, A., Zeller, M., Meencke, H.J., Cavalheiro, E.A., Heinemann, U. and Lehmann, T.N. (2004). Stimulus and potassium-induced epileptiform activity in the human dentate gyrus from patients with and without hippocampal sclerosis. *J. Neurosci.*, 24, p.10416-10430.

- Galarreta, M. and Hestrin, S. (1999). A network of fast-spiking cells in the neocortex connected by electrical synapses. *Nature*, 402, p.72-75.
- Galarreta, M. and Hestrin, S. (2002). Electrical and chemical synapses among parvalbumin fast-spiking GABAergic interneurons in adult mouse neocortex. *Proc. Natl Acad. Sci. USA*, 99, p.12438-12443.
- Garcia Dominguez, L., Wennberg, R.A., Gaetz, W., Cheyne, D., Snead, O.C., III, and Perez Velazquez, J.L. (2005). Enhanced synchrony in epileptiform activity? Local versus distant phase synchronization in generalized seizures. *J. Neurosci.*, 25, p.8077-8084.
- Garthwaite, J., Woodhams, P.L., Collins, M.J. and Balazs, R. (1980). A morphological study of incubated slices of rat cerebellum in relation to postnatal age. *Dev Neurosci.*, 3, p.90-99.
- Geddes, J.W., Gahan, L.D., Cooper, S.M., Kim, R.C., Choi, B.H. and Cotman, C.W. (1990). Altered distribution of excitatory amino acid receptors in temporal lobe epilepsy. *Exp. Neurol.*, 108(3), p.214-220.
- Gillies, M.J., Traub, R.D., LeBeau, F.E., Davies, C.H., Gloveli, T., Buhl, E.H. and Whittington, M.A. (2002). A model of atropine-resistant theta oscillations in the rat hippocampal area CA1. *J Physiol (Lond)*, 543, p.779-793.
- Givens, B.S. and Olton, D.S. (1990). Cholinergic and GABAergic modulation of the medial septal area: effect on working memory. *Behav Neurosci*, 104,p.849-855.
- Glien, M., Brandt, C., Potschka, H., Voigt, H., Ebert, U. and Löscher, W. (2001). Repeated low-dose treatment of rats with pilocarpine: low mortality but high proportion of rats developed epilepsy. *Epilepsy Res*, 46, p.111-119.
- Gloveli, T., Dugladze, T., Saha, S., Monyer, H. and Heinemann, U. (2005) Differential involvement of oriens/pyramidal interneurons in hippocampal network oscillations *in vitro*. *J. Physiol.* 562(1), p.131-147.
- Gnatkovsky, V., Wendling, F. and de Curtis, M. (2007). Cellular correlates of spontaneous periodic events in the medial entorhinal cortex of the *in vitro* isolated guinea pig brain. *Eur J. Neurosci.*, 26, p.302-311.
- Goddard, G.V., McIntyre, D.C. and Leech, C.K. (1969). A permanent change in brain function resulting from daily electrical stimulation. *Exp. Neurol.*, 25, p.295-330.
- Goffin, K., Nissinen, J., Van Laere, K. and Pitkänen, A. (2007). Cyclicity of spontaneous recurrent seizures in pilocarpine model of temporal lobe epilepsy in rat. *Exp Neurol*, 205, p.501-505.
- Goldin, M., Epsztein, J., Jorquera, I., Represa, A., Ben-Ari, Y., Crepel, V. & Cossart, R. (2007). Synaptic kainate receptors tune oriens-lacunosum moleculare interneurons to operate at theta frequency. *J. Neurosci.*, 27, p.9560-9572.
- Gong, X.W., Yang, F., Liu, J.S., Lu, Q.C., Gong, H.Q., Liang, P.J. and Zhang, P.M. (2010). Investigation of The Initiation Site and Propagation of Epileptiform Discharges

- in Hippocampal Slices Using Microelectrode Array. *Progress Biochem Biophys*, 37, p.1240-1247.
- González-Albo, M. C., Gómez-Utrero, E., Sánchez, A., Sola, R. G. and DeFelipe, J. (2001). Changes in the colocalization of glutamate ionotropic receptor subunits in the human epileptic temporal lobe cortex. *Exp. Brain Res.*, 138(3), p.398-402.
- Graebenitz, S., Kedo, O., Speckmann, E. J., Gorji, A., Panneck, H., Hans, V. and Pape, H.C. (2011). Interictal-like network activity and receptor expression in the epileptic human lateral amygdala. *Brain*, 134(10), p.2929-2947.
- Gray, C.M. and Singer, W. (1989). Stimulus-specific oscillations in orientation columns of cat visual cortex. *Proc Natl Acad Sci USA*, 86, p.1698-1702.
- Grenier, F, Timofeev, I. and Steriade, M. (2003). Neocortical very fast oscillations (ripples, 80–200 hz) during seizures: Intracellular correlates. *J Neurophysiol*, 89, p.841-852.
- Griffiths, M. J., Messent, M., MacAllister, R. J. and Evans, T. W. (1993). Aminoguanidine selectively inhibits inducible nitric oxide synthase. *Br.J.Pharmacol.*, 110(3), p.963-968.
- Grigorenko, E., Glazier, S., Bell, W., Tytell, M., Nosel, E., Pons, T. and Deadwyler, S. A. (1997). Changes in glutamate receptor subunit composition in hippocampus and cortex in patients with refractory epilepsy. *J. Neurol. Sci.*, 153(1), p.35-45.
- Gryder, D.S. and Rogawski, M.A., (2003). Selective antagonism of GluR5 kainate-receptor-mediated synaptic currents by topiramate in rat basolateral amygdala neurons. *J. Neurosci.*, 23(18), p.7069-7074.
- Guldvog, B., Loyning, Y., Hauglie-Hanssen, E., Flood, S. and Bjornaes, H. (1994). Surgical treatment for partial epilepsy among Norwegian children and adolescents. *Epilepsia*, 35(3), p.554-565.
- Gulyas, A.I., Miles, R., Sık, A., Toth, K., Tamamaki, N. and Freund, T.F. (1993). Hippocampal pyramidal cells excite inhibitory neurons through a single release site. *Nature*, 366(6456), p.683-687.
- Gulyás, A. I., & Freund, T. T. (2015). Generation of physiological and pathological high frequency oscillations: the role of perisomatic inhibition in sharp-wave ripple and interictal spike generation. *Curr. Opin. Neurobiol.*, 31, 26-32.
- Haider, B., Duque, A., Hasenstaub, A.R. and McCormick, D.A. (2006). Neocortical network activity *in vivo* is generated through a dynamic balance of excitation and inhibition. *J. Neurosci.*, 26(17), p.4535-4545.
- Hajos, F., Garthwaite, J., Garthwaite, G. and Csillag, A. (1989). Morphology of supravital brain slices pre-incubated in a physiological solution prior to fixation. *Acta Morphol Hung*, 37, p.181-199.
- Hájos, N., Katona, I., Naiem, S.S., Mackie, K., Ledent, C., Mody, I. and Freund, T.F. (2000). Cannabinoids inhibit hippocampal GABAergic transmission and network oscillations. *Eur J. Neurosci.*, 12, p.3239-3249.

- Hajos, N., Palhalmi, J., Mann, E.O., Nemeth, B., Paulsen, O. and Freund, T.F. (2004). Spike timing of distinct types of GABAergic interneuron during hippocampal gamma oscillations *in vitro*. *J. Neurosci.*, 24, p.9127-9137.
- Hájos, N. and Paulsen, O. (2009). Network mechanisms of gamma oscillations in the CA3 region of the hippocampus, *Neural Networks*, 22 (8), p.1113-1119.
- Halasy, K., Buhl, E.H., Lorinczi, Z., Tamas G. and Somogyi, P. (1996). Synaptic target selectivity and input of GABAergic basket and bistratified interneurons in the CA1 area of the rat hippocampus. *Hippocampus*, 6, p.306-329.
- Hamani, C. and Mello, L.E. (2002). Spontaneous recurrent seizures and neuropathology in the chronic phase of the pilocarpine and PTX model epilepsy. *Neurol Res.*, 24, p.199-209.
- Hamilton, S.E., Loose, M.D., Qi, M., Levey, A.I., Hille, B. and McKnight, G.S. (1997). Disruption of the m1 receptor gene ablates muscarinic receptor-dependent M current regulation and seizure activity in mice. *Proc Natl Acad Sci USA*, 94, p.13311–13316.
- Hansen, J.J., Nielsen, B., Krosgaard-Larsen, P., Brehm, L., Nielsen, E.Ø. and Curtis, D.R. (1989). Excitatory amino acid agonists. Enzymic resolution, X-ray structure, and enantioselective activities of (R)- and (S)-bromohomoibotenic acid. *J Med Chem*, 32, p.2254-2260.
- Hasenstaub, A., Shu, Y., Haider, B., Kraushaar, U., Duque, A. and McCormick, D.A. (2005). Inhibitory postsynaptic potentials carry synchronized frequency information in active cortical networks. *Neuron*, 47(3), p.423-435.
- Hauser, W.A. (1992). Seizure disorders: the changes with age. *Epilepsia*, 33(s4), p.6-14.
- Heinemann, U., Kann, O. and Schuchmann, S. (2006). An overview of *in vitro* seizure models in acute and organotypic slices. In: Pitkänen A, Schwartzkroin PA, Moshé SL (eds.), *Models of Seizures and Epilepsy*, Burlington, MA: Elsevier Academic, p.35–44.
- Heinemann, U. and Staley, K. J. (2014). What is the clinical relevance of *in vitro* epileptiform activity?. In: *Issues in Clinical Epileptology: A View from the Bench*. Springer Netherlands. p.25-41.
- Heistek, T.S., Timmerman, A.J., Spijker, S., Brussaard, A.B. and Mansvelder, H.D. (2010). GABAergic synapse properties may explain genetic variation in hippocampal network oscillations in mice. *Front Cell Neurosci*, 4, p.18.
- Herrmann, C.S., Munk, M.H. and Engel, A.K. (2004). Cognitive functions of gamma-band activity: memory match and utilization. *Trends Cogn. Sci.*, 8, p.347-355.
- Herrmann, C.S. and Demiralp, T. (2005). Human EEG gamma oscillations in neuropsychiatric disorders. *Clin Neurophysiol*, 116(12), p.2719–2733.
- Higashima, M., Ohno, K., Kinoshita, H. and Koshino, Y. (2000). Involvement of GABAA and GABAB receptors in after discharge generation in rat hippocampal slices. *Brain Res.*, 865, p.186-193.

- Hikiji, M., Tomita, H., Ono, M., Fujiwara, Y. and Akiyama, K. (1993). Increase of kainate receptor mRNA in the hippocampal CA3 of amygdala-kindled rats detected by *in situ* hybridization. *Life sciences*, 53(10), p.857-864.
- Honchar, M.P., Olney, J.W. and Sherman, W.R. (1983). Systemic cholinergic agents induce seizures and brain damage in lithium-treated rats. *Science*, 220, p.323-325.
- Hopfield J.J. (1995). Pattern recognition computation using action potential timing for stimulus representation. *Nature*, 376, p.33-36.
- Hormuzdi, S.G, Pais, I., LeBeau, F.E., Towers, S.K., Rozov, A., Buhl, E.H., Whittington, M.A. and Monyer, H. (2001). Impaired electrical signaling disrupts gamma frequency oscillations in connexin 36-deficient mice. *Neuron*, 31, p.487-495.
- Huang, X., McMahon, J. and Huang, Y. (2012). Rapamycin attenuates aggressive behavior in a rat model of pilocarpine-induced epilepsy. *Neuroscience*, 215, p.90-97.
- Huberfeld, G., Menendez, d.P., Pallud, J., Cohen, I., Le Van Quyen, M., Adam, C., Clemenceau, S., Baulac, M. and Miles, R. (2011). Glutamatergic pre-ictal discharges emerge at the transition to seizure in human epilepsy. *Nat Neurosci*, 14, p.627-634.
- Huber, R., Ghilardi, M.F., Massimini, M. and Tononi, G. (2004). Local sleep and learning. *Nature*, 430(6995), p.78-81.
- Hurtado, J.M., Rubchinsky, L.L. and Sigvardt, K.A. (2004). Statistical method for detection of phaselocking episodes in neural oscillations. *J. Neurophysiol.*, 91, p.1883-1898.
- Hu, Y., Jiang, L., Chen, H. and Zhang, X. (2012). Expression of AMPA receptor subunits in hippocampus after status convulsion. *Child's Nervous System*, 28(6), p.911-918.
- Hwa, G.G.C., Avoli, M., Olivier, A. and Villemure, J.G. (1991). Bicuculline-induced epileptogenesis in the human neocortex maintained *in vitro*. *Exp. Brain Res.*, 83, p.329-339.
- Iber, C., Ancoli-Israel, S., Chesson, A. and Quan, S.F. (2007). The AASM Manual for the Scoring of Sleep and Associated Events: Rules, Terminology and Technical Specifications. Westchester: American Academy of Sleep Medicine.
- Inoue, K., Morimoto, K., Sato, K., Yamada, N. and Otsuki, S. (1992). Mechanisms in the development of limbic status epilepticus and hippocampal neuron loss: an experimental study in a model of status epilepticus induced by kindling-like electrical stimulation of the deep prepyriform cortex in rats. *Acta Med. Okayama*, 46, p.129-139.
- Isomura, Y., Sirota, A., Özen, S., Montgomery, S., Mizuseki, K., Henze, D.A. and Buzsáki, G. (2006). Integration and segregation of activity in entorhinal-hippocampal subregions by neocortical slow oscillations. *Neuron*, 52(5), p.871-882.
- Jackson, G.D., Briellmann, R.S. and Kuzniecky, R.I. (2004). Temporal lobe epilepsy. In: Kuzniecky, R.I. and Jackson, G.D. (eds.) *Magnetic resonance in epilepsy; neuroimaging techniques*. Elsevier, Amsterdam, p.99-176.

- Jacobs, J., LeVan, P., Chander, R., Hall, J., Dubeau, F. and Gotman, J. (2008). Interictal high-frequency oscillations (80–500 Hz). are an indicator of seizure onset areas independent of spikes in the human epileptic brain. *Epilepsia*, 49, p.1893-1907.
- Jane, D.E., Lodge, D. and Collingridge, G.L. (2009). Kainate receptors: pharmacology, function and therapeutic potential. *Neuropharmacol.*, 56, p.90-113.
- Jasper, H.H. and Andrews H.L. (1938). Electroencephalography. III. Normal differentiation of occipital and precentral regions in man. *Arch Neurol Psychiatry*, 39, p.96-115.
- Jefferys, J.G.R. and Haas, H.L. (1982). Synchronized bursting of CA1 pyramidal cells in the absence of synaptic transmission. *Nature*, 300, p.448-450.
- Jensen, M.S. and Yaari, Y. (1988). The relationship between interictal and ictal paroxysms in an *in vitro* model of focal hippocampal epilepsy. *Ann Neurol*, 24, p.591-598.
- Jensen, O., Kaiser, J. and Lachaux, J.P. (2007). Human gamma-frequency oscillations associated with attention and memory. *Trends Neurosci.s*, 30(7), p.317-324.
- Ji, D. and Wilson, M.A. (2006). Coordinated memory replay in the visual cortex and hippocampus during sleep. *Nat. Neurosci.*, 10(1), p.100-107.
- Jones, R.S.G. and Heinemann, U. (1988). Synaptic and intrinsic responses of medial entorhinal cortical cells in normal and magnesium-free medium *in vitro*. *J Neurophysiol.*, 59(5), p.1476-1496.
- Jones, R.S.G. and Lambert, J.D.C. (1990). Synchronous discharges in the rat entorhinal cortex *in vitro*: Site of initiation and the role of excitatory amino acid receptors. *Neurosci.*, 34(3), p.657-670
- Jope, R.S., Morrisett, R.A. and Snead O.C. (1986). III Characterization of lithium potentiation of pilocarpine-induced status epilepticus in rats. *Exp Neurol.*, 91, p.471-480.
- Jutila, L., Ylinen, A., Partanen, K., Alafuzoff, I., Mervaala, E., Partanen, J., and Pitkänen, A. (2001). MR volumetry of the entorhinal, perirhinal, and temporopolar cortices in drug-refractory temporal lobe epilepsy. *Am. J. Neuroradiol.*, 22(8), p.1490-1501.
- Kahana, M.J., Sekuler, R., Caplan, J.B., Kirschen, M. and Madsen, J R. (1999). Human theta oscillations exhibit task dependence during virtual maze navigation. *Nature*, 399(6738), p.781-784.
- Kaminski, R.M., Banerjee, M. and Rogawski, M.A. (2004). Topiramate selectively protects against seizures induced by ATPA, a GluR5 kainate receptor agonist. *Neuropharmacol.*, 46(8), p.1097-1104.
- Kamiya, H. and Ozawa, S. (1998). Kainate receptor-mediated inhibition of presynaptic Ca²⁺ influx and EPSP in area CA1 of the rat hippocampus. *J. Physiol.*, 509(Pt. 3), p.833-845.

- Kamphuis, W., Hendriksen, H., Diegenbach, P.C. and Da Silva, F.H. (1995). N-methyl-d-aspartate and kainate receptor gene expression in hippocampal pyramidal and granular neurons in the kindling model of epileptogenesis. *Neuroscience*, 67(3), p.551-559.
- Kan, P., Van Orman, C. and Kestle, J.R. (2008). Outcomes after surgery for focal epilepsy in children. *Child's Nervous System*, 24(5), p.587-591.
- Karlócai, M. R., Kohus, Z., Káli, S., Ulbert, I., Szabó, G., Máté, Z., ... & Gulyás, A. I. (2014). Physiological sharp wave-ripples and interictal events in vitro: what's the difference?. *Brain*, 137(2), 463-485.
- Katzner, S., Nauhaus, I., Benucci, A., Bonin, V., Ringach, D.L. and Carandini, M. (2009). Local origin of field potentials in visual cortex. *Neuron*, 61, p.35-41.
- Keene, D. L., Higgins, M. J. and Ventureyra, E.C.G. (1997). Outcome and life prospects after surgical management of medically intractable epilepsy in patients under 18 years of age. *Child's Nervous System*, 13(10), p.530-535.
- Kehl, S.J., McLennan, H., Collingridge, G.L. (1984). Effects of folic and kainic acids on synaptic responses of hippocampal neurones. *Neurosci.*, 11(1), p.111-124.
- Khalilov, I., Hirsch, J., Cossart, R., Ben-Ari, Y. (2002). Paradoxical anti-epileptic effects of a GluR5 agonist of kainate receptors. *J Neurophysiol.*, 88, p.523–527
- Khazipov, R. and Holmes, G.L. (2003). Synchronization of kainate-induced epileptic activity via GABAergic inhibition in the superfused rat hippocampus *in vivo*. *J. Neurosci.*, 23, p.5337-5341.
- Kilner, J.M., Baker, S.N., Salenius, S., Jousmaki, V., Hari, R. and Lemon, R.N. (1999). Taskdependent modulation of 15-30 Hz coherence between rectified EMGs from human hand and forearm muscles. *J Physiol*, 516(Pt 2), p.559-570.
- Kirov, S.A., Sorra, K.E. and Harris, K.M. (1999). Slices have more synapses than perfusion-fixed hippocampus from both young and mature rats. *J. Neurosci.*, 19, p.2876-2886.
- Klitgaard, H., Matagne, A., Vanneste-Goemaere, J. and Margineanu, D.G. (2002). Pilocarpine-induced epileptogenesis in the rat: impact of initial duration of status epilepticus on electrophysiological and neuropathological alterations. *Epilepsy Res.*, 51, p.93-107.
- Klostermann, F., Nikulin, V.V., Kuhn, A.A., Marzinzik, F., Wahl, M., Pogosyan, A., Kupsch, A., Schneider, G.H., Brown, P. and Curio, G. (2007). Task- related differential dynamics of EEG alpha- and beta-band synchronization in cortico-basal motor structures. *Eur J. Neurosci.*, 25, p.1604-1615.
- Knopp, A., Kivi, A., Wozny, C., Heinemann, U. and Behr, J. (2005). Cellular and network properties of the subiculum in the pilocarpine model of temporal lobe epilepsy. *J Comp Neurol.*, 483, p.476-488.

- Kobayashi, K., Oka, M., Inoue, T., Ogino, T., Yoshinaga, H. and Ohtsuka, Y. (2005). Characteristics of slow waves on EEG associated with epileptic spasms. *Epilepsia*, 46(7), p.1098-1105.
- Koenig, T., Prichep, L., Dierks, T., Hubl, D., Wahlund, L.O., John, E.R. and Jelic, V. (2005). Decreased EEG synchronization in Alzheimer's disease and mild cognitive impairment. *Neurobiol. Aging*, 26, p.165-171.
- Kohling, R., Schwartzkroin, P.A. and Avoli, M. (2006). Studying Epilepsy in the Human Brain *In vitro*. In: Pitkänen, A., Schwartzkroin, P.A. and Moshé, S.L. (eds.) *Models of Seizures and Epilepsy*. Burlington, MA: Elsevier Academic, p.89-103.
- Konnerth, A., Heinemann, U. and Yaari, Y. (1984). Slow transmission of neural activity in hippocampal area CA1 in absence of active chemical synapses. *Nature*, 307, p.69-71.
- Kortenbruck, G., Berger, E., Speckmann, E. J. and Musshoff, U. (2001). RNA editing at the Q/R site for the glutamate receptor subunits GLUR2, GLUR5, and GLUR6 in hippocampus and temporal cortex from epileptic patients. *Neurobiol. Dis.*, 8(3), p.459-468.
- Kramer, M. A., Eden, U. T., Kolaczyk, E. D., Zepeda, R., Eskandar, E. N. and Cash, S. S. (2010). Coalescence and fragmentation of cortical networks during focal seizures. *J. Neurosci.*, 30(30), p.10076-10085.
- Kreisman, N. R. and Olson, J. E. (2003). Taurine enhances volume regulation in hippocampal slices swollen osmotically. *Neuroscience*, 120(3), p.635-642.
- Krishnan, G.P., Vohs, J.L., Hetrick, W.P., Carroll, C.A., Shekhar, A., Bockbrader, M.A. and O'Donnell, B.F. (2005). Steady state visual evoked potential abnormalities in schizophrenia. *Clin. Neurophysiol*, 116, p.614-624.
- Krueger, J.M., Rector, D.M., Roy, S., Van Dongen, H.P., Belenky, G. and Panksepp, J. (2008). Sleep as a fundamental property of neuronal assemblies. *Nat. Rev. Neurosci.* 9, p.910-919.
- Kurth, S., Ringli, M., Geiger, A., LeBourgeois, M., Jenni, O.G. and Huber, R. (2010). Mapping of cortical activity in the first two decades of life: A high-density sleep electroencephalogram study. *J Neurosci.*, 30, p.13211-13219.
- Kwan, P. and Brodie, M.J. (2000). Early identification of refractory epilepsy. *New Engl. J. Med.*, 342(5), p.314-319.
- Kwon, J.S., O'Donnell, B.F., Wallenstein, G.V., Greene, R.W., Hirayasu, Y., Nestor, P.G., Hasselmo, M.E., Potts, G.F., Shenton, M.E. and McCarley, R.W. (1999). Gamma frequency-range abnormalities to auditory stimulation in schizophrenia. *Arch. Gen. Psychiatry*, 56, p.1001-1005.
- Lachaux, J. P., Rodriguez, E., Martinerie, J. and Varela, F. J. (1999). Measuring phase synchrony in brain signals. *Hum. Brain Mapp.*, 8, p.194-208.

- Lauri, S.E., Bortolotto, Z.A., Bleakman, D., Ornstein, P.L., Lodge, D., Isaac, J.T. and Collingridge, G.L. (2001). A critical role of a facilitatory presynaptic kainate receptor in mossy fiber LTP. *Neuron*, 32, p.697-709.
- Lazarus, M.S. and Huang, Z.J. (2011). Distinct maturation profiles of perisomatic and dendritic targeting GABAergic interneurons in the mouse primary visual cortex during the critical period of ocular dominance plasticity. *J. Neurophysiol.*, 106(2), p.775-787.
- LeBeau, F. E. N., Towers, S. K., Traub, R. D., Whittington, M. A. and Buhl, E. H. (2002). Fast network oscillations induced by potassium transients in the rat hippocampus *in vitro*. *J. Physiol. (Lond.)*, 542, p.167-179.
- Lehericy, S., Semah, F., Hasboun, D., Dormont, D., Clemenceau, S., Granat, O., Marsault, C. and Baulac, M. (1997). Temporal lobe epilepsy with varying severity: MRI study of 222 patients. *Neuroradiology*, 39, p.788-796.
- Lemos, T. and Cavalheiro, E.A. (1995). Suppression of pilocarpine-induced status epilepticus and the late development of epilepsy in rats. *Exp Brain Res.*, 102, p.423-428.
- Lerma, J. and Marques, J.M. (2013). Kainate receptors in health and disease. *Neuron*, 80, p.292-311.
- Le Van Quyen, M., Staba, R., Bragin, A., Dickson, C., Valderrama, M., Fried, I. and Engel, J. (2010). Large-scale microelectrode recordings of high-frequency gamma oscillations in human cortex during sleep. *J. Neurosci.*, 30(23), p.7770-7782.
- Lewis, D.A., Hashimoto, T. and Volk, D.W. (2005). Cortical inhibitory neurons and schizophrenia. *Nat. Rev. Neurosci.*, 6, p.312-324.
- Lisman, J.E. and Idiart, M.A.P. (1995). Storage of 7 6 2 short-term memories in oscillatory subcycles. *Science*, 267, p.15120-1514.
- Lisman, J. E. (1999). Relating hippocampal circuitry to function: recall of memory sequences by reciprocal dentate-CA3 interactions. *Neuron*, 22, p.233-242.
- Lisman, J.E. and Jensen, O. (2013). The theta-gamma neural code. *Neuron.*, 77, p.1002-1016.
- Liu, R.S., Lemieux, L., Bell, G.S., Sisodiya, S.M., Bartlett, P.A., Shorvon, S.D., Sander, J.W. and Duncan, J.S. (2002). The structural consequences of newly diagnosed seizures. *Ann Neurol*, 52, p.573-580.
- Liu, Z., Nagao, T., Desjardins, G.C., Gloor, P. And Avoli, M. (1994). Quantitative evaluation of neuronal loss in the dorsal hippocampus in rats with long-term pilocarpine seizures. *Epilepsy Res.*, 17, p.237-247.
- Löscher, W. and Schmidt, D. (1988). Which animal models should be used in the search for new antiepileptic drugs? A proposal based on experimental and clinical findings. *Epilepsy Res.*, 2, p.145-181.
- Loscher, W., Lehmann, H., Behl, B., Seemann, D., Teschendorf, H.J., Hofmann, H.P., Lubisch, W., Hoger, T., Lemaire, H.G. and Gross, G. (1999). A new pyrrolyl-

- quinoxalinedione series of non-NMDA glutamate receptor antagonists: pharmacological characterization and comparison with NBQX and valproate in the kindling model of epilepsy. *Eur J. Neurosci.*, 11, p.250-262.
- Lu, C. B., Hamilton, J. B., Powell, A. D., Toescu, E. C. and Vreugdenhil, M. (2009). Effect of ageing on CA3 interneuron sAHP and gamma oscillations is activity-dependent. *Neurobiol. Aging.*, 32(5), p.956-965.
- Luczak, A., Barthó, P., Marguet, S.L., Buzsáki, G. and Harris, K.D. (2007). Sequential structure of neocortical spontaneous activity *in vivo*. *Pro. Natl. Acad. Sci.*, 104(1), p.347-352.
- Lytton, W. and Sejnowski, T. (1991). Simulations of cortical pyramidal neurons synchronized by inhibitory interneurons. *J. Neurophysiol*, 66, p.1059-1079.
- Maddochs, J.A., Hodge, R.S. and Rex, J. (1951). Observations on the occurrence of precentral activities in the lower brainstem. *Electroencephalogr Clin Neurophysiol*, 3, p.370.
- Mann, E.O., Radcliffe, C.A. and Paulsen, O. (2005a). Hippocampal gamma frequency oscillations: from interneurons to pyramidal cells, and back. *J. Physiol. (Lond.)*, 562, p.55-63.
- Mann, E.O., Suckling, J.M., Hajos, N., Greenfield, S.A. and Paulsen, O. (2005b). Perisomatic feedback inhibition underlies cholinergically induced fast network oscillations in the rat hippocampus *in vitro*. *Neuron*, 45, p.105-117.
- Mann, E. O., Kohl, M. M. and Paulsen, O. (2009). Distinct roles of GABAA and GABAB receptors in balancing and terminating persistent cortical activity. *J. Neurosci.*, 29(23), p.7513-7518.
- Mann, E. O. and Mody, I. (2010). Control of hippocampal gamma oscillation frequency by tonic inhibition and excitation of interneurons. *Nat. Neurosci.*, 13(2), p.205-212.
- Mares, P. and Kubova, H. (2006). Electrical Stimulation-Induced Models of Seizures. In: edited by Pitkänen, A., Schwartzkroin, P.A. and Moshé, S.L. (eds.) *Models of Seizures and Epilepsy*. Burlington, MA: Elsevier Academic, 2006, p.153-161.
- Margerison, J.H. and Corsellis, J.A. (1966). Epilepsy and the temporal lobes. A clinical, electroencephalographic and neuropathological study of the brain in epilepsy, with particular reference to the temporal lobes. *Brain*, 89, p.499-530.
- Massimini, M., Huber, R., Ferrarelli, F., Hill, S. and Tononi, G. (2004). The sleep slow oscillation as a traveling wave. *J. Neurosci.*, 24, p.6862-6870.
- Masukawa, L.M., Higashima, M., Kim, J.H. and Spencer, D.D. (1989). Epileptiform discharges evoked in hippocampal brain slices from epileptic patients. *Brain Res*, 493, p.168-174.
- Mathern, G.W., Babb, T.L. and Armstrong, D.L. (1997). Hippocampal sclerosis. In: Engel J., Pedley T.A. (eds.). *Epilepsy: a comprehensive textbook*. Lippincott-Raven; Philadelphia: 1997. p.133-155.

- Mathern, G. W., Pretorius, J. K., Kornblum, H. I., Mendoza, D., Lozada, A., Leite, J. P., and Adelson, P. D. (1998). Altered hippocampal kainate-receptor mRNA levels in temporal lobe epilepsy patients. *Neurobiol. Dis.*, 5(3), p.151-176.
- Mathern, G.W., Adelson, P.D., Cahan, L.D. and Leite, J.P. (2002). Hippocampal neuron damage in human epilepsy: Meyer's hypothesis revisited. *Prog Brain Res.*, 135, p.237-251.
- Maton, B., Jayakar, P., Resnick, T., Morrison, G., Ragheb, J. and Duchowny, M. (2008). Surgery for medically intractable temporal lobe epilepsy during early life. *Epilepsia*, 49(1), p.80-87.
- McCormick, D.A., Connors, B.W., Lighthall, J.W. and Prince, D.A. (1985). Comparative electrophysiology of pyramidal and sparsely spiny stellate neurons of the neocortex. *J. Neurophysiol.* 54(4), p.782-806.
- McCormick, D.A. (1989). GABA as an inhibitory neurotransmitter in human cerebral cortex. *J Neurophysiol*, 62(5), p.1018-1027.
- McIntyre, D.C., Kelly, M.E. and Dufresne, C. (1999). FAST and SLOW amygdala kindling rat strains: comparison of amygdala, hippocampal, piriform and perirhinal cortex kindling. *Epilepsy Res.*, 35, p.197-209.
- Mello, L.E., Covolan, L. (1996). Spontaneous seizures preferentially injure interneurons in the pilocarpine model of chronic spontaneous seizures. *Epilepsy Res.*, 26, p.123-129.
- Meyer, A.H., Katona, I., Blatow, M., Rozov, A. and Monyer, H. (2002). *In vivo* labeling of parvalbumin-positive interneurons and analysis of electrical coupling in identified neurons. *J. Neurosci.*, 22, p.7055-7064.
- Middleton, S., Jalics, J., Kispersky, T., LeBeau, F.E.N., Roopun, A.K., Kopell, N.J., Whittington, M.A. and Cunningham, M.O. (2008). NMDA receptor-dependent switching between different gamma rhythm-generating microcircuits in entorhinal cortex. *Proc. Natl. Acad. Sci. U.S.A.*, 105, p.18572-18577.
- Mikkonen, M., Soininen, H., Kalvianen, R., Tapiola, T., Ylinen, A., Vapalahti, M., Paljarvi, L. and Pitkanen, A. (1998). Remodeling of neuronal circuitries in human temporal lobe epilepsy: increased expression of highly polysialylated neural cell adhesion molecule in the hippocampus and the entorhinal cortex. *Ann. Neurol.*, 44, p.923-934.
- Miles, R., Toth, K., Gulyas, A. I., Hajos, N. and Freund, T. F. (1996). Differences between somatic and dendritic inhibition in the hippocampus. *Neuron*, 16, p.815-823.
- Mody, I., Schwartzkroin, P.A. (1997). Acute seizure models (intact animals). In: *Epilepsy: a Comprehensive Textbook*. Eds. Engel J, Pedley TA, Philadelphia, Lippincott-Raven, p.397-404.
- Moghaddam, B. (2003). Bringing order to the glutamate chaos in schizophrenia. *Neuron*, 40, p.881-884.

- Molnár, G., Oláh, S., Komlósi, G., Füle, M., Szabadics, J., Varga, C. and Tamás, G. (2008). Complex events initiated by individual spikes in the human cerebral cortex. *PLoS biology*, 6(9), p.222.
- Monaghan, D.T. and Cotman, C.W. (1982). The distribution of [3H]kainic acid binding sites in rat CNS as determined by autoradiography. *Brain Res.*, 252, p.91-100.
- Montgomery, S.M., Sirota, A. and Buzsaki, G. (2008). Theta and gamma coordination of hippocampal networks during waking and rapid eye movement sleep. *J. Neurosci.*, 28, p.6731-6741.
- More, J.C.A., Nitisco, R., Dolman, N.P., Clarke, V.R.J., Alt, A.J., Ogden, A.M., Buelens, F.P., Troop, H.M., Kelland, E.E., Pilato, F., Bleakman, D., Bortolotto, Z.A., Collingridge, G.L. and Jane, D.E. (2004). Characterisation of UBP296: a novel, potent and selective kainate receptor antagonist. *Neuropharmacol.*, 47, p.46-64.
- Morimoto, K., Fahnestock, M. and Racine, R.J. (2004). Kindling and status epilepticus models of epilepsy: rewiring the brain. *Prog Neurobiol.*, 73, p.1-60.
- Morin, F., Beaulieu, C. and Lacaille, J.C. (1998). Selective loss of GABA neurons in area CA1 of the rat hippocampus after intraventricular 'entate'. *Epilepsy Res.*, 32, p.363-369.
- Morrisett, R.A., Jope, R.S. and Snead, O.C., (1987). III Effects of drugs on the initiation and maintenance of status epilepticus induced by administration of pilocarpine to lithium-pretreated rats. *Exp Neurol.*, 97, p.193-200.
- Moruzzi, G. and Magoun, H.W. (1949) Brainstem reticular formation and activation of the EEG. *Electroencephalogr Clin Neurophysiol*, 1, p.455-473.
- Moser, V., (1988). Comparison of chlordimeform and carbaryl using a functional observational battery. *Fund. Appl. Toxicol.*, 11, p.189-206.
- Moyer, J.R. Jr. and Brown, T.H. (1998). Methods for whole-cell recording from visually preselected neurons of perirhinal cortex in brain slices from young and aging rats. *J. Neurosci. Meth.*, 86, p.35-54.
- Mühlebner, A., Gröppel, G., Dressler, A., Reiter-Fink, E., Kasprian, G., Prayer, D. and Feucht, M. (2014). Epilepsy surgery in children and adolescents with malformations of cortical development—outcome and impact of the new ILAE classification on Focal Cortical Dysplasia. *Epilepsy Res.*
- Mulle, C., Sailer, A., Perez-Otano, I., Dickinson-Anson, H., Castillo, P.E., Bureau, I., Maron, C., Gage, F.H., Mann, J.R., Bettler, B., *et al.* (1998). Altered synaptic physiology and reduced susceptibility to kainate-induced seizures in GluR6-deficient mice. *Nature*, 392, p.601-605.
- Murthy, V.N. and Fetz, E.E. (1992). Coherent 25- to 35-Hz oscillations in the sensorimotor cortex of awake behaving monkeys. *Proc Natl Acad Sci USA*, p. 5670-5674.
- Nadler, J.V., Perry, B. W. and Cotman, C.W. (1978). Intraventricular kainic acid preferentially destroys hippocampal pyramidal cells. *Nature (Land.)*, 271, p.676-677.

- Nadler, J.V. (1981). Minireview. Kainic acid as a tool for the study of temporal lobe epilepsy. *Life Sci.*, 29, p.2031-2042.
- Nadler, J.V. (2003). The recurrent mossy fiber pathway of the epileptic brain. *Neurochem. Res.*, 28, p.1649-1658.
- Navarro Mora, G., Bramanti, P., Osculati, F., Chakir, A., Nicolato, E., Marzola, P., Sbarbati, A. and Fabene, P.F. (2009). Does pilocarpine-induced epilepsy in adult rats require status epilepticus? *PLoS One*, 4, p.5759.
- Neckelmann, D., Amzica, F. and Steriade, M. (1998). Spike-wave complexes and fast components of cortically generated seizures. III. Synchronizing mechanisms. *J Neurophysiol*, 80, p.1480-1494.
- Niedermeyer, E. (1990). Alpha-like rhythmical activity of the temporal lobe. *Clin Electroencephalogr*, 21(4), p.210-24.
- Niedermeyer, E. (1991). The "third rhythm": further observations. *Clin Electroencephalogr*, 22(2), p.83-96.
- Niedermeyer, E. (1997). Alpha rhythms as physiological and abnormal phenomena. *Int J Psychophysiol*, 26(1-3), p.31-49.
- Niedermeyer, E. and da Silva, F. L. (Eds.). (2005). *Electroencephalography: basic principles, clinical applications, and related fields*. Lippincott Williams and Wilkins.
- Nir, Y., Staba, R.J., Andrillon, T., Vyazovskiy, V.V., Cirelli, C., Fried, I. and Tononi, G. (2011). Regional slow waves and spindles in human sleep. *Neuron*, 70, p.153-169.
- Olsen, R.W., Bergman, M.O., Van Ness, P.C., Lummis, S.C., Watkins, A.E., Napias, C. and Greenlee, D.V. (1981). Gamma-Aminobutyric acid receptor binding in mammalian brain. Heterogeneity of binding sites. *Mol Pharmacol*, 19(2), p.217-27.
- Ormandy, G.C., Jope, R.S. and Snead, O.C. III. (1989). Anticonvulsant actions of MK-801 on the lithium-pilocarpine model of status epilepticus in rats. *Exp Neurol*, 106, p.172-180.
- Pakhotin, P. I., Pakhotina, I. D. and Andreev, A. A. (1997). Functional stability of hippocampal slices after treatment with cyclooxygenase inhibitors. *Neuroreport*, 8(7), p.1755-1759.
- Palhalmi, J., Paulsen, O., Freund, T.F. and Hajos, N. (2004). Distinct properties of carbachol- and DHPG-induced network oscillations in hippocampal slices. *Neuropharmacol.*, 47, p.381-389.
- Palomero-Gallagher, N., Schleicher, A., Bidmon, H.-J., Pannek, H.-W., Hans, V., Gorji, A., Speckmann, E.J. and Zilles, K. (2012). Multireceptor analysis in human neocortex reveals complex alterations of receptor ligand binding in focal epilepsies. *Epilepsia*, 53(11), p.1987-1997.
- Paternain, A.V., Morales, M, and Lerma, J. (1995). Selective antagonism of AMPA receptors unmasks kainate receptor mediated responses in hippocampal neurons. *Neuron*, 14(1), p.185-189.

- Peça, J., Feliciano, C., Ting, J. T., Wang, W., Wells, M. F., Venkatraman, T. N., ... & Feng, G. (2011). Shank3 mutant mice display autistic-like behaviours and striatal dysfunction. *Nature*, 472(7344), p. 437-442.
- Pelletier *et al.* (1996). Substituted 1,2-dihydrophthalazines: potent, selective and non-competitive inhibitors of the AMPA receptor. *J.Med.Chem.*, 39, p.343.
- Penfield, W., & Jasper, H. Epilepsy and the functional anatomy of the human brain, 1954. *Little, Brown, Boston*, 896.
- Perrais, D., Pinheiro, P.S., Jane, D.E. and Mulle, C. (2009). Antagonism of recombinant and native GluR7-containing kainate receptors. *Neuropharmacol.*, 56, 131-140.
- Perrais, D., Veran, J. and Mulle, C. (2010). Gating and permeation of kainite receptors: differences unveiled. *Trends Pharmacol. Sci.*, 31, p.516-522.
- Pfurtscheller, G. and Neuper, C. (1992). Simultaneous EEG 10 Hz desynchronization and 40 Hz synchronization during finger movements. *Neuroreport*, p. 1057-1060.
- Pfurtscheller, G., Zalaudek, K. and Neuper, C. (1998). Event-related beta synchronization after wrist, finger and thumb movement. *Electroen. Clin. Neuro./Electromyography and Motor Control*, 109(2), p.154-160.
- Penttonen, M., Kamondi, A., Acsady, L. and Buzsaki, G. (1998). Gamma frequency oscillation in the hippocampus of the rat: intracellular analysis *in vivo*. *Eur. J. Neurosci.*, 10, p.718-728.
- Pietersen, A.N., Lancaster, D.M., Patel, N., Hamilton, J.B. and Vreugdenhil, M. (2009). Modulation of gamma oscillations by endogenous adenosine through A1 and A2A receptors in the mouse hippocampus. *Neuropharmacol.*, 56, p.481-492.
- Pietersen, A. N.J., Patel, N., Jefferys, J. G.R. and Vreugdenhil, M. (2009). Comparison between spontaneous and kainate-induced gamma oscillations in the mouse hippocampus *in vitro*. *Eur. J. Neurosci.*, 29, p.2145-2156.
- Pike, F.G., Goddard, R.S., Suckling, J.M., Ganter, P., Kasthuri, N. and Paulsen, O. (2000). Distinct frequency preferences of different types of rat hippocampal neurones in response to oscillatory input currents. *J. Physiol*, 529, p.205-213.
- Pineau, N., Charriaut-Marlangue, C., Motte, J. and Nehlig, A. (1999). Pentylentetrazol seizures induce cell suffering but not death in the immature rat brain. *Brain Res Dev Brain Res.*, 112, p.139-144.
- Pinheiro, P.S., Perrais, D., Coussen, F., Barhanin, J., Bettler, B., Mann, J.R., Malva, J.O., Heinemann, S.F. and Mulle, C. (2007). GluR7 is an essential subunit of presynaptic kainate autoreceptors at hippocampal mossy fiber synapses. *Proc. Natl. Acad. Sci. USA*, 104, p.12181-12186.
- Pinheiro, P.S., Lanore, F., Veran, J., Artinian, J., Blanchet, C., Crepel, V., Perrais, D. and Mulle, C. (2013). Selective block of postsynaptic kainite receptors reveals their function at hippocampal mossy fiber synapses. *Cereb. Cortex*, 23, p.323-331.

- Pitkänen, A., Schwartzkroin, P.A. and Moshé, S.M. (2006). Models of seizures and epilepsy. *Elsevier Academic Press Burlington*, p. 712.
- Polascheck, N., Bankstahl, M. and Löscher, W. (2010). The COX-2 inhibitor parecoxib is neuroprotective but not antiepileptogenic in the pilocarpine model of temporal lobe epilepsy. *Exp. Neurol.*, 224, p.219-233.
- Porter, B.E., Cui, X.N. and Brooks-Kayal, A.R. (2006). Status epilepticus differentially alters AMPA and kainate receptor subunit expression in mature and immature dentate granule neurons. *Eur. J. Neurosci.*, 23(11), p.2857-2863.
- Proctor, P. H. (2008). Uric acid and neuroprotection, *Stroke*, 39(8), p. E126.
- Prokic, E. (2012). *Modulation of neuronal network activity in the primary motor cortex* (Doctoral dissertation, Aston University).
- Puig, M.V., Ushimaru, M. and Kawaguchi, Y. (2008). Two distinct activity patterns of fast-spiking interneurons during neocortical up states. *Proc Natl Acad Sci USA*, 2008, 105(24), p.8428-8433.
- Racine, R.J. (1972). Modification of seizure activity by electrical stimulation. II. Motor seizure. *Electroenceph Clin Neurophysiol.*, 32, p.281-294.
- Rafiq, A., Zhang, Y.F., DeLorenzo, R.J. and Coulter, D.A. (1995). Long duration self-sustained epileptiform activity in the hippocampal-parahippocampal slice: a model of status epilepticus. *J. Neurophysiol.*, 74, p.2028-2042.
- Rafiq, A., DeLorenzo R. and Coulter, D. A. (1993). Generation and propagation of epileptiform discharges in a combined entorhinal cortex/hippocampal slice. *J. Neurophysiol.*, 70, p.1962-1974.
- Raghavachari, S., Kahana, M.J., Rizzuto, D.S., Caplan, J.B., Kirschen, M.P., Bourgeois, B. and Lisman, J.E. (2001). Gating of human theta oscillations by a working memory task. *J. Neurosci.*, 21(9), p.3175-3183.
- Rajasekaran, K., Todorovic, M. and Kapur, J. (2012). Calcium-permeable AMPA receptors are expressed in a rodent model of status epilepticus. *Ann. Neurol.*, 72(1), p.91-102.
- Represa, A., Tremblay, E. and Ben-Ari, Y. (1987). Kainate binding sites in the hippocampal mossy fibers: localization and plasticity. *Neuroscience*, 20, p.739-748.
- Represa, A., Le Gall La Salle, G. and Ben-Ari, Y. (1989). Hippocampal plasticity in the kindling model of epilepsy in rats. *Neuroscience lett.*, 99(3), p.345-350.
- Ribary, U., *et al.* (1991). Magnetic field tomography of coherent thalamocortical 40-Hz oscillations in humans. *Proc. Natl Acad. Sci. USA*, 88, p.11037-11041.
- Rice, A.C., Floyd, C.L., Lyeth, B.G., Hamm, R.J. and Delorenzo, R.J. (1998). Status Epilepticus Causes Long-Term NMDA Receptor-Dependent Behavioural Changes and Cognitive Deficits. *Epilepsia*, 39, p.1148-1157.

- Rice, M. E., Perezpinzon, M. A. and Lee, E. J. K. (1994). Ascorbic-Acid, But Not Glutathione, Is Taken Up by Brain-Slices and Preserves Cell Morphology. *J. Neurophysiol.*, 71(4), p.1591-1596.
- Rice, M.E. (2000). Ascorbate regulation and its neuroprotective role in the brain, *Trends Neurosci.*, 23(5), p.209-216.
- Rodriguez-Moreno A, Herreras O and Lerma J. (1997). Kainate receptors presynaptically downregulate GABAergic inhibition in the rat hippocampus. *Neuron*, 19(4), p.893-901.
- Rodriguez-Moreno, A. and Lerma, J. (1998). Kainate receptor modulation of GABA release involves a metabotropic function. *Neuron*, 20, p.1211-1218.
- Ronnqvist, K. C., McAllister, C. J., Woodhall, G. L., Stanford, I. M. and Hall, S. D. (2013). A multimodal perspective on the composition of cortical oscillations. *Front. Hum. Neurosci.*, 7, p.132.
- Roopun, A.K., Middleton, S.J., Cunningham, M.O., LeBeau, F.E., Bibbig, A., Whittington, M.A. and Traub, R.D. (2006). A beta2-frequency (20–30 Hz). oscillation in nonsynaptic networks of somatosensory cortex. *Pro. Natl. Acad. Sci.*, 103(42), p.15646-15650.
- Roopun, A.K., Simonotto, J.D., Pierce, M.L., Jenkins, A., Nicholson, C., Schofield, I.S. and Cunningham, M.O. (2010). A nonsynaptic mechanism underlying interictal discharges in human epileptic neocortex. *Pro. Natl. Acad. Sci.*, 107(1), p.338-343.
- Rothman, S. M. (1985). The neurotoxicity of excitatory amino acids is produced by passive chloride influx. *J.Neurosci.*, 5(6), p.1483-1489.
- Russell, W. M. S., Burch, R. L., & Hume, C. W. (1959). The principles of humane experimental technique.
- Rutecki, P.A., Grossman, R.G., Armstrong, D. and Irish-Loewen, S. (1989). Electrophysiological connections between the hippocampus and entorhinal cortex in patients with complex partial seizures. *J. Neurosurg.*, 70(5), p.667-675.
- Sainsbury, R.S., Harris, J.L. and Rowland, G.L. (1987a). Sensitization and hippocampal type 2 theta in the rat. *Physiol Behav*, 41, p.489-493.
- Sainsbury, R.S., Heynen, A. and Montoya, C.P. (1987b). Behavioral correlates of hippocampal type 2 theta in the rat. *Physiol Behav*, 39, p.513- 519.
- Samoriski, G.M. and Applegate, C.D. (1997). Repeated generalized seizures induce time-dependent changes in the behavioral seizure response independent of continued seizure induction. *J. Neurosci.*, 17, p.5581-5590.
- Sanabria, E.R.G., da Silva, A.V., Spreafico, R. and Cavalheiro, E.A. (2002). Damage, reorganization, and abnormal neocortical hyperexcitability in the pilocarpine model of temporal lobe epilepsy. *Epilepsia.*, 43(Suppl 5), p.6-106.
- Sanchez-Vives, M.V. and McCormick, D.A. (2000). Cellular and network mechanisms of rhythmic recurrent activity in neocortex. *Nat Neurosci.*, 3, p.1027-1034.

- Sander, J.W.A.S. (1997). The epidemiology of the epilepsies: future directions. *Epilepsia*, 38(5), p.614-618.
- Sanes, J. N. and Donoghue, J. P. (1993). Oscillations in local field potentials of the primate motor cortex during voluntary movement. *Pro. Natl. Acad. Sci.*, 90(10), p.4470-4474.
- Sarkisian, M.R. (2001). Overview of the current animal models for human seizure and epileptic disorders. *Epilepsy Behav*, 2, p. 201-216.
- Savage, D.D., Nadler, J.V. and McNamara, J. O. (1984). Reduced kainic acid binding in rat hippocampal formation after limbic kindling. *Brain Res.*, 323(1), p.128-131.
- Schwartzkroin, P. A. (1997). Origins of the Epileptic State. *Epilepsia*, 38, p.853-858.
- Schmidt, D. and Stavem, K. (2009). Long-term seizure outcome of surgery versus no surgery for drug-resistant partial epilepsy: A review of controlled studies. *Epilepsia*, 50(6), p.1301-1309.
- Schmitz, D., Frerking, M. and Nicoll, R.A. (2000). Synaptic activation of presynaptic kainate receptors on hippocampal mossy fiber synapses. *Neuron*, 27(2), p.327-338.
- Schmitz, D., Mellor, J. and Nicoll, R.A. (2001). Presynaptic kainate receptor mediation of frequency facilitation at hippocampal mossy fiber synapses. *Science*, 291, p1972-1976.
- Schutz, E. and Muller, H.W. (1951). Uber ein neues Zeichen zentral nervoser Erregbarkeitssteigerung im Elektroenzephalogramm. *Klin Wochenschr*, 29(22-23).
- Segal, M. and Barker, J. L. (1984). Rat hippocampal neurons in culture: voltage-clamp analysis of inhibitory synaptic connections. *J. Neurophysiol.*, 52, p.469-487.
- Semah, F., Picot, M.C., Adam, C., Broglin, D., Arzimanoglou, A., Bazin, B., *et al.* (1998). Is the underlying cause of epilepsy a major prognostic factor for recurrence? *Neurology*, 51, p.1256-1262.
- Semyanov, A and Kullmann, D.M. (2001). Kainate receptor-dependent axonal depolarization and action potential initiation in interneurons. *Nat Neurosci*, 4, p.718-723.
- Senior, T.J., Huxter, J.R., Allen, K., O'Neill, J. and Csicsvari, J. (2008). Gamma oscillatory firing reveals distinct populations of pyramidal cells in the CA1 region of the hippocampus. *J. Neurosci.*, 28, p.2274-2286.
- Shaw, P., Kabani, N.J., Lerch, J.P., Eckstrand, K., Lenroot, R., Gogtay, N. and Wise, S.P. (2008). Neurodevelopmental trajectories of the human cerebral cortex. *J. Neurosci.*, 28(14), p.3586-3594.
- Sheer, D.E. (1989). Focused arousal and the cognitive 40-Hz event-related potentials: differential diagnosis of Alzheimer's disease. *Prog Clin Biol Res*, p.79-94.

- Sheroziya, M.G., von Bohlen Und Halbach, O., Unsicker, K., Egorov, A.V. (2009). Spontaneous bursting activity in the developing entorhinal cortex. *J. Neurosci.*, 29, p.12131–12144.
- Shimono, K., Brucher, F., Granger, R., Lynch, G. and Taketani, M. (2000). Origins and distribution of cholinergically induced beta rhythms in hippocampal slices. *J. Neurosci.*, 20, p.8462-8473.
- Shi, Y.J., Gong, X.W., Gong, H.Q., Liang, P.J., Zhang, P.M. and Lu, Q.C. (2014). Effect of the entorhinal cortex on ictal discharges in low-Mg²⁺-induced epileptic hippocampal slice models. *Neural Plasticity* 2014.
- Shorvon, S. D. (2011). The etiologic classification of epilepsy. *Epilepsia*, 52, p1052-1057.
- Shuai, J., Bikson, M., Hahn, P.J., Lian, J. and Durand, D.M. (2003). Ionic mechanisms underlying spontaneous CA1 neuronal firing in Ca²⁺-free solution. *Biophys J.*, 84(3), p.2099-2111.
- Shu, Y., Hasenstaub, A. and McCormick, D.A. (2003). Turning on and off recurrent balanced cortical activity. *Nature*, 423, p.288-293.
- Siegel, A.M., Wieser, H.G., Wichman, W. and Yasargil, G.M. (1990). Relationships between MR-imaged total amount of tissue removed, resection scores of specific mediobasal limbic subcompartments and clinical outcome following selective amygdalohippocampectomy. *Epilepsy Res*, 6(1), p.56-65.
- Silva, A.V., Sanabria, E.R.G., Cavalheiro, E.A. and Spreafico, R. (2002). Alterations of the neocortical GABAergic system in the pilocarpine model of temporal lobe epilepsy: neuronal damage and immunocytochemical changes in chronic epileptic rats. *Brain Res Bull.*, 58, p.417-421.
- Simon, A., Traub, R.D., Vladimirov, N., Jenkins, A., Nicholson, C., Whittaker, R.G. and Whittington, M.A. (2014). Gap junction networks can generate both ripple-like and fast ripple-like oscillations. *Eur. J. Neurosci.*, 39(1), p.46-60.
- Singer, W. and Gray, C. (1995). Visual feature integration and the temporal correlation hypothesis. *Annu. Rev. Neurosci.*, 18, p.555–586.
- Singer, W. (1999) Neuronal synchrony: a versatile code for the definition of relations? *Neuron*, 24, p.49-65.
- Smolders, I., Bortolotto, Z.A., Clarke, V.R., Warre, R., Khan, G.M., O'Neill, M.J., Ornstein, P.L., Bleakman, D., Ogden, A., Weiss, B., Stables, J.P., Ho, K.H., Ebinger, G., Collingridge, G.L., Lodge, D. and Michotte, Y. (2002). Antagonists of GLU(K5)-containing kainate receptors prevent pilocarpine-induced limbic seizures. *Nat Neurosci.*, 5, p.796-804.
- Sloviter, R. S. (1983). "Epileptic" brain damage in rats induced by sustained electrical stimulation of the perforant path. I. Acute electrophysiological and light microscopic studies. *Brain Res. bulletin*, 10(5), p.675-697.

- Sloviter, R. S. (1987). Decreased hippocampal inhibition and a selective loss of interneurons in experimental epilepsy. *Science*, 235(4784), p.73-76.
- Sloviter, R. S. (1991). Permanently altered hippocampal structure, excitability, and inhibition after experimental status epilepticus in the rat: the "dormant basket cell" hypothesis and its possible relevance to temporal lobe epilepsy. *Hippocampus*, 1(1), p.41-66.
- Sloviter, R.S., Zappone, C.A., Bumanglag, A.V., Norwood, B. and Kudrimoti, H. (2007). On the relevance of prolonged convulsive status epilepticus in animals to the etiology and neurobiology of human temporal lobe epilepsy. *Epilepsia*, 48(8), p.6-10.
- Sloviter, R.S. (2005). The neurobiology of temporal lobe epilepsy: too much information, not enough knowledge. *C R Biol.*, 328, p.143-153.
- Sloviter, R.S. (2008). Hippocampal epileptogenesis in animal models of mesial temporal lobe epilepsy with hippocampal sclerosis: the importance of the "latent period" and other concepts. *Epilepsia*, 49(Suppl. 9), p.85-92.
- Soltesz, I. and Deschênes, M. (1993). Low- and high-frequency membrane potential oscillations during theta activity in CA1 and CA3 pyramidal neurons of the rat hippocampus under ketamine-xylazine anaesthesia. *J. Neurophysiol.*, 70, p.97-116.
- Sowell, E.R., Thompson, P.M. and Toga, A.W. (2004). Mapping changes in the human cortex throughout the span of life. *The Neuroscientist*, 10(4), p.372-392.
- Spencer, S.S. and Spencer, D.D. (1994). Entorhinal-Hippocampal Interactions in Medial Temporal Lobe Epilepsy. *Epilepsia*, 35(4), 721-727.
- Stafstrom, C. E., Schwindt, P. C., Chubb, M. C., & Crill, W. E. (1985). Properties of persistent sodium conductance and calcium conductance of layer V neurons from cat sensorimotor cortex in vitro. *J. Neurophysiol.*, 53(1), p. 153-170.
- Stam, C. J., Jones, B. F., Nolte, G., Breakspear, M., & Scheltens, P. (2007). Small-world networks and functional connectivity in Alzheimer's disease. *Cereb. cortex*, 17(1), 92-99.
- Stanger, H.L., Alford, R., Jane, D.E., Cunningham, M.O. (2008). The role of GLU K5-containing kainate receptors in entorhinal cortex gamma frequency oscillations. *Neural Plast.*, 401645.
- Stanton, P.K, Jones, R.S., Mody, I. and Heinemann, U. (1987). Epileptiform activity induced by lowering extracellular $[Mg^{2+}]$ in combined hippocampal-entorhinal cortex slices: modulation by receptors for norepinephrine and N-methyl-D-aspartate. *Epilepsy Res*, 1, p.53-62.
- Stelzer, A., Slater, N. and Bruggencate, G. (1987). Activation of NMDA receptors blocks GABAergic inhibition in an *in vitro* model of epilepsy. *Nature*, 326, p.698-701.
- Steriade, M., Amzica, F. and Nunez, A. (1993a). Cholinergic and noradrenergic modulation of the slow (0.3 Hz) oscillation in neocortical cells. *J Neurophysiol*, 70, p.1385-1400.

- Steriade, M., Contreras, D., Curró Dossi, R., Nuñez, A. (1993b). The slow (<1 Hz) oscillation in reticular thalamic and thalamocortical neurons: scenario of sleep rhythm generation in interacting thalamic and neocortical networks. *J. Neurosci.*, 13, p.3284-3299.
- Steriade, M., McCormick, D.A. and Sejnowski, T.J. (1993c). Thalamocortical oscillations in the sleeping and aroused brain. *Science*, 262, p.679-685.
- Steriade, M., Nunez, A. and Amzica, F. (1993d). A novel slow (< 1 Hz) oscillation of neocortical neurons *in vivo*: depolarizing and hyperpolarizing components. *J. Neurosci.*, 13, p.3252-3265.
- Steriade, M., Nuñez, A., & Amzica, F. (1993e). Intracellular analysis of relations between the slow (< 1 Hz) neocortical oscillation and other sleep rhythms of the electroencephalogram. *J. Neurosci.*, 13(8), 3266-3283.
- Steriade, M. and Contreras, D. (1995). Relations between cortical and thalamic cellular events during transition from sleep patterns to paroxysmal activity. *J. Neurosci.*, 15, p.623-42.
- Steriade, M., Timofeev, I. and Grenier, F. (2001). Natural waking and sleep states: A view from inside neocortical neurons. *J Neurophysiol.*
- Steriade, M. and Timofeev, I. (2003). Neuronal plasticity in thalamocortical networks during sleep and waking oscillations. *Neuron*, 37(4), p.563-576.
- Steriade, M. (2006). Grouping of brain rhythms in corticothalamic systems. *Neuroscience*, 137, p. 1087–1106.
- Stelzer, A., Slater, N. and Bruggencate, G. (1987). Activation of NMDA receptors blocks GABAergic inhibition in an *in vitro* model of epilepsy. *Nature*, 326, p.698-701.
- Stickgold, R. and Walker, M.P. (2007). Sleep-dependent memory consolidation and reconsolidation. *Sleep Med.*, 8, p.331-343.
- Stringer, J.L. (1994). Pentylentetrazol elicits epileptiform activity in the dentate gyrus of the urethane anesthetized rat by activation of the entorhinal cortex. *Brain Res.*, 636(2), p.221-226.
- Stubblefield, E.A. and Benke, T.A. (2010). Distinct AMPA-type glutamatergic synapses in developing rat CA1 hippocampus. *J. Neurophysiol.*, 104(4), p.1899-1912.
- Sutula, T., He, X.X., Cavazos, J. and Scott, G. (1988). Synaptic reorganization in the hippocampus induced by abnormal functional activity. *Science*, 239, p.1147-1150.
- Sutula, T., Cascino, G., Cavazos, J., Parada, I. and Ramirez, L. (1989). Mossy fiber synaptic reorganization in the epileptic human temporal lobe. *Ann. Neurol.*, 26, p.321-330.

- Syková, E., Mazel, T., Vargová, L., Voříšek, I. and Prokopová-Kubinová, Š. (2000). Extracellular space diffusion and pathological states. *Prog. Brain Res.*, 125, p.155-178.
- Tallon-Baudry, C. and Bertrand, O. (1999). Oscillatory gamma activity in humans and its role in object representation. *Trend Cogn Sci*, 3, p.151-162.
- Tanaka, Y., Tanaka, Y., Furuta, T., Yanagawa, Y. and Kaneko, T. (2008). The effects of cutting solutions on the viability of GABAergic interneurons in cerebral cortical slices of adult mice. *J. Neurosci. Meth.*, 171(1), p.118-125.
- Tang, F.R., Chen, P.M., Tang, Y.C., Tsai, M.C. and Lee, W.L. (2007). Two-methyl-6-phenylethynyl-pyridine (MPEP), a metabotropic glutamate receptor 5 antagonist, with low doses of MK801 and diazepam: a novel approach for controlling status epilepticus. *Neuropharmacol.*, 53(7), p.821-831.
- Tatum, W.O., French, J.A., Benbadis, S.R. and Kaplan, P.W. (2001). The etiology and diagnosis of status epilepticus. *Epilepsy Behav*, 2, p.311-317.
- Teitelbaum, J.S., Zatorre, R.J., Carpenter, S., Gendron, D., Evans, A.C., Gjedde, A. and Cashman, N.R. (1990). Neurologica sequelae of domoic acid intoxication due to the ingestion of contaminated mussels. *N Engl J Med*, 322, p.1781-1787.
- Telfeian, A.E., Federoff, H.J., Leone, P., During, M.J. and Williamson, A. (2000). Overexpression of GluR6 in rat hippocampus produces seizures and spontaneous nonsynaptic bursting *in vitro*. *Neurobiol Dis.*, 7, p.362-374.
- Tian, H., Zhang, G. Y., Li, H. C. and Zhang, Q. G. (2003). Antioxidant NAC and AMPA/KA receptor antagonist DNQX inhibited JNK3 activation following global ischemia in rat hippocampus. *Neurosci. Res.*, 46(2), p.191-197.
- Tiesinga, P. H.E., Fellous, J.-M., José, J. V. and Sejnowski, T. J. (2001). Computational model of carbachol-induced delta, theta, and gamma oscillations in the hippocampus. *Hippocampus*, 11, p.251-274.
- Timofeev, I. and Steriade, M. (1996). Low-frequency rhythms in the thalamus of intact-cortex and decorticated cats. *J Neurophysiol*, 76, p.4152-4168.
- Timofeev, I., Grenier, F., Bazhenov, M., Sejnowski, T.J. and Steriade, M. (2000). Origin of slow cortical oscillations in deafferented cortical slabs. *Cereb Cortex*, 10, p.1185-1199.
- Timofeev, I., Bazhenov, M., Seigneur, J., & Sejnowski, T. (2012). Neuronal synchronization and thalamocortical rhythms in sleep, wake and epilepsy. *Jasper's basic mechanisms of the epilepsies*. JL Noebels, M. Avoli, MA Rogawski, RW Olsen and AV Delgado-Escueta. Bethesda (MD). *National Center for Biotechnology Information*.
- Thompson, S.E., Woodhall, G.L. and Jones R.S.G. (2007). Depression of glutamate and GABA release by presynaptic GABA_B receptors in the entorhinal cortex in normal and chronically epileptic rats. *Neurosignals.*, 15, p.202-216.

- Tolner, E.A., Kloosterman, F., Kalitzin, S.N., Da Silva, F.H.L. and Gorter, J.A. (2005). Physiological changes in chronic epileptic rats are prominent in superficial layers of the medial entorhinal area. *Epilepsia*, 46(s5), p.72-81.
- Tononi, G. and Cirelli, C. (2006). Sleep function and synaptic homeostasis. *Sleep Med. Rev.*, 10, p.49-62.
- Traub, R.D., Whittington, M.A., Collins, S.B., Buzsaki, G. and Jefferys, J.G.R. (1996a). Analysis of gamma rhythms in the rat hippocampus *in vitro* and *in vivo*. *J. Physiol.*, 493, p.471-484.
- Traub, R.D., Whittington, M.A., Stanford, I.M. and Jefferys, J.G. (1996b). A mechanism for generation of long-range synchronous fast oscillations in the cortex. *Nature*, 383(6601), p.621-624.
- Traub, R.D., Bibbig, A., Fisahn, A., LeBeau, F.E.N., Whittington, M.A. and Buhl, E.H. (2000). A model of gamma-frequency network oscillations induced in the rat CA3 region by carbachol *in vitro*. *Eur. J. Neurosci.*, 12, p.4093-4106.
- Traub, R. D., Kopell, N., Bibbig, A., Buhl, E. H., LeBeau, F. E., & Whittington, M. A. (2001a). Gap junctions between interneuron dendrites can enhance synchrony of gamma oscillations in distributed networks. *J. Neurosci.*, 21(23), 9478-9486.
- Traub, R.D., Whittington, M.A., Buhl, E.H., LeBeau, F.E., Bibbig, A., Boyd, S., Cross, H. and Baldeweg, T. (2001b). A possible role for gap junctions in generation of very fast EEG oscillations preceding the onset of, and perhaps initiating, seizures. *Epilepsia*, 42, p.153-170.
- Traub, R.D., Whittington, M.A. and Cunningham, M.O. (2012). Fast Oscillations and Synchronization Examined with *In vitro* Models. *Jasper's Basic Mechanisms of the Epilepsies*, 80, p.286.
- Trevino, M., Vivar, C. and Gutierrez, R. (2007). Beta / gamma oscillatory activity in the CA3 hippocampal area is depressed by aberrant GABAergic transmission from the dentate gyrus after seizures. *J. Neurosci.*, 27, p.251-259.
- Turski, W.A., Czuczwar, S.J., Kleinrok, Z. and Turski L. (1983a). Cholinomimetics produce seizures and brain damage in rats. *Experientia.*, 39, p.1408-1411.
- Turski, W.A., Cavalheiro, E.A., Schwarz, M., Czuczwar, S.L.J., Kleinrok, Z. and Turski, L. (1983b). Limbic seizures produced by pilocarpine I rats: behavioral, electroencephalographic and neuropathological study. *Behav Brain Res.*, 9, p.315-335.
- Turski, W.A., Cavalheiro, E.A., Bortolotto, Z.A., Mello, L.M., Schwarz, M. and Turski, L. (1984). Seizures produced by pilocarpine in mice: a behavioral, electroencephalographic and morphological analysis. *Brain Res.*, 32, p.237-253.
- Turski, L., Ikonomidou, C., Turski, W.A., Bortolotto, Z.A. and Cavalheiro, E.A. (1989). Review: cholinergic mechanisms and epileptogenesis. The seizures induced by pilocarpine: a novel experimental model of intractable epilepsy. *Synapse*, 3, p.154-171.

- Tutak, E., Satar, M., Zorludemir, S., Erdogan, S., Yapicioglu, H. and Narli, N. (2005). Neuroprotective effects of indomethacin and aminoguanidine in the newborn rats with hypoxic-ischemic cerebral injury. *Neurochem. Res.*, 30(8), p.937-942
- Uhlhaas, P.J. and Silverstein, S.M. (2005). Perceptual organization in schizophrenia spectrum disorders: empirical research and theoretical implications. *Psychol. Bull*, 131, p.618-632.
- Uhlhaas, P.J. and Singer, W. (2006). Neural synchrony in brain disorders: Relevance for cognitive dysfunctions and pathophysiology. *Neuron*, 52, p.155-168.
- Ullal, G., Fahnestock, M. and Racine, R. (2005). Time-dependent Effect of Kainate-induced Seizures on Glutamate Receptor GluR5, GluR6, and GluR7 mRNA and Protein Expression in Rat Hippocampus. *Epilepsia*, 46(5), p.616-623.
- Valentin, A., Arunachalam, R., Mesquita-Rodrigues, A., Garcia Seoane, J. J., Richardson, M. P., Mills, K. R., & Alarcon, G. (2008). Late EEG responses triggered by transcranial magnetic stimulation (TMS) in the evaluation of focal epilepsy. *Epilepsia*, 49(3), p. 470-480.
- Vanderwolf, C. H. (1969). Hippocampal electrical activity and voluntary movement in the rat. *Electroen. Clin. Neuro.*, 26(4), p.407-418.
- Vanhatalo, S., Palva, J.M., Holmes, M.D., Miller, J.W., Voipio, J. and Kaila, K. (2004). Infralow oscillations modulate excitability and interictal epileptic activity in the human cortex during sleep. *Proc Natl Acad Sci USA*, 101, p.5053-5057.
- van Putten, M.J. (2003). Nearest neighbor phase synchronization as a measure to detect seizure activity from scalp EEG recordings. *J. Clin. Neurophysiol*, 20, p.320-325.
- Velisek, L. (2006). Models of Chemically-induced Acute Seizures. In: Pitkänen, A., Schwartzkroin PA, Moshé, S.L. (eds) *Models of Seizures and Epilepsy*, Burlington, MA: Elsevier Academic, 2006, p.127-153.
- Veliskova, J., Pitkänen, A., Schwartzkroin, P.A. and Moshé, S.L. (2006). Behavioral characterization of seizures in rats. Models of seizures and epilepsy. *Elsevier Academic Press, Burlington*. p.601-611.
- Vertes, R.P. and Kocsis, B. (1997). Brainstem-diencephalo-septohippocampal systems controlling the theta rhythm of the hippocampus. *Neuroscience*, 81, p.893-926.
- Vignes, M. and Collingridge, G.L. (1997). The synaptic activation of kainite receptors. *Nature*, 388, p.179-182.
- Volgushev, M., Chauvette, S., Mukovski, M. and Timofeev, I. (2006). Precise long-range synchronization of activity and silence in neocortical neurons during slow-wave sleep. *J. Neurosci.*, 26, p.5665-5672.
- Vreugdenhil, M. and Toescu, E.C., (2005). Age-dependent reduction of gamma oscillations in the mouse hippocampus *in vitro*. *Neuroscience*, 132, p.1151-1157.

- Vyazovskiy, V.V., Olcese, U., Lazimy, Y.M., Faraguna, U., Esser, S.K., Williams, J.C. and Tononi, G. (2009). Cortical firing and sleep homeostasis. *Neuron*, 63(6), p.865-878.
- Wallenstein, G.V. and Hasselmo, M.E. (1997). GABAergic modulation of hippocampal activity: Sequence learning, place field development, and the phase precession effect. *J. Neurophysiol.*, 78, p.393-408.
- Walton, N.Y. and Treiman, D.M. (1988). Response of status epilepticus induced by lithium and pilocarpine to treatment with diazepam. *Exp Neurol*, 101, p.267-275.
- Walton, N.Y. and Treiman, D.M. (1991). Motor and electroencephalographic response of refractory experimental status epilepticus in rats to treatment with MK-801, diazepam, or MK-801 plus diazepam. *Brain Res*, 553, p.97-104.
- Wang, S., Chen, X., Kurada, L., Huang, Z. and Lei, S. (2012). Activation of group II metabotropic glutamate receptors inhibits glutamatergic transmission in the rat entorhinal cortex via reduction of glutamate release probability. *Cereb. Cortex*, 22(3), p.584-594.
- Wang, X.J. and Rinzel, J. (1992). Alternating and synchronous rhythms in reciprocally inhibitory model neurons. *Neural Comput.*, 4, p.84-97
- Wang, X.J. and Buzsaki, G. (1996). Gamma oscillation by synaptic inhibition in a hippocampal interneuronal network model. *J. Neurosci.*, 16, p.6402-6413.
- Wass, C. T., Rajala, M. M., Hughes, J. M. and Sharbrough, F. W. (1996). Long-term follow-up of patients treated surgically for medically intractable epilepsy: results in 291 patients treated at mayo clinic rochester between july 1972 and march 1985. *Mayo Clinic Proceedings*, 71(11), p.1105-1113.
- Watkins, J.C. and Evans, R.H., (1981). Excitatory amino acid transmitters. *Annu. Rev. Pharmacol.*, 21, p.165-204.
- West, P.J., Dalpe´-Charron, A., Wilcox, KS. (2007). Differential contribution of kainate receptors to excitatory post-synaptic currents in the superficial layer neurons of the rat medial entorhinal cortex. *Neuroscience*, 146, p.1000–1012.
- Whishaw, I.Q. (1972). Hippocampal electroencephalographic activity in the Mongolian gerbil during natural behaviours and wheel running and in the rat during wheel running and conditioned immobility. *Can J Psychol*, 26, p.219-239.
- Whishaw, I.Q. and Vanderwolf, C.H. (1973). Hippocampal EEG and behavior: change in amplitude and frequency of RSA (theta rhythm). associated with spontaneous and learned movement patterns in rats and cats. *Behavioral biology*, 8(4), p.461-484.
- Whittington, M.A., Traub, R.D. and Jefferys, J.G.R. (1995). Synchronized oscillations in interneuron networks driven by metabotropic glutamate receptor activation. *Nature*, 373, p.612-615.

- Whittington, M. A., Stanford, I. M., Colling, S. B., Jefferys, J. G. R. and Traub, R. D. (1997). Spatiotemporal patterns of gamma frequency oscillations tetanically induced in the rat hippocampal slice. *Journal of Physiology-London*, 502(3), p.591-607.
- Whittington, M. A., Traub, R. D., Kopell, N., Ermentrout, B. and Buhl, E. H. (2000). Inhibition-based rhythms: experimental and mathematical observations on network dynamics. *Int. J. Psychophysiol.* 38, p.315–336.
- Wieser, H.G. (2004). ILAE Commission on Neurosurgery of Epilepsy. ILAE Commission Report. Mesial temporal lobe epilepsy with hippocampal sclerosis. *Epilepsia*, 45, p.695-714.
- Winson, J. (1978). Loss of hippocampal theta rhythm results in spatial memory deficit in the rat. *Science*, 201, p.160-163.
- Wisden, W. and Seeburg, P.H. (1993). A complex mosaic of high-affinity kainite receptors in rat brain. *J. Neurosci.*, 13, p.3582-3598.
- Woodhall, G., Evans, D.I.P. and Jones, R.S.G. (2001). Activation of presynaptic group III metabotropic glutamate receptors depresses spontaneous inhibition in layer V of the rat entorhinal cortex. *Neuroscience*, 105(1), p.71-78.
- Worrell, G.A., Gardner, A.B., Stead, S.M., Hu, S., Goerss, S., Cascino, G.J., Meyer, F.B., Marsh, R. and Litt, B. (2008). High-frequency oscillations in human temporal lobe: Simultaneous microwire and clinical macroelectrode recordings. *Brain*, 131, p.928-937.
- Wozny, C., Gabriel, S., Jandova, K., Schulze, K., Heinemann, U. and Behr, J. (2005). Entorhinal cortex entrains epileptiform activity in CA1 in pilocarpine-treated rats. *Neurobiol. Dis.*, 19(3), p.451-460.
- Wyllie, E., Comair, Y. G., Kotagal, P., Bulacio, J., Bingaman, W. and Ruggieri, P. (1998). Seizure outcome after epilepsy surgery in children and adolescents. *Annals of neurology*, 44(5), p.740-748.
- Xing, D., Yeh, C.I. and Shapley, R.M. (2009). Spatial spread of the local field potential and its laminar variation in visual cortex. *J. Neurosci.*, 29, p.11540-11549.
- Yamamoto, C. and McIlwain, H. (1996). Electrical activities in thin sections from the mammalian brain maintained in chemically-defined media *in vitro*. *J Neurochemistry*, 13, p.1333-1343.
- Yamawaki, N., Stanford, I.M., Hall, S.D. and Woodhall, G.L. (2008). Pharmacological induced and stimulus evoked rhythmic neuronal oscillatory activity in the primary motor cortex (M1). *in vitro. Neuroscience*, 151, p.386-395.
- Yang J., Woodhall G.L. and Jones R.S.G. (2006). Tonic facilitation of glutamate release by presynaptic NR2B-containing NMDA receptors is increased in the entorhinal cortex of chronically epileptic rats. *J. Neurosci.*, 26, p.406-410.
- Ye, J. H., Zhang, J., Xiao, C. and Kong, J. Q. (2006). Patch-clamp studies in the CNS illustrate a simple new method for obtaining viable neurons in rat brain slices:

glycerol replacement of NaCl protects CNS neurons. *J. Neurosci. Meth.*, 158(2), p.251-259.

Yilmazer-Hanke, D. M., Wolf, H. K., Schramm, J., Elger, C. E., Wiestler, O. D. and Blümcke, I. (2000). Subregional pathology of the amygdala complex and entorhinal region in surgical specimens from patients with pharmacoresistant temporal lobe epilepsy. *Journal of Neuropathology and Exp. Neurol.*, 59(10), p.907-920.

Ylinen, A., Sik, A., Bragin, A., Nadasdy, Z., Jando, G., Szabo, I. and Buzsaki, G. (1995). Sharp wave-associated high-frequency oscillation (200 Hz). in the intact hippocampus: network and intracellular mechanisms. *J. Neurosci.*, 15, p.30-46.

Yordanova, J, Banaschewski, T., Kolev, V., Woerner, W., Rothenberger, A. (2001). Abnormal early stages of task stimulus processing in children with attention-deficit hyperactivity disorder evidence from eventrelated gamma oscillations. *Clin Neurophysiol*, 112, p.1096 -1108.

Zhang, C.L., Dreier, J.P., Heinemann, U. (1995). Paroxysmal epileptiform discharges in temporal lobe slices after prolonged exposure to low magnesium are resistant to clinically used anticonvulsants. *Epilepsy Res.*, 20, p.105-111.

Zhang, X., Cui, S.S., Wallace, A.E., Hannesson, D.K., Schmued, L.C. and Saucier, D.M. (2002). Relations between brain pathology and temporal lobe epilepsy. *J. Neurosci.*, 22, p.6052-6061.

Appendix

Appendix 1



National Research Ethics Service

The Black Country Research Ethics Committee

Osprey House
Albert Street
Redditch
Worcestershire
B97 4DE

Telephone: 01527 587573
Facsimile: 01527 587503

30 April 2010

Dr Gavin Woodhall
Reader
Aston University
Biomedical Sciences
Aston Triangle
Birmingham
B47EY

Dear Dr Woodhall

Study Title: Cellular studies in epilepsy
REC reference number: 10/H1202/23
Protocol number: 1.6

Thank you for your letter of 27 April 2010, responding to the Committee's request for further information on the above research and submitting revised documentation.

The further information has been considered on behalf of the Committee by the Vice Chair.

Confirmation of ethical opinion

On behalf of the Committee, I am pleased to confirm a favourable ethical opinion for the above research on the basis described in the application form, protocol and supporting documentation as revised subject to the conditions specified below.

Ethical review of research sites

The favourable opinion applies to all NHS sites taking part in the study, subject to management permission being obtained from the NHS/HSC R&D office prior to the start of the study (see "Conditions of the favourable opinion" below).

Conditions of the favourable opinion

The favourable opinion is subject to the following conditions being met prior to the start of the study.

Management permission or approval must be obtained from each host organisation prior to the start of the study at the site concerned.

For NHS research sites only, management permission for research ("R&D approval") should be obtained from the relevant care organisation(s) in accordance with NHS research governance arrangements. Guidance on applying for NHS permission for research is available in the Integrated Research Application System or at <http://www.rdforum.nhs.uk>.

This Research Ethics Committee is an advisory committee to West Midlands Strategic Health Authority
The National Research Ethics Service (NRES) represents the NRES Directorate within
the National Patient Safety Agency and Research Ethics Committee in England

Figure A.1. Copy of ethical approval for cellular studies in human epilepsy.

Where the only involvement of the NHS organisation is as a Participant Identification Centre, management permission for research is not required but the R&D office should be notified of the study. Guidance should be sought from the R&D office where necessary.

Sponsors are not required to notify the Committee of approvals from host organisations.

It is the responsibility of the sponsor to ensure that all the conditions are complied with before the start of the study or its initiation at a particular site (as applicable).

Approved documents

The final list of documents reviewed and approved by the Committee is as follows:

Document	Version	Date
Covering Letter		19 February 2010
REC application	2.5	19 February 2010
Investigator CV		03 February 2010
Participant Information Sheet: for 6-10 Project overview	2	23 April 2010
Participant Consent Form: For patients	1.6	27 April 2010
Participant Consent Form: For 6-10 years	1.6	27 April 2010
Participant Consent Form: For 11-16 years	1.6	27 April 2010
Referees or other scientific critique report		30 November 2009
Summary/Synopsis	1.1	23 February 2010
Protocol	1.6	23 February 2010
Participant Information Sheet: For 11-16 years project overview	2	23 February 2010
Referees or other scientific critique report		11 February 2010
Letter from Sponsor		16 February 2009
Participant Information Sheet: Information document for patients	1.6	27 April 2010
Participant Information Sheet: Information document for patients [young persons/children 11-16]	1.6	27 April 2010
Participant Information Sheet: Information document for patients [children 6-10 yrs]	1.6	26 April 2010
Response to Request for Further Information		27 April 2010
Participant Information Sheet: Information for Parents of Participants	1.6	27 April 2010

Statement of compliance

The Committee is constituted in accordance with the Governance Arrangements for Research Ethics Committees (July 2001) and complies fully with the Standard Operating Procedures for Research Ethics Committees in the UK.

Figure A.1. Copy of ethical approval for cellular studies in human epilepsy (cont.).

- Notifying substantial amendments
- Adding new sites and investigators
- Progress and safety reports
- Notifying the end of the study

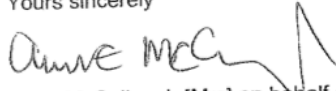
The NRES website also provides guidance on these topics, which is updated in the light of changes in reporting requirements or procedures.

We would also like to inform you that we consult regularly with stakeholders to improve our service. If you would like to join our Reference Group please email referencegroup@nres.npsa.nhs.uk.

10/H1202/23

Please quote this number on all correspondence

Yours sincerely



Anne McCullough [Mrs] on behalf of
Dr Joseph Arumainayagam
Vice Chair

Email: anne.mccullough@westmidlands.nhs.uk

Enclosures: "After ethical review – guidance for researchers"

Copy to: *Dr Nichola Seare*
School of Life and Health sciences
Aston University
Birmingham
B4 7ET

Dr Carol Cummins
R & D Department
Birmingham Children's Hospital
Steelhouse Lane
Birmingham
B4 6NH

Figure A.1. Copy of ethical approval for cellular studies in human epilepsy (cont.).

Appendix 2

Table A.1. Choline chloride-based cutting solution recipe. Adapted from BrainSliceMethods n.d.

Choline Chloride Recovery Solution (JT)					
Recovery period <12 min at 32-34°C (use the shortest possible)					
Excellent for very old mice or for difficult/compact brain areas (CA1, CA3)					
(NOTE: extended exposure can permanently disrupt physiology)					
(NOTE: recommended only if NMDG-HEPES aCSF is not sufficient)					
	mM	MW	g/L	g/500 mL	
Choline chloride	92	139.6	12.85	6.42	
KCl	2.5	74.6	0.19	0.09	
NaH ₂ PO ₄	1.2	138.0	0.17	0.08	
NaHCO ₃	30	84.0	2.52	1.26	
HEPES	20	238.3	4.77	2.38	
Glucose	25	180.2	4.51	2.25	
Sodium ascorbate	5	198.0	0.99	0.50	
Thiourea	2	76.1	0.15	0.08	
Sodium pyruvate	3	110.0	0.33	0.17	
MgSO ₄ ·7H ₂ O	10	246.4 8	5 mL	2.5 mL	(2M stock)
CaCl ₂ ·2H ₂ O	0.5	147.0 1	250 μL	125 μL	(2M stock)

Table A.2. NMDG-based cutting solution recipe. Adapted from BrainSliceMethods n.d.

NMDG-HEPES Recovery Solution (JT)					
Recovery period <15 min at 32-34°C					
Excellent for mouse ages 5 weeks to 1 year old or older					
	mM	MW	g/L	g/500 mL	
NMDG	93	195.2	18.16	9.08	
HCl (see note)	93				(10N stock)
KCl	2.5	74.6	0.19	0.09	
NaH ₂ PO ₄	1.2	138.0	0.17	0.08	
NaHCO ₃	30	84.0	2.52	1.26	
HEPES	20	238.3	4.77	2.38	
Glucose	25	180.2	4.51	2.25	
Sodium ascorbate	5	198.0	0.99	0.50	
Thiourea	2	76.1	0.15	0.08	
Sodium pyruvate	3	110.0	0.33	0.17	
MgSO ₄ ·7H ₂ O	10	246.5	5 mL	2.5 mL	(2M stock)
CaCl ₂ ·2H ₂ O	0.5	147.0	250	125 μL	(2M stock)

			μL		stock)
--	--	--	---------------	--	--------

Table A.3. Modified HEPES holding aCSF recipe. Adapted from BrainSliceMethods n.d.

Modified HEPES Holding aCSF (JT)					
	mM	MW	g/L	g/500 mL	
NaCl	92	58.4	5.38	2.69	
KCl	2.5	74.6	0.19	0.09	
NaH ₂ PO ₄	1.2	138.0	0.17	0.08	
NaHCO ₃	30	84.0	2.52	1.26	
HEPES	20	238.3	4.77	2.38	
Glucose	25	180.2	4.51	2.25	
Sodium ascorbate	5	198.0	0.99	0.50	
Thiourea	2	76.1	0.15	0.08	
Sodium pyruvate	3	110.0	0.33	0.17	
MgSO ₄ .7H ₂ O	2	246.5	1 mL	0.5 mL	(2M stock)
CaCl ₂ .2H ₂ O	2	147.0	1 mL	0.5 mL	(2M stock)

Table A.4 Recording aCSF recipe. Adapted from BrainSliceMethods n.d.

Standard recording aCSF (JT)					
	mM	MW	g/L	g/500mL	
NaCl	124	58.4	7.25	3.62	
KCl	2.5	74.6	0.19	0.09	
NaH ₂ PO ₄	1.2	138.0	0.17	0.08	
NaHCO ₃	24	84.0	2.02	1.01	
HEPES	5	238.3	1.19	0.60	
Glucose	12.5	180.2	2.25	1.13	
MgSO ₄ .7H ₂ O	2	246.5	1 mL	0.5 mL	(2M stock)
CaCl ₂ .2H ₂ O	2	147.0	1 mL	0.5 mL	(2M stock)